

CORONARY PERIVASCULAR ADIPOSE TISSUE AND VASCULAR SMOOTH
MUSCLE FUNCTION: INFLUENCE OF OBESITY

Jillian Nicole Noblet

Submitted to the faculty of the University Graduate School
in partial fulfillment of the requirements
for the degree
Doctor of Philosophy
in the Department of Cellular & Integrative Physiology,
Indiana University

April 2016

Accepted by the Graduate Faculty, Indiana University, in partial fulfillment of the requirements for the degree of Doctor of Philosophy.

Johnathan D. Tune, Ph.D., Chair

Robert V. Considine, Ph.D.

Doctoral Committee

Carmella E. Evans-Molina, M.D., Ph.D.

March 22, 2016

Michael S. Sturek, Ph.D.

DEDICATION

This dissertation is dedicated to my parents for their love, encouragement, and support throughout my education.

ACKNOWLEDGEMENTS

The author would like to express her deepest gratitude to her graduate advisor, Dr. Johnathan D. Tune for his steadfast leadership and support throughout the completion of this work. His mentorship will continue to impact and inspire the author for many years to come. Additionally, the author would like to thank the members of her research committee, Drs. Robert V. Considine, Carmella E. Evans-Molina, and Michael S. Sturek for their invaluable contributions. This work was supported by the National Institutes of Health, National Center for Advancing Translational Sciences, Clinical and Translational Sciences Award TL1 TR001107 and UL1 TR001108 (A. Shekhar), Indiana University Health – Indiana University School of Medicine Strategic Research Initiative (CECARE) and National Institute of Health HL117620 (J.D. Tune-Mather).

CORONARY PERIVASCULAR ADIPOSE TISSUE AND VASCULAR SMOOTH
MUSCLE FUNCTION: INFLUENCE OF OBESITY

Factors released from coronary perivascular adipose tissue (PVAT), which surrounds large coronary arteries, have been implicated in the development of coronary disease. However, the precise contribution of coronary PVAT-derived factors to the initiation and progression of coronary vascular dysfunction remains ill defined. Accordingly, this investigation was designed to delineate the mechanisms by which PVAT-derived factors influence obesity-induced coronary smooth muscle dysfunction. Isometric tension studies of coronary arteries from lean and obese swine demonstrated that both lean and obese coronary PVAT attenuate vasodilation via inhibitory effects on smooth muscle K^+ channels. Specifically, lean coronary PVAT attenuated K_{Ca} and K_v7 channel-mediated dilation, whereas obese coronary PVAT impaired K_{ATP} channel-mediated dilation. Importantly, these effects were independent of alterations in underlying smooth muscle function in obese arteries. The PVAT-derived factor calpastatin impaired adenosine dilation in lean but not obese arteries, suggesting that alterations in specific factors may contribute to the development of smooth muscle dysfunction. Further studies tested the hypothesis that leptin, which is expressed in coronary PVAT and is upregulated in obesity, acts as an upstream mediator of coronary smooth muscle dysfunction. Long-term administration (3 day culture) of obese concentrations of leptin markedly altered the coronary artery proteome, favoring pathways associated with calcium signaling and cellular proliferation. Isometric tension studies demonstrated that short-term (30 min) exposure to leptin potentiated depolarization-induced contraction of coronary arteries and that this effect was augmented following longer-term leptin administration (3 days). Inhibition of Rho kinase reduced leptin-mediated increases in coronary artery contractions.

Acute treatment was associated with increased Rho kinase activity, whereas longer-term exposure was associated with increases in Rho kinase protein abundance. Alterations in Rho kinase signaling were also associated with leptin-mediated increases in coronary vascular smooth muscle proliferation. These findings provide novel mechanistic evidence linking coronary PVAT with vascular dysfunction and further support a role for coronary PVAT in the pathogenesis of coronary disease.

Johnathan D. Tune, Ph.D., Chair

TABLE OF CONTENTS

| | |
|---|----|
| Chapter 1: Introduction | 1 |
| The Global Pandemic of Obesity..... | 2 |
| Obesity and Cardiovascular Disease | 3 |
| Adipose Tissue and Obesity-Induced Coronary Disease..... | 5 |
| Perivascular Adipose Tissue | 10 |
| Coronary Perivascular Adipose Tissue | 11 |
| Obesity and Coronary Vascular Dysfunction | 13 |
| Vascular Effects of Perivascular Adipose Tissue | 19 |
| Expression Profiles in Coronary PVAT..... | 23 |
| Pathways Influenced by Coronary Perivascular Adipose Tissue | 29 |
| Summary and Proposed Experimental Aims | 32 |
| Chapter 2: Lean and obese coronary perivascular adipose tissue impairs vasodilation via differential inhibition of vascular smooth muscle K ⁺ channels..... | 35 |
| Abstract | 36 |
| Introduction | 37 |
| Materials and Methods..... | 38 |
| Results..... | 43 |
| Discussion | 51 |
| Acknowledgements..... | 55 |
| Sources of Funding..... | 55 |
| Disclosures | 56 |
| Significance | 56 |
| Chapter 3: Leptin augments coronary vasoconstriction and smooth muscle proliferation via a Rho kinase dependent pathway..... | 57 |
| Abstract | 58 |

| | |
|---|-----|
| Introduction | 59 |
| Materials and Methods..... | 61 |
| Results..... | 68 |
| Discussion | 76 |
| Disclosures | 83 |
| Chapter 4: Discussion | 84 |
| Summary of Findings | 85 |
| Implications..... | 90 |
| Future Directions and Proposed Studies..... | 92 |
| Concluding Remarks..... | 97 |
| Appendices | 99 |
| Appendix A: Supplemental Table..... | 100 |
| Appendix B: Supplemental Figures | 169 |
| Reference List | 173 |
| Curriculum Vitae | |

LIST OF TABLES

Chapter 1

Table 1.1 Adipokine expression of coronary perivascular relative to subcutaneous adipose tissue in health and coronary artery disease. CAD indicates coronary artery disease; NCAD, no coronary artery disease; NCAD+CAD, group populations. ↑ indicates significant increase in expression in coronary perivascular adipose tissue (PVAT); ↓ indicates significant decrease in expression; TNF- α , tumor necrosis factor-alpha; IL-6, interleukin, 6; IL-1 β , interleukin-1 beta; MCP-1, monocyte chemoattractant protein-1; PAI-1, plasminogen activator inhibitor-1. Modified from Owen et al., *Arterioscler Thromb Vasc Biol*, 2014.¹⁷

Chapter 2

Table 2.1 Phenotypic characteristics of lean and obese Ossabaw swine. Values are mean \pm SE for lean (n=10) and obese (n=10) swine. * P <0.05 vs. lean.

Chapter 3

Table 3.1 Protein expression profile of leptin-treated coronary arteries. Values for fold change in expression of coronary arteries cultured for three days with leptin (30 ng/mL) versus untreated controls (n=4 each group). Ingenuity Pathway Analysis (IPA): ¹Calcium signaling, ²Cell proliferation, ³Cell movement, migration, invasion, ⁴Quantity of smooth muscle cells, ⁵Cell spreading. **Bos taurus* homolog.

LIST OF FIGURES

Chapter 1

Figure 1.1 Pandemic of obesity in men aged 18+. In 2014, more than half a billion adults worldwide were classed as obese (BMI \geq 30 kg/m²).³

Figure 1.2 Global prevalence of overweight and obesity in adults. Age-standardized prevalence of overweight and obesity (BMI \geq 25, A) and obesity (BMI \geq 30, B) increased in both developed and developing countries between 1980 and 2013.¹¹

Figure 1.3 Cardiovascular disease mortality in the United States. Coronary heart disease accounts for nearly half of all cardiovascular related deaths.⁷

Figure 1.4 Components of adipose tissue. Adipocytes and the stromal vascular fraction constitute the main cellular component of adipose tissue. Blood vessels distributed throughout adipose provide oxygen and nutrients to the tissue and allow for the distribution of adipokines.¹³

Figure 1.5 Obesity-induced adipose tissue dysfunction. Chronic inflammation of adipose tissue in obesity markedly alters the adipokine expression profile. Augmented secretion of pro-inflammatory adipokines from adipose tissue triggers endothelial dysfunction and vascular inflammation.⁶

Figure 1.6 Pathogenesis of atherosclerosis. Endothelial dysfunction stimulates chemokine production and the upregulation of leukocyte adhesion molecules on the surface of endothelial cells. These changes, along with increased endothelial permeability, result in migration of leukocytes into the artery wall. Monocytes differentiate into macrophages, which take up modified LDL to form foam cells. Pro-inflammatory chemokines promote proliferation and migration of smooth muscle cells into the developing plaque. A fibrous cap forms over the top of the plaque, providing temporary stabilization and isolation from the circulation. Hypoxia and oxidative stress may cause foam-cell apoptosis and lead to the formation of a lipid-laden necrotic core. As the plaque enlarges, it may become large enough to impede blood flow (i.e., flow limiting stenosis) and/or the fibrous cap thins and ruptures leading to acute thrombosis and occlusion.¹⁴

Figure 1.7 Factors derived from adipose tissue contribute to atherogenesis. Adipokines are known to influence nearly all critical aspects of atherogenesis including endothelial dysfunction, leukocyte recruitment and transmigration, lipid oxidation, foam cell formation, smooth muscle cell proliferation and migration, plaque rupture, and thrombus formation. Red arrows represent pro-inflammatory pathways that are stimulated during obesity. Blue arrows represent anti-inflammatory pathways that are inhibited during obesity. Green arrows represent the stimulation of adipokine secretion.¹²

Figure 1.8 Anatomic locations of perivascular adipose tissue. Types of perivascular adipose tissue (PVAT) can be classified according to anatomic location. Note that PVAT is absent from the murine coronary artery.⁸

Figure 1.9 Coronary perivascular adipose tissue. Representative image of naturally occurring coronary perivascular adipose tissue (PVAT) on the heart. RA, right atrium; LA, left atrium; RV, right ventricle; LV, left ventricle; RCA, right coronary artery; LAD, left anterior descending artery; LCX, left circumflex artery.¹⁵

Figure 1.10 Effects of metabolic syndrome on coronary blood flow. Metabolic syndrome (MetS) diminishes local metabolic control of coronary blood flow, evidenced by decreased coronary blood flow at a given coronary venous PO₂ (left). MetS also results in an imbalance between myocardial oxygen supply and demand, evidenced by the reduction in coronary venous PO₂ relative to alterations in myocardial oxygen consumption (right). Modified from Berwick et al., *J Mol Cell Cardiol*, 2012.⁴

Figure 1.11 K_V channel dysfunction in metabolic syndrome. Whole-cell voltage-dependent K⁺ current was impaired at currents consistent with K_V channel activation (i.e., greater than 0 mV) in coronary smooth muscle from metabolic syndrome (MetS) swine. Modified from Berwick et al., *J Mol Cell Cardiol*, 2012.²¹

Figure 1.12 BK_{Ca} channel dysfunction in metabolic syndrome. Coronary smooth muscle cell current in response to the BK_{Ca} channel agonist, NS1619, was reduced in metabolic syndrome (MetS; left). Reductions in BK_{Ca} channel current correspond to diminished vasodilation to NS1619 in MetS swine (right). Modified from Berwick et al., *J Mol Cell Cardiol*, 2012.⁴

Figure 1.13 Increased Ca_v1.2 channel-mediated coronary vasoconstriction in metabolic syndrome. Contractile responses to the Ca_v1.2 channel agonist, BayK 8644, were augmented in coronary arteries from metabolic syndrome (MetS) swine. Modified from Borbouse et al., *Am J Physiol Heart Circ Physiol*, 2009.¹

Figure 1.14 Perivascular adipose tissue releases a relaxing factor. Contractile responses of rat aortic rings with surrounding fat intact (bottom) were significantly impaired relative to contractions in the absence of fat (top). Modified from Löhn et al., *FASEB J*, 2002.⁵

Figure 1.15 Coronary perivascular adipose tissue potentiates coronary artery contractions. Representative wire myograph tracing of tension generated by coronary arteries in response to prostaglandin F₂α (PGF₂α) and the addition of perivascular adipose tissue (PVAT) to the organ bath (top). Active tension development stimulated by coronary PVAT was proportional to the amount of PVAT added and was significantly augmented in swine with metabolic syndrome (MetS). Modified from Owen et al., *Circulation*, 2013.⁹

Figure 1.16 The coronary vasa vasorum. Epicardial adipokines may be delivered to the vessel wall via paracrine signaling by diffusing through the interstitial fluid (1) or via vasocrine signaling through the network of blood vessels supplying the vessel wall, the vasa vasorum (2).²⁰

Figure 1.17 Leptin impairs coronary endothelial-dependent dilation *in vitro* and *in vivo*. Leptin impaired endothelial-dependent vasodilation of isolated canine coronary arteries to acetylcholine (ACh) at a concentration of 10 ng/mL but not 4 ng/mL (left). In open chest anesthetized dogs, concentrations of leptin in the obese range attenuated coronary vasodilation to acetylcholine (right). Modified from Knudson et al., *Exp Biol Med (Maywood)*, 2007.¹⁶

Figure 1.18 Coronary perivascular adipose-derived leptin exacerbates endothelial dysfunction. Impaired endothelial-dependent vasodilation of coronary arteries from metabolic syndrome (MetS) swine to bradykinin is indicative of endothelial dysfunction.

This endothelial dysfunction was exacerbated in the presence of perivascular adipose tissue (PVAT) from the same animal. Addition of a pegylated leptin antagonist to inhibit leptin signaling significantly improved dilation to bradykinin. Modified from Payne et al., *Arterioscler Thromb Vasc Biol*, 2010.²

Figure 1.19 Imbalance between leptin and adiponectin as an upstream mediator of atherogenesis. In the setting of obesity, increased expression of leptin and diminished expression of adiponectin in coronary PVAT is associated with the activation of several complex atherogenic pathways. CRP, C-reactive protein; IL, interleukin-1 and 6; TNF α , tumor necrosis factor-alpha; oxLDL, oxidized low density lipoprotein.¹⁵

Figure 1.20 Effects of Rho kinase signaling on the vascular effects of coronary PVAT. Addition of the Rho kinase inhibitor, fasudil, significantly reduced the contractile effect of PVAT in isolated coronary arteries from lean, but not obese swine. The difference in tension generated by each isolated porcine coronary artery before and after the addition of perivascular adipose tissue (PVAT) is expressed as delta active tension. Modified by Owen et al., 2013.⁹

Figure 1.21 Alterations in coronary perivascular adipose tissue (PVAT)-derived adipokines and potential downstream effector mechanisms in endothelium and vascular smooth muscle. Coronary PVAT-derived leptin diminishes endothelial nitric oxide synthase (eNOS) activity, reducing nitric oxide (NO)-mediated dilation of vascular smooth muscle via K⁺ channel activation and contributes to the recruitment and retention of macrophages. Adipose-derived constricting factors (ADCF), such as calpastatin and other presently unknown factors, increase vasodilation via activation of Ca_v1.2 channels, inhibition of K⁺ channels, and/or alterations in Rho kinase signaling. Production of other adipokines that may play a role in endothelial and smooth muscle dysfunction include, but are not limited to, increased resistin, chemerin, osteoglycin and osteoprotegerin, and decreased adiponectin. H₂O₂, hydrogen peroxide; TNF, tumor necrosis factor.¹⁷

Chapter 2

Figure 2.1 Representative pictures illustrating the isolation of coronary artery rings and perivascular adipose tissue (PVAT) from lean and obese hearts prior to isometric tension studies. Images adapted from Owen et al.,⁹ with permissions from Wolters Kluwer Health Publishing. Copyright 2013, *Circulation*.

Figure 2.2 Experimental design for isometric tension studies. Illustrations correspond to studies presented in Figure 2.5 and Figure 2.6.

Figure 2.3 Experimental design for crossover isometric tension studies. Illustrations correspond to studies presented in Figure 2.8.

Figure 2.4 Representative images of immunohistochemical analyses of coronary arteries and associated PVAT. Arteries were obtained from humans (n=2), and lean and obese swine (n=4, each group). Hematoxylin and eosin-stained sections (10X) illustrated similarities in perivascular adipocyte morphology between humans and swine (A-C). Verhoeff-van Gieson stained sections (4X) showed evidence of atheroma formation in

human (F) and obese (E) compared to lean (D) arteries. CD163 staining (10X) indicated a marked increase in macrophages in obese (I, arrows) compared to lean (H) arteries relative to isotype control (G).

Figure 2.5 Coronary PVAT attenuates adenosine induced vasodilation. In control arteries cleaned of PVAT (n=6 each group), maximal vasodilation to adenosine was reduced ~25% in lean (A) compared to obese (B) arteries. The presence of PVAT from the same animal (n=6 each group) impaired dilation to a similar extent and constriction with KCl (n=3 each group) abolished adenosine dilation in lean and obese arteries. * $P < 0.05$, PVAT vs. control. † $P < 0.001$, lean vs. obese control.

Figure 2.6 Effect of coronary PVAT on K⁺ channel mediated dilation is altered in obesity. Arteries were incubated in the absence (control) or presence of PVAT from the same animal. PVAT attenuated vasodilation to the K_{Ca} channel agonist NS-1619 in lean (A) but not obese (B) arteries. Dilation to the K_V7 channel agonist L-364,373 was reduced in the presence of PVAT in lean (C) but not obese (D) arteries. In the absence of PVAT, dilation to NS-1619 and L-364,373 was impaired in obese (B, D) relative to lean (A, C) arteries. K_{ATP} channel mediated dilation to cromakalim was unaffected by PVAT in lean (E) arteries but was impaired by PVAT in obese (F) arteries. * $P < 0.05$, PVAT vs. control. † $P < 0.05$, lean vs. obese control.

Figure 2.7 Western blot analysis of coronary artery KCNQ1 and Kir6.1 channel expression. Representative blots of KCNQ1 (A) and Kir6.1 (B) channel expression in lean and obese arteries. Expression levels of both KCNQ1 (C) and Kir6.1 (D) were unaffected by an obese phenotype ($P = 0.11$ and $P = 0.40$, respectively). Average data (n=3 for each group) are expressed as % protein observed in lean swine.

Figure 2.8 Effects of lean versus obese PVAT on coronary K⁺ channel mediated dilation in lean arteries. For comparison purposes, lean control and lean PVAT responses are re-plotted from Figure 2A, 2C and 2E. Obese PVAT had no effect on vasodilation of lean arteries to the K_{Ca} channel agonist NS-1619 (n=4 [A]) or the K_V7 channel agonist L-364,373 (n=3 [B]). Dilation of lean arteries to the K_{ATP} channel agonist cromakalim was attenuated by obese but not lean PVAT (n=3 [C]). * $P < 0.05$ lean PVAT vs. control. † $P < 0.05$, obese PVAT vs. control.

Figure 2.9 Effect of calpastatin on coronary artery vasodilation to adenosine. Incubation with calpastatin (10 μM) attenuated adenosine dilation in lean (A) but not obese (B) arteries. All groups n=5. * $P < 0.05$ vs. control.

Chapter 3

Figure 3.1 Leptin augments depolarization-induced coronary artery contractions. Acute (30 min) exposure to leptin (30 ng/mL) increased KCl-induced contractions ~1.3 g at doses >40 mM (n=9 [A]). Chronic (3 day culture in serum-free media) leptin

administration (30 ng/mL) increased tension development ~2.5 g at doses >40 mM (n=4 [B]).

Figure 3.2 Role of Rho kinase in leptin-mediated coronary contraction. In the absence of leptin, acute (n=9 [A]), but not chronic (n=4 [B]) treatment with the Rho kinase inhibitor, fasudil (1 μ M), diminished vasoconstriction to KCl. Inhibition of Rho kinase reduced the effect of both acute (n=9 [C]) and chronic (n=4 [D]) leptin administration on KCl-induced contractions. However, the fasudil-mediated reduction in tension was greater following acute (C) versus chronic (D) leptin exposure.

Figure 3.3 Effects of acute versus chronic leptin treatment on Rho kinase. Representative blots of Rho kinase protein abundance in coronary arteries following acute (A) and chronic (3 day culture in serum free media) (D) leptin exposure. Average data are expressed as % relative to control. Acute leptin treatment increased Rho kinase activity (C) in the absence of a change in protein abundance (B). Following chronic exposure, protein abundance was significantly elevated in leptin treated arteries (E), while no difference in overall Rho kinase activity was detected relative to untreated control arteries (F). All groups n=3. * P <0.05, leptin vs. control. † P <0.05, vs. acute control.

Figure 3.4 Leptin augments coronary vascular smooth muscle proliferation via effects on Rho kinase. Representative images of α -smooth muscle actin (red) and proliferating cell nuclear antigen (brown) co-immunostaining of untreated, control (A), leptin treated (B), and leptin and fasudil co-treated arteries (C) following chronic, 8 day culture in serum-containing media. The increase in PCNA-positive nuclei in leptin treated, relative to untreated arteries was significantly reduced by inhibition of Rho kinase with fasudil (D). All groups n=5. * P <0.05, leptin vs. control. ** P <0.05 leptin vs. leptin+fasudil.

Figure 3.5 Effects of leptin-induced vascular smooth muscle proliferation on Rho kinase. Representative blot of Rho kinase protein abundance in control versus leptin treated arteries following 8 days of culture in serum-containing media (A). Leptin administration significantly increased Rho kinase activity (C), while only a modest increase in Rho kinase protein abundance was detected (B). The effect of leptin on Rho kinase activity was abolished by co-incubation with fasudil (C) All groups n=5. * P <0.05, leptin vs. control. ** P <0.05 leptin vs. leptin+fasudil.

Chapter 4

Figure 4.1 Factors derived from lean and obese coronary perivascular adipose tissue (PVAT) inhibit K⁺ channel-mediated vasodilation. Coronary PVAT attenuates vasodilation via differential inhibition of vascular smooth muscle K⁺ channels. Lean PVAT-derived factors inhibit K_{Ca} and K_{V7} channels, while obese PVAT-derived factors inhibit K_{ATP} channels. These inhibitory effects occur independently of underlying differences in smooth muscle reactivity in coronary arteries from lean and obese swine.

Figure 4.2 Leptin increases coronary vasoconstriction and smooth muscle proliferation. Leptin promotes progressive increases in coronary vasoconstriction via alterations in Rho kinase signaling. Acute (30 min) leptin administration increases Rho

kinase (ROCK) activity, whereas chronic (3 day culture) leptin exposure increases ROCK protein abundance. Leptin mediated increases in vascular smooth muscle cell proliferation following chronic (8 day culture) administration are associated with increases in Rho kinase activity.

Figure 4.3 Proposed mechanisms of action of coronary PVAT-derived factors on vascular smooth muscle function. Lean and obese PVAT-derived factors attenuate vasodilation via inhibitory effects on vascular smooth muscle K⁺ channels. Inhibitory effects on K⁺ channels serve to increase Ca_v1.2 channel activity, further potentiating contraction. In the setting of obesity, alterations in specific factors are capable of influencing smooth muscle function. Increased leptin promotes progressive increases in coronary vasoconstriction and augments smooth muscle proliferation. These leptin-mediated effects are associated with increases in Rho kinase (ROCK) activity and/or expression. Increased calpastatin promotes vasoconstriction, which is proposed to occur via activation of Ca_v1.2 channels.

Figure 4.4 Lentiviral transfection of coronary PVAT. Representative image of *in vitro* lentiviral GFP (green) transfection of coronary PVAT (top). Confocal image of GFP expression in PVAT following *in vivo* lentiviral injection (bottom).

Figure 4.5 Proposed mechanism of coronary PVAT-derived leptin action on coronary vascular calcification and disease. Leptin has been associated with increased release of osteoprotegerin (OPG) and receptor activator of nuclear factor-κB ligand (RANKL),¹⁰ which could be mediated through leptin-stimulated release from coronary PVAT or inflammatory tumor necrosis factor-α (TNF-α) signaling from coronary endothelial cells. Studies suggest that OPG exacerbates endothelial dysfunction and promotes inflammatory cell infiltration.^{18;19} Leptin has been shown to upregulate RANKL expression and promote osteogenic differentiation and calcification of vascular smooth muscle cells,²² which may also be stimulated via leptin receptor (ObR) signaling. Overall, these promising findings support the hypothesis of leptin as an upstream regulator of the calcification of coronary vascular smooth muscle cells.

Chapter 1

Introduction

The Global Pandemic of Obesity

Over the last several decades, an overabundance of food and an increasingly sedentary lifestyle have contributed to the advancement obesity from a relatively minor health issue to a major threat to public health throughout the world. In fact, the increasing prevalence of overweight and obese individuals has been described as a global pandemic (**Figure 1.1**).^{3;23;24} Recent estimates indicate that approximately 2 billion individuals are overweight (defined as a body mass index, BMI ≥ 25 kg/m²)²⁵ or obese (BMI ≥ 30 kg/m²),²⁵ with at least one-third of the world's adult population considered obese.^{11;26} The Global

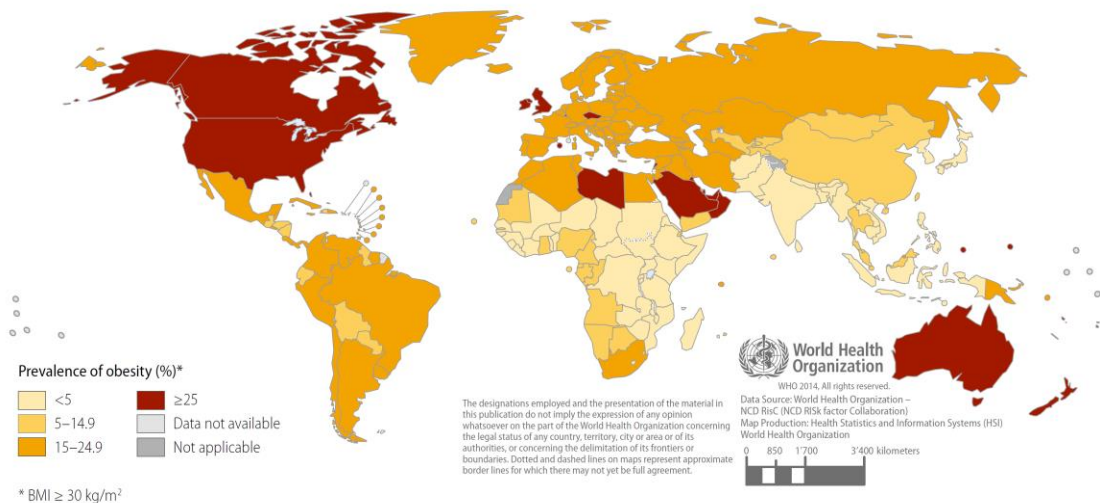


Figure 1.1 Pandemic of obesity in men aged 18+. In 2014, more than half a billion adults worldwide were classed as obese (BMI ≥ 30 kg/m²).³

Burden of Disease Study 2013 further revealed that the proportion of adults with a BMI of 25 or greater increased from 29% to 37% in men and from 30% to 38% in women between 1980 and 2013 (**Figure 1.2**).¹¹ Both developed and developing countries are plagued by the obesity epidemic,²⁵ as no country in the world has had a significant decrease in obesity

in the past 33 years.¹¹ Currently, the United States is among the top 15 countries worldwide in terms of increases in obesity since 1980.¹¹ Although some data suggest that this increase in obesity is levelling off among adults in the United States,²⁷⁻²⁹ cases of severe obesity (BMI ≥ 35 kg/m²)²⁵ are accounting for an increasingly large proportion of the obese population over time, with 1 in 7 Americans now considered severely obese.^{30;31} As evidenced by the substantial increase in prevalence and severity, obesity has clearly become a major national and global health crisis.

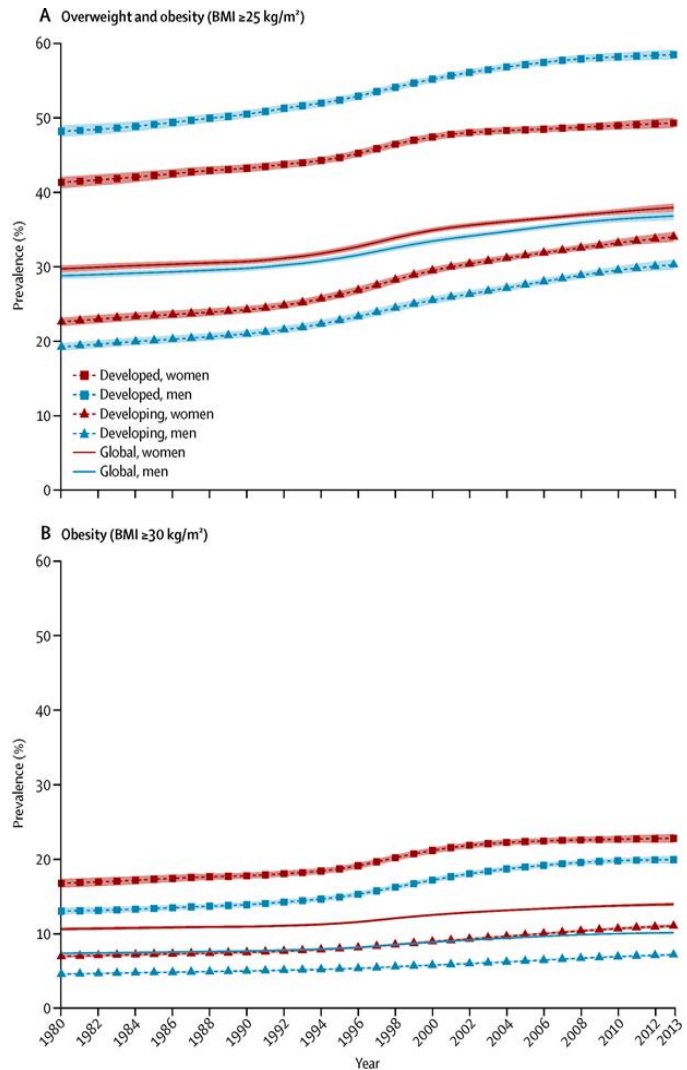


Figure 1.2 Global prevalence of overweight and obesity in adults. Age-standardized prevalence of overweight and obesity (BMI ≥ 25 , A) and obesity (BMI ≥ 25 , B) increased in both developed and developing countries between 1980 and 2013.¹¹

Obesity and Cardiovascular Disease

Perhaps more alarming than the rising prevalence of obesity are the established health risks associated with this condition. Throughout the world, overweight and obesity account for nearly 3.5 million deaths and 95 million disability-adjusted life years (i.e., the number of years lost due to ill-health, disability or early death) per year.³ Medical care costs of obesity and its related health complications reach an estimated \$150 billion dollars

annually in the United States.³² This includes both direct costs related to diagnostic and treatment services as well as indirect costs related to the impact of obesity on morbidity and mortality.^{33;34} Weight gain is associated with numerous comorbidities that contribute to a reduced quality of life including limited mobility, depression, and respiratory ailments such as asthma and sleep apnea.^{35;36} Excess weight also leads to adverse metabolic effects on blood pressure, cholesterol, triglycerides, and insulin resistance.^{13;25;36} Since 1988, investigators have systematically outlined a clustering of several risk factors associated with cardiovascular disease including but not limited to abdominal obesity, hypertension, dyslipidemia, and glucose intolerance which are now referred to as “metabolic syndrome”

(MetS).³⁷⁻³⁹ An estimated 30% of the total U.S. population and near 60% of those considered obese exhibit characteristics of the MetS.^{40;41} Individuals with MetS are at a significantly increased overall risk for developing cardiovascular disease, and each component

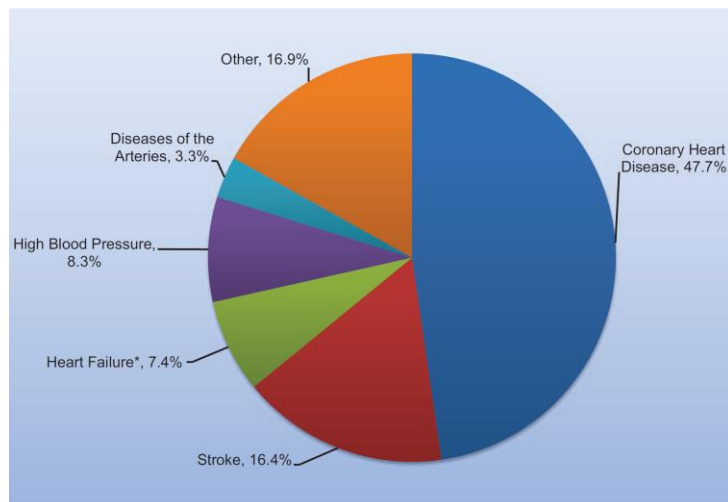


Figure 1.3 Cardiovascular disease mortality in the United States. Coronary heart disease accounts for nearly half of all cardiovascular related deaths.⁷

of the MetS is considered an independent risk factor.^{38;39;42;43} Obesity, in particular, is considered a major risk factor for a cardiovascular event such as a myocardial infarction or stroke.^{44;45} Cardiovascular disease is the leading cause of death in the United States, accounting for 31% of all deaths.⁷ A large proportion of cardiovascular related deaths are a result of coronary artery disease (**Figure 1.3**), the complications of which are responsible for approximately 1 of every 7 deaths in the United States.⁷ Prospective studies provide strong support that obesity alone is associated with increased risk of coronary artery

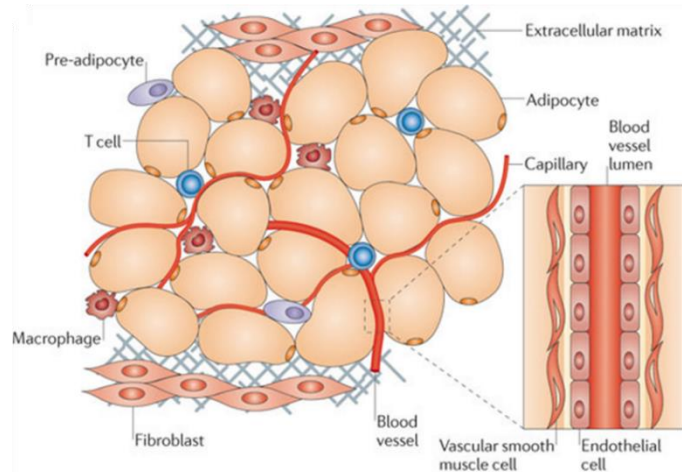
disease, even prior to the development of overt clinical symptoms (i.e., morbid obesity or type 2 diabetes).⁴⁶ Taken together, an even larger proportion of the population may be at increased risk of coronary disease than has been currently identified. These findings highlight the importance of understanding the complex relationship between obesity and coronary disease.

Despite the growing global pandemic of obesity and the incidence of obesity-related cardiovascular disease, the precise mechanisms by which excess adiposity predisposes individuals to coronary disease remain poorly understood. Recent attention has been given to adipose tissue, an active endocrine and paracrine organ that releases a variety of bioactive mediators that may provide a molecular link between obesity and cardiovascular disease.^{13;47-49}

Adipose Tissue and Obesity-induced Coronary Disease

Numerous investigations have focused on the multifaceted relationships between adipose tissue, metabolic dysfunction, chronic inflammation, and cardiovascular disease in the setting of obesity. Historically, adipose tissue was thought simply as lipid-laden connective tissue responsible for insulating the body, storing triglycerides during energy surplus, and releasing energy in the form of free fatty acids during periods of energy shortage.^{50;51} However, it is now commonly accepted that adipose tissue is also an endocrine and paracrine organ capable of secreting a multitude of bioactive proteins and peptides, collectively referred to as adipokines.^{13;47} Adipose tissue is composed of several cell types such as adipocytes, preadipocytes, and the stromal vascular fraction which includes macrophages, leukocytes, and endothelial cells (**Figure 1.4**).^{13;52} The majority of adipokines are released from adipocytes, whereas non-fat cells (i.e., stromal vascular

fraction) secrete inflammatory cytokines.⁵³ Recent studies have identified adipose tissue dysfunction (i.e., heightened inflammatory status) as a defining characteristic of obesity/MetS and its related pathologies.



In the setting of obesity, factors that promote adipogenesis such as lipoprotein lipase and cholesterol ester transfer protein

Figure 1.4 Components of adipose tissue. Adipocytes and the stromal vascular fraction constitute the main cellular component of adipose tissue. Blood vessels distributed throughout adipose provide oxygen and nutrients to the tissue and allow for the distribution of adipokines.¹³

act via paracrine and/or autocrine mechanisms to increase adipose depot size and/or modulate body fat distribution.⁵⁴ Both adipocyte hyperplasia (increase in cell number) and hypertrophy (increase in cell size) have been observed in the obese state.⁵⁵ The persistent state of energy excess exerts an increased burden on adipose tissue causing various effects, predominantly inflammation, within the tissue (**Figure 1.5**).^{6;56} This chronic inflammatory state modifies the cellular composition and/or phenotype of the tissue, resulting in marked alterations in secretory output.^{6;13;48} Adipocyte hypertrophy is associated with a pro-inflammatory adipose secretome, evidenced by a positive correlation between adipocyte size and secretion of pro-inflammatory factors such as tumor necrosis factor- α (TNF- α), monocyte chemoattractant protein (MCP-1), leptin, interleukin-6 (IL-6), and interleukin-8 (IL-8).⁵⁷ Subsequent infiltration of macrophages and lymphocytes are not only a source of inflammation but also contribute to increased secretion of pro-inflammatory adipokines, which further exacerbate the inflammatory status of adipose tissue.^{6;58} This rich source of pro-inflammatory mediators has the

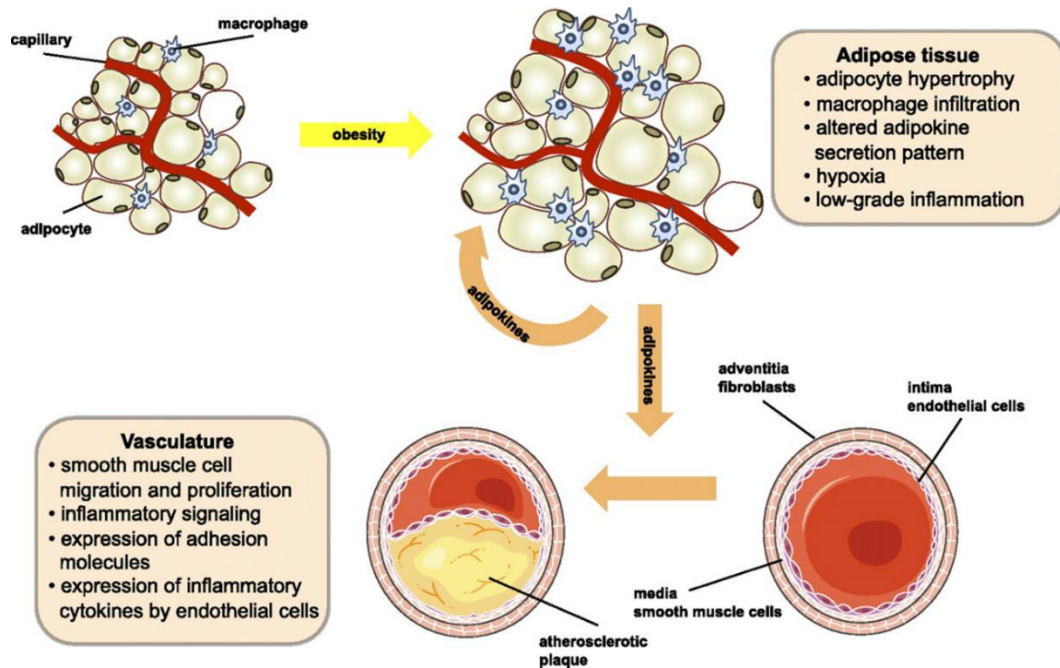


Figure 1.5 Obesity-induced adipose tissue dysfunction. Chronic inflammation of adipose tissue in obesity markedly alters the adipokine expression profile. Augmented secretion of pro-inflammatory adipokines from adipose tissue triggers endothelial dysfunction and vascular inflammation.⁶

potential to contribute to the development of obesity-induced insulin resistance, cardiovascular dysfunction, and atherogenesis.⁴⁸ On the other hand, adipose tissue has been shown to produce adipokines, such as adiponectin, that confer protection against inflammation and vascular injury.⁵⁹⁻⁶² However, several studies have documented that plasma levels of adiponectin and other anti-inflammatory and cardioprotective adipokines is markedly reduced in the setting of obesity.⁶³

The role of adipose tissue in the pathogenesis of coronary artery disease and atherosclerosis has received considerable research interest in recent years. **Figure 1.6** outlines the cascade of events involved in coronary atherosclerotic plaque formation. The initiation of atherosclerosis is triggered by various inflammatory stimuli including increased adiposity, hypercholesterolemia, and insulin resistance.^{6,64} The initiation of atherosclerotic disease begins with endothelial dysfunction, characterized by the adhesion of platelets

and inflammatory cells in the vessel wall.⁶⁵ If the inflammatory stimulus persists, leukocytes migrate and accumulate beneath the endothelial layer.⁶⁶ The subsequent formation of lipid laden foam cells and the proliferation and migration of smooth muscle cells contribute to the formation of an atherosclerotic plaque.^{48;64;67-69} Plaque development continues in the presence of atherogenic stimuli until destabilizing factors (i.e., thinning of the fibrous cap) trigger plaque rupture and thrombus formation, which then have the potential to occlude blood flow and trigger a myocardial infarction.^{67;68}

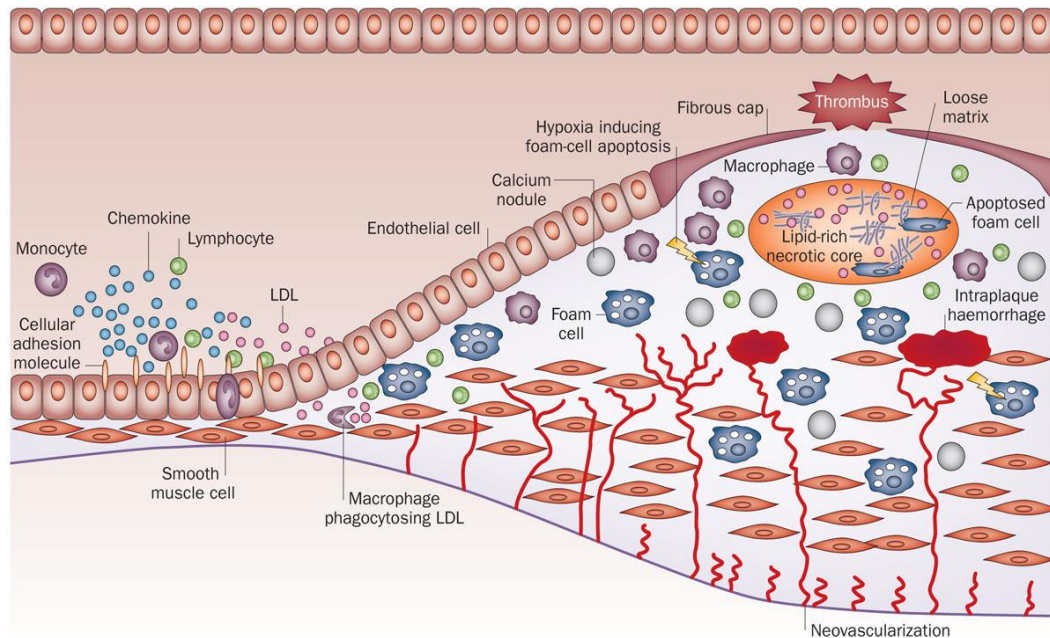


Figure 1.6 Pathogenesis of atherosclerosis. Endothelial dysfunction stimulates chemokine production and the upregulation of leukocyte adhesion molecules on the surface of endothelial cells. These changes, along with increased endothelial permeability, result in migration of leukocytes into the artery wall. Monocytes differentiate into macrophages, which take up modified LDL to form foam cells. Pro-inflammatory chemokines promote proliferation and migration of smooth muscle cells into the developing plaque. A fibrous cap forms over the top of the plaque, providing temporary stabilization and isolation from the circulation. Hypoxia and oxidative stress may cause foam-cell apoptosis and lead to the formation of a lipid-laden necrotic core. As the plaque enlarges, it may become large enough to impede blood flow (i.e., flow limiting stenosis) and/or the fibrous cap thins and ruptures leading to acute thrombosis and occlusion.¹⁴

Recent studies suggest the potential for adipokines to influence various components of atherogenesis (**Figure 1.7**). For example, adipose-derived leptin has been implicated in the development of endothelial dysfunction,^{2,70;71} and the production of MCP-1 by adipocytes has been shown to directly promote leukocyte transmigration.⁶⁵ Adipose-derived factors may also have the potential to induce proliferation and migration of smooth muscle cells.⁶ These early findings indicate the potential for adipose tissue to causally contribute to the development of obesity-associated coronary disease via cross talk between adipokines and the vascular wall. However, several key factors have made elucidating the relationship between adipose tissue and coronary vascular disease an

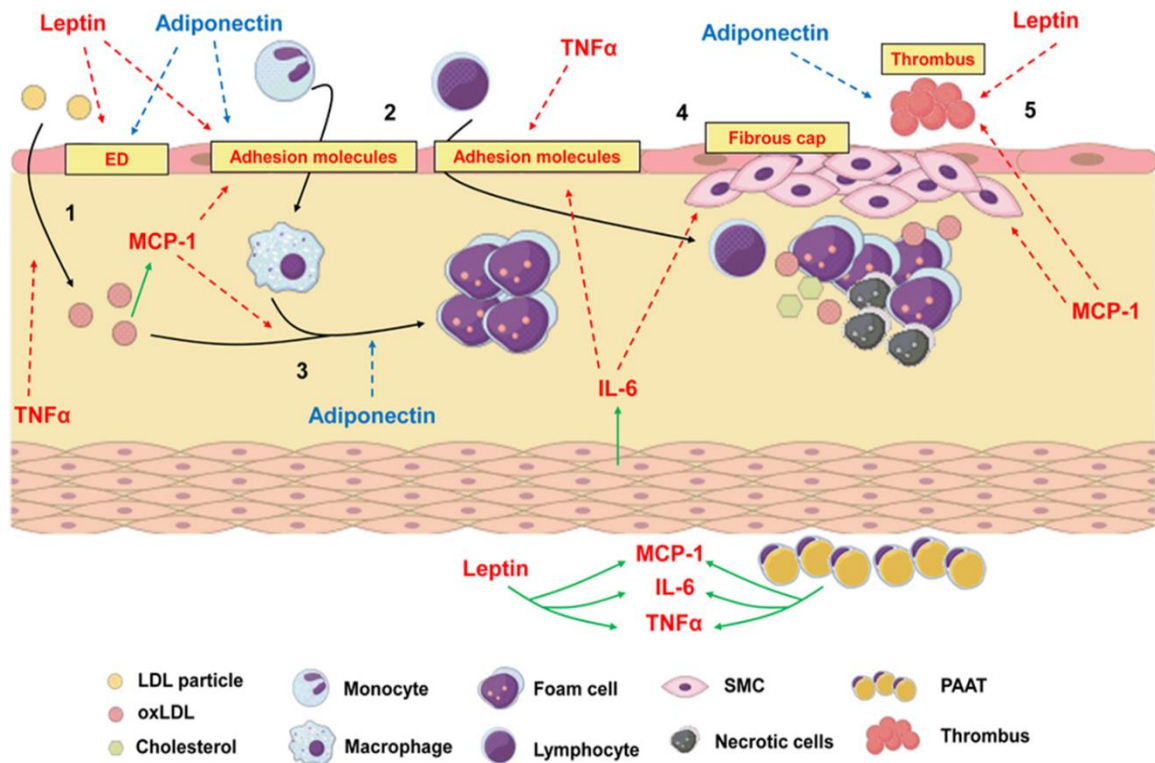


Figure 1.7 Factors derived from adipose tissue contribute to atherogenesis. Adipokines are known to influence nearly all critical aspects of atherogenesis including endothelial dysfunction, leukocyte recruitment and transmigration, lipid oxidation, foam cell formation, smooth muscle cell proliferation and migration, plaque rupture, and thrombus formation. Red arrows represent pro-inflammatory pathways that are stimulated during obesity. Blue arrows represent anti-inflammatory pathways that are inhibited during obesity. Green arrows represent the stimulation of adipokine secretion.¹²

exceptionally complex endeavor. First, the adipokine secretion profile may vary between adipose tissue depots depending on anatomic location.^{13;17;72;73} Second, the secretory status of adipose tissue can vary dramatically depending on the underlying disease state (i.e. obesity, inflammation) and the particular organism being studied.^{9;13;74;75} Finally, novel adipokines are continually being discovered, adding to the list of hundreds of adipose-derived factors identified to date that warrant further investigation.^{13;48;76} It is evident that these issues must be collectively considered in order to better understand the growing paradigm of a role for adipose tissue in obesity-induced coronary disease.

Perivascular Adipose Tissue

The majority of large blood vessels (internal diameter > 100 μm) throughout the body, apart from cerebral and pulmonary arteries, are surrounded by various quantities of perivascular adipose tissue, or PVAT (**Figure 1.8**).^{8;62;77} In particular, PVAT has been described around large arteries (e.g. aorta, coronary, mammary, femoral), veins, small and resistance vessels, and skeletal muscle microvessels.⁷⁸ Similar to other adipose tissue depots, PVAT is a highly vascularized network comprised of several cell types including adipocytes, pre-adipocytes, inflammatory cells, and stem cells capable of producing metabolically active factors.^{62;79;80}

Uniquely, PVAT directly abuts the adventitia of most conduit arteries, due to an absence of a fascial layer

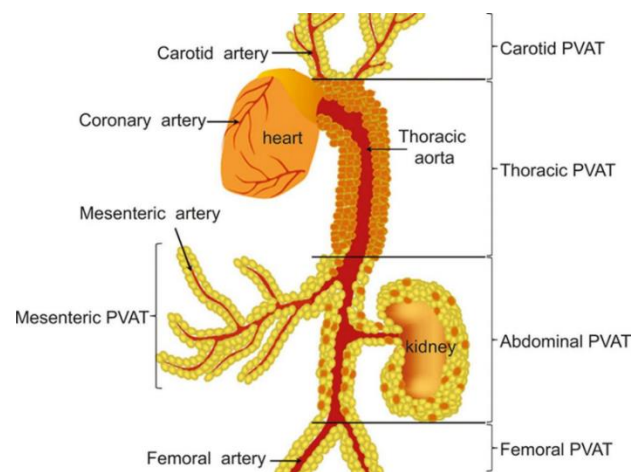


Figure 1.8 Anatomic locations of perivascular adipose tissue. Types of perivascular adipose tissue (PVAT) can be classified according to anatomic location. Note that PVAT is absent from the murine coronary artery.⁸

separating adipocytes from the vessel wall.^{81;82} As a result, adipocytes from PVAT have been shown to infiltrate into the adventitia, providing for direct paracrine physiological and pathophysiological communication with the vasculature.^{75;81;83}

This emerging view of “outside in” signaling between vasoactive factors from PVAT and the vascular wall is supported by evidence that PVAT depots are associated with specific vascular complications depending on the anatomic location of the vascular bed. For example, PVAT surrounding the microcirculation of the gracilis muscle modulates insulin-dependent vascular function and has been associated with insulin resistance.⁸⁴ Additionally, increases in peripheral artery PVAT are associated with peripheral artery disease and vascular calcification.⁸⁵ It is proposed that these differential paracrine effects are related to the unique adipokine profiles of anatomically distinct PVAT depots.^{8;17;78} Perhaps the most physiological and pathophysiological role of a PVAT depot has been described for coronary PVAT.

Coronary Perivascular Adipose Tissue

Coronary PVAT surrounds the major conduit coronary arteries on the surface of the heart (**Figure 1.9**).^{17;86} Studies suggest that coronary PVAT shares characteristics with both white and brown adipose tissue.^{15;17;87} Other data, however, indicate that human coronary perivascular adipocytes display a histologic appearance and gene expression pattern more consistent with white rather than brown adipose tissue.^{73;75;81} Further study of human perivascular adipocytes revealed that those surrounding coronary arteries are smaller in size and exhibit a reduced state of adipogenic differentiation compared to peripheral (subcutaneous and perirenal) adipocytes, evidenced by decreased expression of adipocyte-specific genes.^{73;75} These differences are likely a result of a distinct

developmental origin of PVAT. Although studies of perivascular adipocyte origin are scarce, evidence points towards vascular smooth muscle progenitors, an origin distinct from adipocytes of other depots.^{88;89} Further studies are needed to characterize the developmental origin of perivascular adipocytes and to examine potential differences between peripheral (non-coronary) and coronary PVAT depots.

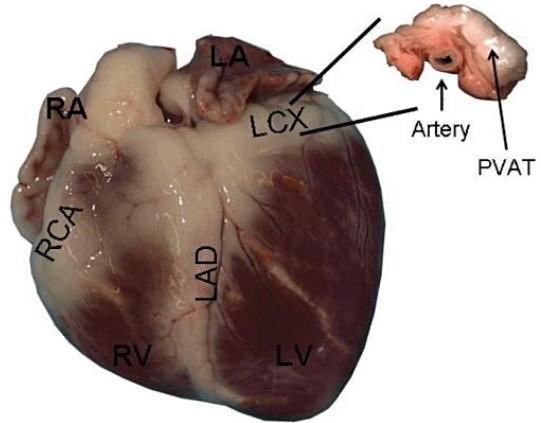


Figure 1.9 Coronary perivascular adipose tissue. Representative image of naturally occurring coronary perivascular adipose tissue (PVAT) on the heart. RA, right atrium; LA, left atrium; RV, right ventricle; LV, left ventricle; RCA, right coronary artery; LAD, left anterior descending artery; LCX, left circumflex artery.¹⁵

Currently, there is some inconsistency in the literature regarding the nomenclature of cardiac fat depots. Coronary PVAT immediately surrounds the coronary arteries and is functionally distinct from the adipose tissue found on the surface of the myocardium, which termed myocardial or epicardial adipose tissue.^{90;90;91} However, the term epicardial adipose tissue is often used to describe both myocardial/epicardial and coronary PVAT depots. Altogether though, cardiac adiposity is highly and directly correlated with abdominal visceral adipose tissue volume^{92;93} and has been shown to expand with obesity.⁹⁴ Epicardial adipose tissue volume also increases with the number of MetS risk factors.⁹⁵⁻⁹⁷ Several studies demonstrate that atherosclerotic plaques occur predominantly in coronary arteries that are encased in PVAT^{20;94;95;98} and that coronary PVAT volume is positively associated with underlying plaque burden.^{99;100} A recent study by McKenney et al. documented that resection of coronary PVAT decreased the progression of coronary atherosclerosis in obese swine, further supporting that PVAT exacerbates the progression

of disease.¹⁰¹ Together, these findings support cardiac adiposity as an independent risk factor for coronary artery disease.^{98;102;103}

Although a positive association between coronary PVAT and coronary artery disease is clear, the precise link between the two is unknown. Recent studies propose that the association between PVAT and vascular disease is related to direct effects of PVAT-derived factors on endothelial and smooth muscle function. In fact, a disruption of normal vascular function (i.e., an imbalance between vasodilation and vasoconstriction) is a central component in the pathogenesis of coronary vascular disease.⁴⁸ In order to comprehend the potential mechanisms by which coronary PVAT could contribute to the development of vascular dysfunction, an understanding of how obesity affects the coronary circulation is important.

Obesity and Coronary Vascular Dysfunction

Coronary arteries are responsible for the delivery of oxygen and energy substrates to the myocardium which generates the pressure necessary to drive blood throughout the circulatory system. Since the myocardium has a limited anaerobic capacity, utilizing a rate of 70-80% oxygen extraction at rest, the heart is highly dependent on a continuous supply of oxygen from the coronary circulation.¹⁰⁴⁻¹⁰⁶ Within seconds, inadequate oxygen delivery (i.e. ischemia) can significantly impair cardiac contractile function.¹⁰⁷⁻¹⁰⁹ Thus, tight control of coronary blood flow is essential for normal cardiac function. As such, during normal physiologic conditions, oxygen delivery (i.e., coronary blood flow) is tightly matched with myocardial oxygen consumption (MVO_2). This process is regulated by affecting one or more of the primary determinants of coronary blood flow including arterial pressure,

myocardial metabolism, neuro-hormonal influences, and extravascular myocardial compression.^{106;110}

Growing evidence supports dysfunction of the control of coronary blood flow as an important contributor to the increased cardiovascular morbidity and mortality associated with obesity/MetS. In the setting of obesity, repeated measures of coronary blood flow reveal little or no difference at rest.^{111;112} However, although myocardial perfusion may be equivalent, myocardial oxygen consumption (MVO_2) is elevated in obesity in proportion to increases in stroke volume, cardiac output, and blood pressure.^{113;114} This “hyperdynamic circulation” results in increased myocardial oxygen demand and is a defining characteristic of the obese coronary circulation. Obesity is also clearly associated with reduced coronary flow reserve, defined as the difference between maximal and resting coronary blood flow.^{111;115;116} Decreases in coronary flow reserve are directly correlated with increases in waist-to-hip ratio, body mass index, blood pressure, and diagnosis of MetS.^{111;112;115;117} The reduction in flow reserve could be due to the effects of diffuse atherosclerosis on fluid dynamics, the extent of focal coronary stenosis, and/or the presence of microvascular dysfunction.^{111;118} The coronary microcirculation regulates vascular resistance in order to balance myocardial oxygen supply and demand. In obesity, coronary blood flow is decreased at a given coronary venous PO_2 (an index of myocardial tissue PO_2 which is a stimulus for metabolic vasodilation)^{104;110} and PO_2 is reduced relative to alterations in MVO_2 (the primary determinant of myocardial perfusion) at rest and during exercise (**Figure 1.10**).⁴ Furthermore, coronary vasodilation in response to myocardial ischemia has also been shown to be impaired by obesity/MetS.^{4;119} Together, these findings indicate that coronary microvascular dysfunction in obesity leads to an imbalance between coronary blood flow and myocardial metabolism. This imbalance likely contributes to the

cardiac contractile dysfunction and high incidence of myocardial ischemia observed in obese subjects.^{42;120}

Several potential

mechanisms underlying alterations in the control of coronary blood flow have been explored including the role of neurohormonal modulation. It is well established that obesity is

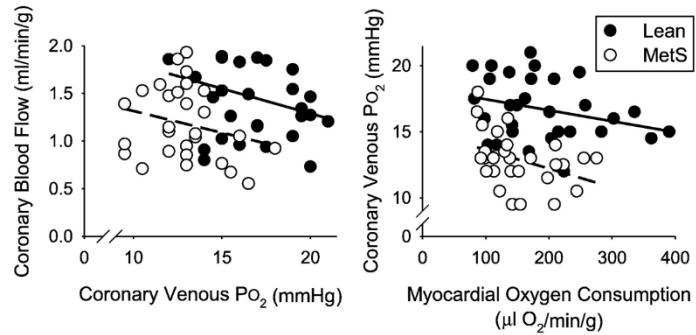


Figure 1.10 Effects of metabolic syndrome on coronary blood flow. Metabolic syndrome (MetS) diminishes local metabolic control of coronary blood flow, evidenced by decreased coronary blood flow at a given coronary venous PO₂ (left). MetS also results in an imbalance between myocardial oxygen supply and demand, evidenced by the reduction in coronary venous PO₂ relative to alterations in myocardial oxygen consumption (right). Modified from Berwick et al., *J Mol Cell Cardiol*, 2012.⁴

associated with increased sympathetic tone.^{121;122} Several studies have documented elevated plasma catecholamines as well as increased sympathetic nerve activity and cardiac autonomic activity in obese subjects.¹²¹⁻¹²⁴ In particular, data from both *in vitro* and *in vivo* studies demonstrate increased coronary α_1 -adrenoceptor signaling and α_1 -adrenoceptor-mediated vasoconstriction, independent of alterations in α_1 -adrenoceptor expression.^{4;125;126} These findings suggest that α_1 -adrenoceptor signaling likely contributes to the myocardial oxygen supply demand imbalance, particularly during heightened sympathetic activity. Substantial evidence also supports a role for the renin-angiotensin-aldosterone system (RAAS) in the regulation of coronary blood flow in obesity. Data indicate an increase in angiotensin II type 1 (AT₁) receptor expression and angiotensin II-mediated vasoconstriction in obese coronary arteries.^{4;114} Additionally, aldosterone produces dose-dependent coronary vasoconstriction *in vitro* and *in vivo* and has been shown to exacerbate contractile dysfunction during myocardial ischemia.^{127;128} Together, present data implicate increased sympathetic activity and upregulation of the RAAS as

potential mechanisms responsible for the dysregulation of coronary blood flow control in obesity.

Alterations in the functional expression of coronary vascular K^+ and Ca^{2+} channels in the setting of obesity is a topic of intense study, as such changes could contribute to coronary vascular dysfunction. In coronary artery smooth muscle cells, K^+ channels dominate membrane conductance and thus determine the resting membrane potential.^{4;129} The equilibrium potential for K^+ is an estimated -83 mV, but due to the balancing depolarizing influence of other ion channels, the resting membrane potential of coronary smooth muscle cells is less negative, typically between -60 mV and -40 mV.¹²⁹ The threshold for L-type ($Ca_v1.2$) Ca^{2+} channels, and thus contraction, is in this range.^{130;131} When K^+ channels open, K^+ moves down its electrochemical gradient, hyperpolarizing the membrane, and smooth muscle relaxes to produce vasodilation. In contrast, when the inhibition of K^+ channels reduces K^+ efflux, the membrane depolarizes, activating $Ca_v1.2$ channels, and the resulting increase in intracellular Ca^{2+} produces vasoconstriction. This interplay between K^+ and voltage-gated Ca^{2+} channels represents electromechanical coupling. A variety of K^+ channels are expressed in coronary smooth muscle including voltage-dependent (K_V), large conductance Ca^{2+} activated (BK_{Ca}), and ATP-sensitive (K_{ATP}) channels, and serve as important regulators of coronary vascular reactivity. K_V channels have been implicated in the control of coronary vascular tone.¹²⁹ Studies in lean, healthy animals demonstrate that K_V channels regulate coronary blood flow at rest, with increasing MVO_2 and during ischemia.^{21;132;133} Recent findings indicate that obesity markedly alters the functional expression of K_V channels, as reductions in smooth muscle K_V current were observed in coronary arteries from swine with the MetS (**Figure 1.11**).²¹ BK_{Ca} channels have been shown to influence coronary endothelial-dependent vasodilation^{134;135} but data fail to support a significant role for BK_{Ca} channels in the

regulation of coronary blood flow in lean, healthy subjects.^{1,136} However, the induction of MetS has been shown to attenuate BK_{Ca} channel-mediated vasodilation (**Figure 1.12**) and induce a paradoxical increase in BK_{Ca} channel expression.¹³⁶ Decreases in spontaneous transient outward currents, which are indicative of BK_{Ca} channel activation have also been reported in coronary smooth muscle cells from diabetic dyslipidemic swine.¹³⁷ Evidence also supports that coronary K_{ATP} channels are altered

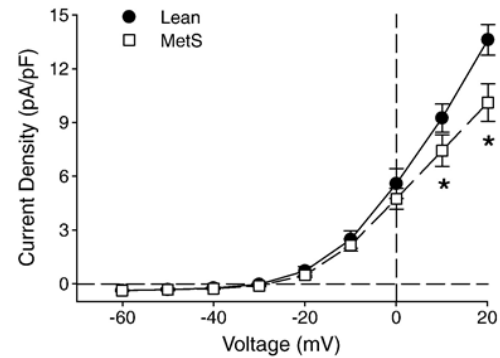
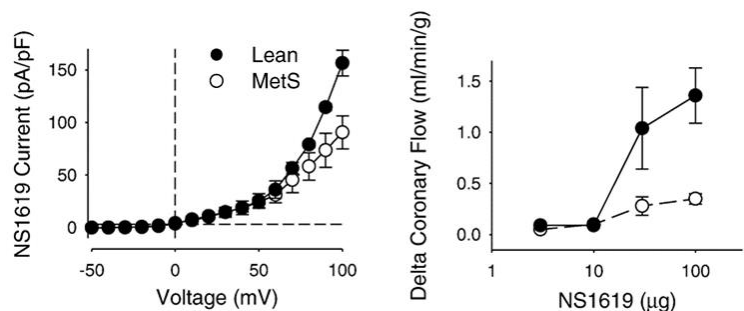


Figure 1.11 K_V channel dysfunction in metabolic syndrome. Whole-cell voltage-dependent K⁺ current was impaired at currents consistent with K_V channel activation (i.e., greater than 0 mV) in coronary smooth muscle cells from metabolic syndrome (MetS) swine. Modified from Berwick et al., *J Mol Cell Cardiol*, 2012.²¹

in the setting of obesity. In particular, the contribution of K_{ATP} channels to coronary vasodilation in response to brief coronary artery occlusion was reduced in obese compared to lean swine.¹¹⁹

In coronary smooth muscle cells, intracellular Ca⁺ regulates both contraction and gene expression. Thus, alterations in Cav1.2 channel activity, the predominant voltage-dependent Ca⁺ channel in smooth muscle cells could contribute significantly to coronary vascular dysfunction. Both decreases



in the functional expression of K⁺ channels and increases in vasoconstrictor pathway (e.g., α₁-adrenoceptor)

Figure 1.12 BK_{Ca} channel dysfunction in metabolic syndrome. Coronary smooth muscle cell current in response to the BK_{Ca} channel agonist, NS1619, was reduced in metabolic syndrome (MetS; left). Reductions in BK_{Ca} channel current correspond to diminished vasodilation to NS1619 in MetS swine (right). Modified from Berwick et al., *J Mol Cell Cardiol*, 2012.⁴

activation, both of which are well documented in obesity, would serve to augment $\text{Ca}_v1.2$ channel-mediated coronary vasoconstriction. Initial studies in coronary smooth muscle from dyslipidemic swine documented reductions in $\text{Ca}_v1.2$ channel current.^{138;139} In contrast, other studies support that MetS is associated with increased $\text{Ca}_v1.2$ channel expression and activity as well as $\text{Ca}_v1.2$ channel agonist-mediated vasoconstriction (Figure 1.13).^{1;4;140;141} Together, the present data support that alterations in the functional expression of both K^+ and Ca^{2+} channels contribute to obesity-induced coronary microvascular dysfunction. At present, the precise mechanisms responsible for these alterations are under active investigation.

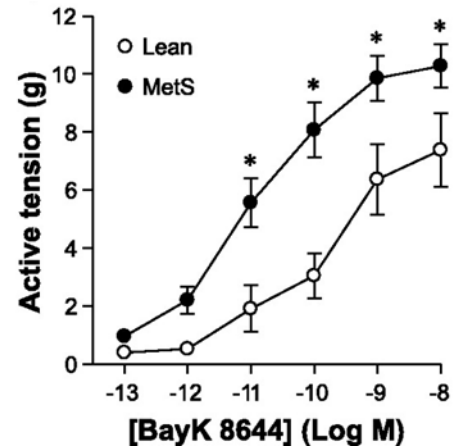


Figure 1.13 Increased $\text{Ca}_v1.2$ channel-mediated coronary vasoconstriction in metabolic syndrome. Contractile responses to the $\text{Ca}_v1.2$ channel agonist, BayK 8644, were augmented in coronary arteries from metabolic syndrome (MetS) swine. Modified from Borbouse et al., *Am J Physiol Heart Circ Physiol*, 2009.¹

An understanding of the factors and cellular pathways that mediate the development of coronary vascular dysfunction is important, as microvascular dysfunction precedes overt atherosclerosis.¹⁴² Although larger conduit vessels, or macrovessels, contribute very little to the regulation of coronary blood flow,¹⁴³ the macrovasculature is more prone to atherosclerosis.⁶⁵ As described above, it is well understood that endothelial dysfunction initiates and exacerbates atherosclerotic disease. However, smooth muscle dysfunction also contributes to the progression of atherosclerosis. It should be noted that obesity is associated with alterations in several mechanisms of Ca^{2+} handling including impaired Ca^{2+} extrusion via the plasmalemma Ca^{2+} ATPase (PMCA), increased Ca^{2+} sequestration by the sarcoplasmic reticulum Ca^{2+} ATPase (SERCA), and increased nuclear Ca^{2+} localization.¹⁴⁴ These changes in Ca^{2+} handling have been implicated in

phenotypic modulation of smooth muscle cells, characterized by enhanced proliferation and migration,^{145;146} in obesity-induced coronary disease.^{144;147;148}

Taken together, it is evident that obesity is associated with numerous deleterious effects on coronary endothelial and smooth muscle function and that the disruption of normal vascular function is central to the initiation and progression of coronary disease. Thus, potential effects of coronary PVAT-derived factors on vascular reactivity provide plausible mechanisms by which adipose tissue could influence the development of obesity-induced coronary disease.

Vascular Effects of Perivascular Adipose Tissue

Peripheral (non-cardiac) PVAT

Initial studies into the vascular effects of PVAT were conducted in peripheral (non-cardiac) tissues. In 1991, Soltis and Cassis were the first to systematically investigate the hypothesis that PVAT influences vascular tone by comparing contractile responses of segments of rat aorta cleaned of adipose with those with the surrounding PVAT still intact. These studies revealed that vessels with PVAT intact were less responsive to norepinephrine, suggesting that PVAT was buffering the degree of vasoconstriction.¹⁴⁹ The next major discovery came in 2002 when Löhn et al. described an adipocyte-derived relaxing factor (ADRF), a vasoactive factor produced by perivascular adipocytes.^{5;150} The inhibitory, or “anti-contractile” effect of PVAT on contractile responses to angiotensin II confirmed the presence of ADRF in intact aortic rings (**Figure 1.14**).^{5;150;151} The presence of ADRF has also been detected in mesenteric arteries.¹⁵²⁻¹⁵⁴ Depending on the vascular bed, PVAT may stimulate endothelial dependent and/or independent vasodilation.^{5;155}

Several transfer experiments have demonstrated that these effects are in fact a result of the paracrine function of the tissue, rather than the absorption or blocking of vasoactive mediators,^{150;156;157} and have established ADRF as a transferrable factor.⁵ While the majority of vasoreactivity studies have been conducted using murine tissues, studies of human internal thoracic and gluteal arteries have consistently documented an anti-contraction response to PVAT.¹⁵⁸⁻¹⁶⁰ Several potential candidates for the anti-contraction factor (ADRF) have been identified including adiponectin,^{160;161} hydrogen sulfide,^{153;155} angiotensin-(1-7), and hydrogen peroxide,¹⁵¹ although it is becoming increasingly apparent that likely more than one factor represents the ADRF. Regardless, it has been established that the end-effector mechanism of ADRF(s) is the opening of vascular smooth muscle K⁺ channels to illicit vasorelaxation.^{5;154;161;162} Furthermore, recent studies have delineated subtypes of K⁺ channels attributed to the anticontractile effect of PVAT, namely voltage-dependent K_v7 (voltage-dependent K) channels,^{153;157;163} BK_{Ca} (large conductance calcium-activated K) channels,^{159;164} and Kir (inward-rectifying K) channels.^{151;165} It should be noted that, alternatively, peripheral PVAT has also been shown to potentiate contraction. Data indicate that PVAT augments contraction of mesenteric arteries to electric field stimulation via increased production of angiotensin II and superoxide.^{156;166} Other studies have also documented that PVAT from obese rodents attenuates endothelial-dependent vasodilation in aorta¹⁶⁷ and mesenteric arteries.^{168;169}

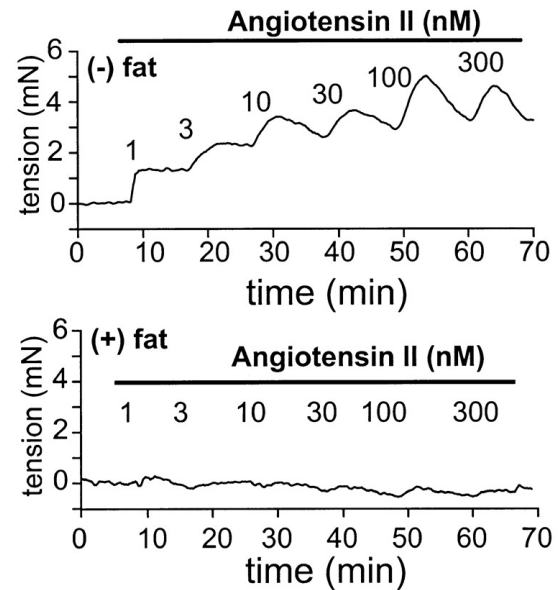


Figure 1.14 Perivascular adipose tissue releases a relaxing factor. Contractile responses of rat aortic rings with surrounding fat intact (bottom) were significantly impaired relative to contractions in the absence of fat (top). Modified from Löhn et al., *FASEB J*, 2002.⁵

The adipokine chemerin has been implicated as a PVAT-derived constricting factor responsible for these effects in mesenteric and aortic vascular beds.¹⁷⁰ Thus, present data support that peripheral (non-cardiac) PVAT is capable of producing factors that illicit both vasodilation and vasoconstriction.

Coronary PVAT

Current data to support the vascular effects of coronary PVAT are rather limited and somewhat conflicting. Initial studies revealed that coronary PVAT diminishes endothelial-dependent dilation *in vitro* and *in vivo* in normal, healthy dogs.^{171;172} In contrast, coronary PVAT appears to have little/no effect on endothelial-dependent dilation in normal, lean swine.^{2;173;174} These disparate findings are likely related to species differences in adipokine expression, although they suggest a potential regulatory role for PVAT-derived factors in the healthy coronary circulation. In contrast, in the setting of coronary disease, Payne et al. demonstrated that MetS coronary PVAT markedly augments underlying endothelial dysfunction of isolated coronary arteries from swine with the MetS.² Studies in both lean and hypercholesterolemic swine show little/no effect of coronary PVAT on contractile responses to endothelin-1, angiotensin II, or the thromboxane A2 mimetic U46619.^{2;173;174} Alternatively, a seminal study by Owen et al. revealed that the addition of lean coronary PVAT to isolated, clean (PVAT free) coronary arteries from lean swine potentiates contractile responses to KCl-induced depolarization and to prostaglandin F2 α (PGF2 α) in direct proportion to the amount of PVAT (**Figure 1.15**).⁹ In this study, the effect of mesenteric PVAT on KCl contractions was similar to that of coronary PVAT, but subcutaneous adipose tissue had no effect on coronary vasoconstriction, highlighting the specificity of the adipose tissue depot.⁹ Bioassay

experiments also support that, similar to peripheral PVAT, the vascular effects of coronary PVAT are mediated via the paracrine production of a transferable factor(s). Interestingly, Owen et al. documented that the contractile effect of coronary PVAT was augmented in coronary arteries from obese versus lean swine.⁹ Regardless of health status, coronary PVAT potentiated coronary artery contractions in both endothelium intact and denuded coronary arteries.⁹ Thus, it is hypothesized that the vascular effects of coronary PVAT are influenced by obesity due to alterations in the adipokine expression profile of PVAT and/or inherent phenotypic differences in coronary vascular smooth muscle.

Taken together, the current literature suggest that the vascular effects of PVAT are highly dependent on the anatomic location of

the artery/adipose tissue depot, the species being studied, the pharmacological agonists used, and the underlying phenotype of the endothelium and smooth muscle in relation to the overall health status of the animal model being studied.^{9;17;175} In general, peripheral PVAT exerts anticontractile effects, while recent data suggest that coronary PVAT induces vasoconstrictor effects on both endothelial-dependent dilation and depolarization-induced

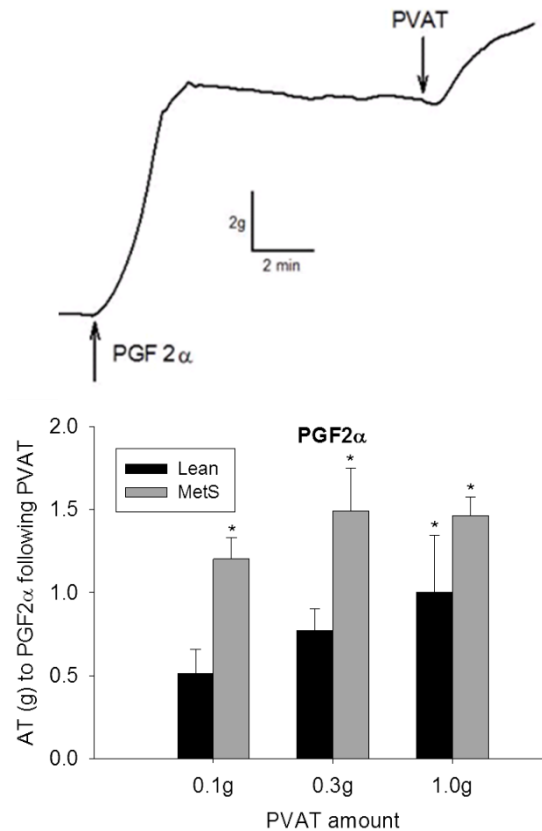


Figure 1.15 Coronary perivascular adipose tissue potentiates coronary artery contractions. Representative wire myograph tracing of tension generated by coronary arteries in response to prostaglandin F_{2α} (PGF_{2α}) and the addition of perivascular adipose tissue (PVAT) to the organ bath (top). Active tension development stimulated by coronary PVAT was proportional to the amount of PVAT added and was significantly augmented in swine with metabolic syndrome (MetS). Modified from Owen et al., *Circulation*, 2013.⁹

contraction, although the specific factors and cellular mechanisms responsible for these effects are not well understood.

Expression Profiles in Coronary PVAT

Recent evidence supports that there are substantial differences in gene and protein expression among adipose tissue depots depending on anatomic location. Results from Baker et al. and Cheng et al. were among the first to document adipokine expression profiles from human coronary PVAT and found augmented expression of leptin, TNF- α , and IL-6 in coronary relative to abdominal adipose tissue.^{176;177} Significant macrophage infiltration was also reported, suggesting an increased inflammation.¹⁷⁷ Recent data from the Weintraub laboratory indicate that adipocytes from human coronary PVAT exhibit augmented gene expression and secretion of pro-inflammatory cytokines such as IL-6, IL-8, and MCP-1 compared to other adipose tissue depots and in the presence of coronary artery disease^{73;75} (**Table 1.1**). Additional studies support that this heightened pro-inflammatory environment of coronary PVAT is markedly exacerbated in the setting of obesity and with the progression of coronary artery disease.^{2;9;48;178}

Overall, evidence is mounting in support of marked upregulation of pro-atherogenic adipokine expression profiles in coronary PVAT in the setting of obesity-induced coronary disease.^{9;15;73;177} In particular, increased expression of pro-atherogenic factors including leptin, resistin, TNF- α , IL-6, chemerin, and calpastatin have been identified to date.^{2;9;170;176;177;179} Interestingly, expression of the osteogenic factors osteoprotegerin and osteoglycin, which have been linked to atherosclerosis and the severity of coronary artery disease,^{18;180} were recently identified in coronary PVAT.^{9;73} Furthermore, diminished expression of potentially vasculoprotective adipokines such as adiponectin, which is

associated with improvements in endothelial function,⁶⁰ is well established in human coronary PVAT in the setting of obesity and coronary artery disease.^{177;181;182} This aberrant regulation of coronary PVAT correlates with the well-documented underlying vascular dysfunction observed in obesity-induced coronary disease.^{4;9;101;171;177;183} Thus, there is a strong and growing body of evidence to support that coronary PVAT has the potential to locally produce factors (i.e., independent of changes in visceral adipose tissue and/or circulating adipokine levels) that directly influence the initiation and progression of coronary vascular dysfunction and disease.

Table 1.1 Adipokine expression of coronary perivascular relative to subcutaneous adipose tissue in health and coronary artery disease.

| Adipokine | Condition | Coronary PVAT Expression Relative to Subcutaneous | References |
|-------------|-----------|---|------------|
| Leptin | NCAD | ↓ mRNA | 75 |
| | CAD | ↓ mRNA | 176 |
| Adiponectin | NCAD | ↓ mRNA, ↓ protein secretion | 75 |
| | CAD | ↑ protein secretion | 177 |
| TNF-α | NCAD+CAD | ↑ mRNA | 179 |
| | CAD | ↑ mRNA, ↑ protein secretion | 184 |
| | | ↓ protein secretion | 177 |
| IL-6 | NCAD | ↑ mRNA | 75 |
| | NCAD+CAD | ↑ mRNA | 179 |
| | CAD | ↓ mRNA | 176 |
| | | ↑ protein secretion | 184 |
| IL-1β | NCAD+CAD | ↑ mRNA | 179 |
| | CAD | ↑ mRNA, ↑ protein secretion | 184 |
| MCP-1 | NCAD | ↑ protein secretion | 75 |
| | NCAD+CAD | ↑ mRNA | 179 |
| | CAD | ↑ mRNA, ↑ protein secretion | 184 |
| PAI-1 | CAD | ↓ mRNA | 176 |

CAD indicates coronary artery disease; NCAD, no coronary artery disease; NCAD+CAD, group populations. ↑ indicates significant increase in expression in coronary perivascular adipose tissue (PVAT); ↓ indicates significant decrease in expression; TNF-α, tumor necrosis factor-alpha; IL-6, interleukin, 6; IL-1β, interleukin-1 beta; MCP-1, monocyte chemoattractant protein-1; PAI-1, plasminogen activator inhibitor-1. Modified from Owen et al., *Arterioscler Thromb Vasc Biol*, 2014.¹⁷

It is important to consider how factors produced by coronary PVAT are able to traverse the arterial wall to influence the endothelium and vascular smooth muscle. The prevailing hypothesis is that the vasa vasorum, a network of small blood vessels that is interspersed within the PVAT and supplies blood to the walls of large blood vessels,¹⁸⁵⁻¹⁸⁷ serves as a potential conduit (**Figure 1.16**). This hypothesis is supported by Herrmann et al.

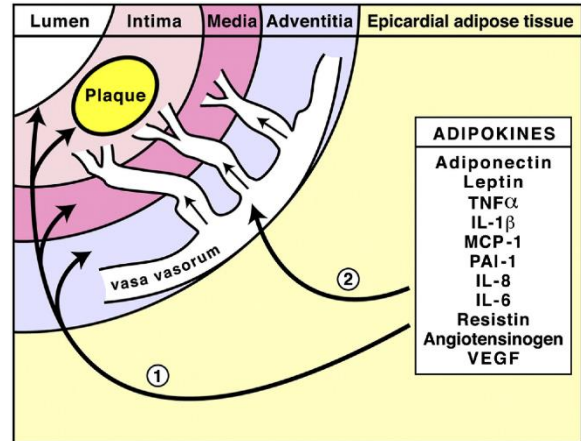


Figure 1.16 The coronary vasa vasorum. Epicardial adipokines may be delivered to the vessel wall via paracrine signaling by diffusing through the interstitial fluid (1) or via vasocrine signaling through the network of blood vessels supplying the vessel wall, the vasa vasorum (2).²⁰

which demonstrated that increases in coronary vasa vasorum neovascularization precede the development of coronary endothelial dysfunction in swine fed a high cholesterol diet.¹⁸⁵ These findings have been confirmed in human patient populations, with several studies documenting an association between neovascularization of the vasa vasorum with the extent of inflammation and coronary disease.^{188;189} Although the association between the expansion of the coronary vasa vasorum and the development of atherosclerosis is intriguing, the transit of PVAT-derived factors across the coronary wall continues to be an active area of research.

One adipose-derived factor that has received significant attention is leptin. Produced and secreted predominantly from adipose tissue, leptin was initially implicated in the regulation of energy balance and metabolism.^{190;191} Since its discovery, a significant research effort has focused on elucidating the effects of leptin on the cardiovascular system. In the setting of obesity, plasma leptin concentrations can rise from normal, healthy levels of 3-5 ng/mL to as high as 90-95 ng/mL (typical range 8-90 ng/mL).¹⁹² An

elevated plasma leptin level (hyperleptinemia) is nearly universal in obese humans¹⁹¹ and is a key component of the MetS.^{38;39} Thus, hyperleptinemia is also independent risk factor for cardiovascular disease.¹⁹³ Importantly, leptin receptors (ObRb) are expressed in endothelial cells and smooth muscle cells and have been detected throughout the wall of diseased coronary arteries.^{2;70;194} Leptin has been implicated in several key aspects of atherogenesis including chemoattraction of circulating myocytes,¹⁹⁵ accumulation of cholesterol esters in foam cells,¹⁹⁶ and vascular smooth muscle cell proliferation.^{197;198} Leptin has also been shown to have vasomotor effects on the coronary circulation. Although initial studies suggested that leptin stimulates endothelium-dependent vasodilation, the vast majority of these studies were conducted using concentrations of leptin well above both physiologic and pathophysiologic plasma concentrations.¹⁶ A study by Knudson et al. revealed that, in the coronary circulation, endothelial-dependent dilation only occurs at concentrations above those documented in obese humans (>160 ng/mL).¹⁹⁴ Interestingly, Knudson et al. also demonstrated that while healthy (normal physiologic) concentrations of leptin have no effect, “obese” concentrations of leptin (i.e. plasma concentrations typically observed in obese subjects) impair endothelial-dependent dilation to acetylcholine both *in vitro* and *in vivo* (**Figure 1.17**).¹⁹⁴

Mounting evidence suggests that PVAT-derived leptin may locally contribute to obesity-associated coronary disease. Several studies have documented increased leptin mRNA and protein expression in coronary PVAT from obese subjects with evidence of coronary artery disease.^{177;179;181;199} Interestingly, no correlation between plasma leptin concentration and PVAT leptin mRNA expression has been observed.^{179;200} This suggests that alterations in the PVAT adipokine profile are not necessarily a result of increased global adiposity and the potential for the effects of local PVAT-derived leptin to occur independently from those of circulating plasma leptin. This is supported by recent studies

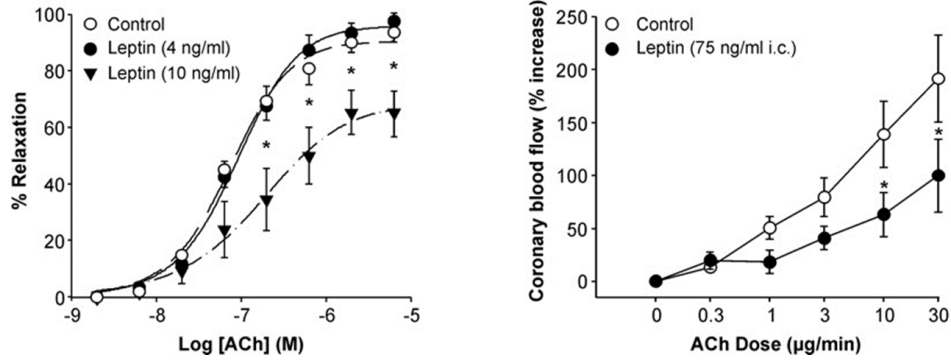


Figure 1.17 Leptin impairs coronary endothelial-dependent dilation *in vitro* and *in vivo*. Leptin impaired endothelial-dependent vasodilation of isolated canine coronary arteries to acetylcholine (ACh) at a concentration of 10 ng/mL but not 4 ng/mL (left). In open chest anesthetized dogs, concentrations of leptin in the obese range attenuated coronary vasodilation to acetylcholine (right). Modified from Knudson et al., *Exp Biol Med* (Maywood), 2007.¹⁶

in obese swine in which the exacerbation of endothelial dysfunction by obese PVAT was significantly reversed by the inhibition of leptin signaling, implicating PVAT-derived leptin in mediating endothelial dysfunction in the coronary circulation (**Figure 1.18**).²

An imbalance between pro-atherogenic adipokines (i.e., leptin) and anti-atherogenic adipokines could activate key regulatory pathways, such as endothelial dysfunction, that promote obesity-induced coronary disease (**Figure 1.19**). The anti-atherogenic adipokine adiponectin has been shown to increase NO bioavailability and stimulate endothelial-dependent vasodilation in gluteal arteries from healthy patients, but data indicate that this effect is lost in the setting of obesity/MetS.¹⁶⁰ This loss of function of adiponectin, along with the reduction in adiponectin expression in obese

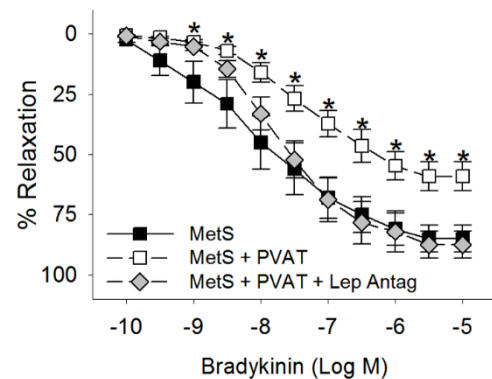


Figure 1.18 Coronary perivascular adipose-derived leptin exacerbates endothelial dysfunction. Endothelial-dependent vasodilation to bradykinin is impaired in coronary arteries from metabolic syndrome (MetS) swine. This endothelial dysfunction was exacerbated in the presence of perivascular adipose tissue (PVAT) from the same animal. Addition of a pegylated leptin antagonist to inhibit leptin signaling significantly improved dilation to bradykinin. Modified from Payne et al., *Arterioscler Thromb Vasc Biol*, 2010.²

coronary PVAT, could facilitate inflammation, endothelial dysfunction and atherogenesis.^{177;182;201}

Recent evidence that recombinant adiponectin administration reversed obese PVAT-mediated

atherogenic changes in endothelial cells, including the increased expression of endothelial cell adhesion

molecules, support this hypothesis.²⁰¹ Together, these findings implicate the down-regulation of coronary PVAT adiponectin expression along with the up-regulation of PVAT-derived leptin expression in the pathogenesis of coronary vascular dysfunction and disease.

Data regarding the effect of leptin on vascular smooth muscle function, particularly in the coronary circulation, are limited. In parallel to the early disparate findings on endothelial function, studies have documented either a modest anti-contractile effect or no effect on smooth muscle contraction in peripheral (non-coronary) arteries.²⁰²⁻²⁰⁴ Evidence also points to effects of leptin on vascular smooth muscle proliferation. Barandier et al. demonstrated that obese PVAT stimulates aortic smooth muscle proliferation in healthy rats but not in leptin-receptor deficient Zucker rats.²⁰⁵ Recent data also suggest that perivascular overexpression of leptin promotes neointima formation after carotid artery wire injury in mice.^{206;207} Although these findings suggest the potential for leptin to

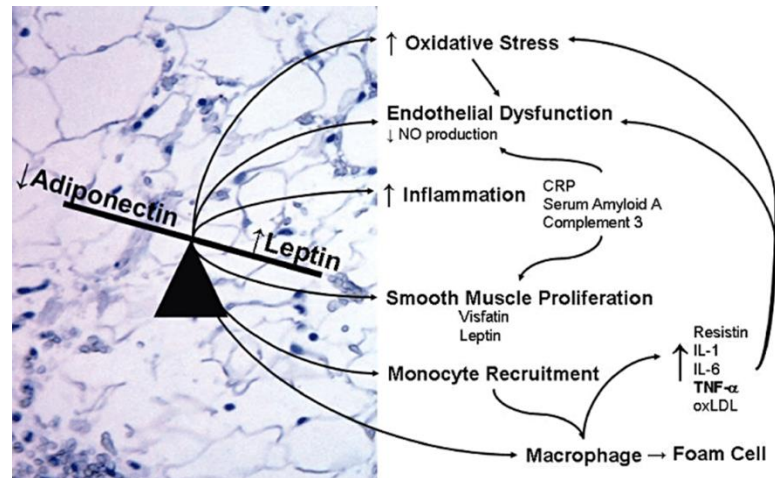


Figure 1.19 Imbalance between leptin and adiponectin as an upstream mediator of atherogenesis. In the setting of obesity, increased expression of leptin and diminished expression of adiponectin in coronary PVAT is associated with the activation of several complex atherogenic pathways. CRP, C-reactive protein; IL, interleukin-1 and 6; TNF α , tumor necrosis factor-alpha; oxLDL, oxidized low density lipoprotein.¹⁵

influence smooth muscle contraction and proliferation, the effects of leptin on coronary vascular smooth muscle function are still unclear. Overall, studies to directly investigate a causal role for PVAT-derived leptin in the pathogenesis of coronary disease are needed.

Another coronary PVAT-derived adipokine of particular interest is calpastatin. A recent global proteomic screening of coronary PVAT in lean versus obese swine revealed a significant upregulation of calpastatin fragments in obese PVAT.⁹ Calpastatin, an endogenous calpain inhibitor, has been suggested to be a partial agonist of Ca_v1.2 channels, although the precise mechanisms by which the peptide interacts with the channel and regulates its activity have not been clearly defined.²⁰⁸⁻²¹⁰ Owen et al. documented that calpastatin dose-dependently augments coronary artery contractions to a similar degree as that observed in response to coronary PVAT.⁹ Although these initial findings suggest that calpastatin is a PVAT-derived constricting factor, the vascular effects of calpastatin warrant further investigation.

Pathways Influenced by Coronary Perivascular Adipose Tissue

Recent investigations provide insight into potential mechanisms responsible for PVAT-induced coronary vascular dysfunction. As outlined above, initial studies of the vascular effects of coronary PVAT demonstrated that adipokines (i.e., leptin, adiponectin) produced by this depot influence endothelial-dependent vasodilation, especially in the setting of obesity.^{2:194} The mechanism of this impairment was initially described as a reduction in nitric oxide (NO) production via the inhibition of endothelial nitric oxide synthase (eNOS).¹⁷¹ Further examination revealed protein kinase C (PKC)- β dependent, site-specific phosphorylation of eNOS at the Thr⁴⁹⁵ inhibitory site.¹⁷² This mechanism is supported by additional studies in which the inhibition of PKC- β with ruboxistaurin

abrogated the endothelial effects of obese coronary PVAT.² These particular findings are consistent with other studies documenting leptin-induced activation of PKC- β ²¹¹ and are corroborated by reported increases in PKC- β activation in the setting of obesity.²¹²⁻²¹⁴ An apparent loss of function of PVAT-derived adiponectin also contributes to endothelial dysfunction in obesity. This loss of function may be a result of decreased adiponectin levels and/or downregulation of adiponectin receptors,²¹⁵ although the exact cause remains unclear. Regardless, several studies demonstrate that administration of adiponectin improves endothelial function via adenosine monophosphate-activated protein kinase (AMPK)-induced phosphorylation of eNOS.^{216;217} Thus, alterations in this signaling pathway may also contribute to the development of endothelial dysfunction.

Evidence regarding the mechanistic effects of coronary PVAT derived factors on vascular smooth muscle are much more limited. Owen et al. proposed that coronary PVAT potentiates coronary artery contractions via activation of voltage-dependent ion channels (i.e., Ca_v1.2 channels). The augmented contractile effect of obese coronary PVAT is consistent with reports of increased coronary vascular smooth muscle Ca_v1.2 current and vasoconstriction in the setting of obesity.^{1;21;141} It has also been proposed that PVAT-derived factors inhibit vascular smooth muscle K⁺ channels. This is supported by studies in which H₂O₂-induced dilation of coronary arteries, which was completely abolished by pre-constriction with KCl, was markedly attenuated in the presence of coronary PVAT.⁹ Importantly, inhibitory effects on K⁺ channels would also serve to activate Ca_v1.2 channels and augment coronary artery contractions. However, the effects of coronary PVAT on smooth muscle K⁺ channels and the precise K⁺ channel subtypes involved warrant further investigation.

A proteomic assessment of coronary PVAT from lean and obese swine indicated that coronary PVAT produces factors capable of influencing several key regulatory

pathways including cellular growth and proliferation, and cellular movement.⁹ Interestingly, RhoA was significantly elevated in samples from obese coronary PVAT.⁹ RhoA is a molecular GTPase regulatory switch that interacts with downstream effectors, such as Rho kinase, to elicit cellular responses.²¹⁸ Rho kinases regulate a variety of cellular functions such as contraction, motility, and proliferation.²¹⁹ In smooth muscle, contraction is regulated by the phosphorylation/dephosphorylation of myosin light chain via Ca²⁺-dependent (i.e., rise in cytosolic Ca²⁺) and Ca²⁺-

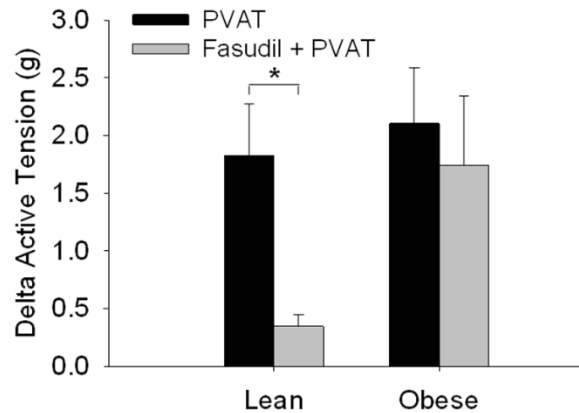


Figure 1.20 Effects of Rho kinase signaling on the vascular effects of coronary PVAT. Addition of the Rho kinase inhibitor, fasudil, significantly reduced the contractile effect of PVAT in isolated coronary arteries from lean, but not obese swine. The difference in tension generated by each isolated porcine coronary artery before and after the addition of perivascular adipose tissue (PVAT) is expressed as delta active tension. Modified from Owen et al., 2013.⁹

independent mechanisms.²²⁰ The inhibitory phosphorylation of myosin light chain phosphatase by Rho kinase sensitizes the contractile apparatus to Ca²⁺ and allows for agonist-induced contraction independent of changes in cytosolic Ca²⁺ concentration.²²¹ Interrogation of the Rho kinase pathway in coronary arteries (**Figure 1.20**) indicated that PVAT-derived factors potentiate vasoconstriction via a Rho kinase-dependent mechanism in lean arteries, while PVAT mediated increases in contraction in the setting of obesity occur via Rho-independent pathways (i.e., functional alterations in Ca_v1.2 and/or K⁺ channels).⁹

Numerous studies also implicate Rho kinase in several mechanisms of atherogenesis including vascular smooth muscle proliferation and migration. In particular, Rho kinase signaling has been implicated in both platelet-derived growth factor(PGDF)-

stimulated and G-protein-coupled receptor (i.e. thrombin)-induced proliferation of vascular smooth muscle cells.^{222;223} A potential mechanism by which Rho kinase may regulate smooth muscle cell proliferation involves the activation of extracellular-regulated kinase 1/2 (ERK 1/2), as inhibition of Rho kinase has been found to suppress PDGF-induced activation of ERK1/2.²²² In animal models of vascular injury, the inhibition of Rho kinase has been shown to reduce intimal hyperplasia via effects on smooth muscle proliferation.^{224;225} Other studies, however, suggest that Rho kinase influences neointimal formation primarily via effects on apoptosis and vascular inflammation and fail to demonstrate a substantial role for Rho kinase in smooth muscle cell proliferation.^{226;227} Importantly, the present studies have been conducted in peripheral (non-coronary) vascular beds and thus the involvement of Rho kinase in coronary smooth muscle cell proliferation remains to be elucidated. Altogether, these observations support that the role of Rho kinase signaling in vascular smooth muscle cell proliferation and the potential upstream atherogenic factors responsible for activating this pathway require further investigation.

Summary and Proposed Experimental Aims

The pandemic of obesity is an urgent global healthcare crisis. Particularly alarming is the dramatically increased risk of cardiovascular disease associated with obesity. While many studies have resulted in significant improvements in the ability to manage and mitigate obesity-induced cardiovascular complications, current understanding of the causal link between obesity and coronary artery disease remains rather limited. Such understanding is needed in order to elucidate potential therapeutic targets for the effective treatment and perhaps prevention of obesity-induced coronary disease.

To that end, many investigations have demonstrated that adipose tissue is an endocrine and paracrine organ, producing adipokines that have the potential to influence several mechanisms of atherogenesis, namely vascular dysfunction, in the setting of obesity. Recent data implicate the adipose tissue depot surrounding the vasculature, PVAT, in the pathogenesis of vascular disease. In particular, coronary PVAT, which immediately surrounds the large coronary arteries of the heart, has been identified as a risk factor for coronary artery disease.

A growing body of evidence supports that changes in the adipokine expression profile of coronary PVAT occur concomitantly with phenotypic alterations in the coronary endothelium and vascular smooth muscle in the setting of obesity (**Figure 1.21**). However, the contribution of PVAT-derived factors (e.g., leptin) to the initiation and progression of coronary vascular dysfunction and disease is still not well understood. Accordingly, the goal of this investigation is to delineate the mechanisms by which PVAT-derived factors influence coronary vascular smooth muscle function and the development of obesity-induced coronary disease. This goal will be directly addressed by the following Specific Aims:

- 1. Delineate the mechanisms by which lean versus obese coronary PVAT influences coronary vascular smooth muscle reactivity.** Rationale for **Aim 1** is based on recent findings suggesting that the vascular effects of coronary PVAT are related to alterations in the functional expression of smooth muscle K^+ channels in the setting of obesity. Studies will test the hypothesis that lean and obese PVAT differentially attenuates K_{Ca} , K_V , and K_{ATP} channel-mediated vasodilation in the coronary circulation.

2. Test the hypothesis that leptin acts as an upstream mediator in the development of coronary vascular smooth muscle dysfunction and disease.

Rationale for **Aim 2** is based on evidence that coronary PVAT-derived factors potentiate contraction of vascular smooth muscle via a Rho kinase-dependent mechanism and that PVAT-derived leptin impairs coronary vasodilation and promotes neointima formation. Studies will test the hypothesis that leptin promotes progressive alterations in coronary smooth muscle contraction via alterations in Rho kinase signaling and markedly alters the coronary artery proteome in favor of pathways associated with the initiation and progression of coronary artery disease.

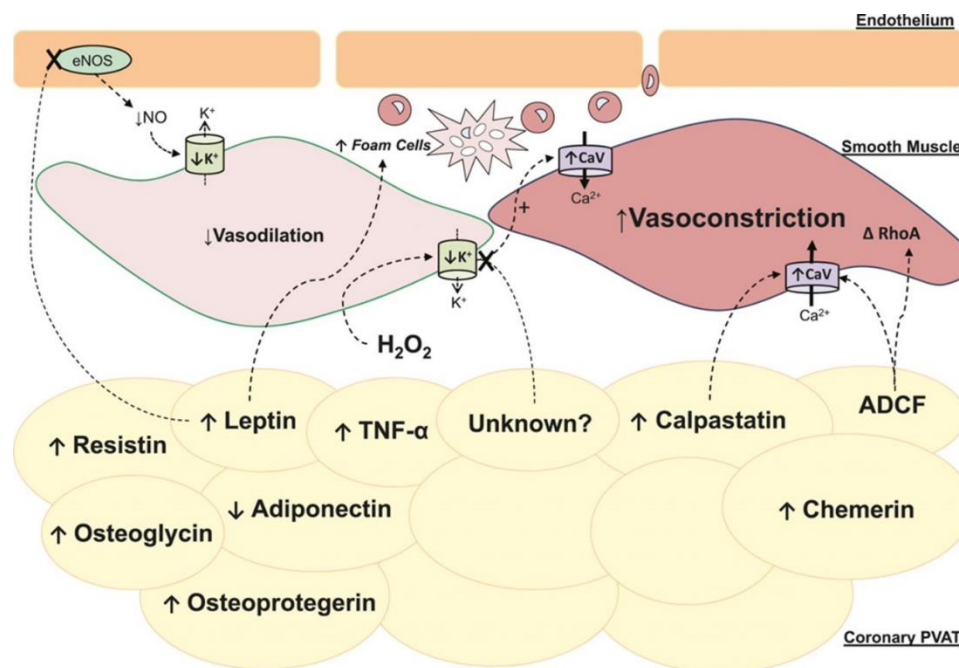


Figure 1.21 Alterations in coronary perivascular adipose tissue (PVAT)-derived adipokines and potential downstream effector mechanisms in endothelium and vascular smooth muscle. Coronary PVAT-derived leptin diminishes endothelial nitric oxide synthase (eNOS) activity, reducing nitric oxide (NO)-mediated dilation of vascular smooth muscle via K^+ channel activation and contributes to the recruitment and retention of macrophages. Adipose-derived constricting factors (ADCF), such as calpastatin and other presently unknown factors, increase vasodilation via activation of $Ca_v1.2$ channels, inhibition of K^+ channels, and/or alterations in Rho kinase signaling. Production of other adipokines that may play a role in endothelial and smooth muscle dysfunction include, but are not limited to, increased resistin, chemerin, osteoglycin and osteoprotegerin, and decreased adiponectin. H_2O_2 , hydrogen peroxide; TNF, tumor necrosis factor.¹⁷

Chapter 2

Lean and obese coronary perivascular adipose tissue impairs vasodilation via differential inhibition of vascular smooth muscle K⁺ channels

Arteriosclerosis, Thrombosis, and Vascular Biology

Volume 35(6), June 2015

Jillian N. Noblet¹, Meredith K. Owen², Adam G. Goodwill¹, Daniel J. Sassoon¹,
and Johnathan D. Tune¹

¹Department of Cellular & Integrative Physiology, Indiana University School of Medicine,
Indianapolis, Indiana

²Department of Cell Biology & Physiology, University of North Carolina School of
Medicine, Chapel Hill, North Carolina

ABSTRACT

Objective – The effects of coronary perivascular adipose tissue (PVAT) on vasomotor tone are influenced by an obese phenotype and are distinct from other adipose tissue depots. The purpose of this investigation was to examine the effects of lean and obese coronary PVAT on end-effector mechanisms of coronary vasodilation and to identify potential factors involved.

Approach and Results – Hematoxylin and eosin staining revealed similarities in coronary perivascular adipocyte size between lean and obese Ossabaw swine. Isometric tension studies of isolated coronary arteries from Ossabaw swine revealed that factors derived from lean and obese coronary PVAT attenuated vasodilation to adenosine. Lean coronary PVAT inhibited K_{Ca} and K_{V7} , but not K_{ATP} channel mediated dilation in lean arteries. In the absence of PVAT, vasodilation to K_{Ca} and K_{V7} channel activation was impaired in obese arteries relative to lean arteries. Obese PVAT had no effect on K_{Ca} or K_{V7} channel mediated dilation in obese arteries. In contrast, obese PVAT inhibited K_{ATP} channel mediated dilation in both lean and obese arteries. The differential effects of obese versus lean PVAT were not associated with changes in either coronary K_{V7} or K_{ATP} channel expression. Incubation with calpastatin attenuated coronary vasodilation to adenosine in lean but not obese arteries.

Conclusions – These findings indicate that lean and obese coronary PVAT attenuates vasodilation via inhibitory effects on vascular smooth muscle K^+ channels and that alterations in specific factors such as calpastatin are capable of contributing to the initiation and/or progression of smooth muscle dysfunction in obesity.

Nonstandard Abbreviations and Acronyms

PVAT – perivascular adipose tissue

INTRODUCTION

Perivascular adipose tissue (PVAT) surrounds large arteries throughout the body and is capable of producing adipokines that act directly upon the adjacent vasculature.^{17;228} PVAT-derived factors have been shown to stimulate chemotaxis, inflammation, and endothelial dysfunction, thereby implicating local PVAT signaling in the initiation and progression of vascular disease.^{2;56;83;91;171;172} Data from recent studies investigating vascular responses to PVAT-derived factors suggest that the endothelial and smooth muscle effects of these substances are highly dependent on anatomic location of the adipose/vascular depot and the underlying disease state of the subjects from which the tissues were obtained.¹⁷ Such discrepant phenotypic effects of PVAT are not surprising given marked differences in protein expression and secretion profiles of adipose tissue depots from lean versus obese subjects.^{9;73;75;101;176;177;181} However, current understanding of how these alterations influence mechanisms of vascular function remains limited.

Differences in the vascular effects of PVAT-derived factors are evident when comparing peripheral (non-cardiac) versus coronary-cardiac PVAT. In particular, aortic,^{150;229} mesenteric,^{153;154} and internal thoracic artery^{158;159} PVAT have been shown to significantly diminish contractile responses to a variety of agonists. This vasodilator or “anti-contractile” effect is attributed to production of adipose-derived relaxing factor(s) (ADRF(s)) that promote endothelial dependent and/or independent vasodilation via activation of voltage-dependent K_v7 channels,¹⁵³ BK_{Ca} channels,^{159;164} and K_{ir} channels.¹⁵¹ In contrast, factors released from coronary PVAT have been shown to attenuate endothelial-dependent dilation^{171;172} and potentiate coronary artery contractions.⁹ These deleterious effects of coronary PVAT are augmented in the setting of obesity and are directly associated with marked alterations in the coronary PVAT proteome and the functional expression of coronary K^+ and Ca^{2+} channels.^{1;9;21} Specifically, our laboratory

has recently demonstrated that the endogenous calpain inhibitor calpastatin^{208,230} is significantly elevated in the secreted protein expression profile of obese coronary PVAT and is sufficient to dose-dependently augment coronary artery contractions in the absence of PVAT.⁹ Obesity has also been found to diminish the contribution of end-effector K⁺ channels to coronary vasodilator responses.⁴ These channels include voltage-dependent (K_V), Ca²⁺-activated (K_{Ca}), and ATP-sensitive (K_{ATP}) channels, which regulate smooth muscle membrane potential and participate in the regulation of coronary vascular resistance.¹²⁹ However, the extent to which coronary PVAT-derived factors modulate the role of these channels has not been investigated.

Accordingly, the purpose of this investigation was to delineate the effects of lean and obese coronary PVAT on end-effector mechanisms of coronary vasodilation and to identify potential PVAT-derived factors involved. Studies were specifically designed to test the hypothesis that lean and obese PVAT differentially attenuate K_{Ca}, K_V, and K_{ATP} channel mediated vasodilation in the coronary circulation and that calpastatin contributes to these effects. Findings from this investigation add to growing evidence supporting a role for PVAT in the pathogenesis of vascular dysfunction in obesity-induced coronary disease.

MATERIALS AND METHODS

Ossabaw Swine Model of Obesity

All experimental protocols and procedures were approved by the Institutional Animal Care and Use Committee in accordance with the *Guide for the Care and Use of Laboratory Animals*. Lean Ossabaw swine (n=30) were fed ~2000 kcal/day standard chow containing 18% kcal from protein, 71% kcal from complex carbohydrates, and 11% kcal from fat. Obese Ossabaw swine (n=28) were fed ≥8000 kcal/day atherogenic diet containing 16% kcal from protein 41% kcal from complex carbohydrates, 43% kcal from fat, and supplemented with 2.0% cholesterol and 0.7% sodium cholate by weight (5L80

and KT324, Purina Test Diet, Richmond, IN). Swine were fed their respective diets for ~6 months prior to sacrifice.

Immunohistochemistry

Immunohistochemical analyses were performed in conjunction with Indiana University Health Pathology Laboratory (Indianapolis, IN). Briefly, hearts from lean and obese swine were excised upon sacrifice and immediately perfused with 4°C, Ca²⁺-free Krebs buffer (131.5 mM NaCl, 5 mM KCl, 1.2 mM NaH₂PO₄, 1.2 mM MgCl₂, 25 mM NaHCO₃, 10 mM glucose) via aortic cannulation. Segments of coronary arteries with perivascular adipose tissue (PVAT) intact were grossly dissected from the heart and placed in 10% Formalin (Fisher Scientific, Fair Lawn, NJ, SF98-4). Similar segments of coronary artery were harvested from a formalin fixed human heart obtained via Indiana University Health Pathology Laboratory (Indianapolis, IN) and with approval of the Institutional Review Board of Indiana University (IRB #1306011568). Fixed artery segments were embedded in paraffin and cross sectioned. Verhoeff-van Gieson (VVG) and Hematoxylin and Eosin (H&E) staining were performed. Additionally, sections were exposed to anti-CD163 antibody (1:100; Abcam, Cambridge, MA, ab87099), a marker for cells of the monocyte/macrophage lineage²³¹ and anti-Rabbit IgG (1:100; Abcam, Cambridge, MA, ab172730) as an isotype control. Slides were imaged at 4X or 10X magnification, as indicated, on a Nikon Eclipse 80i microscope and images captured with a Nikon DS-Fi1 and associated Nikon Elements software. Linear adjustments of contrast, applied equally to all parts of an image, were made using ImageJ software Fiji.²³² Diameters of adipocytes within 500 µm of the vessel wall were determined using Leica image processing system.

Functional Assessment of Isolated Coronary Rings

Functional studies on isolated coronary artery rings were performed as previously described.^{2,9} After the perfusion described above, coronary arteries from lean and obese swine were grossly dissected from the heart (**Figure 2.1A**), removed from the myocardium (**Figure 2.1B**) and cleaned of surrounding coronary PVAT (**Figure 2.1C**). Subsequently, coronary PVAT was cut into ~50 mg pieces and stored in Ca²⁺-free Krebs buffer at 4°C for later use. Cleaned coronary arteries were cut into 3 mm rings and mounted in organ baths filled with Ca²⁺-containing Krebs buffer (131.5 mM NaCl, 5 mM KCl, 1.2 mM NaH₂PO₄, 1.2 mM MgCl₂, 25 mM NaHCO₃, 10 mM glucose, 4mM CaCl₂) at 37°C. Once stabilized at optimal passive tension (~4 g), arteries were subjected to the experimental protocols outlined below.

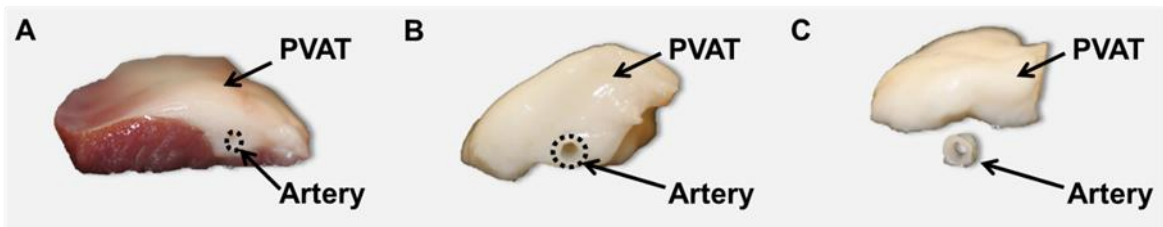


Figure 2.1 Representative pictures illustrating the isolation of coronary artery rings and perivascular adipose tissue (PVAT) from lean and obese hearts prior to isometric tension studies. Images adapted from Owen et al.,⁹ with permissions from Wolters Kluwer Health Publishing. Copyright 2013, *Circulation*.

Lean and obese coronary arteries were incubated with coronary PVAT from the same animal (**Figure 2.2B and 2.2C**), or left untreated as time-control (**Figure 2.2A and 2.2D**) for 30 minutes at 37°C. For arteries incubated with PVAT, 0.3 g of PVAT (~50 mg pieces) was weighed and then added directly to the organ bath, as previously described.^{2,9} Arteries were then pre-constricted with the thromboxane A₂ mimetic, U46619 (1 µM: Santa Cruz Biotechnology, Dallas, TX, sc-201242) or KCl (60 mM: Sigma Aldrich, St. Louis, MO, P9333), indicated as “KCl control” in (**Figure 2.4**). Active tension development (peak tension minus baseline tension) was recorded for each treatment group. Upon stabilization of contractions, arteries were exposed to increasing concentrations of adenosine (10 nM

– 30 μM : Sigma Aldrich, St. Louis, MO, A9251), the K_{Ca} channel agonist NS-1619 (1 μM – 30 μM : Sigma Aldrich, St. Louis, MO, N170), the $\text{K}_{\text{V}7}$ channel agonist L-364,373 (10 nM – 10 μM : Tocris, Minneapolis, MN, Cat.No.2660), or the K_{ATP} channel agonist cromakalim (30 nM – 1 μM : Sigma Aldrich, St. Louis, MO, C1055). For crossover experiments (**Figure 2.8**), lean arteries cleaned of PVAT, indicated as “control” were incubated with known quantities (0.3 g) of either lean PVAT from the same animal, indicated as “lean PVAT,” or obese PVAT from an obese animal sacrificed on the

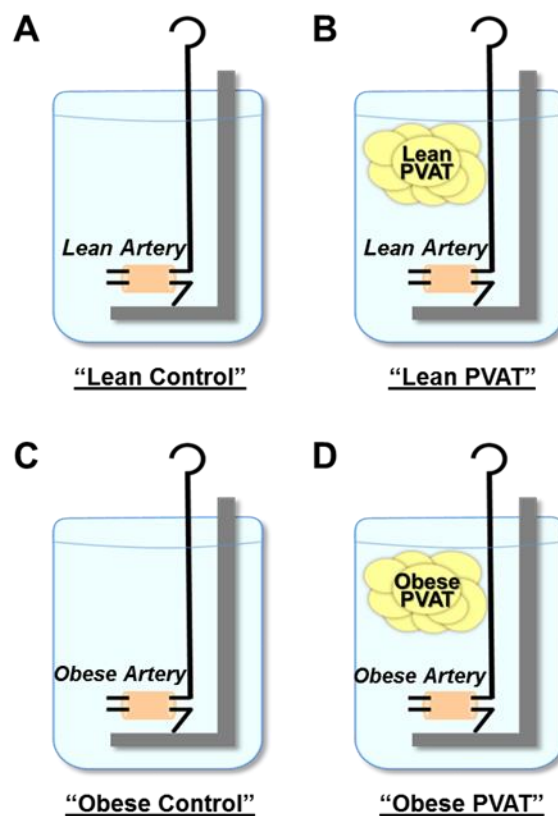


Figure 2.2 Experimental design for isometric tension studies. Illustrations correspond to studies presented in Figure 2.5 and Figure 2.6.

same day, indicated as “obese PVAT” (**Figure 2.2**). For calpastatin studies, both lean and obese coronary arteries cleaned of PVAT were incubated with calpastatin (10 μM : Calbiochem, San Diego, CA, Cat#208902), or left untreated as control for 30 minutes at 37°C. Arteries were then pre-constricted with U46619 (1 μM) and exposed to increasing concentrations of adenosine (10 nM – 30 μM) in the presence or absence of calpastatin. Additional experiments were also conducted in endothelium denuded coronary arteries from lean swine. The endothelium was removed by gently rubbing fine-tip forceps along the lumen of the artery. Denudation was confirmed by <15% relaxation to bradykinin (1 μM : Sigma Aldrich, St. Louis, MO, B3259). Results are reported as the percent relaxation for each animal and rings with the same treatment from the same animal were averaged for

n = 1. One hundred percent relaxation is defined as a return to the level of baseline tension.

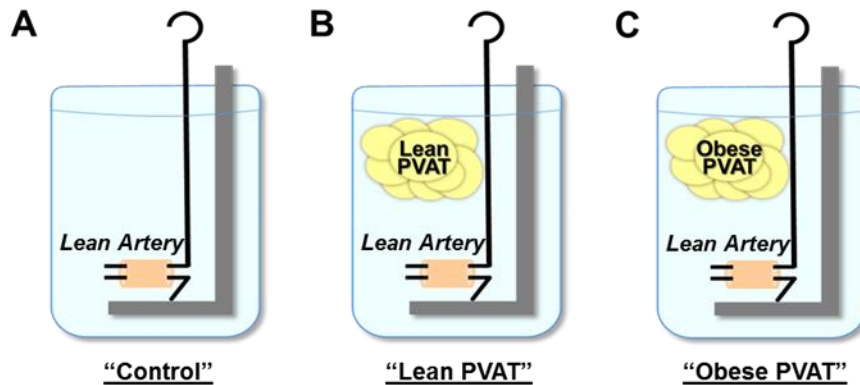


Figure 2.3 Experimental design for crossover isometric tension studies. Illustrations correspond to studies presented in Figure 2.8.

Western Analysis

Coronary arteries from lean (n=3) and obese (n=3) swine were cleaned of adipose tissue, frozen in liquid N₂ and stored at -80°C. Arteries were homogenized and total protein collected and quantified as previously described.²³³ Equivalent amounts of protein were loaded onto 10% polyacrylamide gels (Life Technologies, Carlsbad, CA, NP0302) for electrophoresis and blotting. Membranes were incubated overnight at 4°C with primary antibodies directed against Kir6.1 (1:200, Santa Cruz Biotechnology, Dallas, TX, sc-11224) or KCNQ1 (1:400, Sigma-Aldrich, St. Louis, MO, AV35529). The blots were washed and incubated with donkey anti-goat (1:5000, Santa Cruz Biotechnology, Dallas, TX, sc-2020) or goat anti-rabbit (1:1000, Santa Cruz Biotechnology, Dallas, TX, sc-2004) IgG-horseradish peroxidase secondary antibodies for 1.5 h at ambient temperature. To verify equal protein loading, membranes were washed and incubated with antibody to β -actin (1:200, Santa Cruz Biotechnology, Dallas, TX, sc-1616). Immunoreactivity was visualized using ECL (Thermo Scientific, Rockford, IL, Prod#32106) and the G:BOX system (Syngene). MagicMark XP Western Standard (Life Technologies, Carlsbad, CA, LC5602) was used as a protein ladder. Densitometry analyses were conducted using

ImageJ. Protein levels of KCNQ1, Kir6.1, and β -actin are reported as “% lean;” i.e. protein levels from each sample were normalized to the average level of the respective protein in lean arteries.

Statistical Analysis

Data are presented as mean \pm SE. A t-test was used to compare phenotypic data (lean vs. obese) and densitometry of Western blot analyses. For isometric tension studies, a two-way ANOVA was used to test the effects of PVAT (Factor A) relative to doses of specific treatments (Factor B). If assumptions of normality and equal variance for parametric ANOVA were not met, a Kruskal-Wallis non-parametric ANOVA was performed. Importantly, results of non-parametric ANOVAs were consistent with those of the parametric ANOVA. When statistical differences were found with ANOVA ($P < 0.05$), a Student-Newman-Keuls multiple comparison test was performed. SigmaPlot version 11.0 (Systat Software Inc, San Jose, CA) was used for graphics and statistical analyses.

RESULTS

Phenotype of Lean and Obese Ossabaw Swine

Compared to their lean counterparts, obese swine exhibited significant increases in body weight, fasting glucose, total cholesterol, and triglycerides (**Table 2.1**). Histopathological analyses to examine the morphology of perivascular adipocytes were performed on sections of coronary arteries with the adjacent PVAT intact. Hematoxylin and eosin staining revealed apparent similarities in perivascular adipocyte size between lean (**Figure 2.4A**) and obese (**Figure 2.4B**) swine. Specifically, adipocyte diameter averaged $70 \pm 1 \mu\text{m}$ in lean and $67 \pm 2 \mu\text{m}$ in obese swine ($P = 0.24$). These values are consistent with measures of coronary perivascular adipocyte diameter (**Figure 2.4C**, average = $66 \pm 2 \mu\text{m}$, $n=2$) from human subjects with evidence of coronary artery disease

Table 2.1 Phenotypic characteristics of lean and obese Ossabaw swine

| | Lean | Obese |
|-------------------------------|----------|-----------|
| Body weight (kg) | 62 ± 6 | 100 ± 5* |
| Heart weight (g) | 182 ± 16 | 222 ± 15 |
| Mean arterial pressure (mmHg) | 102 ± 9 | 107 ± 5 |
| Glucose (mg/dL) | 154 ± 14 | 232 ± 21* |
| Insulin (μU/mL) | 12 ± 1 | 14 ± 3 |
| Total cholesterol (mg/dL) | 74 ± 4 | 340 ± 61* |
| Triglycerides (mg/dL) | 46 ± 5 | 78 ± 14* |

Values are mean ± SE for lean (n=10) and obese (n=10) swine. * $P < 0.05$ vs. lean.

(**Figure 2.4F**). Verhoeff-van Gieson elastin stain demonstrated the presence of atheroma formation in obese (**Figure 2.4E**) compared to lean (**Figure 2.4D**) swine. These data are consistent with findings from other studies from our investigative team which documented ~15-20% stenosis of major coronary arteries (using intravascular ultrasound) in obese Ossabaw swine.²³⁴⁻²³⁶ Immunostaining for CD163, a marker for cells of the monocyte/macrophage lineage,²³¹ revealed prominent staining in the medial layer of obese arteries (**Figure 2.4I**) with only modest staining evident in lean arteries (**Figure 2.4H**) relative to isotype control (**Figure 2.4G**). These findings are consistent with prior reports of inflammation in coronary arteries from obese swine.²³⁷

Lean and Obese PVAT Attenuate Coronary Vasodilation

To initially examine the effects of PVAT on vasodilation, coronary arteries cleaned of surrounding PVAT from lean and obese swine were incubated with or without a known quantity of coronary PVAT (0.3 g) from the same animal for 30 min (**Figure 2.5**). Arteries were then pre-constricted with the thromboxane A₂ mimetic U46619 (1 μM). Active tension development of control arteries to U46619 (1 μM) in the absence of PVAT averaged 9.01 ± 0.41 g in lean and 10.20 ± 0.61 g in obese arteries ($P = 0.09$). In arteries treated with PVAT, active tension development averaged 9.61 ± 0.42 g in lean and 9.88 ± 0.53 g in

obese arteries ($P = 0.68$). Vasodilation to adenosine ($30 \mu\text{M}$) was reduced $\sim 25\%$ in obese (Figure 2.5B) compared to lean (Figure 2.5A) arteries in the absence of PVAT ($P < 0.001$). The presence of PVAT significantly attenuated adenosine relaxation at concentrations $>3 \mu\text{M}$ in arteries from both lean and obese swine. Although maximal responses to adenosine were lower in obese arteries, the overall degree of PVAT

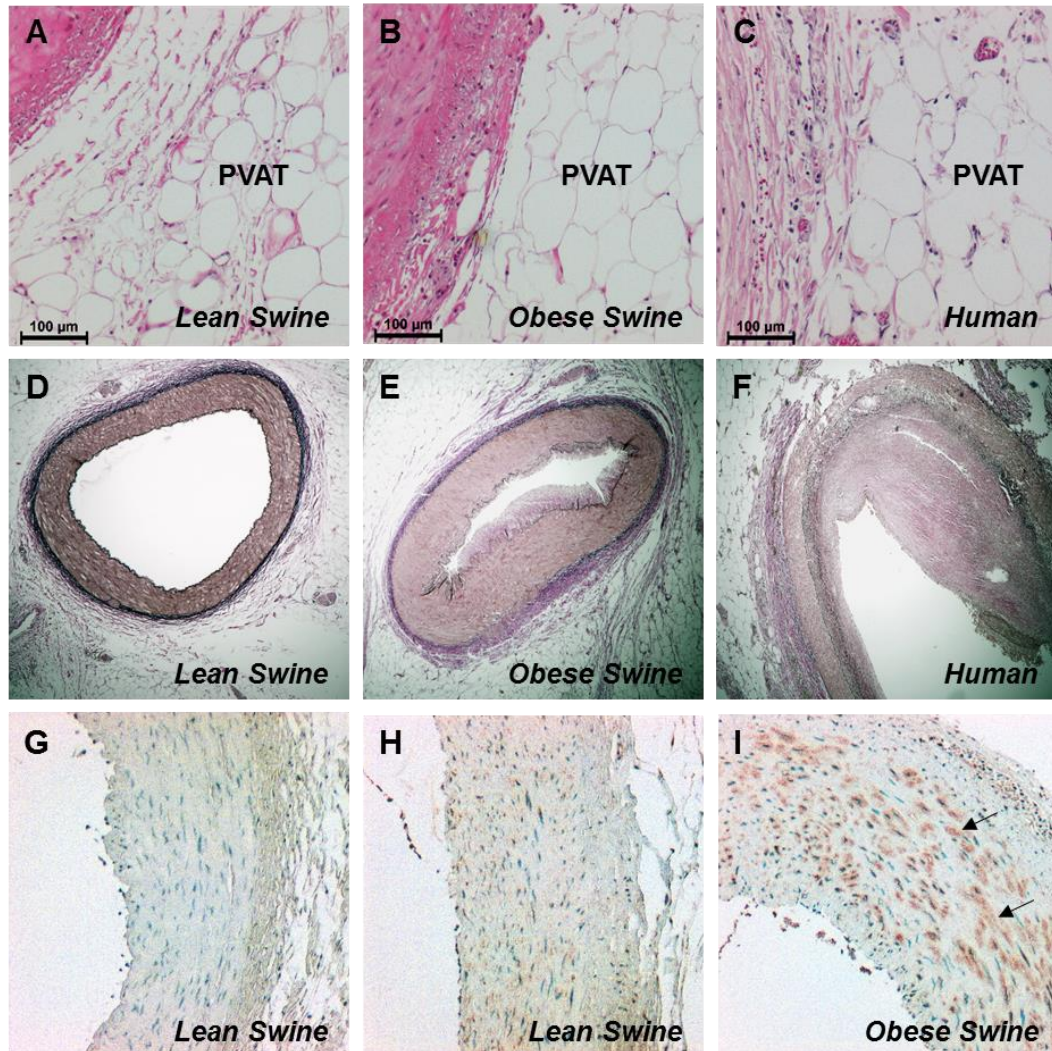


Figure 2.4 Representative images of immunohistochemical analyses of coronary arteries and associated PVAT. Arteries were obtained from humans ($n=2$), and lean and obese swine ($n=4$, each group). Hematoxylin and eosin-stained sections (10X) illustrated similarities in perivascular adipocyte morphology between humans and swine (A-C). Verhoeff-van Gieson stained sections (4X) showed evidence of atheroma formation in human (F) and obese (E) compared to lean (D) arteries. CD163 staining (10X) indicated a marked increase in macrophages in obese (I, arrows) compared to lean (H) arteries relative to isotype control (G).

inhibition on maximal adenosine-induced dilation (30 μ M) was similar in lean (~31%) and obese (~32%) arteries (**Figure 2.5A** vs. **Figure 2.5B**). Pre-constriction with KCl (60 mM), which averaged 7.19 ± 0.22 g in lean and 8.27 ± 0.90 g in obese arteries ($P = 0.36$), essentially abolished dilation to adenosine in both lean and obese arteries. Additional experiments in endothelium denuded coronary arteries demonstrated that adenosine-induced dilation was unaffected by removal of the endothelium in both control ($P = 0.94$) and PVAT treated ($P = 0.99$) arteries. Denudation was confirmed in these studies by <15% relaxation to bradykinin (1 μ M).

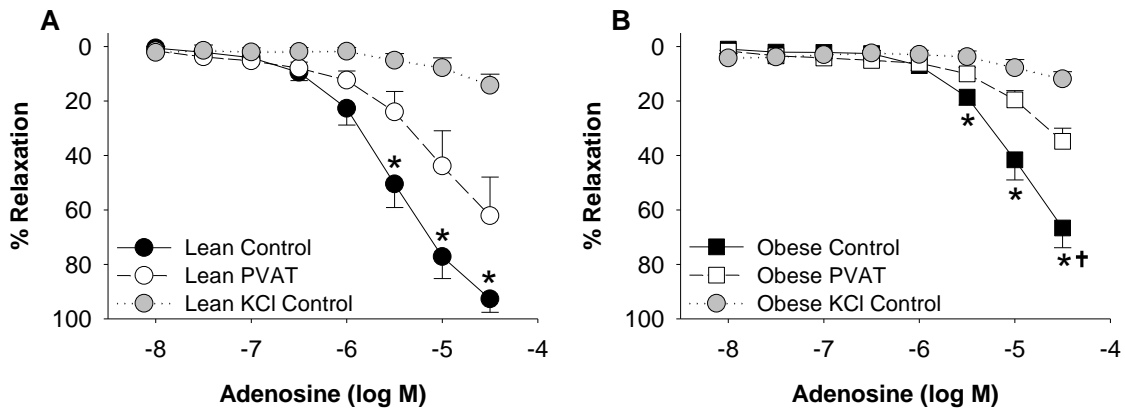


Figure 2.5 Coronary PVAT attenuates adenosine induced vasodilation. In control arteries cleaned of PVAT (n=6 each group), maximal vasodilation to adenosine was reduced ~25% in lean (**A**) compared to obese (**B**) arteries. The presence of PVAT from the same animal (n=6 each group) impaired dilation to a similar extent and constriction with KCl (n=3 each group) abolished adenosine dilation in lean and obese arteries. * $P < 0.05$, PVAT vs. control. † $P < 0.001$, lean vs. obese control.

Lean Coronary PVAT Inhibits K_{Ca} and K_{V7} Channels

The contribution of K_{Ca} channels to coronary vasodilation in lean and obese hearts was examined by comparing responses to the K_{Ca} channel agonist NS1619 (1 μ M – 30 μ M). Overall responses to NS-1619 (30 μ M) were reduced ~30% in obese compared to lean control arteries in the absence of PVAT ($P = 0.01$; **Figure 2.6A** vs. **Figure 2.6B**). Compared to control responses, the addition of PVAT attenuated dilator responses to the NS-1619 (30 μ M) by ~30% in lean arteries ($P < 0.001$; **Figure 2.6A**). In contrast, NS-1619

mediated dilation was unaffected by the addition of PVAT in obese arteries ($P = 0.90$; **Figure 2.6B**).

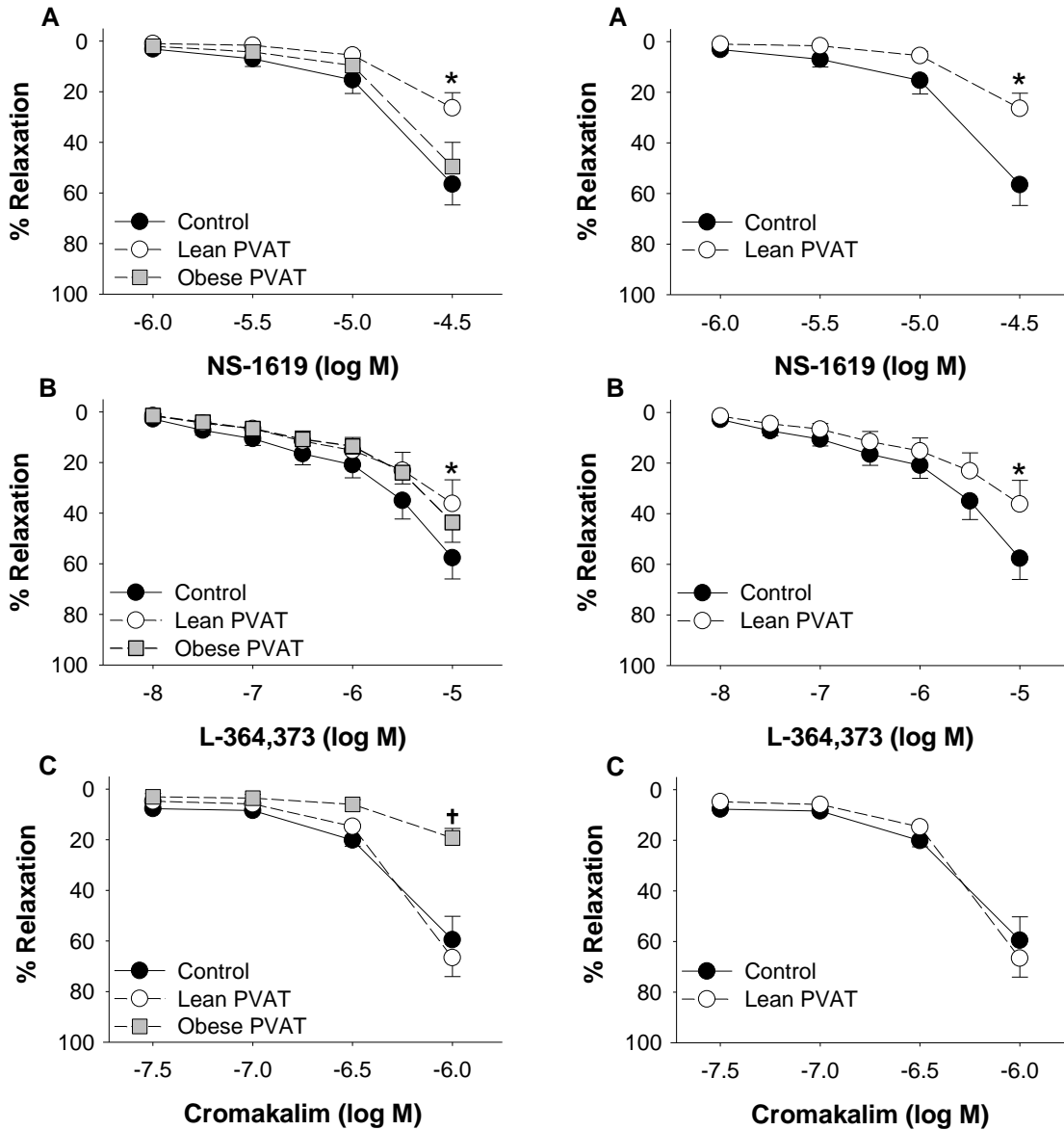


Figure 2.6 Effect of coronary PVAT on K^+ channel mediated dilation is altered in obesity. Arteries were incubated in the absence (control) or presence of PVAT from the same animal. PVAT attenuated vasodilation to the K_{Ca} channel agonist NS-1619 in lean (**A**) but not obese (**B**) arteries. Dilation to the K_v7 channel agonist L-364,373 was reduced in the presence of PVAT in lean (**C**) but not obese (**D**) arteries. In the absence of PVAT, dilation to NS-1619 and L-364,373 was impaired in obese (**B, D**) relative to lean (**A, C**) arteries. K_{ATP} channel mediated dilation to cromakalim was unaffected by PVAT in lean (**E**) arteries but was impaired by PVAT in obese (**F**) arteries. * $P < 0.05$, PVAT vs. control. † $P < 0.05$, lean vs. obese control.

To investigate the role of K_v7 channels in coronary vasodilation, responses to the K_v7 channel agonist L-364,373 (10 nM – 10 μ M) were examined in lean and obese arteries. Dilation to L-364,373 was significantly attenuated at doses >3 μ M in obese compared to lean control arteries in the absence of PVAT ($P < 0.05$; **Figure 2.6C** vs. **Figure 2.6D**). The presence of PVAT attenuated L-364,373 mediated dilation (10 μ M) by ~20% in lean arteries ($P = 0.02$; **Figure 2.6C**) but had no effect in obese arteries ($P = 0.98$; **Figure 2.6D**). Western blot analyses of K_v7 channel (KCNQ1) protein indicated that the abundance of KCNQ1 was not significantly different in lean versus obese coronary arteries ($P = 0.11$; **Figure 2.7A** and **2.7C**). Abundance of β -actin was not significantly

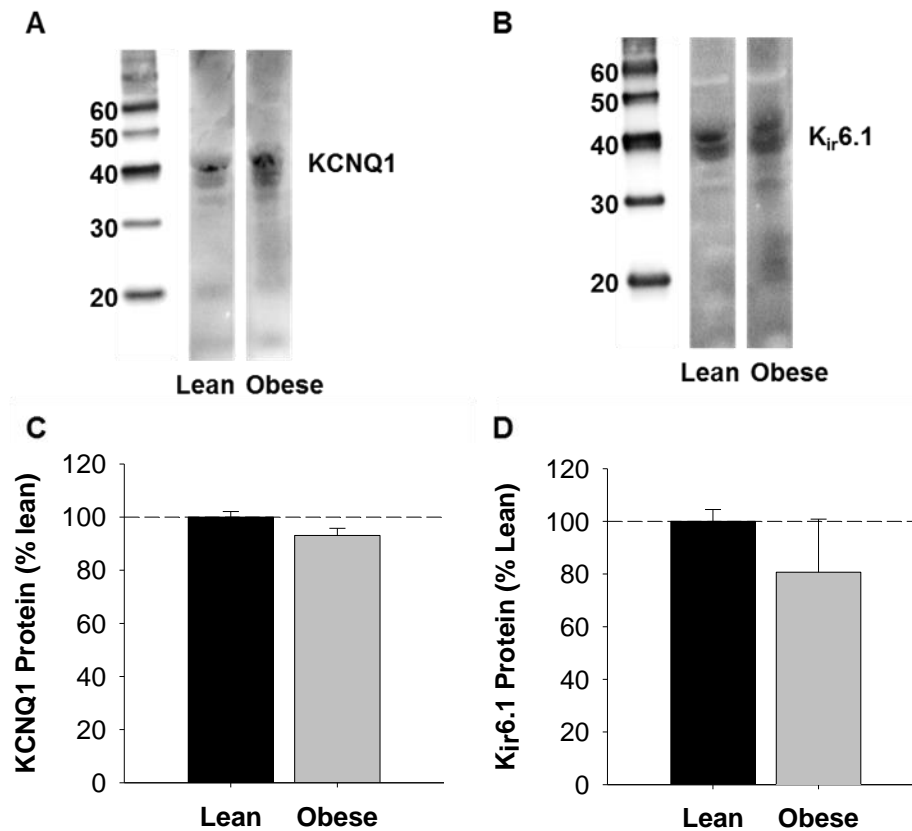


Figure 2.7 Western blot analysis of coronary artery KCNQ1 and Kir6.1 channel expression. Representative blots of KCNQ1 (**A**) and Kir6.1 (**B**) channel expression in lean and obese arteries. Expression levels of both KCNQ1 (**C**) and Kir6.1 (**D**) were unaffected by an obese phenotype ($P=0.11$ and $P=0.40$, respectively). Average data ($n=3$ for each group) are expressed as % protein observed in lean swine.

different in lean versus obese arteries ($P = 0.91$), indicating equal protein loading between samples.

Obese coronary PVAT Inhibits K_{ATP} Channels

Studies to investigate the effect of coronary PVAT on K_{ATP} channel mediated dilation were performed by comparing responses to the K_{ATP} channel agonist cromakalim (30 nM – 1 μ M) in lean and obese arteries. Control responses to cromakalim (1 μ M) were not significantly different in lean versus obese arteries in the absence of PVAT ($P = 0.90$; **Figure 2.6E and 2.6F**). The presence of coronary PVAT from the same animal had no effect on dilation to cromakalim (1 μ M) in lean arteries ($P = 0.57$; **Figure 2.6E**). In contrast, PVAT significantly attenuated dilation to cromakalim in obese arteries ($P = 0.02$; **Figure 2.6F**). Western blot analyses show that abundance of K_{ATP} channel pore forming unit (K_{ir} 6.1) protein was not different in obese compared to lean arteries ($P = 0.40$; **Figure 2.7B and 2.7D**). Abundance of β -actin was not significantly different in lean versus obese arteries ($P = 0.34$), indicating equal protein loading between samples.

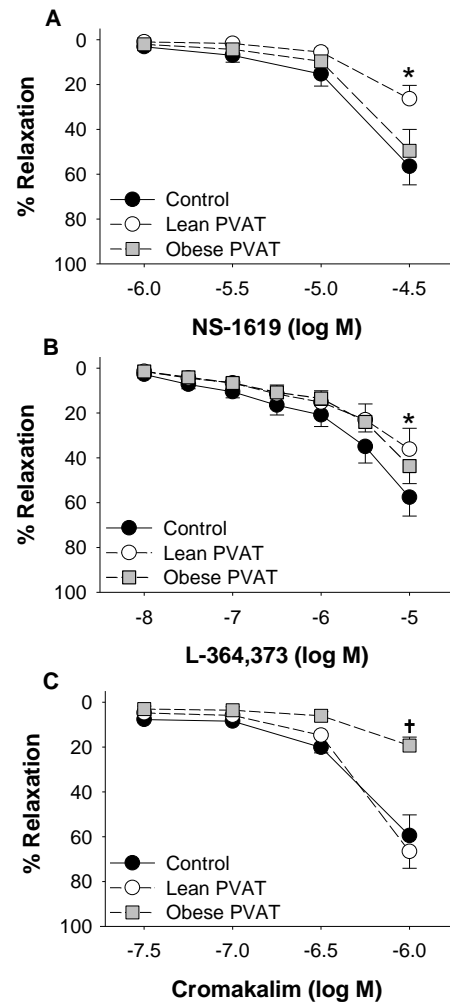


Figure 2.8 Effects of lean versus obese PVAT on coronary K^+ channel mediated dilation in lean arteries. For comparison purposes, lean control and lean PVAT responses are re-plotted from Figure 2A, 2C and 2E. Obese PVAT had no effect on vasodilation of lean arteries to the K_{Ca} channel agonist NS-1619 ($n=4$ [A]) or the K_V7 channel agonist L-364,373 ($n=3$ [B]). Dilation of lean arteries to the K_{ATP} channel agonist cromakalim was attenuated by obese but not lean PVAT ($n=3$ [C]). * $P < 0.05$ lean PVAT vs. control. † $P < 0.05$, obese PVAT vs. control.

Differential Effects of Lean versus Obese Coronary PVAT

In order to evaluate the specific effects of lean versus obese PVAT on K⁺ channel function, independent of differences in coronary artery responsiveness, control coronary arteries (cleaned of PVAT) from lean swine were incubated with known quantities of PVAT (0.3 g) from either lean or obese swine sacrificed on the same day. In contrast to the inhibitory effects of lean PVAT, obese PVAT had no effect on relaxation to NS-1619 (30 μ M) or L-364,373 (10 μ M) in lean arteries ($P = 0.40$; **Figure 2.8A** and $P = 0.10$; **Figure 2.8B**). Alternatively, obese PVAT significantly attenuated relaxation to cromakalim (1 μ M) ($P < 0.001$; **Figure 2.8C**) while lean PVAT had no effect ($P = 0.57$).

Based on previous findings,⁹ additional proof-of-principle studies were performed to investigate the effects of calpastatin (10 μ M) on coronary vasodilation. Incubation with calpastatin significantly attenuated vasodilation to adenosine (from 3 μ M to 10 μ M) in lean arteries cleaned of PVAT ($P = 0.001$; **Figure 2.9A**). In contrast, exposure to calpastatin had no effect on adenosine dilation in obese arteries cleaned of PVAT ($P = 0.30$; **Figure 2.9B**).

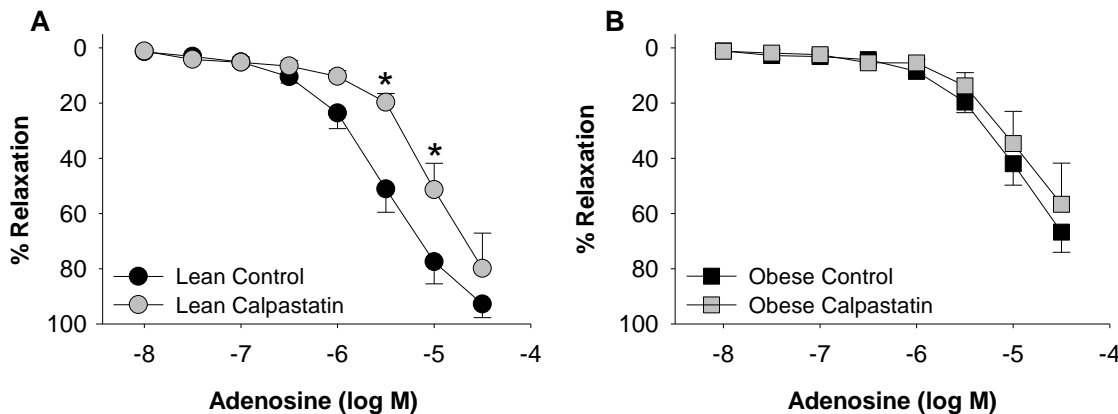


Figure 2.9 Effect of calpastatin on coronary artery vasodilation to adenosine. Incubation with calpastatin (10 μ M) attenuated adenosine dilation in lean (**A**) but not obese (**B**) arteries. All groups $n=5$. * $P < 0.05$ vs. control.

DISCUSSION

This investigation was designed to delineate the effects of lean and obese coronary PVAT on end-effector mechanisms of coronary vasodilation and to identify potential factors involved. The major new findings of this study are: (1) diameters of adipocytes in epicardial coronary PVAT are similar in lean and obese swine (2) factors derived from lean and obese coronary PVAT attenuate vasodilation in response to adenosine; (3) lean coronary PVAT inhibits K_{Ca} and K_v7 channel mediated dilation but has no effect on K_{ATP} channel mediated dilation in lean arteries; (4) coronary vasodilation to K_{Ca} and K_v7 channel activation is impaired in obese relative to lean arteries in the absence of PVAT; (5) obese PVAT has no effect on K_{Ca} or K_v7 channel activation in obese arteries; (6) obese PVAT inhibits K_{ATP} channel mediated vasodilation in both lean and obese coronary arteries; (7) calpastatin attenuates coronary vasodilation to adenosine in lean but not obese arteries. These findings provide novel evidence that lean and obese PVAT-derived factors attenuate coronary vasodilation via differential inhibition of K^+ channels and implicate a mechanistic link between alterations in PVAT-derived factors, such as calpastatin, and diminished functional expression of coronary K^+ channels in the setting of obesity.

Although the ability of PVAT to produce transferrable factors that influence the vasculature is well established, current understanding regarding the nature of this effect in specific adipose tissue depots remains rather limited. While the majority of studies on peripheral (non-cardiac) PVAT support the production of ADRF(s) and an overall “anti-*contractile*” effect,^{152-155;158;159;164;229;238;239} recent data indicate that coronary PVAT is unique relative to these other adipose depots both in its expression profile and effects on the vasculature.^{2;9;73} In particular, factors derived from coronary PVAT have been found to attenuate endothelial-dependent dilation and potentiate coronary artery contractions, especially in the setting of obesity.^{2;9;171;172} Other studies in lean or hypercholesterolemic

swine show little/no anti-contractile effect of coronary PVAT in response to endothelin-1, angiotensin II, or the thromboxane A2 mimetic U46619.^{2;173;174} Results from the present study further support the distinct vascular effects of coronary PVAT in that lean and obese coronary PVAT significantly attenuate coronary vasodilator responses to adenosine. This impaired dilator response is directly related to effects of PVAT-derived factors on smooth muscle K⁺ channels, as adenosine-induced dilation was unaffected by endothelial denudation and was essentially abolished by pre-constriction with KCl (**Figure 2.5A and 2.5B**). Inhibitory effects of PVAT on K⁺ channels have significant (patho)physiologic implications as prior studies have clearly demonstrated the contribution of K_V and K_{ATP} channels to the regulation of coronary microvascular tone^{129;240} and K_{Ca} channels in endothelial-dependent dilation.^{134;135}

The present findings provide novel evidence that lean and obese PVAT have distinct inhibitory effects on specific K⁺ channel subtypes in lean and obese coronary arteries. Specifically, factors derived from lean coronary PVAT impair K_{Ca} and K_{V7} channel mediated dilation, while factors derived from obese coronary PVAT attenuate K_{ATP} channel mediated dilation (**Figure 2.6**). The lack of effect of obese coronary PVAT on K_{Ca} and K_{V7} channels was observed in both obese (**Figure 2.6**) and lean (**Figure 2.8**) coronary arteries and is thus not related to intrinsic differences in smooth muscle phenotype of lean versus obese swine. Therefore, the “cross-over” studies in which lean arteries (i.e. with normal vascular smooth muscle function) were incubated with lean and obese PVAT, strongly support that lean and obese PVAT-derived factors differentially affect K_{Ca}, K_{V7}, and K_{ATP} channels. This distinction is important as we found that coronary vasodilation in response to K_{Ca} and K_{V7} channel agonists is attenuated in obese relative to lean arteries in the absence of PVAT (**Figure 2.6**). These data are consistent with prior work from our laboratory and others which demonstrated the functional down-regulation of BK_{Ca} and K_V channels in the coronary circulation^{1;21;137;241;242} and suggest the potential for PVAT-

derived factors to contribute to the initiation and progression of coronary vascular dysfunction in the setting of obesity.

There are several potential mechanisms that could contribute to the effects of PVAT-derived factors on coronary K⁺ channels. In particular, it does not appear that differences in K⁺ channel expression levels are responsible for the divergent effects of PVAT, as Western analyses revealed similar levels of K_V7 (KCNQ1) and K_{ATP} (K_{ir}6.1) channels in coronary arteries of lean and obese swine (**Figure 2.7**). Previous studies from our group also found augmented expression of BK_{Ca} channel subunits in coronary arteries of obese swine.¹ However, it is possible that expression of other channel subtypes and/or subunits could be altered in the setting of obesity. The potential for direct effects of PVAT-derived factors on specific coronary K⁺ channels is supported by prior evidence that NS-1619, L-364,373, and cromakalim directly open K_{Ca}, K_V, and K_{ATP} channels (i.e. without activating transmembrane signaling pathways), as these agonists have been shown to bind to sites on channel subunits and increase the open probability of excised membrane patches.²⁴³⁻²⁴⁵ Additionally, cellular signaling pathways also influence the response of these K⁺ channels to their respective agonists. For example, ischemic stimuli and Rho kinase signaling influence the response of K_{Ca} channels to NS-1619,^{246;247} while the effects of L-364,373 on K_V7 channels may intersect with ERK signaling²⁴⁸ and PKC alters the K_{ATP} channel response to cromakalim.²⁴⁹ Therefore, it is possible that cellular signaling, including post-translational modifications such as phosphorylation, influences the response of vascular smooth muscle K⁺ channel activation in the presence of PVAT.¹⁶³ Such effects are in line with previous studies from our laboratory which demonstrated that coronary PVAT influences both PKC and Rho kinase signaling.^{2;9} Whether coronary PVAT-derived factors interact with K⁺ channels directly and/or influence their function indirectly through intracellular signaling pathways warrants further investigation.

Identification of the precise factors responsible for the vascular effects of coronary PVAT remains a daunting task. Recent studies by the Weintraub laboratory have established that adipocytes from human coronary PVAT have a distinct phenotype and exhibit elevated expression of pro-inflammatory genes and genes associated with angiogenesis, coagulation, and vascular morphology.^{73;75;250;251} Evidence of macrophage infiltration (**Figure 2.4I**) and atheroma formation (**Figure 2.4E**) in obese arteries support a potential role for inflammatory cross-talk between PVAT and the artery wall in the pathogenesis of atherosclerosis. A previous global proteomic assessment revealed the up-regulation of proteins associated with cellular growth, proliferation, and movement in obese versus lean coronary PVAT from swine.⁹ These differences appear to be independent of gross changes in morphology, as similarities in adipocyte diameter were found between lean and obese PVAT (**Figure 2.4A and 2.4B**). Of particular interest is the endogenous calpain inhibitor, calpastatin, which we have shown to be significantly elevated in supernatant of obese coronary PVAT and to dose-dependently augment coronary artery contractions.⁹ Findings from the current investigation further support that calpastatin is capable of mimicking the effects of coronary PVAT in that it acts to impair smooth muscle dilation in response to adenosine in lean coronary arteries (**Figure 2.9A**). The loss of this effect in obese coronary arteries (**Figure 2.9B**) is consistent with the lack of effect of obese PVAT on K_{Ca} and K_V7 channel mediated dilation in obese arteries (**Figure 2.6B and 2.6D**), and suggests that chronic local exposure of the coronary circulation to factors such as calpastatin could contribute to the impairment of smooth muscle function in the setting of obesity.

It is important to recognize that although a differential effect of lean versus obese PVAT on vascular function was demonstrated in lean, healthy arteries, the effect of lean PVAT on obese arteries was not examined in this investigation. Additionally, findings of the present study were produced following short-term (~30 min) exposure to PVAT ex

vivo. Thus, a critical question remains as to whether chronic exposure of the coronary vasculature to the PVAT milieu directly contributes to the altered functional expression of K^+ channels in the setting of obesity. We propose that as the severity of obesity and other cardiovascular risk factors (insulin resistance, hypercholesterolemia, hypertension) progresses, changes in the secretion profile of coronary PVAT adversely influences the function and expression of coronary ion channels. However, the extent to which phenotypic alterations in coronary PVAT causally contribute to mechanistic alterations in the obese coronary circulation merits further study.

In summary, the current findings demonstrate that although coronary perivascular adipocytes from lean and obese swine share similar morphology, lean and obese PVAT-derived factors impair vasodilation via differential inhibition of vascular smooth muscle K^+ channels. Specifically, our data are the first to demonstrate that lean coronary PVAT attenuates K_{Ca} and K_v7 channel mediated dilation, while obese coronary PVAT impairs K_{ATP} channel mediated dilation. These results further support the paradigm of distinct “outside to inside” signaling influences of coronary PVAT and that alterations in specific factors such as calpastatin are capable of contributing to the initiation and/or progression of smooth muscle dysfunction in the setting of obesity.

ACKNOWLEDGEMENTS

None

SOURCES OF FUNDING

This publication was made possible in part by the Indiana University Health – Indiana University School of Medicine Strategic Research Initiative (CECARE); HL117620 (Tune-Mather); TL1 TR000162 (Noblet; Sassoon); 13POST1681001813 (Goodwill)

DISCLOSURES

None

SIGNIFICANCE

Coronary perivascular adipose tissue (PVAT) normally surrounds the major coronary arteries of the heart. Evidence is mounting to support the potential for factors derived from coronary PVAT to influence the pathogenesis of coronary vascular disease. In particular, recent studies indicate that coronary PVAT-derived factors initiate/potentiate contraction of vascular smooth muscle, a property distinct from other adipose tissue depots, and that this effect is significantly augmented in the setting of obesity. However, the effects of coronary PVAT on vasodilation have not been clearly defined. Results from this investigation indicate that coronary PVAT attenuates dilation via inhibitory effects on vascular K⁺ channels and that the mechanisms and factors involved in mediating these effects are markedly altered in the setting of obesity. These findings provide new insights into the unique vasoactive properties of coronary PVAT and the potential role of PVAT-derived factors in obesity-induced coronary disease.

Chapter 3

Leptin augments coronary vasoconstriction and smooth muscle proliferation via a Rho kinase dependent pathway

Basic Research in Cardiology

In Press

Jillian N. Noblet,¹ Adam G. Goodwill,¹ Daniel J. Sassoon,¹ Alexander M. Kiel,^{1,2}

Johnathan D. Tune¹

¹Department of Cellular & Integrative Physiology, Indiana University School of Medicine, Indianapolis, Indiana

²Weldon School of Biomedical Engineering, Purdue University, West Lafayette, Indiana

ABSTRACT

Leptin has been implicated as a key upstream mediator of pathways associated with coronary vascular dysfunction and disease. The purpose of this investigation was to test the hypothesis that leptin modifies the coronary artery proteome and promotes increases in coronary smooth muscle contraction and proliferation via influences on Rho kinase signaling. Global proteomic assessment of coronary arteries from lean swine cultured with obese concentrations of leptin (30 ng/mL) for 3 days revealed significant alterations in the coronary artery proteome (68 proteins) and identified an association between leptin treatment and calcium signaling/contraction (4 proteins) and cellular growth and proliferation (35 proteins). Isometric tension studies demonstrated that both acute (30 min) and chronic (3 day, serum-free media) exposure to obese concentrations of leptin potentiated depolarization-induced contraction of coronary arteries. Inhibition of Rho kinase significantly reduced leptin-mediated increases in coronary artery contractions. The effects of leptin on the functional expression of Rho kinase were time-dependent, as acute treatment increased Rho kinase activity while chronic (3 day) exposure was associated with increases in Rho kinase protein abundance. Proliferation assays following chronic leptin administration (8 day, serum-containing media) demonstrated that leptin augmented coronary vascular smooth muscle proliferation and increased Rho kinase activity. Inhibition of Rho kinase significantly reduced these effects of leptin. Taken together, these findings demonstrate that leptin promotes increases in coronary vasoconstriction and smooth muscle proliferation and indicate that these phenotypic effects are associated with alterations in the coronary artery proteome and dynamic effects on the Rho kinase pathway.

INTRODUCTION

Numerous studies have suggested that factors derived from adipose tissue have the potential to influence several key mechanisms of obesity-induced coronary disease including the promotion of vascular dysfunction and smooth muscle proliferation.^{2;13;48;207} For example, recent studies support that alterations in the adipokine secretion profile of coronary perivascular adipose tissue (PVAT), which surrounds the large conduit arteries of the heart, contribute to impaired endothelial-dependent dilation and augmented smooth muscle contraction in the setting of obesity^{2;9;171;172;177;184} Specifically, coronary PVAT has been shown to potentiate coronary artery contractions and attenuate vasodilation via effects on Rho kinase signaling and smooth muscle Ca_v1.2 and K⁺ channels^{2;141;172;252} While these effects are in contrast with the anti-contractile effects of peripheral PVAT,^{8;62;157;162} they are consistent with reported increases in pro-inflammatory and pro-atherogenic factors in coronary PVAT of subjects with documented atherosclerotic disease.^{48;73;75;253} However, the specific adipokines and pathways responsible for these deleterious influences remain ill defined.

A growing body of evidence implicates a role for the adipose tissue hormone, leptin, as a key upstream mediator of pathways associated with coronary vascular dysfunction and the initiation and progression of coronary disease in obesity.^{70;254} Plasma concentrations and expression of leptin in coronary PVAT are markedly elevated in obese subjects^{2;177;179;191;251} and leptin receptors (ObR) are highly expressed throughout the wall of diseased coronary arteries.^{2;202;255;256} Increases in leptin levels (30 – 90 ng/mL) have been associated with the activation of a number of pro-inflammatory pathways (e.g. monocyte chemoattractant protein-1; tumor necrosis factor- α),^{195;257} attenuation of endothelial-dependent dilation, and further impairment of obesity-induced endothelial dysfunction.^{2;255;258} However, the effects of leptin on coronary vascular smooth muscle

remain equivocal, as leptin either attenuates or has no effect on contractile responses to a variety of agonists in isolated rat aorta.²⁰²⁻²⁰⁴ Importantly, the majority of these studies were conducted following acute, short-term exposure to leptin (30-60 min). Therefore, understanding of the vascular effects of longer-term leptin exposure is rather limited.

Several studies suggest an interrelationship between leptin signaling and the RhoA/Rho kinase pathway, a known regulator of vascular smooth muscle contraction.²⁵⁹⁻²⁶¹ Recent findings demonstrate that perivascular overexpression of leptin promotes neointima formation after carotid artery injury²⁰⁷ and that exogenous administration of leptin stimulates proliferation of isolated vascular smooth muscle cells from rodents.^{198;206;262} Interestingly, activation of the RhoA/Rho kinase pathway has been implicated in leptin-mediated increases in vascular smooth muscle cell proliferation and hypertrophy.²⁶⁰ However, contrasting studies have found that leptin produces dose-dependent decreases in proliferation²⁵⁶ and have failed to support a role for RhoA/Rho kinase in mediating vascular smooth muscle proliferation.^{226;263} Thus, further studies are required to identify the effects of short-term and long-term leptin administration on coronary vascular smooth muscle contraction and proliferation and to elucidate the precise mechanisms involved.

Accordingly, the purpose of this investigation was to test the hypothesis that leptin promotes (1) marked alterations in the coronary proteomic expression profile that favor pathways associated with vascular smooth muscle contraction and proliferation; and (2) increases in coronary smooth muscle contraction and proliferation via a Rho kinase dependent pathway. Findings from this investigation provide novel evidence that leptin contributes to mechanistic alterations in coronary vascular function and support the growing paradigm that leptin acts as an upstream mediator in the development of obesity-induced coronary disease.

MATERIALS AND METHODS

All experimental procedures and protocols in this investigation were approved by the Institutional Animal Care and Use Committee in accordance with the *Guide for the Care and Use of Laboratory Animals*. Upon sacrifice, hearts from domestic swine (body weight ~50 kg) were excised and perfused via aortic cannulation with 4°C, Ca²⁺-free Krebs buffer (131.5 mM NaCl, 5mM KCl, 1.2 mM NaH₂PO₄, 1.2 mM MgCl₂, 25mM NaHCO₃, 10 mM glucose). Coronary arteries were grossly dissected from the adjacent myocardium and epicardial adipose tissue. Arteries were then further isolated from the surrounding perivascular adipose tissue and adventitia using a dissecting microscope before being cut into 3 mm rings and subjected to the protocols outlined below.

Proteomics

Coronary arteries were cut into 3 mm rings and were placed in 12-well tissue culture dishes with serum-free, low glucose (100 mg/dL) Dulbecco's Modified Eagle Medium (DMEM: Corning Cellgro, Manassas, VA, 10014CM) containing penicillin (100 U/mL) and streptomycin (100 µg/mL) (MP Biomedicals, 1670249). Arteries were maintained in a 5% CO₂ atmosphere at 37°C for three days of incubation without (control) or with leptin (30 ng/mL: Sigma Aldrich, St. Louis, MO, L4146) for 3 days. Following the culture period, arteries were frozen in liquid N₂ and delivered on dry ice to the Ohio State University Proteomics Core for protein extraction. Tissues were homogenized in 1:10 w/v in ice cold Buffer A (1% digitonin, 0.05% NP-40, NaCl 150 mM, Tris 50 mM, pH 7.4) with Complete Protease Inhibitors and PhosSTOP (Roche Diagnostics) using a polytron homogenizer (Power Gen 700, Fisher Scientific). Proteins were extracted on ice for 1 hr, centrifuged at 80,000g for 30 min, and protein concentration of supernatant was

determined with the Dc Protein Assay (Bio-Rad). Proteins were eluted in Laemmli Reducing Sample Buffer for 1D gel electrophoresis.

In-Gel Digestion

Each band was cut into 8 fractions based on relative protein abundance and placed in 96 well plates for in-gel digestion. Briefly, gel pieces were washed in 100 μ l of 50% methanol/5% acetic acid for 30 min. The wash step was repeated a total of 3 times and slices were left in a storage solution of 50 μ l of 50% methanol/5% acetic acid until digestion. Digestion was carried out by adding 100 μ l 50 mM ammonium bicarbonate (ABC) for 10 min followed by 100 μ l acetonitrile for 10 min. The gel bands were rehydrated with dithiothreitol (DTT) (prepared as 5 mg/ml in 50 mM ABC) and incubated for 30 min followed by a 30 min incubation with iodoacetamide (prepared as 15 mg/ml iodoacetamide in 50 mM ABC) in the dark. The gel bands were washed again with 2 cycles of acetonitrile and 50 mM ABC in 10 and 5 min increments, respectively and then dried for 10 min. The protease was driven into the gel pieces by rehydrating them in 50 μ L of sequencing grade modified trypsin from Promega (Madison, WI, prepared at 5 μ g/ml with 0.01% ProteaseMAX Surfactant in 50 mM ABC) and incubated at room temperature overnight. The peptides were extracted from the polyacrylamide with 50 μ l 50% acetonitrile and 5% formic acid for 10 min a total of 3 times and a final extraction with 50 μ l of acetonitrile for 10 min and then pooled together. The extracted pools were dried completely and resuspended in 20 μ l of 50 mM acetic acid.

Mass Spectrometry

The final digests were analyzed using capillary-liquid chromatography-nanospray tandem mass spectrometry (Capillary-LC/MS/MS) of global protein. Identification was performed on a Thermo Finnigan LTQ orbitrap mass spectrometer equipped with a

microspray source (Michrom Bioresources Inc, Auburn, CA) operated in positive ion mode. Samples (6.4 μ l from each fraction) were separated on a capillary column (0.2X150mm Magic C18AQ 3 μ 200A, Michrom Bioresources Inc, Auburn, CA) using an UltiMate™ 3000 HPLC system (LC-Packings A Dionex Co, Sunnyvale, CA). Each sample was injected into the μ -Precolumn Cartridge (Dionex, Sunnyvale, CA) and desalted with 50 mM acetic acid for 5 min. The injector port was then switched to injection mode and the peptides were eluted off of the trap onto the column. Mobile phase A was 50mM acetic acid in water and acetonitrile was used as mobile phase B. Flow rate was set at 2 μ l/min. Mobile phase B was increased from 2% to 5% in 5 min and again from 5% to 30% in 30 min, then from 30% to 50% in 8 min. The gradient was increased again from 50% to 85% in 3 min and then kept at 85% for another 1 min before being brought back to 2% in 0.1 min. The column was equilibrated at 2% of mobile phase B (or 98% A) for 10 min before the next sample injection. MS/MS data was acquired with a spray voltage of 2.2 kV and a capillary temperature of 175 °C. The scan sequence of the mass spectrometer was based on the data dependent TopTen™ method in preview mode; the analysis was programmed for a full scan recorded between 350-2,000 Da and a MS/MS scan to generate product ion spectra to determine amino acid sequence in consecutive scans of the ten most abundant peaks in the spectrum. The full scan resolution was set at 30,000 to achieve high mass accuracy MS determination. The CID fragmentation energy was set to 35%. Dynamic exclusion is enabled with a repeat count of 1 within 18 s, a mass list size limit of 500, exclusion duration of 10 s and a low mass width and high mass width were set at 30ppm.

Protein Identification and Quantitation

Sequence information from the MS/MS data was processed by converting the .raw files into a mgf files using MsConvert (ProteoWizard) and later merged into a merged file (.mgf) using an in-house program, RAW2MZXML_n_MGF_batch ([merge.pl](#), a Perl script) and searched using Mascot Daemon by Matrix Science version 2.3.2 (Boston, MA) against the NCBI nr Other Mammalia Database (version 20150104, 1,412,788 sequences). Trypsin was used as the enzyme and four missed cleavages were permitted. Considered variable modifications were oxidation (Met), carbamidomethylation (Cys) and deamination (Asn, Gln). The mass accuracy of the precursor ions were set to 20ppm and the fragment mass accuracy was set to 0.8 Da. One ¹³C peak was included in the search in case of the accidental pick of ¹³C peaks. A decoy database was also searched to determine the false discovery rate (FDR) and peptides were filtered according to the FDR. The significance threshold was set at $P < 0.05$. Percolator score was used to further validate the search results and the actual FDR was less than 1% after using percolator scores.

Label-free quantitation was performed using the spectral count approach, in which the relative protein quantitation is measured by comparing the number of MS/MS spectra identified from the same protein in each of the multiple LC/MSMS datasets. Scaffold was used for quantitation analysis. The protein filter was set at 99% to ensure the false discovery rate is less than 1% and the peptide filter was set at 95%.

Functional Assessment of Isolated Coronary Arteries

Isometric tension studies on coronary artery rings were performed as previously described.^{9:252} Briefly, 3 mm coronary artery rings (without PVAT) were mounted in organ baths filled with Ca²⁺-containing Krebs buffer (131.5 mM NaCl, 5mM KCl, 1.2 mM

NaH₂PO₄, 1.2 mM MgCl₂, 25mM NaHCO₃, 10 mM glucose, 4mM CaCl₂) and maintained at 37°C. Once stabilized at optimal passive tension (~4 g), arteries were incubated without (control) or with leptin (30 ng/mL: Sigma Aldrich, L4146) and/or fasudil (1 μM: Sigma Aldrich, H139) for 30 minutes (acute exposure) and then exposed to increasing concentrations of KCl (10 – 60 mM) and to the thromboxane A₂ receptor agonist, U46619 (1 μM: Tocris, 1932). Coronary arteries cultured in serum-free media for 3 days with or without leptin (30 ng/mL: Sigma Aldrich, L4146) and/or fasudil (1 μM: Sigma Aldrich, H139) (chronic exposure) were also mounted in organ baths and exposed to increasing concentrations of KCl (10 – 60 mM) and to U46619 (1 μM: Tocris, 1932). Acute and chronic studies were also conducted in endothelium denuded coronary arteries in which the endothelium was removed by gently rubbing fine-tip forceps along the lumen. Active tension development (peak tension minus baseline tension) was recorded at each concentration for each group. Endothelial denudation was confirmed by <15% relaxation to bradykinin (1 μM: Sigma Aldrich, B3259).

Western Analysis

Following acute (30 minute) or chronic (3 day culture) incubation with or without leptin, coronary arteries were frozen in liquid N₂ and stored at -80°C. Arteries were homogenized in 70 μL of Tissue Protein Extraction Reagent (Thermo Scientific, 78510) and total protein was quantified as previously described.²³³ Equivalent amounts of protein (50 μg) were loaded onto 10% polyacrylamide gels (Life Technologies, NP0302) for electrophoresis and blotting. Membranes were incubated with primary antibody directed against Rho kinase (Rock-2, 1:200, Santa Cruz Biotechnology, sc-1851) overnight at 4°C and donkey anti-goat IRDye 800CW secondary antibody (1:15,000, Li-Cor, 926-32214) for 1 hour at room temperature. To verify equal protein loading, membranes were washed

and incubated with antibody to β -actin (1:200, Santa Cruz Biotechnology, sc-1616). Immunoreactivity was visualized using a Li-Cor Odyssey CLx imaging system. Chameleon Duo (Li-Cor) was used as a protein ladder. Densitometry analyses were conducted using Li-Cor Image Studio Lite, version 5.2. Protein levels were normalized to levels of β -actin and reported as “% control,” i.e. protein levels from each sample were normalized to the average level of the protein in control arteries within the same condition.

Rho Kinase Activity Assay

Protein homogenates of the samples outlined above were subjected to a commercially available enzyme immunoassay for the detection of active Rho kinase (Rho-associated Kinase (ROCK) Activity Assay, Millipore, CSA001). Briefly, equal amounts of protein (50 μ g) from each sample were added to plates pre-coated with recombinant MYPT1. A detection antibody specific for phosphorylated MYPT1 and a HRP-conjugated secondary antibody were added, respectively. The amount of phosphorylated substrate was measured by adding the chromogenic substrate tetramethylbenzidine and reading the absorbance signal at 450 nm. Absorbance values were then normalized to a standard curve of active recombinant ROCK-II enzyme.

Proliferation Assays

Additional culture studies were conducted in which arteries were incubated in serum-containing (30% fetal bovine serum, Gibco, 10437-028), low glucose (100 mg/dL) Dulbecco's Modified Eagle Medium (DMEM: Corning Cellgro, 10014CM) containing penicillin (100 U/mL) and streptomycin (100 μ g/mL) (MP Biomedicals, 1670249) at 37°C in a 5% CO₂ atmosphere. Arteries were incubated with or without leptin (30 ng/mL: Sigma

Aldrich, L4146) and/or fasudil (1 μ M: Sigma Aldrich, H139) for 8 days, with media changes conducted every 2 days. To confirm functional responses at this time point, both intact and denuded arteries were subjected to the isometric tension studies outlined above. In a subset of untreated and leptin treated arteries, 5-Bromo-2'-deoxyuridine (BrdU; 20 μ mol/L) was added to the culture medium for the final 6 hours of culture. Arteries were then fixed in 10% formalin, paraffin embedded, and processed for BrdU labeling in nuclei utilizing an immunohistochemical detection assay (BrdU Labeling and Detection Kit II, Roche, 11299964001). Arteries left untreated with BrdU were used as negative controls for the immunohistochemical procedure. Positive staining for BrdU-labeled nuclei indicates DNA synthesis, a marker of cellular proliferation. To specifically investigate vascular smooth muscle proliferation, arteries from all treatment groups were formalin fixed, paraffin embedded, and processed for co-immunostaining with anti- α smooth muscle actin (1:50, Abcam, ab5694) and anti-proliferating cell nuclear antigen (PCNA, 1:2,000, Abcam, ab29). Mach 2 Double Stain 2 (Biocare Medical, MRCT525) was used as secondary with chromogens Vulcan Fast Red and 3,3'-diaminobenzidine, respectively. Immunohistochemistry was performed in conjunction with the Indiana University Health Pathology Laboratory (Indianapolis, IN). Slides were imaged at 20X magnification. Four distinct fields of view were captured per artery and data were averaged for n=1. Quantitation of positive staining was performed using the open source modification of Image J (Fiji) ²³² and a custom modification of the trichrome quantification macro (The University of Chicago Integrated Light Microscopy Core Facility). Positive PCNA staining was quantitated in artery regions also staining positively for α -smooth muscle actin. Data are reported as "% control," i.e. percent positive staining from each sample was normalized to the average level of positive staining in untreated, control arteries.

Statistical Analyses

Statistical comparisons of proteomic results were performed on proteins which met Scaffold false discovery rate (FDR) criterion by Student's t-test. Proteins with $P < 0.05$ were considered significantly different between treatment groups. Protein lists and corresponding expression values were uploaded onto the Ingenuity Pathway Analysis software server (content version: 24718999) and analyzed to interpret cellular functions and canonical pathways associated with alterations in the proteomic profile between treatment groups. For isometric tension studies, a two-way ANOVA was used to test the effects of leptin and/or inhibitors (Factor A) relative to concentrations of specific agonists (Factor B). When statistical differences were found with ANOVA ($P < 0.05$), a Student-Newman-Keuls multiple comparison test was performed. A Student's t-test was used to compare the results of Western blot, Rho Kinase activity, and proliferation assays. Data are presented as mean \pm SE with "n" equal to number of pigs studied. SigmaPlot version 11.0 (Systat Software Inc, San Jose, CA) was used for all statistical analyses and generation of figures.

RESULTS

Effect of leptin exposure on the coronary proteomic expression profile

To investigate potential factors and pathways affected by leptin exposure, global proteomic profiling was performed on coronary arteries cultured in the presence or absence of leptin (30 ng/mL) for 3 days. This non-biased target discovery approach detected significant alterations in 69 proteins ($P \leq 0.05$) in leptin treated arteries. A complete list of the 793 detected proteins is provided in **Appendix B, Table I**. The top 15 unique upregulated and downregulated proteins are listed in **Table 3.1**. Ingenuity Pathway Analysis (IPA) software identified significant associations ($P < 0.001$) between leptin

treatment and numerous cellular functions, namely calcium signaling (4 proteins) and cellular growth and proliferation (35 proteins).

Table 3.1 Protein expression profile of leptin-treated coronary arteries

| Gene Name | Protein Name | Fold Change | P Value | IPA |
|-------------------------------|---|-------------|---------|-------|
| <i>Upregulated Proteins</i> | | | | |
| MYOZ2 | Calsarcin-1 (myozenin-2) | 5.8 | 0.02 | 4 |
| RAB21 | Ras-related protein, Rab-21 | 4.8 | 0.0002 | |
| SORBS1 | Sorbin and SH3 domain-containing protein 1, isoform 1 | 4.4 | 0.007 | 5 |
| LASP1 | LIM and SH3 domain protein 1 | 3.2 | 0.05 | 2,3 |
| EIF6 | Eukaryotic translation initiation factor 6, isoform X1 | 1.6 | 0.05 | 2 |
| ADIRF* | Adipogenesis regulatory factor | 1.5 | 0.02 | |
| Cald1 | Non-muscle caldesmon, isoform X1 | 1.5 | 0.005 | |
| MTPN | Myotrophin | 1.5 | 0.03 | 2 |
| S100A11 | Protein S100-A11 | 1.4 | 0.04 | 2,3 |
| RPL12 | 60S ribosomal protein L12 | 1.3 | 0.01 | |
| TPM4 | Tropomyosin alpha-4 chain, isoform X3 | 1.3 | 0.02 | 1 |
| TPM4 | Tropomyosin alpha-4 chain, isoform X2 | 1.3 | 0.03 | 1 |
| TPM4 | Tropomyosin alpha-4 chain, isoform X1 | 1.3 | 0.02 | 1 |
| TUBA1C | Tubulin alpha chain-like | 1.2 | 0.02 | 2,3 |
| TPM2 | Tropomyosin beta chain, isoform X1 | 1.2 | 0.03 | 1 |
| <i>Downregulated Proteins</i> | | | | |
| MYOF | Myoferlin | 7.6 | 0.03 | 2,4 |
| ALDH4A1 | Delta-1-pyrroline-5-carboxylate dehydrogenase, mitochondrial | 6.1 | 0.009 | |
| ATPIF1 | ATPase inhibitor, mitochondrial precursor | 4.9 | 0.00003 | 2 |
| SRI | Sorcic | 4.8 | 0.00003 | |
| SSR4 | Translocon-associated protein subunit delta, isoform X1 | 2.6 | 0.04 | |
| PRKAR2A | cAMP-dependent protein kinase type II-alpha regulatory subunit | 2.6 | 0.04 | 1,2,3 |
| CSPG4 | Chondroitin sulfate proteoglycan 4 | 2.4 | 0.03 | 2,3,5 |
| HSP90AA1 | Heat shock protein HSP 90-alpha | 2.3 | 0.02 | 2,3 |
| SLC25A3 | Phosphate carrier protein, mitochondrial | 2.3 | 0.02 | |
| FBN1 | Fibrillin-1 | 2.2 | 0.02 | 2,3,5 |
| PDIA4 | Protein disulfide-isomerase A4 precursor | 2.1 | 0.04 | |
| RNH1 | Ribonuclease inhibitor | 2.1 | 0.03 | 2,3 |
| RPN2 | Dolichyl-diphosphooligosaccharide-protein glycosyltransferase subunit 2 precursor | 2.0 | 0.02 | |
| GLUD1 | Glutamate dehydrogenase 1, mitochondrial precursor | 1.8 | 0.0004 | |
| IGTA1* | Integrin alpha 1 | 1.8 | 0.04 | |

Values for fold change in expression of coronary arteries cultured for three days with leptin (30 ng/mL) versus untreated controls (n=4 each group). Ingenuity Pathway Analysis (IPA): ¹Calcium signaling, ²Cell proliferation, ³Cell movement, migration, invasion, ⁴Quantity of smooth muscle cells, ⁵Cell spreading. *Bos taurus homolog.

These findings are of interest, as previous studies have suggested a potential link between leptin and vascular reactivity^{2;202;203;255} and proliferation.^{198;207} Additional cellular pathways/processes identified include cellular movement, migration, and invasion (25 proteins), cell spreading (6 proteins) and quantity of smooth muscle cells (4 proteins).

Acute and chronic leptin administration augments coronary artery contractions

The effects of leptin on coronary vascular reactivity were examined by comparing KCl-induced contractions of coronary arteries following short-term, acute (30 min) and long-term, chronic (3 day, serum-free culture) exposure to “obese” concentrations of leptin (30 ng/mL), i.e., plasma concentrations typically reported in obese subjects.^{192;264} Overall contractile responses of acute leptin treated arteries were significantly augmented ($P = 0.04$), with maximal tension development increased by 1.5 ± 0.2 g at 60 mM KCl (**Figure 3.1A**). Chronic exposure to leptin also augmented overall active tension development to KCl ($P < 0.001$), with an increase of 2.7 ± 0.49 g at 60 mM (**Figure 3.1B**). Control responses to KCl were reduced following 3 days of culture ($P = 0.006$, **Figure 3.1B vs 3.1A**). This reduction in contraction was also observed in response to the thromboxane A_2 receptor

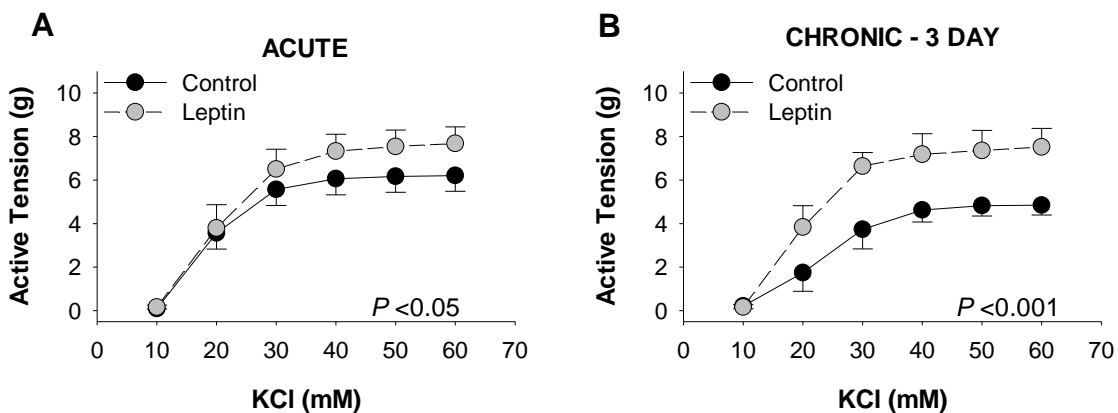


Figure 3.1 Leptin augments depolarization-induced coronary artery contractions. Acute (30 min) exposure to leptin (30 ng/mL) increased KCl-induced contractions ~ 1.3 g at doses > 40 mM ($n=9$ [A]). Chronic (3 day culture in serum-free media) leptin administration (30 ng/mL) increased tension development ~ 2.5 g at doses > 40 mM ($n=4$ [B]).

agonist, U46619 (1 μ M, $P = 0.04$), although leptin had no effect on U46619 contractions following acute ($P = 0.58$) or chronic ($P = 0.34$) exposure (**Appendix B, Figure I**). KCl contractions in control and leptin treated arteries were unaffected by removal of the endothelium, and similar effects of leptin were observed in endothelium denuded arteries (confirmed by <15% relaxation to 1 μ M bradykinin) following both acute (**Appendix B, Figure IIA**) and chronic (**Appendix B, Figure IID**) exposure.

Role of Rho kinase in leptin-mediated coronary contraction

To investigate the role of Rho kinase signaling in mediating the functional effects of leptin, coronary arteries were co-incubated with/without leptin (30 ng/mL) and/or the Rho kinase inhibitor, fasudil (1 μ M). Acute fasudil treatment significantly reduced vasoconstriction to KCl (10 – 60 mM) compared to untreated (control) arteries ($P < 0.001$, **Figure 3.2A**). In contrast, fasudil treatment had no effect on contractile responses to KCl (10 – 60 mM) in untreated (control) arteries cultured for 3 days ($P = 0.50$, **Figure 3.2B**). Fasudil administration significantly decreased the effect of acute ($P < 0.001$, **Figure 3.2C**) and chronic ($P = 0.01$, **Figure 3.2D**) leptin exposure on KCl-induced contractions. However, this effect of fasudil was markedly greater following acute (~3.8 g at concentrations >40 mM) versus chronic exposure (~1.4 g at concentrations >40 mM) to leptin ($P < 0.001$). KCl contractions in arteries treated with leptin and/or fasudil were unaffected by removal of the endothelium, and similar effects of fasudil were observed in endothelium denuded arteries following both acute (**Appendix B, Figure IIB and IIC**) and chronic (**Appendix B, Figure IIE and IIF**) exposure.

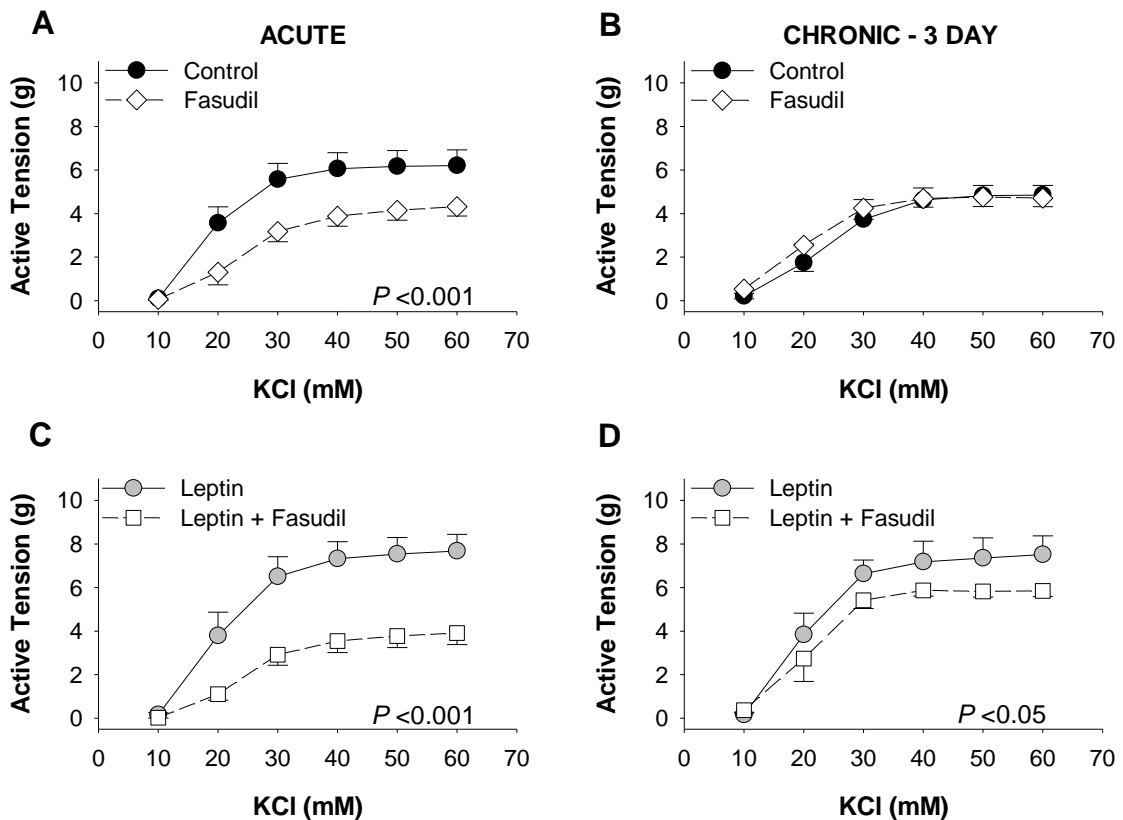


Figure 3.2 Role of Rho kinase in leptin-mediated coronary contraction. In the absence of leptin, acute (n=9 [A]), but not chronic (n=4 [B]) treatment with the Rho kinase inhibitor, fasudil (1 μ M), diminished vasoconstriction to KCl. Inhibition of Rho kinase reduced the effect of both acute (n=9 [C]) and chronic (n=4 [D]) leptin administration on KCl-induced contractions. However, the fasudil-mediated reduction in tension was greater following acute (C) versus chronic (D) leptin exposure.

Effects of leptin on Rho kinase expression and activity

Further analyses were conducted to examine the effects of leptin on Rho kinase abundance and activity. Western blot analyses revealed no difference in normalized protein abundance of Rho kinase in acute leptin treated arteries ($P = 0.61$, **Figure 3.3A and 3.3B**). A commercially available Rho-associated kinase (ROCK) activity assay demonstrated that acute leptin exposure significantly increased the level of Rho kinase activity from $0.50 \pm 0.07 \mu\text{U}/\mu\text{L}$ in untreated arteries to $1.61 \pm 0.25 \mu\text{U}/\mu\text{L}$ in leptin treated arteries ($P = 0.01$, **Figure 3.3C**). Following chronic exposure to leptin (3 day, serum-free culture), the abundance of Rock-2 protein was increased ~ 3.5 -fold relative to untreated

cultured arteries ($P = 0.009$, **Figure 3.3D and 3.3E**). While Rho kinase activity level was increased relative to acute untreated arteries following 3 days of culture, chronic exposure to leptin did not affect overall Rho kinase activity, relative to untreated time-control ($1.73 \pm 0.36 \mu\text{U}/\mu\text{L}$ in untreated versus $1.60 \pm 0.16 \mu\text{U}/\mu\text{L}$ in leptin treated arteries; $P = 0.92$, **Figure 3.3F**).

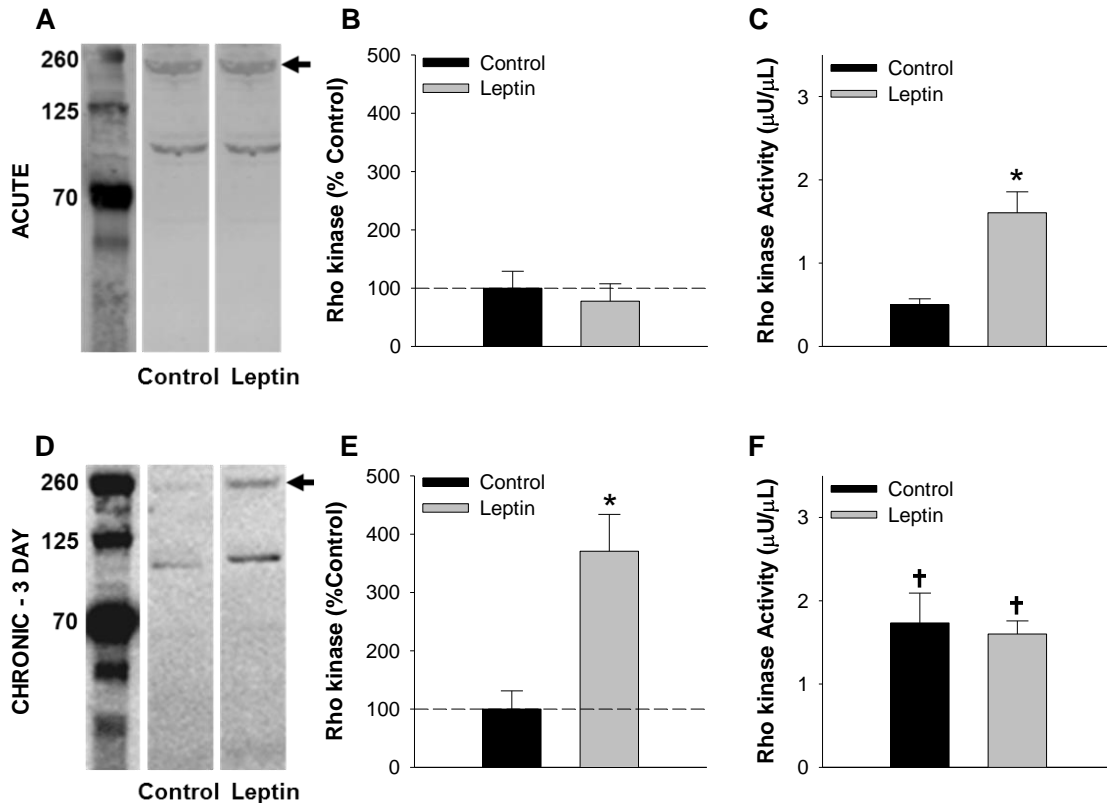


Figure 3.3 Effects of acute versus chronic leptin treatment on Rho kinase. Representative blots of Rho kinase protein abundance in coronary arteries following acute (A) and chronic (3 day culture in serum free media) (D) leptin exposure. Average data are expressed as % relative to control. Acute leptin treatment increased Rho kinase activity (C) in the absence of a change in protein abundance (B). Following chronic exposure, protein abundance was significantly elevated in leptin treated arteries (E), while no difference in overall Rho kinase activity was detected relative to untreated control arteries (F). All groups $n=3$. * $P<0.05$, leptin vs. control. † $P<0.05$, vs. acute control.

Leptin and vascular smooth muscle cell proliferation

Additional studies were conducted to directly investigate the effects of leptin on coronary vascular proliferation. In initial experiments, coronary arteries were cultured in

serum-containing media for 8 days in the presence or absence of leptin, with 5-Bromo-2'-deoxyuridine (BrdU) added to the media for the final six hours of culture. Systematic quantitation of the BrdU staining pattern using ImageJ revealed a ~32% increase in BrdU-positive nuclei in leptin treated relative to untreated, control arteries ($P = 0.02$, **Appendix B, Figure III**). Based on these findings, further studies were conducted in arteries cultured with or without leptin (30 ng/mL) and/or fasudil (1 μ M) for 8 days. The functional effects of leptin and/or fasudil were conserved in both endothelium intact (**Appendix B, Figure IVA-C**) and endothelium denuded arteries (**Appendix B, Figure IVD-F**) at this time point. Overall KCl-induced vasoconstriction in untreated, control arteries was reduced following 8 days of culture ($P < 0.001$, **Appendix B, Figure IVA versus 3.1B**). This reduction in contraction was also observed in response to U46619 (1 μ M, $P = 0.002$), although leptin had no effect on U46619 contractions following chronic, 8 day exposure ($P = 0.61$, **Appendix B, Figure I**).

To investigate the role of Rho kinase on leptin-mediated increases in vascular smooth muscle proliferation, arteries were co-immunostained for α -smooth muscle actin and proliferating cell nuclear antigen (PCNA). Systematic quantitation of the PCNA staining pattern within the vascular smooth muscle layer revealed a ~22% increase in PCNA-positive nuclei in leptin treated (Figure 4B) relative to untreated, control arteries ($P = 0.04$, **Figure 3.4A**). Treatment with fasudil alone had no effect on proliferation relative to untreated control arteries ($P = 0.50$). Co-treatment with leptin and fasudil (**Figure 3.4C**) significantly reduced the effect of leptin on vascular smooth muscle proliferation ($P = 0.002$, **Figure 3.4D**).

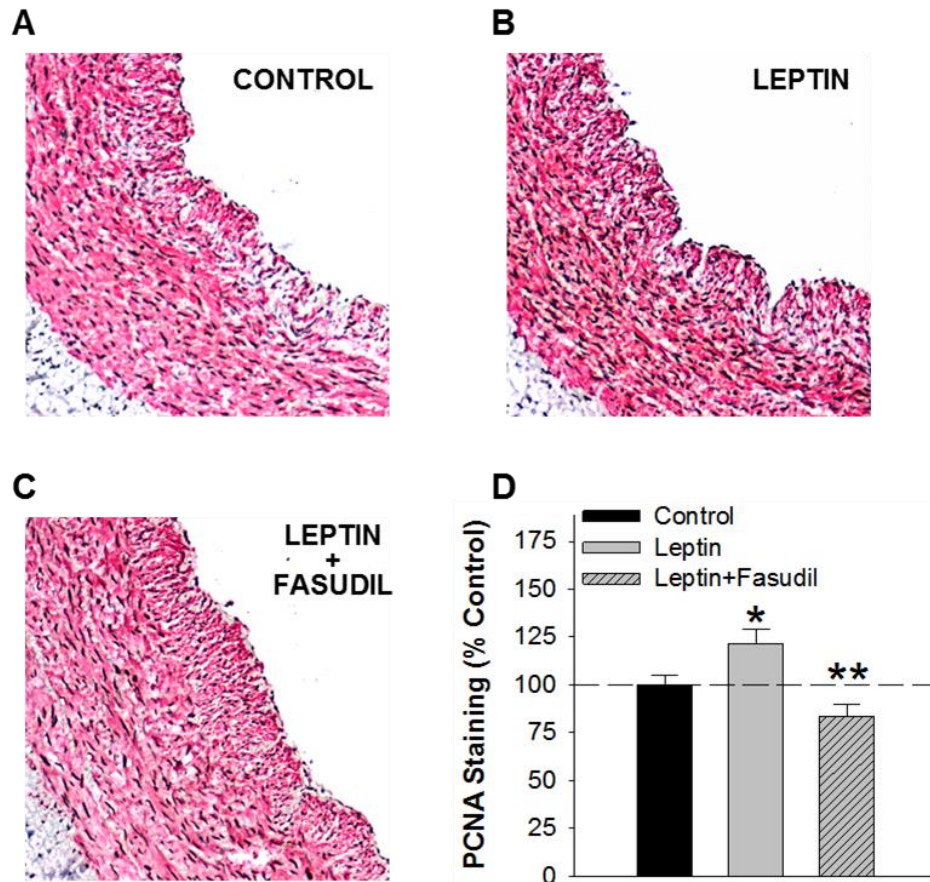


Figure 3.4 Leptin augments coronary vascular smooth muscle proliferation via effects on Rho kinase. Representative images of α -smooth muscle actin (red) and proliferating cell nuclear antigen (brown) co-immunostaining of untreated, control (A), leptin treated (B), and leptin and fasudil co-treated arteries (C) following chronic, 8 day culture in serum-containing media. The increase in PCNA-positive nuclei in leptin treated, relative to untreated arteries was significantly reduced by inhibition of Rho kinase with fasudil (D). All groups n=5. * P <0.05, leptin vs. control. ** P <0.05 leptin vs. leptin+fasudil.

Increases in proliferation with leptin treatment (8 day, serum-containing culture) were associated with a modest increase in Rho kinase protein abundance ($P = 0.18$, **Figure 3.5A and 3.5B**) and a significant increase in Rho kinase activity, averaging $1.52 \pm \mu\text{U}/\mu\text{L}$ in untreated and $2.40 \pm 0.12 \mu\text{U}/\mu\text{L}$ in leptin treated arteries ($P = 0.03$, **Figure 3.5C**). The effect of leptin on Rho kinase activity was significantly reduced by co-incubation with fasudil ($P = 0.002$, **Figure 3.5C**).

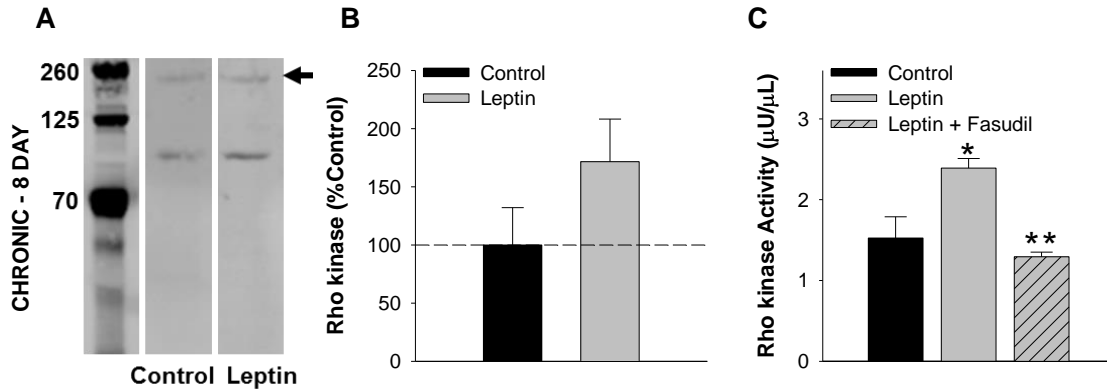


Figure 3.5 Effects of leptin-induced vascular smooth muscle proliferation on Rho kinase. Representative blot of Rho kinase protein abundance in control versus leptin treated arteries following 8 days of culture in serum-containing media (**A**). Leptin administration significantly increased Rho kinase activity (**C**), while only a modest increase in Rho kinase protein abundance was detected (**B**). The effect of leptin on Rho kinase activity was abolished by co-incubation with fasudil (**C**). All groups n=5. * $P < 0.05$, leptin vs. control. ** $P < 0.05$ leptin vs. leptin+fasudil.

DISCUSSION

The purpose of this investigation was to test the hypothesis that leptin modifies the coronary proteomic expression profile and promotes increases in coronary smooth muscle contraction and proliferation via influences on Rho kinase signaling. The major new findings are: (1) chronic exposure to obese concentrations of leptin (30 ng/mL, 3 day culture) induces marked alterations in the coronary artery proteome (68 proteins) with a significant influence on calcium signaling/contraction and cellular growth and proliferation; (2) acute (30 min) and chronic (3 day, serum-free media) exposure to leptin potentiates voltage-dependent contraction of isolated coronary arteries; (3) acute and chronic leptin-mediated increases in coronary vasoconstriction occur concomitantly with increases in activity and protein abundance of Rho kinase, respectively; (4) chronic leptin administration (8 day, serum-containing media) augments vascular smooth muscle proliferation via increases in Rho kinase activity; and (5) the contractile and proliferative effects of leptin exposure were abolished by the Rho kinase inhibitor fasudil. Taken together, these findings provide novel

evidence in support of the paradigm of leptin as an upstream mediator that contributes to marked phenotypic alterations in coronary smooth muscle in the setting of obesity.

Leptin as an upstream mediator of coronary vascular disease

Although recent findings have implicated leptin as an upstream paracrine mediator of a key network of pathways associated with obesity-induced coronary vascular disease, no study has systematically investigated the potential factors and/or pathways involved. Accordingly, we conducted a global proteomic assessment of coronary arteries with and without chronic (3 day) exposure to “obese” concentrations of leptin, i.e., plasma concentrations typically reported in obese subjects (30 ng/ml).^{192;264} This non-biased discovery approach revealed that leptin administration markedly influences the abundance of numerous proteins (**Table 3.1**). These data support that leptin signaling alters the expression of a large number of factors which have the potential to mediate additional paracrine effects within the vascular wall. Indeed, Ingenuity Pathway Analysis (IPA) identified alterations within several key cellular processes in leptin treated arteries. Specifically, IPA revealed that the detected changes in the proteomic expression profile corresponded to pathways associated with calcium signaling (e.g., calreticulin, cAMP-dependent protein kinase type II, tropomyosin) and cellular growth and proliferation (e.g., myotrophin, myoferlin, fibrillin-1). These findings are consistent with a previous proteomics assessment from our laboratory which documented an altered secretion profile of coronary PVAT in obese swine which corresponded with pathways associated with cellular growth and proliferation and cellular movement.⁹ Furthermore, these alterations in the secretion profile were also associated with increases in vascular smooth muscle contraction.⁹ Together with reports of elevated expression of leptin in obese coronary PVAT,² the current proteomic findings support a role for leptin in coronary vascular contraction and proliferation in the setting of obesity.

These findings have significant (patho)physiologic implications. Recent studies from our laboratory and others indicate that obesity augments coronary smooth muscle $\text{Ca}_V1.2$ current and voltage dependent increases in intracellular Ca^{2+} concentration.^{9;141;265} Changes in intracellular Ca^{2+} handling are known to influence both contraction and phenotypic modulation of coronary smooth muscle (i.e. development of a proliferative and/or osteogenic phenotype).^{144;266;267} Recent data also indicate that leptin increases proliferation of isolated smooth muscle cells^{197;198} and that perivascular leptin overexpression promotes neointimal formation in peripheral (non-coronary) arteries.²⁰⁷ Taken together, the present findings and those of others support the growing paradigm regarding a mechanistic role for heightened levels of leptin in obesity-induced coronary disease.

Leptin and coronary smooth muscle contraction

Current understanding of the effects of leptin on vasoconstriction is rather limited and conflicting. Acute leptin administration has been shown to inhibit angiotensin (Ang) II-induced contractions of isolated rat aorta by diminishing the increase in cytosolic $[\text{Ca}^{2+}]$ in smooth muscle cells.²⁰² In contrast, other studies fail to demonstrate an effect of leptin on contractile responses to Ang II, noradrenaline, or endothelin-1.²⁰² Chronic systemic leptin administration in normal rats has been shown to produce modest increases in phenylephrine-induced contractions of aortic rings.²⁶⁸ These disparate findings are likely related to differences in the concentration of leptin used (0.01 – 100 nmol/L), duration of treatment, vascular bed being studied, and/or the overall health status of the animal model. Results from this study demonstrate that “obese” concentrations of leptin (30 ng/mL) potentiate depolarization-induced contraction of coronary arteries following acute (30 min, **Figure 3.1A**) and chronic administration (3 day culture, **Figure 3.1B**). These distinct coronary vascular effects of leptin are consistent with recent studies documenting

a unique contractile effect of coronary PVAT on vascular smooth muscle compared to other artery/adipose tissue depots that is further augmented in the setting of obesity.⁹ Results also demonstrate that leptin has little to no effect on thromboxane A₂ receptor-mediated contractions (**Appendix B, Figure II**), suggesting that the functional effects of leptin observed in this study are specifically related to depolarization-induced contraction. This effect of leptin is consistent with reports of augmented coronary vasoconstriction in the setting of obesity⁴ and, together with both elevated plasma leptin concentration^{191;192} and increased local (coronary PVAT) leptin production^{2;177} in the setting of obesity, support the potential for leptin (plasma and/or local PVAT-derived) to contribute to the development of coronary vascular smooth muscle dysfunction.

Rho kinase and coronary smooth muscle contraction

The mechanisms by which leptin influences coronary vascular smooth muscle function remain ill defined. Recent studies suggest a connection between leptin and RhoA/Rho kinase signaling,²⁵⁹⁻²⁶¹ which is a well-known major regulator of smooth muscle contraction and vascular tone.²²⁰ However, whether RhoA/Rho kinase contributes to the coronary vascular effects of leptin has not been determined. Data from this investigation support a role for Rho kinase in leptin-mediated increases in depolarization-induced coronary artery contraction. These findings are consistent with previous studies from our laboratory which found marked increases in RhoA expression in obese coronary PVAT and that inhibition of Rho kinase attenuates PVAT-mediated increases in coronary vascular smooth muscle contraction.⁹ We propose the effects of leptin occur independent of influences on coronary endothelium as studies in endothelium denuded arteries (**Appendix B, Figure II**) were directionally consistent with studies in endothelium intact arteries.

The present findings also indicate that the effects of leptin on the Rho kinase pathway are time-dependent. Acutely, inhibition of Rho kinase significantly inhibits coronary artery contractions both in the presence (**Figure 3.2C**) and absence (**Figure 3.2A**) of leptin, whereas following chronic culture for 3 days, the inhibition of Rho kinase significantly inhibits coronary artery contractions only in the presence of leptin (**Figure 3.2D**). It is important to note that, in the absence of leptin, the contribution of Rho kinase to KCl-induced contractions was reduced following organ culture (**Figure 3.2B versus 3.2A**) and that the effects of the Rho kinase inhibitor, fasudil, on contractile responses following chronic (**Figure 3.2D**) compared to acute (**Figure 3.2C**) leptin exposure were relatively modest. Interestingly, these findings are consistent with previous reports of a reduced contribution of Rho kinase to maximal KCl contractions in obese compared to lean arteries.⁹

The time-dependent effects of leptin on Rho kinase are further highlighted data indicating that acute (30 min) leptin treatment increased Rho kinase activity (**Figure 3.3C**), independent of changes in Rho kinase expression (**Figure 3.3A and 3.3B**), while chronic exposure to leptin (3 day culture) was associated with increased Rho kinase protein abundance (**Figure 3.3D and 3.3E**) with little/no change in overall Rho kinase activity (**Figure 3.3F**). It should be noted, however, that overall Rho kinase activity of cultured arteries was significantly elevated relative to untreated, acute controls (**Figure 3.3F versus Figure 3.3C**). Altogether, these findings indicate that the coronary vascular actions of leptin are mediated, at least in part, via time-dependent influences on Rho kinase activity (acute) and expression (chronic) and are consistent with phenotypic changes observed in coronary artery disease.

Although the proteomic analyses in this study indicated alterations in pathways involved in the regulation of vascular tone, no significant alterations in proteins involved in the regulation of Rho kinase activation (e.g., RhoA, rho GDP-dissociation inhibitor, rho

GTPase activating protein) or in Rho kinase substrates involved in contraction (e.g., MYPT-1, CPI-17, myosin light chain MLC) were detected by Ingenuity Pathway Analysis following chronic, 3 day leptin treatment (**Appendix A, Table I**). However, it is important to consider that the proteomics approach used in this study excludes the examination of the phosphorylation status of key regulatory proteins in this cascade as well as the examination of potential lipid mediators. Despite the lack of detection of a direct connection, the proteomic analyses provide valuable insights into the complex cellular processes and pathways influenced by chronic leptin exposure.

Leptin and coronary vascular smooth muscle proliferation

Based on the current and prior evidence supporting that leptin is associated with cellular growth and proliferation pathways, additional experiments were performed to directly investigate the effects of leptin on coronary proliferation. In these studies, coronary arteries were cultured in serum-containing media for 8 days. Quantitation of co-immunostaining for PCNA and α -smooth muscle actin revealed a significant increase in PCNA-positive vascular smooth muscle cells in arteries exposed to leptin (30 ng/ml) that was inhibited by co-incubation with fasudil (**Figure 3.4**). The leptin-induced increase in coronary proliferation reported in this study was associated with a modest increase in Rho kinase protein abundance (**Figure 3.5A and 3.5B**) and a significant increase in Rho kinase activity (**Figure 3.5C**) relative to untreated, controls. These data further support that the effects of leptin on Rho kinase protein abundance and activity are dependent, at least in part, on the time-course of administration (e.g., acute, 3 day, 8 day) and culture condition (e.g., serum-free versus serum-containing). Although the precise molecular mechanisms responsible for this dynamic effect of leptin on Rho kinase signaling are presently unknown, we postulate that these effects occur independently of influences on coronary endothelium, as endothelial denudation had little to no effect on functional

responses following chronic, 8 day treatment with leptin and/or fasudil (**Appendix B, Figure IV**). However, the possibility that the observed effects of leptin on proliferation are mediated by factors released from endothelial cells cannot be ruled out. Our findings are consistent with other studies which have documented leptin-induced vascular smooth muscle hypertrophy,^{260;269} smooth muscle proliferation,^{197;198;207} and neointimal formation^{206;207} in rodent models, although contrasting evidence in rat aortic smooth muscle cells exposed to Ang II²⁷⁰ and in a human smooth muscle cell line²⁵⁶ have also been reported. However, to our knowledge, the present data are the first to demonstrate that (patho)physiologically relevant (“obese”) concentrations of leptin are capable of promoting vascular smooth muscle proliferation and to provide evidence in support of a mechanistic linkage between Rho kinase and leptin-mediated increases in proliferation in the coronary circulation.

Limitations

Although this investigation utilizes arteries from the translationally relevant porcine coronary circulation, relevant obese concentrations of leptin, and a time course (i.e., acute and chronic) of leptin administration, it is presently unclear to what extent these findings translate to the human condition. However, the present study is among the first to systematically investigate the factors and pathways involved in leptin-induced phenotypic alterations of coronary arteries (i.e., increased contraction and proliferation). While functional data support that the vascular smooth muscle layer is responsible for the observed effects of leptin, the precise factors and cell types involved remain to be definitively determined. Additionally, a pharmacologic approach was utilized to interrogate the Rho kinase pathway in this study. Based on reported IC₅₀ values for fasudil,²⁷¹⁻²⁷³ a concentration of 1 μM was chosen to potently inhibit Rho kinase and minimize off target effects. Although the possibility of non-specific effects cannot be ruled out, data in which

fasudil diminishes Rho kinase activity in this study (**Figure 3.5C**) support the specificity and efficacy of this pharmacologic approach. However, future genetic knockdown (e.g. antisense oligonucleotides) studies to confirm the present findings are warranted.

Conclusions & Implications

The present data provide novel evidence that relevant obese concentrations of leptin promote increases in coronary vasoconstriction and smooth muscle proliferation and that these phenotypic effects are directly associated with alterations in the coronary artery proteome and dynamic effects on the Rho kinase pathway. Although the current studies were conducted using (patho)physiologically relevant (“obese”) concentrations of leptin, a critical question remains as to the extent to which locally produced versus circulating leptin contributes to the initiation and progression of coronary disease *in vivo*. Future studies to directly investigate the mechanisms responsible for the time-dependent effects of leptin on Rho kinase protein abundance and activity are also warranted. Regardless, this investigation provides novel evidence in support of leptin as an upstream mediator of the hypercontractile and proliferative coronary smooth muscle phenotype reported in obesity-induced coronary disease.

DISCLOSURES

On behalf of all authors, the corresponding author states that there is no conflict of interest.

Chapter 4

Discussion

Summary of Findings

The World Health Organization has described obesity as one of the most visible, yet most neglected, public health crises in recent history, as increased adiposity is a significant risk factor for cardiovascular disease, the leading cause of death throughout the world.^{274;275} A recent World Health Organization agreement challenged healthcare systems throughout the world to develop innovative strategies to address the burden of cardiovascular disease being fueled by the obesity pandemic.²⁷⁶ However, despite significant advances in research over the past several decades, the precise mechanism(s) linking increased adiposity and cardiovascular disease remain poorly understood.

There is a growing body of evidence to support a role for local epicardial adipose tissue in the development of obesity-induced cardiovascular disease. In particular, recent findings implicate the adipose tissue immediately surrounding the major coronary arteries, known as coronary perivascular adipose tissue (PVAT), in the initiation and progression of coronary artery disease. Coronary PVAT has been shown to be one of the best predictors of the presence and severity of coronary artery disease, even more so than other visceral adipose tissue depots (e.g., abdominal adipose).²⁷⁷ This supports a novel paracrine pathway for the development of coronary vascular disease that may function independently of alterations in circulating adipokine levels. This “outside-in” hypothesis is supported by recent studies that reveal an upregulation of pro-atherogenic adipokines released from coronary PVAT in the setting of obesity and demonstrate effects of these adipokines on inflammation, endothelial and smooth muscle function, and atherogenesis.^{2;9;15;176;177} Although prior findings implicate coronary PVAT in the pathogenesis of vascular dysfunction, the precise mechanisms by which specific coronary PVAT-derived factors influence smooth muscle function and the progression of atherogenesis have not been established.

Accordingly, the central focus of this work was to examine the potential role of PVAT in the development of coronary vascular dysfunction in the setting of obesity. Specifically, the goal of this investigation was to delineate the mechanisms by which PVAT-derived factors (e.g., leptin) influence coronary vascular smooth muscle function and the pathogenesis of obesity-induced coronary disease. The findings of the following Specific Aims are summarized below:

Aim 1. Delineate the mechanisms by which lean vs. obese coronary PVAT influences coronary vascular smooth muscle reactivity.

Studies were designed to examine the effects of lean and obese coronary PVAT on end-effector mechanisms of coronary vasodilation and to identify potential PVAT-derived factors involved. An initial examination of the effects of PVAT on vasodilation revealed that the presence of coronary PVAT attenuated adenosine relaxation in coronary arteries from both lean and obese swine (**Figure 2.5**). Adenosine-induced dilation was nearly abolished by pre-constriction with KCl and was unaffected by removal of the endothelium in both control and PVAT-treated arteries, suggesting that these particular effects of PVAT on coronary vasodilation are mediated by endothelial-independent influences on coronary artery K^+ channels.

Further studies provided novel evidence that lean and obese PVAT have distinct inhibitory effects on specific coronary artery K^+ channel subtypes. In arteries from the same animal, lean coronary PVAT impaired K_{Ca} and K_V7 channel-mediated dilation while obese coronary PVAT impaired K_{ATP} but not K_{Ca} or K_V7 channel-mediated dilation (**Figure 2.3**). In the absence of PVAT, vasodilation to K_{Ca} and K_V7 channel activation was attenuated in obese relative to lean coronary arteries. However, cross-over studies in

which lean arteries (i.e., normal, healthy vascular reactivity) were incubated with lean and obese PVAT also revealed a lack of effect of obese PVAT on K_{Ca} and K_V7 channels (**Figure 2.8**). These findings strongly support that lean and obese PVAT-derived factors differentially affect K_{Ca} , K_V7 and K_{ATP} channels. **Figure 4.1** illustrates these important findings.

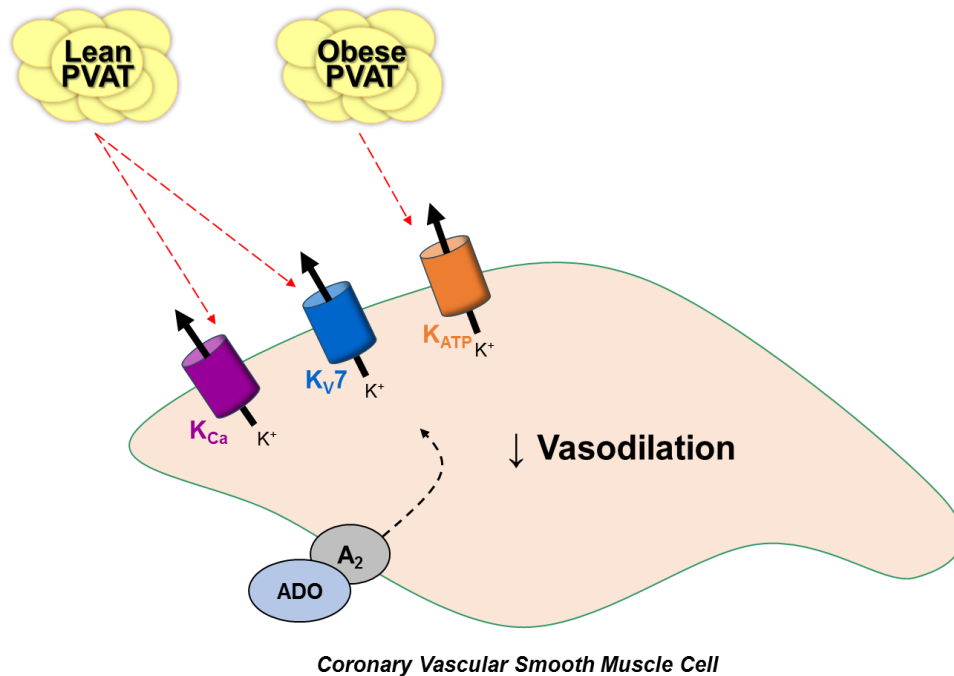


Figure 4.1 Factors derived from lean and obese coronary perivascular adipose tissue (PVAT) inhibit K^+ channel-mediated vasodilation. Coronary PVAT attenuates vasodilation via differential inhibition of vascular smooth muscle K^+ channels. Lean PVAT-derived factors inhibit K_{Ca} and K_V7 channels, while obese PVAT-derived factors inhibit K_{ATP} channels. These inhibitory effects occur independently of underlying differences in smooth muscle reactivity in coronary arteries from lean and obese swine.

Previous reports of a pro-atherogenic and pro-inflammatory adipokine profile of obese coronary PVAT were supported by evidence of atheroma formation (**Figure 2.4E**) and macrophage infiltration (**Figure 2.4I**) in obese coronary arteries surrounded by PVAT. Despite these characteristics, similarities in coronary perivascular adipocyte diameter were documented in lean and obese swine (**Figure 2.4A and 2.4B**), suggesting that

phenotypic differences in coronary PVAT occur independently of gross changes in morphology. Additional studies were designed to examine the potential for the recently identified coronary perivascular adipokine, calpastatin, to influence coronary vasodilation. Calpastatin mimicked the effects of lean coronary PVAT, attenuating adenosine dilation in lean coronary arteries (**Figure 2.9A**). This effect of calpastatin was lost in obese arteries (**Figure 2.9B**), mimicking the lack of effect of obese PVAT on K_{Ca} and K_v7 channel-mediated dilation.

Taken together, these findings demonstrate that although coronary perivascular adipocytes from lean and obese swine share similar morphology, lean and obese PVAT-derived factors impair vasodilation via differential inhibition of vascular smooth muscle K^+ channels. These results further support the paradigm of distinct “outside to inside” signaling influences of coronary PVAT and that alterations in specific factors such as calpastatin are capable of contributing to the initiation and/or progression of smooth muscle dysfunction in the setting of obesity.

Aim 2. Test the hypothesis that leptin acts as an upstream mediator in the development of coronary vascular smooth muscle dysfunction and disease.

Global proteomic analysis performed on coronary arteries chronically exposed to elevated levels of leptin (i.e., plasma concentrations typically observed in obese subjects) identified significant alterations in the coronary artery proteome relative to untreated, control arteries (**Table 3.1**). Overall, significant alterations in 69 proteins ($P \leq 0.05$) were detected in leptin treated arteries. Further analysis with Ingenuity Pathway Analysis software revealed that leptin treatment was associated with alterations in numerous cellular functions, including calcium signaling (4 proteins) and cellular growth and proliferation (35 proteins).

The mechanistic effects of leptin on coronary vascular reactivity were examined by comparing KCl-induced contractions of coronary arteries following acute (30 min) and chronic (3 day serum-free culture) exposure to obese concentrations of leptin (30 ng/mL). Both acute (**Figure 3.1A**) and chronic (**Figure 3.1B**) leptin administration potentiated KCl contraction of isolated coronary arteries. Importantly, the inhibition of Rho kinase significantly reduced leptin-mediated increases in depolarization-induced coronary contraction (**Figure 3.2**). The effects of leptin on the functional expression of Rho kinase were time-dependent, as acute treatment increased Rho kinase activity (**Figure 3.3C**) while chronic (3 day) exposure was associated with increases in Rho kinase protein abundance (**Figure 3.3D and 3.3E**).

Studies were also conducted to directly investigate the effects of obese concentrations of leptin (30 ng/mL) on coronary vascular proliferation. Quantitation of both BrdU incorporation and co-immunostaining for PCNA and α -smooth muscle actin revealed a significant increase in cellular proliferation in coronary arteries chronically exposed to leptin (8 day, serum-containing culture, **Figure 3.4**). This increase in proliferation was associated with a significant increase in Rho kinase activity (**Figure 3.5C**) and a modest increase in Rho kinase protein abundance (**Figure 3.5A and 3.5B**). Inhibition of Rho kinase significantly reduced leptin-mediated increases in proliferation and Rho kinase activity (**Figure 3.4D and 3.5C**).

Taken together, these studies indicate that pathophysiologic, obese concentrations of leptin promote increases in coronary vasoconstriction and smooth muscle proliferation and that these phenotypic effects are associated with alterations in the coronary artery proteome and dynamic effects on the Rho kinase pathway. **Figure 4.2** illustrates these findings.

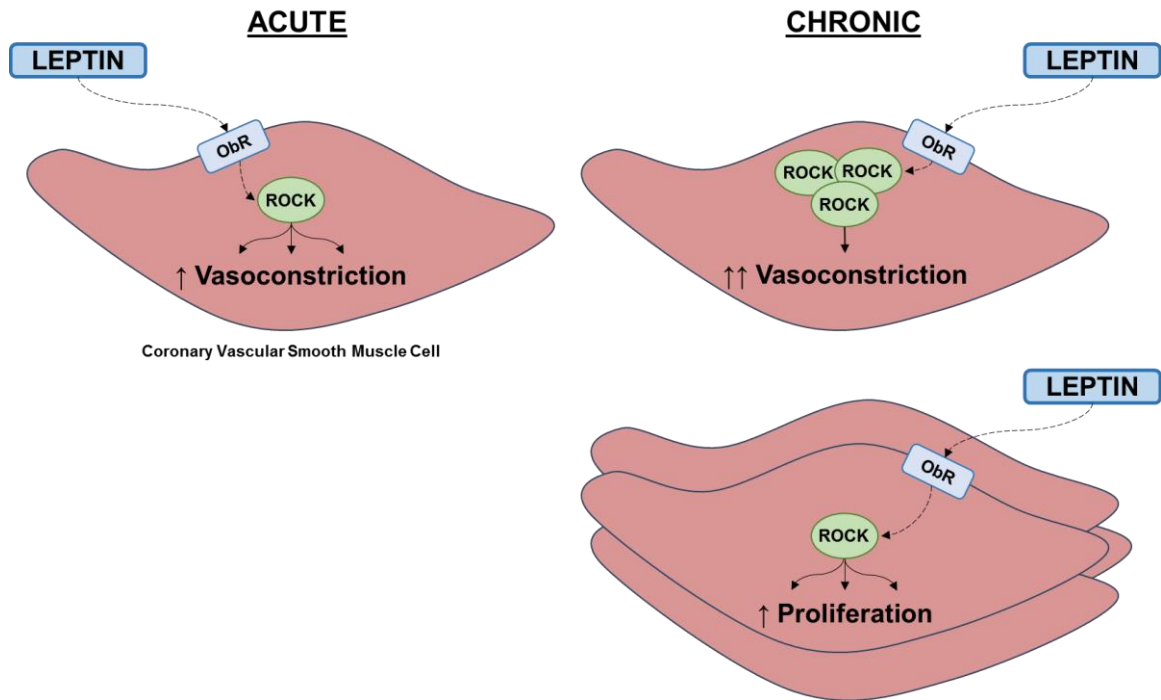


Figure 4.2 Leptin increases coronary vasoconstriction and smooth muscle proliferation. Leptin promotes progressive increases in coronary vasoconstriction via alterations in Rho kinase signaling. Acute (30 min) leptin administration increases Rho kinase (ROCK) activity, whereas chronic (3 day culture) leptin exposure increases ROCK protein abundance. Leptin mediated increases in vascular smooth muscle cell proliferation following chronic (8 day culture) administration are associated with increases in Rho kinase activity.

Implications

Findings from this investigation substantially contribute to the growing body of evidence that changes in the phenotype of coronary PVAT occur concomitantly with mechanistic alterations in endothelium and smooth muscle in the setting of obesity-induced coronary disease. The present findings also support the paradigm of outside-to-inside signaling influences of coronary PVAT and that alterations of specific factors, such as leptin and calpastatin, are capable of contributing to the initiation and/or progression of smooth muscle dysfunction in the setting of obesity. In particular, results from this investigation demonstrate that coronary perivascular adipokines have the potential to augment coronary vasoconstriction, diminish vasodilation, and promote vascular smooth

muscle proliferation in the setting of obesity. These phenotypic effects are related to alterations in the coronary artery proteome, Rho kinase signaling, and the functional expression of smooth muscle K^+ channels. Taken together, we submit that factors derived from coronary PVAT causally contribute to the development of coronary vascular smooth muscle dysfunction (i.e., altered vascular reactivity) in the setting of obesity and propose that obese coronary PVAT-derived leptin is a critical upstream modulator of the development of the hypercontractile and proliferative smooth muscle phenotype reported in obesity-induced coronary disease (see schematic diagram in **Figure 4.3** below).

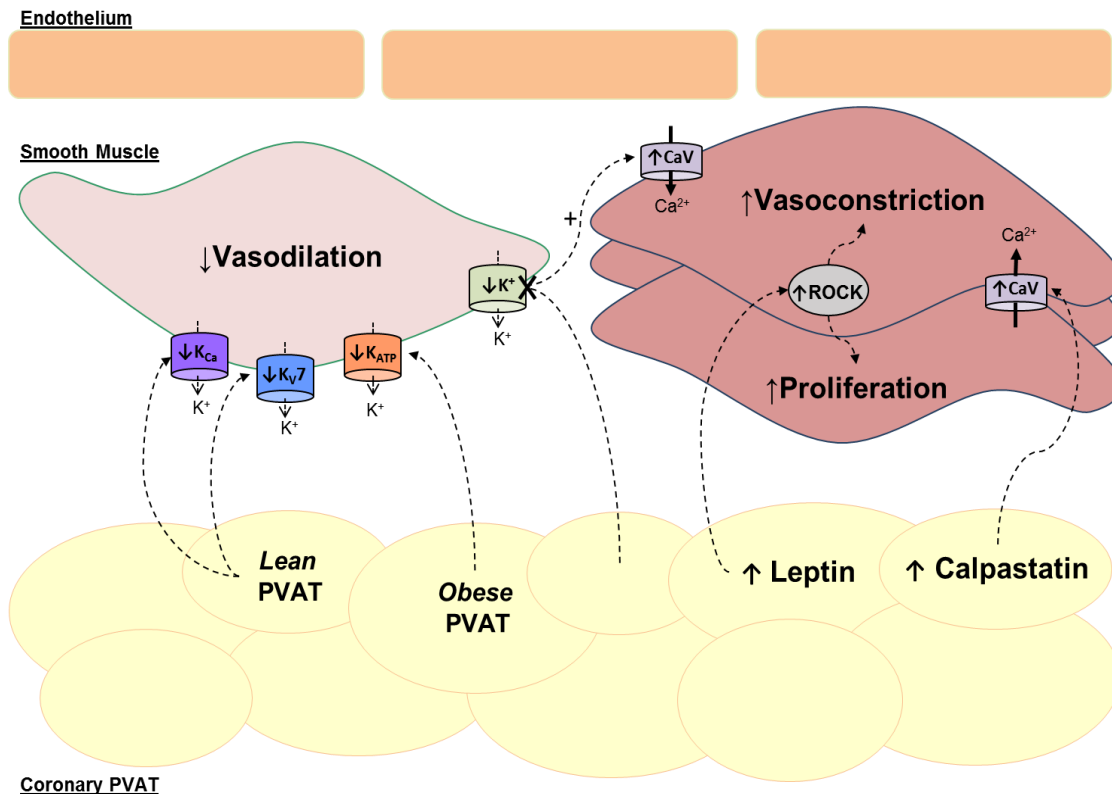


Figure 4.3 Proposed mechanisms of action of coronary PVAT-derived factors on vascular smooth muscle function. Lean and obese PVAT-derived factors attenuate vasodilation via inhibitory effects on vascular smooth muscle K^+ channels. Inhibitory effects on K^+ channels serve to increase $Ca_v1.2$ channel activity, further potentiating contraction. In the setting of obesity, alterations in specific factors are capable of influencing smooth muscle function. Increased leptin promotes progressive increases in coronary vasoconstriction and augments smooth muscle proliferation. These leptin-mediated effects are associated with increases in Rho kinase (ROCK) activity and/or expression. Increased calpastatin promotes vasoconstriction, which is proposed to occur via activation of $Ca_v1.2$ channels.

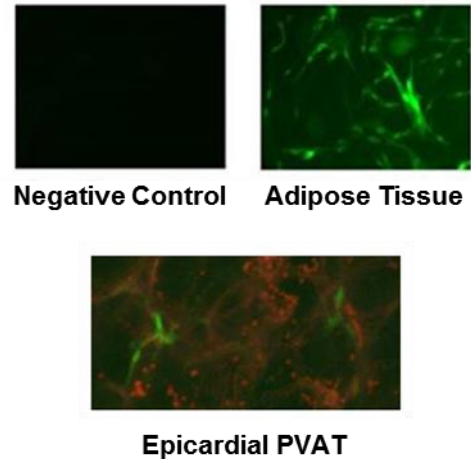
Future Directions and Proposed Studies

This investigation produced several novel observations regarding the effects of coronary perivascular adipokines on coronary smooth muscle function. However, it is important to identify remaining questions as well as logical future directions of this research work in order to continue to advance our understanding of the role of coronary PVAT in obesity-induced coronary disease.

Causal Role for Coronary PVAT-derived Factors in Vivo

Present findings clearly demonstrate the potential for obese PVAT and relevant obese concentrations of adipokines (i.e., leptin) to influence coronary smooth muscle reactivity via influences on K⁺ channels and Rho kinase signaling. These findings are consistent with alterations in the functional expression of K⁺ channels and Rho kinase-dependent contraction in obese coronary arteries. However, a critical question remains as to whether chronic exposure of the coronary vasculature to the PVAT milieu directly contributes to these phenotypic alterations of coronary arteries in the setting of obesity. Thus, there is a need to further characterize a causal link between coronary PVAT-derived factors and the initiation and/or progression of coronary vascular dysfunction and disease. An experimental approach that could selectively overexpress a specific target in coronary PVAT would examine the potential for a causal relationship *in vivo*. The use of lentiviral vectors to selectively overexpress these factors in coronary PVAT would address this critical question. Preliminary “proof of principle” experiments were performed to assess the feasibility of transfecting porcine coronary PVAT both *in vitro* and *in vivo*. Successful *in vivo* transfection of coronary PVAT was confirmed *in vitro* following injection of

lentivirus expressing GFP (150 μ L virus, infectious titer 1×10^9 per mL) and *in vivo* 8 days after injection of lentiviral GFP (350 μ L virus, infectious titer 1×10^9 per mL) (**Figure 4.4**).



The identification of the precise factor(s) responsible for the vascular effects of coronary PVAT remains an ongoing endeavor. Based on recent data implicating a role for leptin and calpastatin in the development of coronary vascular dysfunction in obesity, there is rationale for investigating the effects these factors on the

Figure 4.4 Lentiviral transfection of coronary PVAT. Representative image of *in vitro* lentiviral GFP (green) transfection of coronary PVAT (top). Confocal image of GFP expression in PVAT following *in vivo* lentiviral injection (bottom).

development of coronary vascular dysfunction and atherogenesis *in vivo*. In particular, there is substantial rationale to support the hypothesis that overexpression of leptin in coronary PVAT accelerates the development of a hypercontractile and proliferative coronary smooth muscle phenotype in the setting of obesity. However, although present studies were conducted using relevant, obese concentrations of leptin (**Chapter 3**), the extent to which locally produced (i.e., PVAT-derived) versus circulating plasma leptin contributes to the progression of coronary artery disease *in vivo* has not been addressed. Accordingly, the overexpression of leptin in specific PVAT depots would allow for direct comparisons between regions of the coronary tree that receive lentiviral transfection (e.g., circumflex artery region), null vector transfection (e.g., right coronary artery region), or no injection (e.g., left anterior descending coronary artery region) in the same animal, such that each animal would serve as its own control. Following the injections, swine could be placed on a normal caloric diet (i.e., normal, healthy plasma leptin concentration) or a high-calorie, atherogenic diet (i.e., elevated plasma leptin concentration) for a period of 3-

6 months. Throughout several months of leptin overexpression with or without atherogenic diet, the degree of atherosclerotic disease and plaque morphology among the different artery regions could be mapped using intravascular ultrasound. Subsequently, these tissues could support several *in vitro*, immunohistochemical, and molecular studies including: isometric tension studies to assess vascular reactivity to K⁺ and Ca²⁺ channel agonists, immunohistochemistry to assess vascular smooth muscle proliferation (BrdU) and the degree of macrophage infiltration-foam cell formation (serum response antigen), and Western blot analyses to determine effects on signaling pathways (e.g., Rho kinase, PKC) and ion channels (e.g., K⁺ and Ca²⁺). Results from these studies would elucidate the effects of coronary PVAT-derived leptin on coronary vascular function and atherogenesis in the presence and absence of systemically elevated leptin. Furthermore, these studies would be the first to systematically investigate a potential causal contribution of PVAT-derived factors to the initiation and development of coronary disease *in vivo*.

Coronary PVAT and Coronary Artery Calcification

Strong and growing evidence supports that coronary PVAT displays a unique phenotype relative to other adipose tissue depots and is capable of locally producing factors with the potential to influence the development of coronary disease. Recent studies have identified the expression of osteogenic factors including osteoprotegerin and osteoglycin in coronary PVAT, particularly in obese subjects with coronary artery disease.^{9;73} This unique expression profile is directly associated with the severity of coronary artery disease and the degree of underlying artery calcification.^{18;100;180} Interestingly, numerous studies implicate a role for leptin in the production of osteogenic factors such as osteoprotegerin, receptor activator of nuclear factor- κ B ligand (RANKL), and osteocalcin.^{10;278-281} Furthermore, recent evidence suggests that there is a distinct

relationship between serum RANKL and osteoprotegerin levels (i.e., increased RANKL/osteoprotegerin ratio) with the severity of atherosclerotic disease in humans.^{19;281-283} Despite these promising findings, there is still no unifying hypothesis regarding the contribution of coronary PVAT-derived factors to the development of coronary vascular calcification and atherogenesis. Accordingly, future studies should explore a potential mechanistic link between coronary PVAT-derived factors, such as leptin and osteoprotegerin, and coronary vascular calcification in the setting of obesity. In accordance with the findings of the current investigation of leptin as an upstream mediator of coronary vascular dysfunction and disease, future studies should investigate the hypothesis that leptin released from coronary PVAT promotes coronary vascular calcification via influences on the RANKL/osteoprotegerin signaling axis (see schematic diagram in **Figure 4.5** below).

Both *in vitro* and *in vivo* approaches should be utilized to investigate this hypothesis. Similar to the culture studies described in **Chapter 3**, coronary arteries could be cultured in a pro-calcification media containing fetal bovine serum, PO_4^{3-} , and alkaline phosphatase with/without relevant, obese concentrations of leptin, osteoprotegerin, or RANKL for a period of 2-8 days. Following the culture period, coronary arteries could be subjected to a variety of relevant analyses, including isometric tension studies to assay vascular reactivity, histologic analysis of artery calcification using Von Kossa staining, and Western blot analyses to probe relevant downstream signaling pathways such as bone morphogenic protein-4, nuclear factor- κB , and Rho kinase. Additionally, measures of osteoprotegerin and RANKL in leptin treated arteries, as well as the surrounding culture media, should be performed in order to investigate the potential for leptin signaling to regulate the production of these factors. Co-culture studies of leptin and osteoprotegerin/RANKL should also be considered to assay a possible interrelationship

of these factors in mediating vascular calcification. The use of lentiviral vectors to overexpress these factors in coronary PVAT *in vivo* and subsequent *in vitro* and molecular analyses could be performed, as described above. Results from these experiments would provide critical examination of the functional relevance of PVAT-derived leptin, osteoprotegerin, and/or RANKL in the development of coronary vascular calcification and atherogenesis *in vivo*.

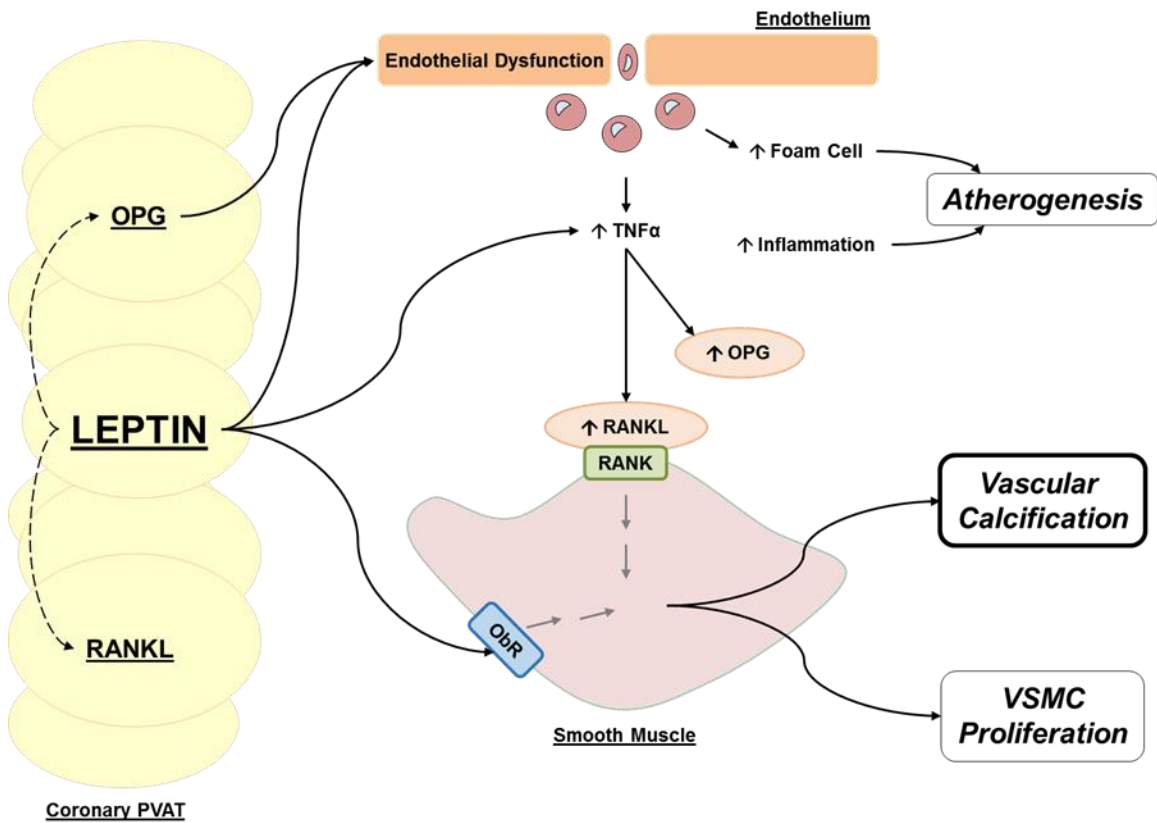


Figure 4.5 Proposed mechanism of coronary PVAT-derived leptin action on coronary vascular calcification and disease. Leptin has been associated with increased release of osteoprotegerin (OPG) and receptor activator of nuclear factor- κ B ligand (RANKL),¹⁰ which could be mediated through leptin-stimulated release from coronary PVAT or inflammatory tumor necrosis factor- α (TNF- α) signaling from coronary endothelial cells. Studies suggest that OPG exacerbates endothelial dysfunction and promotes inflammatory cell infiltration.^{18;19} Leptin has been shown to upregulate RANKL expression and promote osteogenic differentiation and calcification of vascular smooth muscle cells,²² which may also be stimulated via leptin receptor (ObR) signaling. Overall, these promising findings support the hypothesis of leptin as an upstream regulator of the calcification of coronary vascular smooth muscle cells.

An investigation regarding a potential mechanistic link between PVAT-derived factors, such as leptin, and the initiation and/or progression of vascular calcification is warranted based on recent findings and is a logical extension of the present work which supports leptin as an upstream mediator of coronary vascular disease. Findings from these studies would substantially advance current knowledge regarding the functional mechanistic effects of coronary PVAT in the context of obesity-related coronary disease.

Concluding Remarks

Despite the alarming obesity pandemic and the growing body of evidence implicating coronary PVAT, the adipose tissue immediately surrounding large coronary arteries, in the initiation and progression of coronary disease, the mechanisms underlying the link between coronary PVAT and vascular dysfunction and the precise PVAT-derived factors involved remain poorly understood. The central goal of this work was to delineate the mechanisms by which PVAT-derived factors influence coronary vascular smooth muscle function and the development of obesity-induced coronary disease. Results from these investigations clearly illustrate that factors released from lean and obese coronary PVAT influence vascular smooth muscle reactivity via differential inhibition of smooth muscle K⁺ channels. Data also support that alterations in specific factors, such as leptin and calpastatin, are capable of contributing to the development of smooth muscle dysfunction in the setting of obesity. In particular, chronic exposure to elevated levels of leptin markedly alters the coronary artery proteome and progressively augments coronary artery contractions. Further studies implicated leptin-induced alterations in Rho kinase signaling in the development of a hypercontractile and proliferative smooth muscle phenotype. Taken together, findings from this investigation provide novel mechanistic evidence linking coronary PVAT and vascular dysfunction. Above all, the present findings

support a role for coronary PVAT in the initiation and progression of coronary disease and highlight specific PVAT-derived factors as potential targets for therapeutic intervention.

Appendices

APPENDIX A: Supplemental Table

Table I. Complete list of protein changes detected in leptin-treated coronary arteries

| Protein Name | Control MEAN | Control SEM | Leptin MEAN | Leptin SEM | Ratio (Leptin/Control) | P value |
|---|-------------------------|------------------------|------------------------|-----------------------|-----------------------------------|----------------|
| calsarcin 1 [Sus scrofa] | 0.258 | 0.258 | 1.490 | 0.281 | 5.784 | 0.02224 |
| ras-related protein Rab-21 [Bos taurus] | 0.258 | 0.258 | 1.231 | 0.215 | 4.780 | 0.00024 |
| PREDICTED: sorbin and SH3 domain-containing protein 1 isoform 1 [Ceratotherium simum simum] | 1.291 | 0.975 | 5.667 | 0.915 | 4.391 | 0.00710 |
| PREDICTED: LIM and SH3 domain protein 1 isoform X1 [Loxodonta africana] | 1.004 | 0.421 | 3.247 | 0.778 | 3.234 | 0.04793 |
| PREDICTED: eukaryotic translation initiation factor 6 isoform X1 [Equus caballus] | 1.260 | 0.258 | 1.994 | 0.052 | 1.582 | 0.04877 |
| adipose specific 2 [Sus scrofa] | 3.586 | 1.391 | 5.547 | 1.081 | 1.547 | 0.01758 |
| PREDICTED: non-muscle caldesmon isoform X1 [Sus scrofa] | 34.882 | 3.369 | 52.065 | 4.141 | 1.493 | 0.00491 |
| myotrophin [Homo sapiens] | 4.024 | 0.424 | 5.947 | 0.589 | 1.478 | 0.02820 |
| protein S100-A11 [Sus scrofa] | 4.309 | 0.562 | 6.181 | 0.802 | 1.435 | 0.03670 |
| 60S ribosomal protein L12 [Mus musculus] | 6.139 | 1.680 | 8.180 | 1.548 | 1.333 | 0.01125 |
| PREDICTED: tropomyosin alpha-4 chain isoform 3 [Trichechus manatus latirostris] | 83.834 | 6.385 | 109.518 | 7.208 | 1.306 | 0.01805 |
| PREDICTED: tropomyosin alpha-4 chain isoform 2 [Trichechus manatus latirostris] | 96.952 | 7.387 | 123.493 | 7.044 | 1.274 | 0.02291 |

| Protein Name | Control MEAN | Control SEM | Leptin MEAN | Leptin SEM | Ratio (Leptin/Control) | P value |
|--|--------------|-------------|-------------|------------|------------------------|---------|
| hypothetical protein CB1_000172007 [Camelus ferus] | 92.690 | 7.586 | 116.227 | 7.239 | 1.254 | 0.02265 |
| PREDICTED: tubulin alpha chain-like [Canis lupus familiaris] | 17.534 | 0.968 | 20.608 | 1.172 | 1.175 | 0.01756 |
| PREDICTED: tropomyosin beta chain isoform 1 [Canis lupus familiaris] | 185.488 | 11.935 | 215.973 | 5.359 | 1.164 | 0.03469 |
| PREDICTED: tubulin alpha-1A chain-like [Equus caballus] | 75.314 | 3.450 | 82.436 | 3.646 | 1.095 | 0.00926 |
| PREDICTED: transitional endoplasmic reticulum ATPase [Ovis aries] | 10.398 | 1.452 | 11.243 | 1.614 | 1.081 | 0.03649 |
| PREDICTED: LOW QUALITY PROTEIN: myoferlin [Sus scrofa] | 1.984 | 0.550 | 0.261 | 0.261 | -7.590 | 0.02799 |
| PREDICTED: delta-1-pyrroline-5-carboxylate dehydrogenase, mitochondrial [Equus caballus] | 1.476 | 0.448 | 0.243 | 0.243 | -6.080 | 0.00918 |
| ATPase inhibitor, mitochondrial precursor [Sus scrofa] | 1.267 | 0.272 | 0.259 | 0.259 | -4.894 | 0.00003 |
| sorcic [Bos taurus] | 1.260 | 0.258 | 0.261 | 0.261 | -4.821 | 0.00003 |
| PREDICTED: translocon-associated protein subunit delta isoformX1 [Sus scrofa] | 2.483 | 0.425 | 0.954 | 0.551 | -2.603 | 0.04270 |
| cAMP-dependent protein kinase type II-alpha regulatory subunit [Sus scrofa] | 1.267 | 0.272 | 0.493 | 0.285 | -2.569 | 0.04252 |
| PREDICTED: LOW QUALITY PROTEIN: chondroitin sulfate proteoglycan 4 [Sus scrofa] | 4.764 | 0.933 | 1.976 | 0.384 | -2.411 | 0.02713 |
| heat shock protein 90 alpha [Equus caballus] | 16.304 | 0.884 | 6.962 | 2.030 | -2.342 | 0.02046 |

| Protein Name | Control MEAN | Control SEM | Leptin MEAN | Leptin SEM | Ratio (Leptin/Control) | P value |
|--|--------------|-------------|-------------|------------|------------------------|---------|
| phosphate carrier protein, mitochondrial [Sus scrofa] | 5.769 | 0.721 | 2.487 | 0.280 | -2.319 | 0.01566 |
| PREDICTED: fibrillin-1 [Erinaceus europaeus] | 31.725 | 6.279 | 14.566 | 8.410 | -2.178 | 0.01951 |
| protein disulfide isomerase family A, member 4 precursor [Sus scrofa] | 5.769 | 0.721 | 2.706 | 0.399 | -2.132 | 0.03800 |
| RecName: Full=Ribonuclease inhibitor; AltName: Full=Ribonuclease/angiogenin inhibitor 1 [Sus scrofa] | 5.783 | 0.492 | 2.724 | 0.433 | -2.123 | 0.00433 |
| PREDICTED: LOW QUALITY PROTEIN: fibrillin-1 [Felis catus] | 45.016 | 9.359 | 21.334 | 12.353 | -2.110 | 0.03330 |
| dolichyl-diphosphooligosaccharide--protein glycosyltransferase subunit 2 precursor [Sus scrofa] | 7.757 | 0.711 | 3.934 | 0.724 | -1.972 | 0.01836 |
| Chain A, Structure Of Glutamate Dehydrogenase Complexed With Bithionol | 4.519 | 0.253 | 2.471 | 0.227 | -1.828 | 0.00041 |
| PREDICTED: integrin alpha-1 [Sus scrofa] | 11.781 | 0.983 | 6.486 | 0.868 | -1.816 | 0.04630 |
| Chain A, Crystal Structure Of Porcine Aldehyde Reductase Ternary Complex | 6.535 | 0.654 | 3.676 | 0.745 | -1.778 | 0.00017 |
| hypothetical protein PANDA_012129 [Ailuropoda melanoleuca] | 1.755 | 0.245 | 0.997 | 0.026 | -1.760 | 0.04256 |
| PREDICTED: ATP synthase subunit b, mitochondrial [Sus scrofa] | 3.020 | 0.069 | 1.736 | 0.238 | -1.740 | 0.01894 |

| Protein Name | Control MEAN | Control SEM | Leptin MEAN | Leptin SEM | Ratio (Leptin/Control) | P value |
|--|--------------|-------------|-------------|------------|------------------------|---------|
| PREDICTED: calreticulin [Equus caballus] | 9.489 | 1.636 | 5.628 | 1.584 | -1.686 | 0.01366 |
| PREDICTED: prostacyclin synthase isoform X1 [Sus scrofa] | 12.396 | 1.539 | 7.377 | 1.684 | -1.680 | 0.02832 |
| PREDICTED: collagen alpha-1(XIV) chain isoform X1 [Sus scrofa] | 78.779 | 3.063 | 47.471 | 4.658 | -1.660 | 0.01278 |
| PREDICTED: LOW QUALITY PROTEIN: ubiquitin-like modifier activating enzyme 1 [Sus scrofa] | 12.607 | 1.346 | 7.704 | 1.591 | -1.637 | 0.03853 |
| hypothetical protein PANDA_019876 [Ailuropoda melanoleuca] | 2.766 | 0.254 | 1.724 | 0.440 | -1.604 | 0.04743 |
| PREDICTED: LOW QUALITY PROTEIN: neuroblast differentiation-associated protein AHNAK [Capra hircus] | 26.261 | 2.876 | 17.150 | 2.095 | -1.531 | 0.00744 |
| calpain-2 catalytic subunit [Sus scrofa] | 12.114 | 1.105 | 7.959 | 0.335 | -1.522 | 0.03649 |
| RecName: Full=L-lactate dehydrogenase A chain; Short=LDH-A; AltName: Full=LDH muscle subunit; Short=LDH-M [Sus scrofa] | 16.064 | 1.286 | 10.635 | 1.669 | -1.510 | 0.02359 |
| PREDICTED: transmembrane protein 109-like [Ailuropoda melanoleuca] | 7.509 | 0.498 | 5.013 | 0.520 | -1.498 | 0.02765 |
| dermatopontin precursor [Bos taurus] | 7.035 | 0.922 | 4.725 | 0.207 | -1.489 | 0.04980 |

| Protein Name | Control MEAN | Control SEM | Leptin MEAN | Leptin SEM | Ratio (Leptin/Control) | P value |
|--|--------------|-------------|-------------|------------|------------------------|---------|
| alpha-crystallin B chain [Oryctolagus cuniculus] | 27.360 | 1.370 | 18.690 | 1.113 | -1.464 | 0.01028 |
| protein disulfide-isomerase A3 precursor [Sus scrofa] | 20.767 | 1.652 | 14.538 | 2.162 | -1.429 | 0.04491 |
| lumican precursor [Sus scrofa] | 34.624 | 4.503 | 24.337 | 3.975 | -1.423 | 0.00826 |
| PREDICTED: LOW QUALITY PROTEIN: neuroblast differentiation-associated protein AHNAK [Ovis aries] | 27.025 | 3.273 | 19.104 | 1.750 | -1.415 | 0.01529 |
| Moesin [Pteropus alecto] | 34.832 | 2.058 | 25.027 | 1.669 | -1.392 | 0.03728 |
| glyceraldehyde-3-phosphate dehydrogenase [Sus scrofa] | 38.195 | 3.502 | 27.918 | 2.370 | -1.368 | 0.00487 |
| hypothetical protein CB1_001341009 [Camelus ferus] | 18.356 | 0.507 | 13.443 | 1.192 | -1.366 | 0.01312 |
| Chain A, Structure Of Pig Muscle Pkg Complexed With Mgatp | 32.384 | 1.055 | 24.059 | 1.313 | -1.346 | 0.00197 |
| PREDICTED: elongation factor 2 [Sus scrofa] | 26.117 | 1.288 | 19.803 | 2.247 | -1.319 | 0.03958 |
| PREDICTED: LOW QUALITY PROTEIN: neuroblast differentiation-associated protein AHNAK [Tursiops truncatus] | 24.972 | 2.460 | 19.120 | 2.026 | -1.306 | 0.00849 |
| PREDICTED: 78 kDa glucose-regulated protein-like [Ailuropoda melanoleuca] | 28.360 | 1.661 | 22.023 | 1.574 | -1.288 | 0.01731 |
| PREDICTED: T-complex protein 1 subunit zeta isoformX1 [Equus caballus] | 7.347 | 0.884 | 5.732 | 0.620 | -1.282 | 0.01049 |
| PREDICTED: LOW QUALITY PROTEIN: AHNAK nucleoprotein [Sus scrofa] | 33.820 | 3.865 | 26.585 | 2.561 | -1.272 | 0.02246 |

| Protein Name | Control MEAN | Control SEM | Leptin MEAN | Leptin SEM | Ratio (Leptin/Control) | P value |
|---|--------------|-------------|-------------|------------|------------------------|-------------|
| PREDICTED: elongation factor 1-delta isoform X4 [Sus scrofa] | 4.047 | 0.633 | 3.269 | 0.545 | -1.238 | 0.01977 |
| Chain A, X-Ray Structure Of Full-Length Annexin 1 | 57.789 | 3.069 | 46.700 | 2.254 | -1.237 | 0.00267 |
| annexin A2 [Sus scrofa] | 81.978 | 4.401 | 68.049 | 4.666 | -1.205 | 0.02374 |
| PREDICTED: WD repeat-containing protein 1 isoform X2 [Mustela putorius furo] | 24.342 | 1.691 | 20.421 | 2.096 | -1.192 | 0.00872 |
| thioredoxin-dependent peroxide reductase, mitochondrial [Sus scrofa] | 7.023 | 0.292 | 5.983 | 0.156 | -1.174 | 0.02274 |
| PREDICTED: vinculin isoform X1 [Sus scrofa] | 119.348 | 4.302 | 106.039 | 5.949 | -1.126 | 0.02628 |
| PREDICTED: EH domain-containing protein 2 [Sus scrofa] | 26.506 | 2.799 | 23.891 | 2.757 | -1.109 | 0.00404 |
| heat shock protein 70kDa protein 8 [Capra hircus] | 18.079 | 0.613 | 17.123 | 0.848 | -1.056 | 0.03843 |
| reticulocalbin 2, EF-hand calcium binding domain precursor [Sus scrofa] | 1.476 | 0.448 | 0.000 | 0.000 | 0.000 | 0.04580 |
| PREDICTED: cytochrome b-c1 complex subunit 1, mitochondrial isoform X1 [Sus scrofa] | 1.476 | 0.448 | 0.000 | 0.000 | 0.000 | 0.04580 |
| | | | | | | |
| MULTISPECIES: nitrogen regulatory protein P-II 1 [Pseudomonas] | 0.23493 | 0.23493 | 1.9427 | 1.9427 | 8.269271698 | 0.391002219 |
| PREDICTED: synaptopodin-2 isoform X1 [Orycteropus afer afer] | 0.488805 | 0.28263531 | 4.01695 | 1.27273008 | 8.217898753 | 0.082955279 |

| Protein Name | Control MEAN | Control SEM | Leptin MEAN | Leptin SEM | Ratio (Leptin/Control) | P value |
|--|--------------|-------------|-------------|------------|------------------------|-------------|
| PREDICTED: synemin isoform X1 [Lipotes vexillifer] | 0.260075 | 0.260075 | 1.231365 | 0.21457457 | 4.734653465 | 0.085621219 |
| PREDICTED: collagen alpha-2(IV) chain [Sus scrofa] | 1.007805 | 0.72902688 | 4.7238 | 1.12860976 | 4.687216277 | 0.055005478 |
| PREDICTED: filamin-A isoform X1 [Ornithorhynchus anatinus] | 78.0625 | 78.0625 | 322.545 | 1.93813699 | 4.131881505 | 0.050705015 |
| similar to cytoplasmic dynein light chain 1 [Bos taurus] | 0.260075 | 0.260075 | 1.04305 | 0.73940262 | 4.010573873 | 0.391899516 |
| hypothetical protein PANDA_002907 [Ailuropoda melanoleuca] | 0.488805 | 0.28263531 | 1.490165 | 0.28137997 | 3.048587883 | 0.172658966 |
| PREDICTED: LOW QUALITY PROTEIN: laminin subunit alpha-5 [Bos taurus] | 0.77405 | 0.49698584 | 2.34755 | 1.72776503 | 3.032814418 | 0.391903963 |
| PREDICTED: SUN domain-containing protein 2 isoform X1 [Sus scrofa] | 0.253875 | 0.253875 | 0.744475 | 0.46804115 | 2.93244707 | 0.499101166 |
| dolichyl-diphosphooligosaccharide--protein glycosyltransferase subunit DAD1 [Sus scrofa] | 0.5177 | 0.29890093 | 1.5040775 | 0.67349178 | 2.905307128 | 0.375166859 |
| PREDICTED: laminin subunit alpha-5 [Ceratotherium simum simum] | 1.507725 | 0.66091962 | 4.323375 | 1.42480154 | 2.867482465 | 0.225458215 |
| PREDICTED: glycine--tRNA ligase isoform X1 [Sus scrofa] | 0.260075 | 0.260075 | 0.7271 | 0.4533045 | 2.795732 | 0.392505995 |
| PREDICTED: 40S ribosomal protein S14-like [Sarcophilus harrisii] | 1.006505 | 0.02283821 | 2.734865 | 1.03865183 | 2.717189681 | 0.189377295 |
| TPA: cellular retinoic acid-binding protein 1 [Bos taurus] | 1.02545 | 0.41462076 | 2.705575 | 0.39869136 | 2.638427032 | 0.091648916 |

| Protein Name | Control MEAN | Control SEM | Leptin MEAN | Leptin SEM | Ratio (Leptin/Control) | P value |
|---|--------------|-------------|-------------|------------|------------------------|-------------|
| Chain A, Structural Basis Of The 70-Kilodalton Heat Shock Cognate Protein Atp Hydrolytic Activity, Ii. Structure Of The Active Site With Adp Or Atp Bound To Wild Type And Mutant Atpase Fragment | 6.343 | 6.343 | 16.4375 | 5.52484271 | 2.591439382 | 0.263224284 |
| PREDICTED: cellular nucleic acid-binding protein isoform X2 [Ornithorhynchus anatinus] | 0.492555 | 0.28497986 | 1.231365 | 0.21457457 | 2.49995432 | 0.05436688 |
| Ribosomal protein L3 [Bos taurus] | 0.51395 | 0.29677235 | 1.2746025 | 0.50326453 | 2.480012647 | 0.058569339 |
| PREDICTED: small nuclear ribonucleoprotein Sm D1 [Equus caballus] | 0.5115 | 0.29533054 | 1.24875 | 0.60687726 | 2.441348974 | 0.444372388 |
| unconventional myosin-Ic isoform b [Camelus ferus] | 6.751625 | 4.40886367 | 16.311525 | 2.62500349 | 2.415940607 | 0.248428968 |
| PREDICTED: 40S ribosomal protein S21 [Ornithorhynchus anatinus] | 0.77405 | 0.49698584 | 1.7602775 | 0.27651465 | 2.274113429 | 0.090337268 |
| tubulin beta-6 chain [Bos taurus] | 7.2135 | 7.2135 | 15.48925 | 8.94971651 | 2.147258612 | 0.340052857 |
| collagen alpha-1(IV) chain precursor [Bos taurus] | 1.52423 | 0.31599565 | 3.269 | 0.5450397 | 2.14468945 | 0.050983207 |
| PREDICTED: nexilin isoformX1 [Equus caballus] | 1.0292 | 0.42073099 | 2.2013 | 0.56323131 | 2.138845705 | 0.070796767 |
| hypothetical protein PANDA_015940 [Ailuropoda melanoleuca] | 1.1936 | 0.88796798 | 2.5213 | 1.45764816 | 2.112349196 | 0.27468909 |
| D-dopachrome decarboxylase [Sus scrofa] | 0.5115 | 0.29533054 | 1.037825 | 0.73200165 | 2.028983382 | 0.597589397 |

| Protein Name | Control MEAN | Control SEM | Leptin MEAN | Leptin SEM | Ratio (Leptin/Control) | P value |
|--|--------------|-------------|-------------|------------|------------------------|-------------|
| hypothetical protein PANDA_001588 [Ailuropoda melanoleuca] | 0.74643 | 0.24960188 | 1.49279 | 0.2864035 | 1.99990622 | 0.054829328 |
| ubiquitin-conjugating enzyme E2 D2 [Sus scrofa] | 1.25793 | 0.49381205 | 2.508565 | 0.67382356 | 1.99420079 | 0.094704976 |
| leiomodin-1 [Bos taurus] | 3.077675 | 1.25067503 | 6.11965 | 1.31619116 | 1.988400335 | 0.195584174 |
| matrin-3 [Bos taurus] | 0.77405 | 0.49698584 | 1.5334025 | 0.67642755 | 1.981012209 | 0.058559222 |
| Copper transport protein ATOX1, partial [Bos mutus] | 0.771575 | 0.25724221 | 1.5174425 | 0.3254179 | 1.966681787 | 0.076545378 |
| TPA: elongin B-like [Bos taurus] | 0.51395 | 0.29677235 | 0.988525 | 0.38354477 | 1.923387489 | 0.3837056 |
| galectin-3 [Sus scrofa] | 1.02545 | 0.41462076 | 1.969775 | 0.36453145 | 1.92088839 | 0.173083485 |
| calcium/calmodulin-dependent protein kinase type II subunit gamma [Oryctolagus cuniculus] | 1.521755 | 0.52368543 | 2.74355 | 0.88718926 | 1.802885484 | 0.312661824 |
| PREDICTED: laminin subunit alpha-5 [Pteropus alecto] | 1.965175 | 0.6423131 | 3.54175 | 0.95017397 | 1.802256796 | 0.237217836 |
| PREDICTED: sorbin and SH3 domain-containing protein 2 isoform X5 [Sus scrofa] | 14.2028 | 2.6755844 | 25.43625 | 5.63425141 | 1.79093207 | 0.065176462 |
| PREDICTED: polypyrimidine tract-binding protein 1 isoform X1 [Sorex araneus] | 1.546925 | 0.66745894 | 2.746175 | 0.50194035 | 1.775247669 | 0.113055905 |
| Chain A, Refined Structure Of Porcine Cytosolic Adenylate Kinase At 2.1 Angstroms Resolution | 1.52423 | 0.31599565 | 2.69425 | 0.78564622 | 1.767613812 | 0.117340448 |
| PREDICTED: thioredoxin domain-containing protein 17 isoform 1 [Sus scrofa] | 2.008125 | 0.84254326 | 3.505775 | 0.68487716 | 1.745795207 | 0.21637304 |

| Protein Name | Control MEAN | Control SEM | Leptin MEAN | Leptin SEM | Ratio (Leptin/Control) | P value |
|---|--------------|-------------|-------------|------------|------------------------|-------------|
| Leiomodin-1 [Tupaia chinensis] | 2.262 | 0.88215829 | 3.9369 | 0.58914 | 1.740450928 | 0.07525657 |
| PREDICTED: transcriptional activator protein Pur-alpha-like, partial [Ailuropoda melanoleuca] | 1.2818 | 0.76585626 | 2.228575 | 0.1965077 | 1.738629271 | 0.354120077 |
| PREDICTED: poly [ADP-ribose] polymerase 6 isoform X2 [Sus scrofa] | 39.84425 | 23.2293831 | 69.26025 | 4.59655199 | 1.738274657 | 0.240371352 |
| PREDICTED: keratin, type I cytoskeletal 14 isoform X1 [Galeopterus variegatus] | 4.5088 | 1.89907393 | 7.75565 | 2.68631712 | 1.720113999 | 0.357797129 |
| PREDICTED: translocon-associated protein subunit alpha isoform X1 [Monodelphis domestica] | 1.2893 | 0.49657962 | 2.192615 | 0.86717125 | 1.70062437 | 0.238883247 |
| heart fatty acid-binding protein [Sus scrofa] | 2.54968 | 0.53687186 | 4.290875 | 0.84929843 | 1.682907267 | 0.09331917 |
| PREDICTED: B-cell receptor-associated protein 31 isoform X1 [Sus scrofa] | 1.49905 | 0.27457939 | 2.498675 | 0.31019821 | 1.666838998 | 0.124311312 |
| PREDICTED: keratin, type I cytoskeletal 19-like [Galeopterus variegatus] | 3.038475 | 0.44727697 | 5.039175 | 1.16511484 | 1.658455311 | 0.07505649 |
| PREDICTED: 40S ribosomal protein S8 [Equus caballus] | 0.765375 | 0.48680041 | 1.2647 | 0.47925842 | 1.652392618 | 0.606466474 |
| PREDICTED: tryptophan--tRNA ligase, cytoplasmic isoformX1 [Sus scrofa] | 0.755105 | 0.49427151 | 1.231365 | 0.21457457 | 1.630720231 | 0.505692042 |
| PREDICTED: dynactin subunit 2 isoformX2 [Equus caballus] | 1.543175 | 0.51449313 | 2.5073525 | 0.64249711 | 1.624801141 | 0.435830313 |

| Protein Name | Control MEAN | Control SEM | Leptin MEAN | Leptin SEM | Ratio (Leptin/Control) | P value |
|--|--------------|-------------|-------------|------------|------------------------|-------------|
| extracellular superoxide dismutase precursor [Sus scrofa] | 0.765375 | 0.48680041 | 1.231365 | 0.21457457 | 1.608838805 | 0.407883873 |
| leukotriene A-4 hydrolase [Sus scrofa] | 1.991625 | 0.55919918 | 3.179925 | 0.78088465 | 1.596648465 | 0.072458048 |
| hypothetical protein PANDA_018340 [Ailuropoda melanoleuca] | 1.546925 | 0.66745894 | 2.426765 | 1.09341726 | 1.56876707 | 0.235371407 |
| fatty acid binding protein 4 [Sus scrofa] | 3.610275 | 1.37406546 | 5.569275 | 2.01228983 | 1.542617945 | 0.27818017 |
| PREDICTED: septin-9-like isoform X1 [Sus scrofa] | 1.776955 | 1.14867041 | 2.74009 | 0.60774177 | 1.542014288 | 0.413519855 |
| PREDICTED: coronin-1B [Sus scrofa] | 0.9851 | 0.56995448 | 1.5174425 | 0.3254179 | 1.540394376 | 0.593919161 |
| interleukin enhancer-binding factor 2 [Mus musculus] | 1.266605 | 0.27209125 | 1.9425 | 0.63780214 | 1.533627295 | 0.459408797 |
| thrombospondin 1 precursor [Sus scrofa] | 6.63105 | 1.66591513 | 10.111 | 1.14489085 | 1.524796224 | 0.12336597 |
| heterogeneous nuclear ribonucleoproteins A2/B1 isoform B1 [Homo sapiens] | 4.847925 | 1.11369535 | 7.37835 | 1.10650044 | 1.521960426 | 0.24418042 |
| PREDICTED: cysteine and glycine-rich protein 2 isoform X1 [Sus scrofa] | 7.57495 | 1.40920328 | 11.51795 | 1.43420852 | 1.520531489 | 0.110276528 |
| PREDICTED: laminin subunit beta-2-like [Odobenus rosmarus divergens] | 7.206 | 1.83984677 | 10.825975 | 2.6690736 | 1.502355676 | 0.437927026 |
| protein SET isoform 2 [Homo sapiens] | 0.520175 | 0.520175 | 0.779025 | 0.49602796 | 1.497620993 | 0.396468174 |
| PREDICTED: protein DJ-1 [Camelus ferus] | 0.939725 | 0.939725 | 1.4049 | 1.4049 | 1.495011839 | 0.825346305 |

| Protein Name | Control MEAN | Control SEM | Leptin MEAN | Leptin SEM | Ratio (Leptin/Control) | P value |
|--|--------------|-------------|-------------|------------|------------------------|-------------|
| 40S ribosomal protein S12 [Homo sapiens] | 1.53043 | 0.67716146 | 2.2804775 | 0.52714099 | 1.490089387 | 0.468677593 |
| chitinase-3-like protein 1 precursor [Sus scrofa] | 1.002755 | 0.41514941 | 1.4841 | 0.61443455 | 1.480022538 | 0.593770093 |
| glycogenin-1 [Oryctolagus cuniculus] | 1.037875 | 0.73563086 | 1.5334025 | 0.67642755 | 1.477444297 | 0.420607147 |
| PREDICTED: 60S ribosomal protein L38 isoform X1 [Monodelphis domestica] | 2.053375 | 0.93260476 | 3.026165 | 0.75548118 | 1.47375175 | 0.064054278 |
| cystatin B protein [Sus scrofa] | 2.553455 | 0.68677109 | 3.76195 | 0.67617061 | 1.473278362 | 0.13238317 |
| PREDICTED: collagen alpha-1(VI) chain isoform X2 [Mustela putorius furo] | 10.528875 | 2.5107948 | 15.4846 | 3.97701308 | 1.470679441 | 0.194501553 |
| proteasome 26S non-ATPase subunit 11 [Bos taurus] | 0.495005 | 0.28652777 | 0.7271 | 0.4533045 | 1.468874052 | 0.720305909 |
| PREDICTED: keratin, type I cytoskeletal 10-like [Ailuropoda melanoleuca] | 19.756 | 4.69138395 | 28.9255 | 1.70821527 | 1.464137477 | 0.175508717 |
| PREDICTED: plectin isoform 1 [Ceratotherium simum simum] | 2.846175 | 1.6554083 | 4.1299 | 1.78220671 | 1.451035161 | 0.190155206 |
| PREDICTED: smoothelin isoform X1 [Sus scrofa] | 11.674325 | 2.58558251 | 16.8645 | 3.27450929 | 1.444580308 | 0.431351248 |
| PREDICTED: collagen alpha-1(VI) chain [Physeter catodon] | 10.03385 | 2.57262692 | 14.4561 | 3.00627103 | 1.440733118 | 0.120999911 |
| EIF6 protein [Bos taurus] | 1.031675 | 0.42476168 | 1.481475 | 0.61209667 | 1.435990016 | 0.384936899 |
| EH-domain containing 1 [Bos taurus] | 1.5507 | 0.98751958 | 2.223325 | 0.86807199 | 1.433755723 | 0.468684667 |
| PREDICTED: purine nucleoside phosphorylase isoform X1 [Sus scrofa] | 1.0292 | 0.42073099 | 1.471575 | 0.49222164 | 1.429824135 | 0.546759582 |

| Protein Name | Control MEAN | Control SEM | Leptin MEAN | Leptin SEM | Ratio (Leptin/Control) | P value |
|---|--------------|-------------|-------------|------------|------------------------|-------------|
| NADH dehydrogenase [ubiquinone] 1 alpha subcomplex subunit 4 [Sus scrofa] | 1.7554 | 0.24539619 | 2.47869 | 0.60705176 | 1.412037143 | 0.418220519 |
| PREDICTED: tropomyosin alpha-1 chain-like isoform X1 [Bos mutus] | 129.185 | 43.7592934 | 180.0475 | 2.95107713 | 1.393718311 | 0.345376335 |
| PREDICTED: PRKC apoptosis WT1 regulator protein [Orcinus orca] | 1.26038 | 0.25786916 | 1.75419 | 0.50465304 | 1.391794538 | 0.179006114 |
| PREDICTED: LOW QUALITY PROTEIN: laminin subunit beta-2 [Sus scrofa] | 13.027775 | 1.84186083 | 18.108 | 4.10386604 | 1.389953388 | 0.371397769 |
| aldose 1-epimerase [Sus scrofa] | 2.530725 | 0.33377169 | 3.50315 | 0.52935184 | 1.384247597 | 0.113946917 |
| PREDICTED: keratin, type I cytoskeletal 10 [Chrysochloris asiatica] | 15.651725 | 3.877081 | 21.64425 | 2.39614275 | 1.382866745 | 0.292309369 |
| Sorting nexin-12 [Tupaia chinensis] | 2.533175 | 0.54416157 | 3.489825 | 0.67297229 | 1.377648603 | 0.452985295 |
| PREDICTED: dual specificity protein phosphatase 3 isoform 2 [Sus scrofa] | 3.441575 | 1.07050772 | 4.72725 | 0.22616664 | 1.373571693 | 0.292557331 |
| PREDICTED: chloride intracellular channel protein 4 [Erinaceus europaeus] | 3.064955 | 0.86015343 | 4.1957 | 0.52022727 | 1.368927113 | 0.172684508 |
| 40S ribosomal protein S15a [Homo sapiens] | 2.03198 | 0.43064859 | 2.773425 | 0.54024765 | 1.364887942 | 0.2403883 |
| PREDICTED: palladin [Sus scrofa] | 10.2162 | 2.65349535 | 13.8811 | 2.06534778 | 1.358734167 | 0.3753886 |
| PREDICTED: perilipin-4 [Sus scrofa] | 0.767825 | 0.48725115 | 1.04045 | 0.60071938 | 1.355061375 | 0.359980012 |

| Protein Name | Control MEAN | Control SEM | Leptin MEAN | Leptin SEM | Ratio (Leptin/Control) | P value |
|---|--------------|-------------|-------------|------------|------------------------|-------------|
| PREDICTED: KN motif and ankyrin repeat domain-containing protein 2 isoformX1 [Canis lupus familiaris] | 1.804575 | 0.88158463 | 2.44415 | 0.57821994 | 1.35441863 | 0.463770462 |
| PREDICTED: SH3 domain-binding glutamic acid-rich-like protein-like [Sus scrofa] | 12.750675 | 3.23306656 | 17.18675 | 0.29984451 | 1.347909032 | 0.259086153 |
| T-complex protein 1 subunit delta [Tupaia chinensis] | 3.32618 | 1.16688007 | 4.470475 | 0.84414999 | 1.344026781 | 0.338577461 |
| 40S ribosomal protein S28 [Homo sapiens] | 2.78705 | 0.52494877 | 3.743375 | 0.50890497 | 1.343131627 | 0.061700102 |
| PREDICTED: integrin alpha-5 isoform 1 [Sus scrofa] | 3.816275 | 0.69668978 | 5.12245 | 1.34118798 | 1.342264381 | 0.484314315 |
| PREDICTED: histone H2A type 1-E-like [Equus caballus] | 9.501725 | 3.37631706 | 12.72675 | 4.28976902 | 1.339414685 | 0.651800203 |
| hypothetical protein PANDA_004938 [Ailuropoda melanoleuca] | 1.5028 | 0.65435142 | 2.01039 | 0.43822103 | 1.337762843 | 0.615573943 |
| PREDICTED: coronin-1C isoform X1 [Sus scrofa] | 5.036325 | 0.44775143 | 6.735 | 0.53687657 | 1.337284627 | 0.064926766 |
| polymerase I and transcript release factor isoform 2 [Bos taurus] | 21.03875 | 2.96604645 | 28.04 | 3.0381976 | 1.332778801 | 0.141552484 |
| protein DJ-1 [Sus scrofa] | 4.279925 | 0.28083418 | 5.70325 | 0.561163 | 1.332558398 | 0.187209781 |
| protein S100-A6 [Sus scrofa] | 2.81108 | 0.89857662 | 3.728615 | 0.98125638 | 1.326399462 | 0.13910146 |
| PREDICTED: uncharacterized protein LOC102248938 [Myotis brandtii] | 35.76475 | 5.85671562 | 46.956 | 9.83965082 | 1.312912854 | 0.455225418 |
| coactosin-like protein [Bos taurus] | 1.518005 | 0.30559001 | 1.98834 | 0.57278126 | 1.309837583 | 0.184420273 |

| Protein Name | Control MEAN | Control SEM | Leptin MEAN | Leptin SEM | Ratio (Leptin/Control) | P value |
|---|--------------|-------------|-------------|------------|------------------------|-------------|
| PREDICTED: EF-hand domain-containing protein D1 [Sus scrofa] | 3.04225 | 0.45866798 | 3.977525 | 0.56060922 | 1.307428712 | 0.112362335 |
| PREDICTED: 26S protease regulatory subunit 6B isoform 1 [Equus caballus] | 0.775325 | 0.4937467 | 1.0105525 | 0.73241178 | 1.303392126 | 0.746981565 |
| heterogeneous nuclear ribonucleoprotein A/B [Sus scrofa] | 1.49155 | 0.64528063 | 1.939875 | 0.76614252 | 1.300576581 | 0.770070384 |
| Chain A, Dextrin, Nmr, Minimized Average Structure | 10.606525 | 1.12625845 | 13.71595 | 2.59087894 | 1.293161521 | 0.202319846 |
| PREDICTED: vimentin [Pantholops hodgsonii] | 227.3375 | 76.875569 | 293.21 | 16.7337623 | 1.289756419 | 0.438023043 |
| PREDICTED: ATP synthase subunit gamma, mitochondrial isoform X2 [Equus caballus] | 4.054975 | 0.64959546 | 5.2016 | 0.36583681 | 1.282769931 | 0.183054568 |
| PREDICTED: fatty acid-binding protein, heart isoform X2 [Pantholops hodgsonii] | 2.553455 | 0.68677109 | 3.275075 | 0.69090141 | 1.282605333 | 0.527725063 |
| PREDICTED: basal cell adhesion molecule isoform X1 [Sus scrofa] | 4.521075 | 0.26841515 | 5.785075 | 1.01727916 | 1.279579525 | 0.285037185 |
| PREDICTED: thioredoxin domain-containing protein 5, partial [Sus scrofa] | 0.771575 | 0.25724221 | 0.9859 | 0.57063117 | 1.277775978 | 0.677580829 |
| PREDICTED: LOW QUALITY PROTEIN: transcriptional activator protein Pur-beta [Canis lupus familiaris] | 10.62235 | 2.16909059 | 13.5705 | 1.77825952 | 1.277542163 | 0.336544375 |

| Protein Name | Control MEAN | Control SEM | Leptin MEAN | Leptin SEM | Ratio (Leptin/Control) | P value |
|--|--------------|-------------|-------------|------------|------------------------|-------------|
| PREDICTED: T-complex protein 1 subunit epsilon [Monodelphis domestica] | 2.530725 | 0.33377169 | 3.225775 | 0.18039649 | 1.274644618 | 0.07329543 |
| hypothetical protein PANDA_008751 [Ailuropoda melanoleuca] | 4.3013 | 0.80003162 | 5.479 | 0.28951373 | 1.273800944 | 0.214683206 |
| PREDICTED: keratin, type I cytoskeletal 14 [Myotis brandtii] | 6.32065 | 1.33241743 | 8.04195 | 2.76458309 | 1.272329586 | 0.559425712 |
| PREDICTED: LOW QUALITY PROTEIN: NADH dehydrogenase [ubiquinone] 1 alpha subcomplex subunit 6 [Oryctolagus cuniculus] | 0.771575 | 0.25724221 | 0.9812525 | 0.39721785 | 1.271752584 | 0.759416369 |
| PREDICTED: hypothetical protein LOC100468944 [Ailuropoda melanoleuca] | 79.379 | 27.6583902 | 100.915 | 33.6530805 | 1.271306013 | 0.708948754 |
| 60S ribosomal protein L23 [Pongo abelii] | 2.025755 | 0.72446126 | 2.5738275 | 1.24715816 | 1.270552214 | 0.685368718 |
| PREDICTED: histone H2A type 1-like [Equus caballus] | 90.69825 | 17.8658617 | 115.07925 | 20.6674042 | 1.268814448 | 0.514641686 |
| PREDICTED: alpha/beta hydrolase domain-containing protein 14B [Equus caballus] | 2.547255 | 0.67892223 | 3.23185 | 0.47715041 | 1.268757937 | 0.567034803 |
| 40S ribosomal protein S4 [Bos taurus] | 1.807 | 0.77825968 | 2.28395 | 1.13690856 | 1.263945766 | 0.744415125 |
| PREDICTED: SH3 domain-binding glutamic acid-rich-like protein-like isoform X1 [Equus caballus] | 11.428775 | 1.95312085 | 14.41075 | 0.29299015 | 1.260918165 | 0.206290878 |

| Protein Name | Control MEAN | Control SEM | Leptin MEAN | Leptin SEM | Ratio (Leptin/Control) | P value |
|--|--------------|-------------|-------------|------------|------------------------|-------------|
| PREDICTED: protein-glutamine gamma-glutamyltransferase 2 [Sus scrofa] | 61.02275 | 8.48150406 | 76.54025 | 6.9991197 | 1.254290408 | 0.17770027 |
| dynein light chain roadblock-type 1 [Rattus norvegicus] | 1.00898 | 0.42538844 | 1.2612425 | 0.66449335 | 1.250017344 | 0.794736677 |
| PREDICTED: importin-5 isoform X1 [Monodelphis domestica] | 1.006505 | 0.02283821 | 1.2560175 | 0.27241258 | 1.247899911 | 0.410953137 |
| PREDICTED: lysine--tRNA ligase isoform X2 [Sorex araneus] | 1.006505 | 0.02283821 | 1.2560175 | 0.27241258 | 1.247899911 | 0.410953137 |
| PREDICTED: plectin [Lipotes vexillifer] | 3.5637 | 1.01671112 | 4.431925 | 1.70669267 | 1.243630216 | 0.394339605 |
| PREDICTED: PDZ and LIM domain protein 7-like [Ailuropoda melanoleuca] | 14.794075 | 2.77525033 | 18.359 | 2.31226314 | 1.24096978 | 0.378847811 |
| PREDICTED: plectin [Vicugna pacos] | 3.8816 | 2.24962597 | 4.8163 | 2.34113035 | 1.240802762 | 0.59853346 |
| PREDICTED: carbonyl reductase [NADPH] 1-like, partial [Sus scrofa] | 2.785925 | 0.79005233 | 3.438725 | 0.8148219 | 1.234320737 | 0.476211292 |
| heterogeneous nuclear ribonucleoprotein D0 [Bos taurus] | 1.9941 | 0.37085747 | 2.4601 | 0.60135043 | 1.233689384 | 0.467889234 |
| PREDICTED: platelet-activating factor acetylhydrolase IB subunit beta [Equus caballus] | 1.807 | 0.77825968 | 2.228575 | 0.1965077 | 1.233301051 | 0.574429779 |
| PREDICTED: adenylyl cyclase-associated protein 2, partial [Sus scrofa] | 1.006505 | 0.02283821 | 1.2400525 | 0.23550094 | 1.232038092 | 0.431761829 |

| Protein Name | Control MEAN | Control SEM | Leptin MEAN | Leptin SEM | Ratio (Leptin/Control) | P value |
|--|--------------|-------------|-------------|------------|------------------------|-------------|
| Chain B, Crystal Structure Of The Mammalian 20s Proteasome At 2.75 A Resolution | 4.84925 | 1.18917601 | 5.96205 | 0.68521504 | 1.229478785 | 0.47872135 |
| Keratin, type II cytoskeletal 1 [Pteropus alecto] | 40.3265 | 3.48275204 | 49.4775 | 4.35272107 | 1.226922743 | 0.235063617 |
| F-actin-capping protein subunit beta [Bos taurus] | 4.843 | 1.10250498 | 5.940025 | 0.42900206 | 1.226517654 | 0.456361893 |
| laminin subunit gamma-1 precursor [Sus scrofa] | 17.15375 | 2.85096274 | 20.92625 | 4.45260778 | 1.219922757 | 0.616231791 |
| PREDICTED: LOW QUALITY PROTEIN: chloride intracellular channel protein 1 [Sus scrofa] | 0.769125 | 0.49267537 | 0.9366 | 0.9366 | 1.21774744 | 0.784314392 |
| PREDICTED: zyxin isoform X1 [Sus scrofa] | 6.354525 | 1.42574826 | 7.73685 | 1.42119916 | 1.217533962 | 0.200222494 |
| Galectin-1, partial [Tupaia chinensis] | 7.32945 | 1.21369013 | 8.915725 | 0.73158932 | 1.216424834 | 0.464394676 |
| proteasome subunit alpha type-6 [Ovis aries] | 2.247975 | 0.19068227 | 2.732825 | 0.23111146 | 1.215683004 | 0.166515154 |
| RecName: Full=UMP-CMP kinase; AltName: Full=Deoxycytidylate kinase; Short=CK; Short=dCMP kinase; AltName: Full=Nucleoside-diphosphate kinase; AltName: Full=Uridine monophosphate/cytidine monophosphate kinase; Short=UMP/CMP kinase; Short=UMP/CMPK [Sus scrofa] | 2.060875 | 0.73224263 | 2.487375 | 0.27982541 | 1.206950931 | 0.464925018 |

| Protein Name | Control MEAN | Control SEM | Leptin MEAN | Leptin SEM | Ratio (Leptin/Control) | P value |
|---|--------------|-------------|-------------|------------|------------------------|-------------|
| PREDICTED: F-actin-capping protein subunit alpha-1 [Capra hircus] | 0.77288 | 0.77288 | 0.9366 | 0.9366 | 1.21184 | 0.391 |
| prelamin-A/C [Sus scrofa] | 42.78225 | 2.77303334 | 51.59225 | 2.34840192 | 1.205926523 | 0.057785816 |
| calumenin isoform 2 precursor [Oryctolagus cuniculus] | 1.235225 | 0.46689688 | 1.48754 | 0.66119014 | 1.204266429 | 0.836218043 |
| ubiquitin-conjugating enzyme E2N-like [Bos taurus] | 4.5614 | 0.92941628 | 5.481625 | 0.30698353 | 1.20174179 | 0.349888496 |
| PREDICTED: LOW QUALITY PROTEIN: ribosomal protein S19 [Bos mutus] | 6.86095 | 1.15715389 | 8.244225 | 1.13779425 | 1.201615665 | 0.492356667 |
| PREDICTED: biglycan [Sus scrofa] | 42.489 | 5.49115156 | 51.003 | 7.52154533 | 1.200381275 | 0.195546575 |
| thioredoxin [Sus scrofa] | 9.36775 | 1.27117254 | 11.2335 | 0.79139566 | 1.199167356 | 0.366628784 |
| PREDICTED: proteasome activator complex subunit 1-like [Ailuropoda melanoleuca] | 1.0292 | 0.42073099 | 1.22874 | 0.47432116 | 1.193878741 | 0.712578513 |
| PREDICTED: histone H1.1-like [Ochotona princeps] | 74.49175 | 16.1394595 | 88.91375 | 12.814068 | 1.193605332 | 0.61338643 |
| long-chain 3-ketoacyl-CoA thiolase [Sus scrofa] | 2.252875 | 0.87022431 | 2.686975 | 0.68511265 | 1.192687122 | 0.757444135 |
| dynein light chain 2, cytoplasmic [Mus musculus] | 2.547255 | 0.67892223 | 3.03485 | 0.65082687 | 1.191419783 | 0.640460409 |
| PREDICTED: LOW QUALITY PROTEIN: profilin-2 [Oryctolagus cuniculus] | 2.526975 | 0.32394161 | 3.0102 | 0.4622025 | 1.191226664 | 0.179612141 |

| Protein Name | Control MEAN | Control SEM | Leptin MEAN | Leptin SEM | Ratio (Leptin/Control) | P value |
|---|--------------|-------------|-------------|------------|------------------------|-------------|
| PREDICTED: glycogen phosphorylase, brain form isoform X1 [Pteropus alecto] | 1.266605 | 0.27209125 | 1.50875 | 0.50531196 | 1.191176413 | 0.633578133 |
| PREDICTED: serine/threonine-protein phosphatase 2A activator [Leptonychotes weddellii] | 1.035425 | 0.59781643 | 1.231365 | 0.21457457 | 1.189236304 | 0.721837265 |
| Peptidyl-prolyl cis-trans isomerase NIMA-interacting 1 [Myotis brandtii] | 1.26038 | 0.25786916 | 1.4988525 | 0.29511734 | 1.189206827 | 0.656472165 |
| PREDICTED: cullin-associated NEDD8-dissociated protein 1-like [Monodelphis domestica] | 4.57515 | 1.04412008 | 5.43575 | 0.5038974 | 1.188103122 | 0.480778418 |
| Chain A, Crevice-Forming Mutants In The Rigid Core Of Bovine Pancreatic Trypsin Inhibitor: Crystal Structures Of F22a, Y23a, N43g, And F45a | 4.296425 | 0.79184256 | 5.078575 | 1.39602843 | 1.182046702 | 0.682662587 |
| PREDICTED: 40S ribosomal protein S16 [Anolis carolinensis] | 4.298875 | 0.67442198 | 5.072525 | 1.27654156 | 1.179965689 | 0.466138671 |
| RecName: Full=Transforming growth factor-beta-induced protein ig-h3; Short=Beta ig-h3; AltName: Full=Kerato-epithelin; AltName: Full=RGD-containing collagen-associated protein; Short=RGD-CAP; Flags: Precursor [Sus scrofa] | 5.492475 | 0.78738755 | 6.476775 | 1.36578225 | 1.179208827 | 0.264589329 |
| PREDICTED: UTP--glucose-1-phosphate uridylyltransferase isoformX2 [Equus caballus] | 1.26413 | 0.26648333 | 1.490165 | 0.28137997 | 1.178806768 | 0.46830929 |

| Protein Name | Control MEAN | Control SEM | Leptin MEAN | Leptin SEM | Ratio (Leptin/Control) | P value |
|--|--------------|-------------|-------------|------------|------------------------|-------------|
| PREDICTED: astrocytic phosphoprotein PEA-15 [Monodelphis domestica] | 2.7846 | 0.30212183 | 3.275075 | 0.69090141 | 1.176138404 | 0.532130403 |
| hypothetical protein CB1_000606063 [Camelus ferus] | 32.53325 | 3.24208918 | 38.063 | 3.6659892 | 1.169972259 | 0.344357648 |
| PREDICTED: PDZ and LIM domain protein 3 isoform X1 [Sus scrofa] | 8.075125 | 1.64654425 | 9.44065 | 0.51786431 | 1.169102645 | 0.528783167 |
| PREDICTED: proteasome subunit alpha type-5 [Monodelphis domestica] | 2.765675 | 0.25413744 | 3.23185 | 0.47715041 | 1.168557405 | 0.264359223 |
| PREDICTED: collagen alpha-2(VI) chain [Sus scrofa] | 21.704775 | 6.06120125 | 25.34625 | 2.8813512 | 1.16777299 | 0.538906978 |
| RecName: Full=Gelsolin; AltName: Full=Actin-depolymerizing factor; Short=ADF; AltName: Full=Brevin; Flags: Precursor, partial [Sus scrofa] | 44.84425 | 2.93491506 | 52.36625 | 4.5699961 | 1.167736109 | 0.165225148 |
| hypothetical protein PANDA_003128 [Ailuropoda melanoleuca] | 7.0822 | 1.30338013 | 8.25775 | 0.79313502 | 1.165986558 | 0.149295125 |
| septin-7 isoform 2 [Homo sapiens] | 7.0947 | 1.19324901 | 8.184575 | 0.44011937 | 1.153618194 | 0.275939425 |
| PREDICTED: phosphoglucomutase-like protein 5 [Equus przewalskii] | 29.19225 | 1.9147396 | 33.58775 | 3.19927399 | 1.150570785 | 0.215533548 |

| Protein Name | Control MEAN | Control SEM | Leptin MEAN | Leptin SEM | Ratio (Leptin/Control) | P value |
|---|--------------|-------------|-------------|------------|------------------------|-------------|
| PREDICTED: histone H2B type 1-B-like [Ceratotherium simum simum] | 38.324 | 5.57846251 | 43.975 | 9.85522613 | 1.147453293 | 0.666416865 |
| serine/threonine-protein phosphatase 2A catalytic subunit beta isoform [Bos taurus] | 1.514255 | 0.51124989 | 1.735625 | 0.23786866 | 1.146190701 | 0.656661828 |
| Keratin, type II cytoskeletal 5 [Myotis davidii] | 17.22625 | 6.1305061 | 19.7375 | 7.45241035 | 1.145780422 | 0.826868341 |
| peptidyl-prolyl cis-trans isomerase FKBP2 isoform 1 [Bos taurus] | 1.518005 | 0.30559001 | 1.738225 | 0.64794714 | 1.145071986 | 0.696446641 |
| PREDICTED: keratin, type II cytoskeletal 1 [Loxodonta africana] | 37.066 | 4.24267795 | 42.40425 | 4.78551734 | 1.144020126 | 0.535495959 |
| PREDICTED: elongation factor 1-gamma [Sus scrofa] | 1.270355 | 0.50040816 | 1.44955 | 0.602617 | 1.141058995 | 0.827928896 |
| PREDICTED: keratin, type II cytoskeletal 1 [Mustela putorius furo] | 40.87075 | 4.6208469 | 46.6275 | 4.73014534 | 1.140852566 | 0.520209353 |
| PREDICTED: 3-hydroxyacyl-CoA dehydrogenase type-2 isoform 2 [Sus scrofa] | 6.066675 | 0.80607318 | 6.9126 | 0.73376624 | 1.139437995 | 0.613744691 |
| hypothetical protein PANDA_001716 [Ailuropoda melanoleuca] | 1.781855 | 0.50834451 | 2.0297925 | 1.4118414 | 1.139145722 | 0.867830067 |
| ras-related protein Rab-5B [Bos taurus] | 8.787175 | 1.09329727 | 9.995375 | 1.16939645 | 1.137495839 | 0.544999332 |
| elongation factor 1-beta [Oryctolagus cuniculus] | 1.52423 | 0.31599565 | 1.733 | 0.23271051 | 1.136967518 | 0.494165352 |
| catechol O-methyltransferase [Sus scrofa] | 1.511805 | 0.66268013 | 1.71705 | 0.44468545 | 1.135761557 | 0.826407178 |

| Protein Name | Control MEAN | Control SEM | Leptin MEAN | Leptin SEM | Ratio (Leptin/Control) | P value |
|---|--------------|-------------|-------------|------------|------------------------|-------------|
| programmed cell death protein 5 [Bos taurus] | 3.29855 | 0.53104064 | 3.746 | 0.2941983 | 1.135650513 | 0.163879593 |
| galectin-1 [Sus scrofa] | 25.35725 | 4.96405599 | 28.762 | 1.29962065 | 1.134271264 | 0.606390857 |
| protein phosphatase 1 regulatory subunit 14A [Sus scrofa] | 6.995275 | 0.67180323 | 7.934475 | 0.38174402 | 1.134262055 | 0.118943323 |
| PREDICTED: histidine triad nucleotide-binding protein 1-like [Sus scrofa] | 1.746725 | 0.63618883 | 1.978475 | 0.38611276 | 1.132676867 | 0.668194913 |
| hydroxyacyl-coenzyme A dehydrogenase/3-ketoacyl-coenzyme A thiolase/enoyl-coenzyme A hydratase alpha subunit [Sus scrofa] | 9.649425 | 1.50633661 | 10.9256 | 1.54813276 | 1.132253994 | 0.375670977 |
| PREDICTED: alpha-actinin-3 [Sorex araneus] | 25.796 | 3.67551849 | 29.2065 | 3.13021643 | 1.13221042 | 0.242941591 |
| PREDICTED: flavin reductase (NADPH) [Sus scrofa] | 3.307225 | 1.01129631 | 3.743375 | 0.50890497 | 1.131877934 | 0.518734721 |
| cytochrome c [Bos taurus] | 2.014325 | 0.73071291 | 2.274415 | 0.67958931 | 1.129120177 | 0.839672126 |
| heterogeneous nuclear ribonucleoprotein K [Oryctolagus cuniculus] | 6.85325 | 1.76415191 | 7.6903 | 1.13070146 | 1.122139131 | 0.528616568 |
| rho GDP-dissociation inhibitor 1 [Bos taurus] | 7.04315 | 0.43823997 | 7.898575 | 0.85935234 | 1.121454889 | 0.254294058 |
| PREDICTED: lysozyme C [Chrysochloris asiatica] | 2.2682 | 0.65524251 | 2.5419025 | 0.70391636 | 1.120669474 | 0.84071795 |
| PREDICTED: 60S ribosomal protein L31-like [Chrysochloris asiatica] | 2.039505 | 0.74145197 | 2.2778775 | 0.67185046 | 1.116877625 | 0.851154337 |

| Protein Name | Control MEAN | Control SEM | Leptin MEAN | Leptin SEM | Ratio (Leptin/Control) | P value |
|---|--------------|-------------|-------------|------------|------------------------|-------------|
| PREDICTED: calcium-binding protein 39 isoform X1 [Equus caballus] | 1.778105 | 0.27964838 | 1.98574 | 0.37929463 | 1.116773194 | 0.334446264 |
| septin 2 [Sus scrofa] | 3.7722 | 0.25830315 | 4.211675 | 0.69226697 | 1.116503632 | 0.458639266 |
| PREDICTED: filamin-C isoformX1 [Sus scrofa] | 65.54525 | 3.79476333 | 73.08825 | 6.10449208 | 1.115080803 | 0.180313109 |
| PREDICTED: myosin-9 [Dasypus novemcinctus] | 92.7255 | 3.38214632 | 103.36725 | 5.36620871 | 1.114766165 | 0.15265488 |
| filamin-A [Sus scrofa] | 51.5625 | 5.20962779 | 57.47075 | 3.4937609 | 1.114584242 | 0.074065937 |
| calpain small subunit 1 [Oryctolagus cuniculus] | 5.795475 | 0.79626803 | 6.44165 | 0.52478918 | 1.111496469 | 0.614146065 |
| glutathione S-transferase mu 2 [Sus scrofa] | 4.254775 | 0.42590501 | 4.72725 | 0.22616664 | 1.111045825 | 0.105667983 |
| alpha-actinin-1 [Sus scrofa] | 115.883 | 10.8352274 | 128.3 | 11.5450891 | 1.107151178 | 0.158117808 |
| PREDICTED: LOW QUALITY PROTEIN: bromodomain adjacent to zinc finger domain protein 1A [Oryctolagus cuniculus] | 11.902125 | 1.71310656 | 13.16915 | 1.34342271 | 1.106453679 | 0.425037782 |
| PREDICTED: dihydropyrimidinase-related protein 3 isoform 1 [Ceratotherium simum simum] | 26.24275 | 2.57663739 | 28.86525 | 1.6589642 | 1.099932362 | 0.343598809 |
| profilin-1 [Sus scrofa] | 55.1165 | 5.29946426 | 60.622 | 2.5720382 | 1.099888418 | 0.325798338 |
| PREDICTED: ATP synthase subunit delta, mitochondrial-like isoform 1 [Sus scrofa] | 2.2731 | 0.28541387 | 2.496075 | 0.30248977 | 1.098092913 | 0.477569494 |
| PREDICTED: NAD(P)H-hydrate epimerase [Equus caballus] | 2.03818 | 0.44531691 | 2.237275 | 0.23089851 | 1.097682737 | 0.775376708 |

| Protein Name | Control MEAN | Control SEM | Leptin MEAN | Leptin SEM | Ratio (Leptin/Control) | P value |
|---|--------------|-------------|-------------|------------|------------------------|-------------|
| PREDICTED: guanine nucleotide-binding protein G(I)/G(S)/G(T) subunit beta-1 isoform X1 [Equus caballus] | 6.554325 | 0.57770388 | 7.187375 | 0.45924546 | 1.096585079 | 0.094199315 |
| PREDICTED: uncharacterized protein LOC101365636 [Odobenus rosmarus divergens] | 5.54535 | 0.91900348 | 6.076975 | 1.70217388 | 1.095868611 | 0.822312031 |
| PREDICTED: pyruvate kinase PKM [Ornithorhynchus anatinus] | 20.91425 | 2.08962299 | 22.90625 | 1.76328313 | 1.095246064 | 0.458722057 |
| PREDICTED: LanC lantibiotic synthetase component C-like 1 [Sus scrofa] | 2.288305 | 0.77675231 | 2.50594 | 0.51680876 | 1.095107514 | 0.725868444 |
| actin, cytoplasmic 1 [Camelus ferus] | 79.59875 | 2.41055939 | 87.14725 | 1.66523964 | 1.094831891 | 0.119447522 |
| PREDICTED: EH domain-containing protein 4 [Pteropus alecto] | 4.797625 | 0.34718232 | 5.2495 | 1.15191 | 1.094187228 | 0.660667028 |
| prohibitin-2 [Bos taurus] | 2.4891 | 0.6032175 | 2.721525 | 0.42832117 | 1.093377124 | 0.781981315 |
| PREDICTED: 3-hydroxybutyrate dehydrogenase type 2-like isoform 1 [Sus scrofa] | 2.285855 | 0.64932137 | 2.496075 | 0.30248977 | 1.091965588 | 0.820826869 |
| PREDICTED: unconventional myosin-Ic [Sus scrofa] | 22.6025 | 3.57810198 | 24.67525 | 4.35537496 | 1.091704457 | 0.680428527 |
| PREDICTED: myosin-9 [Felis catus] | 111.4875 | 0.91799033 | 121.61 | 4.62177996 | 1.090794932 | 0.107402993 |
| PREDICTED: filamin-A isoform X2 [Bos mutus] | 553.145 | 15.2830879 | 603.2 | 8.21748846 | 1.090491643 | 0.056319923 |
| PREDICTED: filamin-A isoform 2 [Trichechus manatus latirostris] | 533.665 | 14.7728543 | 580.8575 | 9.06294597 | 1.088430945 | 0.05469397 |
| PREDICTED: filamin-A isoform X2 [Pteropus alecto] | 581.04 | 16.0971369 | 631.38 | 10.1905405 | 1.086637753 | 0.070615551 |

| Protein Name | Control MEAN | Control SEM | Leptin MEAN | Leptin SEM | Ratio (Leptin/Control) | P value |
|---|--------------|-------------|-------------|------------|------------------------|-------------|
| PREDICTED: filamin-A isoform 2 [Canis lupus familiaris] | 587.8475 | 16.2863754 | 637.7625 | 9.7739376 | 1.084911478 | 0.084979188 |
| ubiquitin carboxyl-terminal hydrolase isozyme L1 [Sus scrofa] | 2.280955 | 1.06315581 | 2.4726 | 0.98331121 | 1.084019632 | 0.806931595 |
| proteasome (prosome, macropain) subunit, alpha type [Sus scrofa] | 2.045705 | 0.9520061 | 2.217265 | 0.71017819 | 1.083863509 | 0.613353384 |
| PREDICTED: ATP-dependent RNA helicase DDX3X isoform X1 [Galeopterus variegatus] | 5.0301 | 0.42781927 | 5.433125 | 0.77968441 | 1.080122662 | 0.668850776 |
| non-specific lipid-transfer protein [Sus scrofa] | 3.0158 | 0.41391385 | 3.25305 | 0.31587818 | 1.07866901 | 0.263941308 |
| PREDICTED: 14-3-3 protein theta isoform X1 [Monodelphis domestica] | 7.865 | 1.0925427 | 8.47325 | 0.34298231 | 1.0773363 | 0.578377479 |
| PREDICTED: calpain-2 catalytic subunit-like [Oryctolagus cuniculus] | 1.545775 | 1.545775 | 1.665125 | 0.97625674 | 1.077210461 | 0.920044005 |
| PREDICTED: cysteine and glycine-rich protein 1-like isoform 1 [Sus scrofa] | 78.18575 | 8.35505995 | 84.20575 | 2.01887004 | 1.076996128 | 0.431408645 |
| PREDICTED: filamin-A [Sorex araneus] | 515.105 | 12.1973307 | 554.6625 | 6.91957414 | 1.076795022 | 0.051417459 |
| PREDICTED: LOW QUALITY PROTEIN: filamin-A [Equus caballus] | 571.795 | 13.0916497 | 615.625 | 9.97395316 | 1.076653346 | 0.075390125 |
| hypothetical protein PANDA_005634 [Ailuropoda melanoleuca] | 11.3304 | 0.94679677 | 12.19175 | 0.52417274 | 1.076021147 | 0.472052855 |

| Protein Name | Control MEAN | Control SEM | Leptin MEAN | Leptin SEM | Ratio (Leptin/Control) | P value |
|--|--------------|-------------|-------------|------------|------------------------|-------------|
| PREDICTED: myosin light chain kinase, smooth muscle [Ursus maritimus] | 13.8345 | 1.37748711 | 14.871 | 1.6063071 | 1.074921392 | 0.68482649 |
| PREDICTED: prohibitin [Oryctolagus cuniculus] | 6.003675 | 0.83774931 | 6.451575 | 0.36082733 | 1.074604305 | 0.701972403 |
| PREDICTED: filamin-A [Odobenus rosmarus divergens] | 541.91 | 16.0226772 | 582.3225 | 16.9593491 | 1.074574191 | 0.138609386 |
| proteasome activator complex subunit 2 [Sus scrofa] | 2.27555 | 0.6660169 | 2.44415 | 0.57821994 | 1.074091978 | 0.884541193 |
| PREDICTED: tubulin beta chain-like [Tursiops truncatus] | 57.8905 | 2.14919948 | 62.1595 | 3.77151721 | 1.073742669 | 0.366724161 |
| SH3 domain-binding glutamic acid-rich-like protein 3 [Homo sapiens] | 3.273425 | 0.27149294 | 3.514475 | 0.57458207 | 1.073638467 | 0.504061753 |
| beta-actin [Oryctolagus cuniculus] | 145.2225 | 7.9113077 | 155.43 | 4.41626728 | 1.070288695 | 0.232248219 |
| PREDICTED: 2-oxoglutarate dehydrogenase, mitochondrial-like [Ailuropoda melanoleuca] | 0.729925 | 0.45489984 | 0.779025 | 0.49602796 | 1.067267185 | 0.947583602 |
| desmin [Sus scrofa] | 266.23 | 12.0357419 | 284.055 | 4.32476685 | 1.066953386 | 0.320722843 |
| PREDICTED: collagen alpha-1(I) chain isoform 1 [Ceratotherium simum simum] | 6.886825 | 2.10183644 | 7.339525 | 1.66854868 | 1.06573421 | 0.892126711 |
| ras-related protein Rap-1A precursor [Homo sapiens] | 16.085 | 0.31829206 | 17.1235 | 0.9693273 | 1.064563258 | 0.269964172 |
| glutathione peroxidase 1 [Sus scrofa] | 3.057405 | 0.84509252 | 3.250425 | 0.30453486 | 1.06313197 | 0.83461508 |
| Chain A, Refined Crystal Structure Of Cytoplasmic Malate Dehydrogenase At 2.5-Angstroms Resolution | 6.76035 | 0.5267832 | 7.186525 | 1.3172269 | 1.063040375 | 0.711633973 |

| Protein Name | Control MEAN | Control SEM | Leptin MEAN | Leptin SEM | Ratio (Leptin/Control) | P value |
|--|--------------|-------------|-------------|------------|------------------------|-------------|
| PREDICTED: myosin-11-like, partial [Sus scrofa] | 95.7635 | 7.03697218 | 101.47575 | 1.97985809 | 1.059649553 | 0.458999714 |
| PREDICTED: collagen alpha-3(VI) chain isoformX2 [Sus scrofa] | 104.42875 | 21.0385481 | 110.433 | 18.6325441 | 1.05749614 | 0.802750381 |
| PREDICTED: T-complex protein 1 subunit eta [Sarcophilus harrisii] | 3.050875 | 0.76592902 | 3.225775 | 0.18039649 | 1.057327816 | 0.833519327 |
| PREDICTED: talin-1 [Camelus ferus] | 117.6355 | 8.13962327 | 124.305 | 5.19469682 | 1.05669632 | 0.1941455 |
| ATP synthase, H+ transporting, mitochondrial Fo complex, subunit d [Sus scrofa] | 7.04805 | 0.46521602 | 7.444125 | 0.80002689 | 1.056196395 | 0.762877979 |
| PREDICTED: mitochondrial fission 1 protein [Equus caballus] | 3.30475 | 0.69172677 | 3.4872 | 0.2922566 | 1.055208412 | 0.827192145 |
| ATP synthase subunit f, mitochondrial [Sus scrofa] | 4.045 | 0.46439077 | 4.2636 | 0.70049605 | 1.054042027 | 0.756295952 |
| PREDICTED: poly(rC)-binding protein 1 isoform X1 [Sus scrofa] | 3.79245 | 0.79946386 | 3.98015 | 0.37608683 | 1.049493072 | 0.778053669 |
| PREDICTED: alpha-actinin-4 isoformX2 [Sus scrofa] | 96.687 | 11.0438724 | 101.31425 | 14.4406351 | 1.047858037 | 0.421831439 |
| PREDICTED: guanine nucleotide-binding protein subunit beta-2-like 1 [Trichechus manatus latirostris] | 3.074905 | 1.27936489 | 3.214475 | 0.70079436 | 1.04539002 | 0.831336635 |
| PREDICTED: phosphatidylethanolamine-binding protein 1 [Sus scrofa] | 27.20875 | 1.51188714 | 28.338 | 0.58650504 | 1.041503193 | 0.370896738 |
| PREDICTED: nucleolin-like [Sus scrofa] | 4.2886 | 0.68195489 | 4.4632 | 0.45369991 | 1.040712587 | 0.814924039 |

| Protein Name | Control MEAN | Control SEM | Leptin MEAN | Leptin SEM | Ratio (Leptin/Control) | P value |
|--|--------------|-------------|-------------|------------|------------------------|-------------|
| PDZ and LIM domain protein 1 [Sus scrofa] | 13.91705 | 1.5453354 | 14.481 | 0.65814829 | 1.040522237 | 0.711837576 |
| RecName: Full=Tubulin beta chain; AltName: Full=Beta-tubulin [Sus scrofa] | 44.465 | 0.68683186 | 46.14625 | 2.07191322 | 1.037810638 | 0.369871172 |
| PREDICTED: ras-related protein Rab-5A [Monodelphis domestica] | 3.6078 | 1.36941737 | 3.743375 | 0.50890497 | 1.037578303 | 0.909219577 |
| PREDICTED: tropomyosin alpha-3 chain-like, partial [Bubalus bubalis] | 50.8085 | 2.24638408 | 52.70225 | 0.63518939 | 1.037272307 | 0.515079117 |
| RecName: Full=Actin, cytoplasmic 1; AltName: Full=Beta-actin; Contains: RecName: Full=Actin, cytoplasmic 1, N-terminally processed [Bos grunniens] | 759.3025 | 23.0702039 | 786.86 | 18.2428365 | 1.036293177 | 0.464742184 |
| PREDICTED: LOW QUALITY PROTEIN: talin-1 [Sus scrofa] | 117.1105 | 8.12752506 | 121.3175 | 5.80936367 | 1.035923337 | 0.346893093 |
| PREDICTED: myosin-11 isoform 1 [Dasypus novemcinctus] | 409.3675 | 37.4415434 | 423.8775 | 17.9360207 | 1.035444924 | 0.588460147 |
| ras suppressor protein 1 [Ovis aries] | 17.72525 | 2.25756518 | 18.33625 | 1.22885261 | 1.0344706 | 0.721147869 |
| PREDICTED: collagen alpha-1(XVIII) chain, partial [Sus scrofa] | 7.309425 | 0.57117644 | 7.559875 | 1.36303208 | 1.034263981 | 0.87260921 |
| PREDICTED: cysteine-rich protein 2 [Orcinus orca] | 11.363625 | 1.17595829 | 11.74215 | 0.82964448 | 1.033310233 | 0.455974522 |
| PREDICTED: polyubiquitin-B-like [Elephantulus edwardii] | 18.70025 | 2.21261205 | 19.28325 | 2.46988422 | 1.031176054 | 0.774019783 |

| Protein Name | Control MEAN | Control SEM | Leptin MEAN | Leptin SEM | Ratio (Leptin/Control) | P value |
|--|--------------|-------------|-------------|------------|------------------------|-------------|
| PREDICTED: prolargin isoform X1 [Sus scrofa] | 37.17225 | 3.76657985 | 38.28075 | 1.5915955 | 1.029820632 | 0.695980185 |
| PREDICTED: creatine kinase B-type [Canis lupus familiaris] | 25.561 | 1.39036368 | 26.29925 | 1.62741735 | 1.02888189 | 0.822472656 |
| PREDICTED: myosin-11 isoform X1 [Camelus ferus] | 481.145 | 46.075851 | 493.52 | 22.189093 | 1.025719897 | 0.721919941 |
| PREDICTED: cell division control protein 42 homolog [Equus caballus] | 7.27155 | 1.07075706 | 7.45485 | 0.42612188 | 1.025207831 | 0.809061989 |
| PREDICTED: tubulointerstitial nephritis antigen-like 1 isoform X1 [Sus scrofa] | 4.2156 | 0.92422259 | 4.314675 | 1.42388903 | 1.023501993 | 0.960395363 |
| PREDICTED: actin, alpha cardiac muscle 1, partial [Ovis aries] | 1167.65 | 34.353566 | 1194.55 | 50.8746417 | 1.023037725 | 0.697189911 |
| PREDICTED: 60S ribosomal protein L15 isoform X3 [Gallus gallus] | 1.002755 | 0.41514941 | 1.02449 | 0.42727959 | 1.021675285 | 0.248971411 |
| beta-actin, partial [Eubalaena glacialis] | 810.49 | 23.6480024 | 828.025 | 18.3145154 | 1.02163506 | 0.643088375 |
| tenascin precursor [Sus scrofa] | 1.940025 | 1.00866848 | 1.981075 | 0.71548314 | 1.021159521 | 0.953802824 |
| transgelin [Sus scrofa] | 405.495 | 31.3765065 | 413.9625 | 34.1881535 | 1.020881885 | 0.760187956 |
| PREDICTED: myosin-11 isoform 1 [Ceratottherium simum simum] | 453.2575 | 42.0935746 | 462.49 | 17.095224 | 1.020369216 | 0.78111452 |
| PREDICTED: sepiapterin reductase [Sus scrofa] | 8.532275 | 0.83841287 | 8.701475 | 0.97388836 | 1.019830584 | 0.806245496 |
| PREDICTED: protein kinase C delta-binding protein-like [Sus scrofa] | 11.85065 | 1.38848759 | 12.073625 | 2.30546031 | 1.018815424 | 0.871722529 |

| Protein Name | Control MEAN | Control SEM | Leptin MEAN | Leptin SEM | Ratio (Leptin/Control) | P value |
|---|--------------|-------------|-------------|------------|------------------------|-------------|
| PREDICTED: haloacid dehalogenase-like hydrolase domain-containing protein 2 isoform X1 [Equus caballus] | 0.765375 | 0.48680041 | 0.779025 | 0.49602796 | 1.017834395 | 0.986172946 |
| PREDICTED: heat shock cognate 71 kDa protein [Loxodonta africana] | 28.618 | 1.09609078 | 29.089 | 0.67896183 | 1.016458173 | 0.468032315 |
| PREDICTED: myosin-11 isoform X2 [Mustela putorius furo] | 466.81 | 42.2603603 | 474.3125 | 21.6496183 | 1.016071849 | 0.791903312 |
| PREDICTED: myosin-11 isoform X3 [Bubalus bubalis] | 493.7775 | 44.4286464 | 501.3925 | 21.9039283 | 1.015421926 | 0.825630595 |
| transaldolase [Sus scrofa] | 6.598425 | 0.97889853 | 6.69705 | 0.52799021 | 1.014946749 | 0.933594724 |
| PREDICTED: myosin-11 isoform X2 [Bubalus bubalis] | 503.525 | 45.2117803 | 510.3625 | 21.1845484 | 1.013579266 | 0.845497809 |
| PREDICTED: beta-actin-like protein 2 [Sarcophilus harrisii] | 574.9525 | 21.8765759 | 582.335 | 8.8715552 | 1.012840191 | 0.797849738 |
| PREDICTED: LOW QUALITY PROTEIN: calponin 1, basic, smooth muscle [Dasypus novemcinctus] | 17.7025 | 3.37865075 | 17.922 | 1.90815386 | 1.012399379 | 0.963187102 |
| PREDICTED: 14-3-3 protein epsilon isoform X1 [Oryctolagus cuniculus] | 7.60865 | 1.17255664 | 7.69365 | 1.27219129 | 1.011171496 | 0.930927139 |
| 15 kDa selenoprotein precursor [Sus scrofa] | 0.74888 | 0.25054158 | 0.7570025 | 0.49656999 | 1.010846197 | 0.989658351 |
| PREDICTED: inter-alpha-trypsin inhibitor heavy chain H5-like [Sus scrofa] | 4.33775 | 1.10838832 | 4.3799425 | 1.99113501 | 1.009726817 | 0.985849628 |
| PREDICTED: myosin regulatory light polypeptide 9 isoform X2 [Elephantulus edwardii] | 34.9375 | 5.60404634 | 35.23025 | 2.68430902 | 1.008379249 | 0.945990554 |

| Protein Name | Control MEAN | Control SEM | Leptin MEAN | Leptin SEM | Ratio (Leptin/Control) | P value |
|---|--------------|-------------|-------------|------------|------------------------|-------------|
| actin related protein 2/3 complex subunit 1B [Bos taurus] | 0.74643 | 0.24960188 | 0.7517525 | 0.49187288 | 1.007130608 | 0.994560992 |
| PREDICTED: myosin-11 isoform X31 [Canis lupus familiaris] | 478.2975 | 43.3625667 | 481.6825 | 20.076938 | 1.007077185 | 0.910067121 |
| PREDICTED: myosin-11 isoform X4 [Physeter catodon] | 477.3425 | 42.7105862 | 479.9275 | 19.3345767 | 1.005415399 | 0.934532054 |
| PREDICTED: phosphatidylethanolamine-binding protein 1 [Ovis aries] | 18.335 | 1.39998661 | 18.43075 | 1.30662398 | 1.005222253 | 0.960720388 |
| PREDICTED: myosin-11 [Felis catus] | 469.2275 | 39.9691678 | 471.6775 | 19.507573 | 1.005221348 | 0.927346831 |
| neuroplastin precursor [Bos taurus] | 0.9838 | 0.38450823 | 0.988525 | 0.38354477 | 1.004802805 | 0.995465867 |
| high mobility group protein B2 [Homo sapiens] | 0.51525 | 0.51525 | 0.5176 | 0.5176 | 1.004560893 | 0.997951554 |
| PREDICTED: laminin subunit beta-1 isoform X1 [Sus scrofa] | 1.76535 | 0.64901617 | 1.772775 | 0.88997059 | 1.004205965 | 0.996249334 |
| PREDICTED: LOW QUALITY PROTEIN: laminin subunit alpha-4 [Sus scrofa] | 6.491125 | 1.25621669 | 6.516825 | 0.97721846 | 1.003959252 | 0.985502692 |
| 40S ribosomal protein S9 [Homo sapiens] | 1.5407 | 0.66266705 | 1.54469 | 0.67863814 | 1.002589732 | 0.997158433 |
| TPA: alpha-actinin-2 [Bos taurus] | 22.3635 | 8.05206591 | 22.404 | 8.1956671 | 1.001810987 | 0.984826227 |
| Chain A, Structure Of Camp-Dependent Protein Kinase Complexed With A- 443654 | 2.48665 | 0.59955131 | 2.489975 | 0.28816698 | 1.00133714 | 0.996983515 |
| CLTLB protein [Bos taurus] | 0 | 0 | 0.7271 | 0.4533045 | #DIV/0! | 0.207050872 |
| PREDICTED: chaperonin CPN60-1, mitochondrial-like, partial [Lipotes vexillifer] | 0 | 0 | 0.485675 | 0.485675 | #DIV/0! | 0.391002219 |

| Protein Name | Control MEAN | Control SEM | Leptin MEAN | Leptin SEM | Ratio (Leptin/Control) | P value |
|--|--------------|-------------|-------------|------------|------------------------|-------------|
| ELAV-like protein 1 [Sus scrofa] | 0 | 0 | 0.4683 | 0.4683 | #DIV/0! | 0.391002219 |
| PREDICTED: lamin-B1 isoform X1 [Sus scrofa] | 0 | 0 | 0.4683 | 0.4683 | #DIV/0! | 0.391002219 |
| fatty acid synthase [Sus scrofa] | 6.160875 | 2.88207528 | 0.5176 | 0.5176 | -11.90277241 | 0.098587972 |
| PREDICTED: delta-1-pyrroline-5-carboxylate dehydrogenase, mitochondrial [Galeopterus variegatus] | 1.24765 | 0.47406619 | 0.24284 | 0.24284 | -5.137745017 | 0.099491641 |
| ERO1-like protein alpha precursor [Sus scrofa] | 1.238975 | 0.47177585 | 0.2588 | 0.2588 | -4.78738408 | 0.261005804 |
| fibrinogen A-alpha-chain [Sus scrofa] | 1.237675 | 0.46654509 | 0.261425 | 0.261425 | -4.734340633 | 0.084691496 |
| PREDICTED: LOW QUALITY PROTEIN: prolown-density lipoprotein receptor-related protein 1 [Oryctolagus cuniculus] | 3.28095 | 0.66484621 | 0.763065 | 0.25488478 | -4.299699239 | 0.069659192 |
| PREDICTED: adenosine deaminase [Sus scrofa] | 0.98755 | 0.38462955 | 0.2341525 | 0.2341525 | -4.217550528 | 0.187408776 |
| Chain A, C28s Mutant Of Succinyl-Coa:3-Ketoacid Coa Transferase From Pig Heart | 4.20285 | 1.33200503 | 0.9972175 | 0.026037 | -4.214577061 | 0.095570026 |
| cAMP-dependent protein kinase type I-alpha regulatory subunit [Bos taurus] | 1.01273 | 0.42542412 | 0.24284 | 0.24284 | -4.170359084 | 0.222501527 |
| PREDICTED: ribonuclease UK114 isoform 1 [Sus scrofa] | 1.023 | 0.59066107 | 0.2588 | 0.2588 | -3.952859351 | 0.393940074 |
| calnexin precursor [Sus scrofa] | 2.702625 | 1.1711954 | 0.7384175 | 0.24718843 | -3.660022954 | 0.19165605 |
| fumarate hydratase [Sus scrofa] | 1.75165 | 0.63701833 | 0.4955775 | 0.28698701 | -3.534563212 | 0.18470584 |

| Protein Name | Control MEAN | Control SEM | Leptin MEAN | Leptin SEM | Ratio (Leptin/Control) | P value |
|---|--------------|-------------|-------------|------------|------------------------|-------------|
| Chain A, Fructose-1,6-Bisphosphatase (Mutant Y57w) ProductZN COMPLEX (R-State) | 1.746725 | 0.63618883 | 0.4955775 | 0.28698701 | -3.524625311 | 0.072520899 |
| PREDICTED: atlastin-3 [Sus scrofa] | 0.775325 | 0.4937467 | 0.2341525 | 0.2341525 | -3.311196763 | 0.18217009 |
| phospholipase C, delta 1 [Sus scrofa] | 0.77405 | 0.49698584 | 0.2341525 | 0.2341525 | -3.305751594 | 0.467192101 |
| PREDICTED: elongation factor Tu, mitochondrial [Equus caballus] | 0.77405 | 0.49698584 | 0.2341525 | 0.2341525 | -3.305751594 | 0.467192101 |
| PREDICTED: endoplasmic reticulum resident protein 29 [Sus scrofa] | 0.772875 | 0.772875 | 0.2341525 | 0.2341525 | -3.300733496 | 0.391002219 |
| Dihydrolipoyl dehydrogenase, mitochondrial [Tupaia chinensis] | 3.237975 | 0.69689868 | 0.9859 | 0.57063117 | -3.284283396 | 0.093472785 |
| dihydrolipoyl dehydrogenase, mitochondrial precursor [Sus scrofa] | 4.523525 | 0.66128086 | 1.46814 | 0.61851502 | -3.081126459 | 0.096019624 |
| PREDICTED: lysosome-associated membrane glycoprotein 1 isoform X1 [Sus scrofa] | 2.97415 | 0.75157072 | 0.96994 | 0.38307126 | -3.06632369 | 0.140625466 |
| heat shock protein 90 beta [Equus caballus] | 12.534 | 1.05647772 | 4.177775 | 2.41222845 | -3.000161569 | 0.053270731 |
| PREDICTED: 14 kDa phosphohistidine phosphatase isoform X2 [Sus scrofa] | 0.769125 | 0.49267537 | 0.2588 | 0.2588 | -2.97188949 | 0.498788177 |
| PREDICTED: LOW QUALITY PROTEIN: cytoplasmic dynein 1 heavy chain 1 [Sus scrofa] | 7.75825 | 4.64716656 | 2.67125 | 2.67125 | -2.904351895 | 0.49233898 |

| Protein Name | Control MEAN | Control SEM | Leptin MEAN | Leptin SEM | Ratio (Leptin/Control) | P value |
|--|--------------|-------------|-------------|------------|------------------------|-------------|
| PREDICTED: tubulointerstitial nephritis antigen-like isoform X1 [Lipotes vexillifer] | 3.725475 | 1.28550436 | 1.294 | 1.294 | -2.879037867 | 0.188312399 |
| LIM and cysteine-rich domains protein 1 [Sus scrofa] | 4.493775 | 1.6794797 | 1.675015 | 1.03056686 | -2.682826721 | 0.184931023 |
| PREDICTED: cytochrome P450 1B1-like, partial [Sus scrofa] | 5.94365 | 2.76569313 | 2.257875 | 1.13238106 | -2.632408791 | 0.111360356 |
| Chain B, Structure Determination Of Aquomet Porcine Hemoglobin At 2.8 Angstrom Resolution | 87.1385 | 38.5343127 | 33.2095 | 8.28249482 | -2.623902799 | 0.216870632 |
| hemoglobin subunit beta [Sus scrofa] | 86.90725 | 38.7152766 | 33.16875 | 7.65392652 | -2.620154513 | 0.225976476 |
| RecName: Full=Hemoglobin subunit alpha; AltName: Full=Alpha-globin; AltName: Full=Hemoglobin alpha chain [Sus scrofa] | 39.1875 | 11.9733243 | 15.188975 | 3.3727781 | -2.579996346 | 0.131069506 |
| RecName: Full=Aminopeptidase N; Short=AP-N; Short=pAPN; AltName: Full=Alanyl aminopeptidase; AltName: Full=Aminopeptidase M; Short=AP-M; AltName: Full=Microsomal aminopeptidase; AltName: Full=gp130; AltName: CD_antigen=CD13 [Sus scrofa] | 4.330225 | 0.92479788 | 1.6837 | 0.79391971 | -2.571850686 | 0.17785867 |

| Protein Name | Control MEAN | Control SEM | Leptin MEAN | Leptin SEM | Ratio (Leptin/Control) | P value |
|---|--------------|-------------|-------------|------------|------------------------|-------------|
| Chain A, Crystallographic Refinement And Atomic Models Of Two Different Forms Of Citrate Synthase At 2.7 And 1.7 Angstroms Resolution | 4.47815 | 1.27738105 | 1.75419 | 0.50465304 | -2.552830651 | 0.185699335 |
| ribosomal protein S6 (predicted) [Dasypus novemcinctus] | 1.279325 | 0.63761448 | 0.5176 | 0.5176 | -2.471647991 | 0.445736625 |
| Syntenin-1 [Pteropus alecto] | 1.7616 | 0.49606935 | 0.7357925 | 0.2461123 | -2.394153243 | 0.0870198 |
| clusterin precursor [Sus scrofa] | 2.9704 | 1.04180222 | 1.269925 | 0.77265852 | -2.33903577 | 0.106090262 |
| PREDICTED: integrin alpha-8 [Sus scrofa] | 5.181775 | 1.4286791 | 2.231175 | 0.47160187 | -2.322442211 | 0.16969718 |
| PREDICTED: UDP-glucose 6-dehydrogenase isoform 1 [Sus scrofa] | 4.5387 | 1.00265705 | 1.95584 | 0.88140816 | -2.320588596 | 0.205792828 |
| 3-ketoacyl-CoA thiolase, mitochondrial [Sus scrofa] | 1.76405 | 0.88658111 | 0.763065 | 0.25488478 | -2.311795194 | 0.269627441 |
| PREDICTED: 40S ribosomal protein S2 [Equus caballus] | 1.788375 | 1.05135134 | 0.779025 | 0.49602796 | -2.295658034 | 0.479719854 |
| PREDICTED: high mobility group protein B1 isoform X2 [Monodelphis domestica] | 2.243075 | 0.86308633 | 0.9859 | 0.57063117 | -2.275154681 | 0.343963829 |
| vesicle-associated membrane protein 3 [Bos taurus] | 2.7846 | 0.30212183 | 1.23399 | 0.47744521 | -2.256582306 | 0.060640028 |
| dihydrolipoamide dehydrogenase [Sus scrofa] | 2.250425 | 0.46706264 | 0.9998425 | 0.42778425 | -2.250779498 | 0.197948978 |
| apolipoprotein A-I [Sus scrofa] | 2.238 | 0.73921755 | 0.9972175 | 0.026037 | -2.244244611 | 0.186946687 |

| Protein Name | Control MEAN | Control SEM | Leptin MEAN | Leptin SEM | Ratio (Leptin/Control) | P value |
|--|--------------|-------------|-------------|------------|------------------------|-------------|
| S-phase kinase-associated protein 1 isoform b [Homo sapiens] | 0.520175 | 0.520175 | 0.2341525 | 0.2341525 | -2.221522299 | 0.684174184 |
| PREDICTED: cytochrome b-c1 complex subunit 2, mitochondrial-like [Sus scrofa] | 2.18115 | 1.15239462 | 0.987325 | 0.68704532 | -2.209150989 | 0.12445382 |
| PREDICTED: annexin A8-like [Monodelphis domestica] | 0.51525 | 0.51525 | 0.2341525 | 0.2341525 | -2.200488998 | 0.391002219 |
| heterogeneous nuclear ribonucleoprotein H3 isoform a [Homo sapiens] | 1.031675 | 0.42476168 | 0.4769925 | 0.27548309 | -2.162874678 | 0.456668256 |
| PREDICTED: spectrin beta chain, non-erythrocytic 1 isoform X1 [Equus caballus] | 4.018225 | 1.25488674 | 1.939875 | 0.76614252 | -2.071383465 | 0.241379766 |
| 60S ribosomal protein L9 [Homo sapiens] | 1.539425 | 0.65784292 | 0.744475 | 0.46804115 | -2.067799456 | 0.495705299 |
| signal peptidase complex catalytic subunit SEC11A isoform 6 [Homo sapiens] | 1.01273 | 0.42542412 | 0.4929525 | 0.28531688 | -2.054417008 | 0.154625988 |
| PREDICTED: fumarylacetoacetate hydrolase domain-containing protein 2-like [Sus scrofa] | 1.543175 | 0.51449313 | 0.7543775 | 0.25265658 | -2.045627024 | 0.058477265 |
| RPL35 [Sus scrofa] | 1.02545 | 0.41462076 | 0.50164 | 0.28991501 | -2.04419504 | 0.477810785 |
| actin-related protein 2/3 complex subunit 2 [Sus scrofa] | 2.5345 | 0.6831894 | 1.2400525 | 0.23550094 | -2.043865078 | 0.206727527 |
| PREDICTED: peptidyl-prolyl cis-trans isomerase D [Equus caballus] | 2.014325 | 0.73071291 | 0.9972175 | 0.026037 | -2.019945498 | 0.270492921 |

| Protein Name | Control MEAN | Control SEM | Leptin MEAN | Leptin SEM | Ratio (Leptin/Control) | P value |
|--|--------------|-------------|-------------|------------|------------------------|-------------|
| PREDICTED: malectin [Equus caballus] | 0.98755 | 0.38462955 | 0.4955775 | 0.28698701 | -1.992725658 | 0.491216636 |
| 2,4-dienoyl-CoA reductase 1 [Sus scrofa] | 0.520175 | 0.520175 | 0.261425 | 0.261425 | -1.98976762 | 0.719397173 |
| annexin A7 [Bos taurus] | 5.40275 | 2.19368687 | 2.748775 | 0.27861618 | -1.96551191 | 0.353795202 |
| PREDICTED: pre-B-cell leukemia transcription factor-interacting protein 1 [Sus scrofa] | 1.52913 | 0.9072751 | 0.779025 | 0.49602796 | -1.962876673 | 0.230846412 |
| surfeit locus protein 4 [Bos taurus] | 1.48505 | 0.85960435 | 0.76044 | 0.49303655 | -1.952882542 | 0.20488549 |
| delta-sarcoglycan [Sus scrofa] | 0.50775 | 0.50775 | 0.261425 | 0.261425 | -1.942239648 | 0.391002219 |
| PREDICTED: fibrinogen beta chain isoform X2 [Sus scrofa] | 0.46985 | 0.46985 | 0.24284 | 0.24284 | -1.934813046 | 0.391002219 |
| glycogen phosphorylase, liver form [Sus scrofa] | 4.784925 | 0.66381636 | 2.489975 | 0.28816698 | -1.92167592 | 0.081124968 |
| PREDICTED: dihydrolipoyl dehydrogenase, mitochondrial isoform X1 [Eptesicus fuscus] | 3.751925 | 0.72770203 | 1.98574 | 0.37929463 | -1.889434166 | 0.18441278 |
| ras-related protein Rap-2b precursor [Mus musculus] | 2.2731 | 0.28541387 | 1.206715 | 0.58504704 | -1.883709078 | 0.271383643 |
| PREDICTED: heat shock protein HSP 90-beta-like [Leptonychotes weddellii] | 3.216875 | 1.15546044 | 1.713 | 0.99761333 | -1.877918856 | 0.51026988 |
| Calpain-2 catalytic subunit [Myotis davidii] | 5.83305 | 0.86020099 | 3.2072 | 0.40886266 | -1.818735969 | 0.069826564 |
| guanine nucleotide-binding protein G(I)/G(S)/G(T) subunit beta-2 [Mus musculus] | 2.846175 | 1.6554083 | 1.568525 | 1.568525 | -1.814555076 | 0.685301003 |
| PREDICTED: myosin-10 isoform X5 [Camelus ferus] | 100.2375 | 34.0291371 | 55.46175 | 32.7072011 | -1.807326671 | 0.187828002 |

| Protein Name | Control MEAN | Control SEM | Leptin MEAN | Leptin SEM | Ratio (Leptin/Control) | P value |
|--|--------------|-------------|-------------|------------|------------------------|-------------|
| histone H1.0 [Bos taurus] | 1.79705 | 0.64165417 | 0.9972175 | 0.026037 | -1.802064244 | 0.293040893 |
| PREDICTED: very long-chain specific acyl-CoA dehydrogenase, mitochondrial-like isoform X3 [Sus scrofa] | 1.780555 | 0.51064514 | 0.9972175 | 0.026037 | -1.785523218 | 0.207928031 |
| Spectrin alpha chain, brain [Myotis brandtii] | 9.282 | 1.36351891 | 5.20365 | 1.37619799 | -1.783747946 | 0.079628982 |
| dolichyl-diphosphooligosaccharide--protein glycosyltransferase subunit 1 precursor [Sus scrofa] | 6.96365 | 1.30327525 | 3.97145 | 0.7585914 | -1.753427589 | 0.206486857 |
| 40S ribosomal protein S3 isoform 1 [Homo sapiens] | 3.0839 | 1.10860328 | 1.7602775 | 0.27651465 | -1.75193968 | 0.375746643 |
| hypothetical protein PANDA_006316 [Ailuropoda melanoleuca] | 1.78705 | 1.12360856 | 1.02709 | 0.73963131 | -1.739915684 | 0.304683022 |
| aspartate aminotransferase, mitochondrial precursor [Sus scrofa] | 12.930525 | 3.15164855 | 7.446175 | 0.5367193 | -1.736532515 | 0.211204304 |
| PREDICTED: prenylcysteine oxidase 1 isoform X1 [Sus scrofa] | 3.445325 | 1.07245777 | 1.994425 | 0.05207953 | -1.727477844 | 0.279273618 |
| thy-1 membrane glycoprotein precursor [Sus scrofa] | 2.526975 | 0.32394161 | 1.465515 | 0.44839593 | -1.724291461 | 0.206306058 |
| hypothetical protein PANDA_002264 [Ailuropoda melanoleuca] | 2.9844 | 0.89501823 | 1.735625 | 0.23786866 | -1.719495859 | 0.175885816 |
| albumin [Sus scrofa] | 12.107375 | 3.56451879 | 7.057025 | 1.21945976 | -1.715648591 | 0.239224044 |
| integrin alpha-7 [Bos taurus] | 5.15045 | 1.79271426 | 3.002925 | 0.59975777 | -1.715144401 | 0.256087414 |

| Protein Name | Control MEAN | Control SEM | Leptin MEAN | Leptin SEM | Ratio (Leptin/Control) | P value |
|---|--------------|-------------|-------------|------------|------------------------|-------------|
| PREDICTED: ATP synthase subunit beta, mitochondrial [Sus scrofa] | 43.737 | 7.77338482 | 25.5665 | 2.38792562 | -1.710715194 | 0.094175489 |
| GTP-binding protein SAR1a [Mus musculus] | 2.547255 | 0.67892223 | 1.490165 | 0.28137997 | -1.709377821 | 0.186016784 |
| Chain E, Structure Of Bovine Heart Cytochrome C Oxidase At The Fully Oxidized State | 2.51425 | 0.6619073 | 1.471575 | 0.49222164 | -1.708543567 | 0.077002703 |
| PREDICTED: transmembrane emp24 domain-containing protein 9 [Equus caballus] | 2.50805 | 0.27385404 | 1.4829025 | 0.47769807 | -1.691311465 | 0.105311968 |
| PREDICTED: membrane primary amine oxidase [Sus scrofa] | 81.58075 | 13.950869 | 48.797 | 8.10738263 | -1.671839457 | 0.108289056 |
| PREDICTED: LOW QUALITY PROTEIN: oligoribonuclease, mitochondrial [Canis lupus familiaris] | 2.4602 | 0.78436331 | 1.4742 | 0.25083635 | -1.668837336 | 0.272196413 |
| collagen, type I, alpha 2 precursor [Sus scrofa] | 5.182925 | 1.76495656 | 3.10799 | 1.65908684 | -1.667613152 | 0.45305447 |
| PREDICTED: fibrillin-1 isoform 1 [Orcinus orca] | 48.58975 | 10.3163756 | 29.29875 | 11.5011143 | -1.658423994 | 0.126457917 |
| PREDICTED: microfibril-associated glycoprotein 4 [Equus caballus] | 13.1784 | 2.0368127 | 7.967025 | 1.11113631 | -1.654118068 | 0.069421647 |
| PREDICTED: cytoplasmic FMR1-interacting protein 1 isoform 1 [Monodelphis domestica] | 1.2439 | 0.47465323 | 0.7543775 | 0.25265658 | -1.6489092 | 0.484483449 |
| PREDICTED: glucose-6-phosphate 1-dehydrogenase X-like isoform X1 [Sus scrofa] | 0.771575 | 0.25724221 | 0.4683 | 0.4683 | -1.647608371 | 0.550591044 |

| Protein Name | Control MEAN | Control SEM | Leptin MEAN | Leptin SEM | Ratio (Leptin/Control) | P value |
|--|--------------|-------------|-------------|------------|------------------------|-------------|
| plasma membrane Ca ²⁺ -ATPase isoform 4xb [Bos taurus] | 1.99035 | 0.36721019 | 1.212775 | 0.45380868 | -1.641153553 | 0.283772312 |
| 3-hydroxyisobutyrate dehydrogenase, mitochondrial precursor [Bos taurus] | 2.013025 | 0.04569851 | 1.22874 | 0.47432116 | -1.638283933 | 0.185806354 |
| PREDICTED: mitochondrial 2-oxoglutarate/malate carrier protein [Monodelphis domestica] | 1.245175 | 0.4708367 | 0.763065 | 0.25488478 | -1.631807251 | 0.518306661 |
| isocitrate dehydrogenase [NADP], mitochondrial [Sus scrofa] | 5.206925 | 1.16942107 | 3.201125 | 0.54474672 | -1.626592214 | 0.257010539 |
| PREDICTED: sideroflexin-3 isoform X1 [Canis lupus familiaris] | 2.01055 | 0.42105586 | 1.2426775 | 0.48719316 | -1.617917762 | 0.243460632 |
| PREDICTED: fibrillin-1 [Oryctolagus cuniculus] | 29.81475 | 12.4498705 | 18.47175 | 10.6884779 | -1.614072841 | 0.066145988 |
| PREDICTED: serpin H1 isoform X1 [Leptonychotes weddellii] | 11.484975 | 1.41216371 | 7.13815 | 1.10783476 | -1.608956803 | 0.087063905 |
| PREDICTED: fibrillin-1-like [Physeter catodon] | 35.98725 | 15.1869706 | 22.37725 | 12.9915466 | -1.608206996 | 0.069876657 |
| COP9 complex subunit 7a [Bos taurus] | 0.74888 | 0.25054158 | 0.4683 | 0.4683 | -1.599145847 | 0.722146909 |
| cytosolic non-specific dipeptidase [Sus scrofa] | 1.549375 | 0.67189723 | 0.96994 | 0.38307126 | -1.597392622 | 0.43624171 |
| PREDICTED: nidogen-2 [Sus scrofa] | 9.238175 | 1.22680194 | 5.837325 | 2.25145449 | -1.582604189 | 0.190963744 |
| Chain A, Structure Of Full Length Grp94 With Amp-Pnp Bound | 10.018525 | 1.27971735 | 6.379575 | 1.70023357 | -1.570406336 | 0.30329757 |
| PREDICTED: sushi domain-containing protein 2 [Sus scrofa] | 1.968925 | 0.64445403 | 1.2586425 | 0.27833549 | -1.564324262 | 0.452746172 |

| Protein Name | Control MEAN | Control SEM | Leptin MEAN | Leptin SEM | Ratio (Leptin/Control) | P value |
|--|--------------|-------------|-------------|------------|------------------------|-------------|
| PREDICTED: receptor expression-enhancing protein 5 [Sus scrofa] | 4.54625 | 0.57081005 | 2.92234 | 1.2392042 | -1.55568825 | 0.33775244 |
| PREDICTED: CD109 antigen isoformX1 [Sus scrofa] | 0.765375 | 0.48680041 | 0.4955775 | 0.28698701 | -1.544410309 | 0.341969737 |
| fibrillin-1 precursor [Sus scrofa] | 53.63 | 11.4266967 | 34.78075 | 10.5058638 | -1.541944898 | 0.102293382 |
| dolichyl-diphosphooligosaccharide--protein glycosyltransferase 48 kDa subunit precursor [Sus scrofa] | 3.001925 | 0.91254926 | 1.96715 | 0.36175354 | -1.526027502 | 0.189842154 |
| PREDICTED: aflatoxin B1 aldehyde reductase member 2-like [Sarcophilus harrisii] | 1.52048 | 0.30981711 | 0.9972175 | 0.026037 | -1.52472254 | 0.164268007 |
| PREDICTED: tumor protein D54 [Ochotona princeps] | 1.518005 | 0.30559001 | 0.9998425 | 0.42778425 | -1.518244123 | 0.210424098 |
| Chain A, Crystal Structure Of Pig Phosphoglucose Isomerase | 15.48825 | 2.45353291 | 10.220175 | 0.91843838 | -1.515458395 | 0.16336746 |
| PREDICTED: aconitate hydratase, mitochondrial [Oryctolagus cuniculus] | 7.90645 | 2.32859981 | 5.2408 | 1.38364799 | -1.508634178 | 0.244033665 |
| PRA1 family protein 2 [Bos taurus] | 1.539425 | 0.65784292 | 1.021865 | 0.42296105 | -1.50648569 | 0.478776288 |
| lactadherin precursor [Sus scrofa] | 42.047 | 3.42527267 | 28.00125 | 4.80928585 | -1.501611535 | 0.061125083 |
| PREDICTED: guanine nucleotide-binding protein G(k) subunit alpha [Monodelphis domestica] | 7.3107 | 1.09889986 | 4.8743 | 1.88306845 | -1.499846132 | 0.461689393 |
| calmodulin | 3.369875 | 2.38182598 | 2.257875 | 1.13238106 | -1.492498478 | 0.480047268 |

| Protein Name | Control MEAN | Control SEM | Leptin MEAN | Leptin SEM | Ratio (Leptin/Control) | P value |
|---|--------------|-------------|-------------|------------|------------------------|-------------|
| Chain A, Refinement And Comparison Of The Crystal Structures Of Pig Cytosolic Aspartate Aminotransferase And Its Complex With 2-Methylaspartate | 6.288025 | 0.88714647 | 4.222975 | 0.16682193 | -1.489003605 | 0.076628192 |
| caveolin-2 [Sus scrofa] | 3.022 | 0.43428616 | 2.043725 | 0.8459223 | -1.478672522 | 0.101384505 |
| prolyl 4-hydroxylase beta polypeptide [Sus scrofa] | 19.397 | 2.96928215 | 13.1419 | 1.58337236 | -1.475966184 | 0.226457793 |
| glutaredoxin-1 [Sus scrofa] | 0.771575 | 0.25724221 | 0.52285 | 0.52285 | -1.475710051 | 0.655834607 |
| neutral alpha-glucosidase AB precursor [Sus scrofa] | 2.5056 | 0.26573937 | 1.699665 | 0.68244269 | -1.474172852 | 0.222411534 |
| FAH protein [Bos taurus] | 0.729925 | 0.45489984 | 0.4955775 | 0.28698701 | -1.472877602 | 0.768747872 |
| PREDICTED: LOW QUALITY PROTEIN: nucleosome assembly protein 1-like 4 [Sus scrofa] | 1.778105 | 0.27964838 | 1.212775 | 0.45380868 | -1.466145823 | 0.444821955 |
| cytoskeleton-associated protein 4 [Sus scrofa] | 6.8309 | 0.95490761 | 4.675325 | 0.72326458 | -1.46105351 | 0.069109656 |
| sorting nexin-3 isoform a [Homo sapiens] | 1.75915 | 0.25198929 | 1.206715 | 0.58504704 | -1.457800723 | 0.433243947 |
| aldehyde dehydrogenase, mitochondrial precursor [Sus scrofa] | 5.6019 | 1.2883994 | 3.91695 | 1.29318158 | -1.430168881 | 0.056634917 |
| PREDICTED: extended synaptotagmin-1 isoform 1 [Ceratotherium simum simum] | 6.0226 | 0.54357822 | 4.211675 | 0.69226697 | -1.429977384 | 0.123765089 |
| protein Niban-like [Sus scrofa] | 4.28825 | 1.95238654 | 3.027 | 1.42114528 | -1.416666667 | 0.226421458 |
| PREDICTED: coatomer subunit zeta-1 [Oryctolagus cuniculus] | 1.02545 | 0.41462076 | 0.7271 | 0.4533045 | -1.410328703 | 0.658777445 |

| Protein Name | Control MEAN | Control SEM | Leptin MEAN | Leptin SEM | Ratio (Leptin/Control) | P value |
|--|--------------|-------------|-------------|------------|------------------------|-------------|
| rho GTPase-activating protein 1 [Canis lupus familiaris] | 1.02545 | 0.41462076 | 0.729725 | 0.45390642 | -1.405255404 | 0.556722786 |
| rab GDP dissociation inhibitor beta [Sus scrofa] | 13.5266 | 1.5036395 | 9.6501 | 0.86438785 | -1.401705682 | 0.07609482 |
| hypothetical protein PANDA_017913 [Ailuropoda melanoleuca] | 1.034125 | 0.73565295 | 0.7384175 | 0.24718843 | -1.400461121 | 0.779669575 |
| hypothetical protein PANDA_002275 [Ailuropoda melanoleuca] | 4.3126 | 0.82271623 | 3.08415 | 1.3478422 | -1.398310718 | 0.525413753 |
| protein disulfide-isomerase A6 precursor [Sus scrofa] | 11.6906 | 1.76495462 | 8.375425 | 1.08108163 | -1.395821705 | 0.174062673 |
| Golgi-associated plant pathogenesis-related protein 1 [Bos taurus] | 2.78085 | 0.50726747 | 1.994425 | 0.05207953 | -1.394311644 | 0.186706 |
| PREDICTED: LOW QUALITY PROTEIN: serine/threonine-protein kinase WNK4-like [Ailuropoda melanoleuca] | 1.01273 | 0.42542412 | 0.7271 | 0.4533045 | -1.392834548 | 0.565376584 |
| PREDICTED: ADP/ATP translocase 1 isoform 2 [Sus scrofa] | 9.071125 | 0.9083301 | 6.51945 | 0.78101791 | -1.391394213 | 0.070693095 |
| PREDICTED: cytosol aminopeptidase [Odobenus rosmarus divergens] | 3.74085 | 0.57168406 | 2.696875 | 0.6628564 | -1.387105446 | 0.276631903 |
| 60S ribosomal protein L7 [Homo sapiens] | 3.52485 | 0.66774685 | 2.5506 | 0.89486815 | -1.381968948 | 0.448410546 |
| progesterone receptor membrane component 2 [Sus scrofa] | 2.03573 | 0.43950094 | 1.4742 | 0.25083635 | -1.380904898 | 0.362304787 |

| Protein Name | Control MEAN | Control SEM | Leptin MEAN | Leptin SEM | Ratio (Leptin/Control) | P value |
|--|--------------|-------------|-------------|------------|------------------------|-------------|
| PREDICTED: EGF-containing fibulin-like extracellular matrix protein 1 [Ornithorhynchus anatinus] | 1.004055 | 0.42126092 | 0.7271 | 0.4533045 | -1.38090359 | 0.601226645 |
| 60S ribosomal protein L6 [Sus scrofa] | 2.80385 | 1.91722074 | 2.033 | 0.93658249 | -1.379168716 | 0.670400232 |
| PREDICTED: fatty aldehyde dehydrogenase isoform X1 [Sus scrofa] | 0.98755 | 0.38462955 | 0.7198275 | 0.46356545 | -1.371925913 | 0.378173608 |
| PREDICTED: ATP-citrate synthase isoformX1 [Equus caballus] | 3.757 | 0.93601953 | 2.74355 | 0.88718926 | -1.369393669 | 0.348024802 |
| alpha-parvin [Bos taurus] | 9.102825 | 1.80262959 | 6.664525 | 0.89588824 | -1.365862533 | 0.207311423 |
| hydroxyacyl-coenzyme A dehydrogenase, mitochondrial precursor [Sus scrofa] | 5.7852 | 0.27226689 | 4.236325 | 0.76683572 | -1.365617605 | 0.071489812 |
| PREDICTED: 60 kDa heat shock protein, mitochondrial [Equus caballus] | 14.7845 | 1.50989395 | 10.87875 | 1.22417679 | -1.359025623 | 0.182320414 |
| PREDICTED: myosin-11 isoform X2 [Ochotona princeps] | 411.165 | 33.3527591 | 302.7425 | 102.903688 | -1.358134388 | 0.310995941 |
| PREDICTED: myosin-11-like, partial [Bos mutus] | 326.11 | 28.5793238 | 240.64 | 81.0810974 | -1.355177859 | 0.314296069 |
| dihydropteridine reductase [Sus scrofa] | 3.017125 | 0.42208794 | 2.228575 | 0.1965077 | -1.353835971 | 0.064844498 |
| decorin precursor [Sus scrofa] | 39.3584 | 10.3158506 | 29.135 | 4.92463791 | -1.350897546 | 0.414573314 |
| ATP synthase subunit g, mitochondrial [Sus scrofa] | 5.0388 | 0.45921264 | 3.730025 | 0.22716198 | -1.350875664 | 0.152236076 |

| Protein Name | Control MEAN | Control SEM | Leptin MEAN | Leptin SEM | Ratio (Leptin/Control) | P value |
|--|--------------|-------------|-------------|------------|------------------------|-------------|
| hypothetical protein PANDA_001608 [Ailuropoda melanoleuca] | 2.013025 | 0.04569851 | 1.49279 | 0.2864035 | -1.348498449 | 0.149497727 |
| hypothetical protein PANDA_002799 [Ailuropoda melanoleuca] | 8.24785 | 0.96477213 | 6.151575 | 1.36308221 | -1.340770453 | 0.348158449 |
| copine-1 [Sus scrofa] | 3.28715 | 0.89551721 | 2.4601 | 0.60135043 | -1.336185521 | 0.073716604 |
| PREDICTED: vacuolar protein sorting-associated protein 35, partial [Sus scrofa] | 2.292055 | 0.51141417 | 1.715625 | 0.79802261 | -1.335988342 | 0.518727324 |
| PREDICTED: BAG family molecular chaperone regulator 2 isoform X1 [Sus scrofa] | 0.9838 | 0.38450823 | 0.7384175 | 0.24718843 | -1.332308619 | 0.631033022 |
| gi 585690381-DECOY | 1.01273 | 0.42542412 | 0.76044 | 0.49303655 | -1.33176845 | 0.402741576 |
| guanine nucleotide-binding protein G(i) subunit alpha-2 [Sus scrofa] | 11.386975 | 1.51222918 | 8.553625 | 1.61578465 | -1.331245525 | 0.288724258 |
| programmed cell death protein 6 [Bos taurus] | 5.273725 | 0.46128626 | 3.964175 | 0.33012865 | -1.330346163 | 0.16807527 |
| PREDICTED: LOW QUALITY PROTEIN: neuroblast differentiation-associated protein AHNAK [Canis lupus familiaris] | 31.3815 | 4.31393989 | 23.59825 | 2.13276051 | -1.329823186 | 0.053492617 |
| PREDICTED: integral membrane protein 2B-like [Echinops telfairi] | 1.006505 | 0.02283821 | 0.7570025 | 0.49656999 | -1.329592703 | 0.645789549 |
| integrin beta-1 precursor [Sus scrofa] | 36.688 | 4.26264667 | 27.66775 | 0.99726454 | -1.326020367 | 0.155336418 |
| ras-related protein Rab-5C [Bos taurus] | 6.3029 | 0.55768437 | 4.765225 | 0.83204873 | -1.322686757 | 0.126649183 |

| Protein Name | Control MEAN | Control SEM | Leptin MEAN | Leptin SEM | Ratio (Leptin/Control) | P value |
|--|--------------|-------------|-------------|------------|------------------------|-------------|
| hypothetical protein PANDA_002213 [Ailuropoda melanoleuca] | 3.55995 | 0.70628341 | 2.705575 | 0.39869136 | -1.315783151 | 0.292963937 |
| farnesyl pyrophosphate synthase precursor [Sus scrofa] | 1.262855 | 0.49649909 | 0.96125 | 0.66273479 | -1.313763329 | 0.795599411 |
| PREDICTED: 4-trimethylaminobutyraldehyde dehydrogenase [Sus scrofa] | 3.2445 | 0.7291109 | 2.477475 | 0.63192311 | -1.309599491 | 0.541985267 |
| PREDICTED: myosin-11 [Loxodonta africana] | 441.7825 | 41.0335293 | 337.4625 | 113.921156 | -1.309130644 | 0.355796909 |
| parathymosin [Bos taurus] | 8.350075 | 0.98524629 | 6.388425 | 1.37132552 | -1.307063165 | 0.334332752 |
| PREDICTED: 40S ribosomal protein S10-like isoform 1 [Ailuropoda melanoleuca] | 3.585105 | 1.01481746 | 2.746175 | 0.50194035 | -1.305490364 | 0.311123918 |
| Chain A, Atomic Structure Of Fkbp12, An Immunophilin Binding Protein | 7.093425 | 0.84510035 | 5.481625 | 0.30698353 | -1.294036896 | 0.127449517 |
| PREDICTED: annexin A6 isoform X1 [Ochotona princeps] | 27.26825 | 6.78341323 | 21.0745 | 1.19657355 | -1.293897839 | 0.446971547 |
| PREDICTED: translationally-controlled tumor protein [Equus caballus] | 0.9838 | 0.38450823 | 0.76044 | 0.49303655 | -1.293724686 | 0.670805317 |
| Chain A, Structure Of Calmodulin Bound To A Calcineurin Peptide: A New Way Of Making An Old Binding Mode | 7.389725 | 2.12033643 | 5.74245 | 1.41039447 | -1.286859267 | 0.188854332 |
| PREDICTED: selenium-binding protein 1 [Sus scrofa] | 4.532175 | 1.37565 | 3.522575 | 1.25562693 | -1.286608518 | 0.253229016 |
| PREDICTED: importin subunit beta-1 [Monodelphis domestica] | 3.818725 | 0.92291576 | 2.969015 | 1.13645257 | -1.286192559 | 0.434592888 |

| Protein Name | Control MEAN | Control SEM | Leptin MEAN | Leptin SEM | Ratio (Leptin/Control) | P value |
|--|--------------|-------------|-------------|------------|------------------------|-------------|
| PREDICTED: adenylyl cyclase-associated protein 1 isoform 1 [Dasyopus novemcinctus] | 13.65175 | 1.55256881 | 10.62155 | 1.05018815 | -1.285287929 | 0.192257436 |
| PREDICTED: annexin A11 isoform X1 [Sus scrofa] | 6.7514 | 1.02596667 | 5.25475 | 0.79402083 | -1.284818498 | 0.436706849 |
| EF-hand domain-containing protein D2 [Bos taurus] | 3.768425 | 0.24132537 | 2.94315 | 0.98444329 | -1.280405348 | 0.503506406 |
| PREDICTED: RNA binding motif (RNP1, RRM) protein 3 isoform X2 [Sus scrofa] | 5.036325 | 0.44775143 | 3.943 | 0.63575269 | -1.277282526 | 0.096377669 |
| PREDICTED: annexin A1 isoform X1 [Sus scrofa] | 42.4065 | 14.5571938 | 33.27175 | 11.2756871 | -1.274549731 | 0.090754502 |
| CD81 [Sus scrofa] | 3.7735 | 0.8788462 | 2.964375 | 0.34109145 | -1.27294961 | 0.257322884 |
| PREDICTED: fibromodulin [Tupaia chinensis] | 14.096 | 0.93043637 | 11.0783 | 1.8690696 | -1.272397389 | 0.16743862 |
| smooth muscle protein SM22 homolog - bovine (fragments) | 340.115 | 30.1063887 | 267.6225 | 90.8107283 | -1.270875954 | 0.339347464 |
| amine oxidase [flavin-containing] A [Sus scrofa] | 2.809755 | 0.67448333 | 2.2112 | 0.95887857 | -1.270692384 | 0.497805534 |
| PREDICTED: fibulin-5 isoformX1 [Sus scrofa] | 9.249525 | 0.72096609 | 7.28425 | 1.79291086 | -1.269797852 | 0.452921438 |
| PREDICTED: uncharacterized protein LOC100739300 [Sus scrofa] | 1.26413 | 0.26648333 | 0.9972175 | 0.026037 | -1.267657256 | 0.419460284 |
| PREDICTED: 60S ribosomal protein L22 isoform X1 [Ursus maritimus] | 2.54348 | 0.67035068 | 2.01039 | 0.43822103 | -1.265167455 | 0.480455973 |
| UDP-N-acetylhexosamine pyrophosphorylase [Bos taurus] | 1.26038 | 0.25786916 | 0.9972175 | 0.026037 | -1.263896793 | 0.356654368 |

| Protein Name | Control MEAN | Control SEM | Leptin MEAN | Leptin SEM | Ratio (Leptin/Control) | P value |
|--|--------------|-------------|-------------|------------|------------------------|-------------|
| glutathione S-transferase omega-1 [Sus scrofa] | 3.76465 | 0.63134118 | 2.98555 | 0.57279261 | -1.260956943 | 0.431948136 |
| PREDICTED: annexin A6 isoform X1 [Equus caballus] | 35.884 | 9.844228 | 28.5245 | 1.34860796 | -1.258006275 | 0.494243173 |
| PREDICTED: adenylyl cyclase-associated protein 1 isoform X1 [Physeter catodon] | 8.081 | 0.72299192 | 6.435625 | 0.4884483 | -1.255666699 | 0.178612314 |
| PREDICTED: S-methyl-5'-thioadenosine phosphorylase [Oryctolagus cuniculus] | 1.518005 | 0.30559001 | 1.212775 | 0.45380868 | -1.251679001 | 0.662192658 |
| ADP/ATP translocase 3 [Pteropus alecto] | 12.86985 | 1.59773262 | 10.302225 | 1.8815333 | -1.249230142 | 0.317927805 |
| PREDICTED: musculoskeletal embryonic nuclear protein 1 [Oryctolagus cuniculus] | 2.54103 | 0.89580115 | 2.0350425 | 0.75140786 | -1.248637313 | 0.736945541 |
| laminin receptor precursor [Oryctolagus cuniculus] | 5.56515 | 1.34435887 | 4.470475 | 0.84414999 | -1.244867715 | 0.285429436 |
| TPA: calcium channel, voltage-dependent, alpha 2/delta subunit 1 [Bos taurus] | 1.241425 | 0.21271946 | 0.9998425 | 0.42778425 | -1.241620555 | 0.65356975 |
| PREDICTED: annexin A6-like [Sus scrofa] | 38.04 | 11.126893 | 30.67275 | 2.40523822 | -1.240188767 | 0.499768779 |
| versican [Sus scrofa] | 4.302925 | 1.84010039 | 3.476475 | 1.29591227 | -1.237726433 | 0.478333944 |
| PREDICTED: heat shock protein beta-6 [Sus scrofa] | 5.8306 | 0.95102941 | 4.715925 | 0.40849298 | -1.236364022 | 0.144482594 |
| PREDICTED: asporin isoform X1 [Sus scrofa] | 22.2115 | 3.45933526 | 17.989 | 2.55937307 | -1.234726777 | 0.351739383 |
| PREDICTED: 60S ribosomal protein L8 [Loxodonta africana] | 1.26038 | 0.25786916 | 1.021865 | 0.42296105 | -1.233411458 | 0.659027211 |

| Protein Name | Control MEAN | Control SEM | Leptin MEAN | Leptin SEM | Ratio (Leptin/Control) | P value |
|--|--------------|-------------|-------------|------------|------------------------|-------------|
| PREDICTED: alpha-enolase isoform X3 [Bos taurus] | 31.031 | 4.31426809 | 25.19225 | 2.36803584 | -1.231767706 | 0.067641133 |
| L-lactate dehydrogenase B chain [Sus scrofa] | 14.8275 | 0.83297984 | 12.04095 | 1.97062707 | -1.23142277 | 0.360367085 |
| RecName: Full=Protein S100-A10; AltName: Full=Calpactin I light chain; AltName: Full=Calpactin-1 light chain; AltName: Full=Cellular ligand of annexin II; AltName: Full=S100 calcium-binding protein A10; AltName: Full=p10 protein; AltName: Full=p11 [Sus scrofa] | 1.543175 | 0.51449313 | 1.2560175 | 0.27241258 | -1.228625397 | 0.597065538 |
| PREDICTED: LOW QUALITY PROTEIN: dicarbonyl/L-xylulose reductase [Lipotes vexillifer] | 1.521755 | 0.52368543 | 1.2400525 | 0.23550094 | -1.227169817 | 0.701070815 |
| PREDICTED: annexin A5 [Sarcophilus harrisii] | 16.65225 | 1.55984189 | 13.5795 | 1.31843572 | -1.226278582 | 0.116014441 |
| thioredoxin reductase [Sus scrofa] | 1.507725 | 0.66091962 | 1.231365 | 0.21457457 | -1.22443386 | 0.735560948 |
| PREDICTED: annexin A6 isoform X1 [Panthera tigris altaica] | 34.9115 | 8.91736319 | 28.51475 | 1.57800942 | -1.224331267 | 0.478112118 |
| cadherin-13 precursor [Equus caballus] | 1.237675 | 0.46654509 | 1.0131775 | 0.42339583 | -1.22157766 | 0.775930589 |
| PREDICTED: 6-phosphogluconate dehydrogenase, decarboxylating [Sus scrofa] | 1.779405 | 0.78119128 | 1.456825 | 0.80162773 | -1.221426733 | 0.247554694 |

| Protein Name | Control MEAN | Control SEM | Leptin MEAN | Leptin SEM | Ratio (Leptin/Control) | P value |
|--|--------------|-------------|-------------|------------|------------------------|-------------|
| PREDICTED: basement membrane-specific heparan sulfate proteoglycan core protein [Sus scrofa] | 62.70375 | 6.62593037 | 51.3585 | 12.6552016 | -1.220903064 | 0.584729897 |
| phosphatidylinositol-binding clathrin assembly protein [Bos taurus] | 1.75425 | 0.87775855 | 1.43824 | 0.8050132 | -1.219719935 | 0.550789744 |
| PREDICTED: alpha-enolase isoform X1 [Sus scrofa] | 34.02675 | 5.21988841 | 27.9025 | 2.77665667 | -1.219487501 | 0.151990668 |
| plasminogen activator inhibitor 1 RNA-binding protein [Felis catus] | 1.52423 | 0.31599565 | 1.24995 | 0.47477813 | -1.219432777 | 0.61394988 |
| ribosomal protein L7a, partial [Equus caballus] | 1.5407 | 0.66266705 | 1.2647 | 0.47925842 | -1.218233573 | 0.821283941 |
| PREDICTED: collagen alpha-1(XVIII) chain isoform X1 [Equus caballus] | 4.048775 | 0.47811445 | 3.3235525 | 1.18946319 | -1.218207024 | 0.624313588 |
| elongation factor 1-alpha 1 [Equus caballus] | 27.91775 | 3.4072849 | 22.968 | 3.3848888 | -1.215506357 | 0.442729277 |
| PREDICTED: fibronectin isoformX2 [Sus scrofa] | 23.835 | 2.73066698 | 19.6285 | 5.73129189 | -1.214305729 | 0.270310187 |
| PREDICTED: ras-related protein Rab-1A isoform X1 [Loxodonta africana] | 10.84795 | 1.25421776 | 8.939 | 0.55504782 | -1.21355297 | 0.234607685 |
| PREDICTED: serpin peptidase inhibitor, clade B (ovalbumin), member 1 isoform X1 [Sus scrofa] | 4.54245 | 0.70082381 | 3.743375 | 0.50890497 | -1.213463786 | 0.235018698 |
| hypothetical protein PANDA_004987 [Ailuropoda melanoleuca] | 1.52048 | 0.30981711 | 1.2560175 | 0.27241258 | -1.210556382 | 0.353848941 |

| Protein Name | Control MEAN | Control SEM | Leptin MEAN | Leptin SEM | Ratio (Leptin/Control) | P value |
|--|--------------|-------------|-------------|------------|------------------------|-------------|
| ras-related protein Rab-1B [Bos taurus] | 11.10555 | 1.17013816 | 9.18185 | 0.42180876 | -1.209511155 | 0.198134515 |
| peptidyl-prolyl cis-trans isomerase B [Equus caballus] | 11.2724 | 1.63583832 | 9.3441 | 1.99440196 | -1.206365514 | 0.597177309 |
| ras-related protein Rab-6A [Rattus norvegicus] | 3.60405 | 1.2298058 | 2.991625 | 0.07809964 | -1.204713158 | 0.649041657 |
| PREDICTED: transforming growth factor beta-1-induced transcript 1 protein isoform 1 [Ovis aries] | 6.569525 | 0.73249273 | 5.4596 | 0.93841886 | -1.203297861 | 0.21488821 |
| ras-related protein Rab-14 [Rattus norvegicus] | 6.875 | 1.41224521 | 5.715775 | 0.41304117 | -1.202811517 | 0.362175913 |
| PREDICTED: acyl-coenzyme A thioesterase 2, mitochondrial-like, partial [Sus scrofa] | 1.476375 | 0.44763738 | 1.231365 | 0.21457457 | -1.198974309 | 0.695834925 |
| electron-transfer-flavoprotein, alpha polypeptide [Sus scrofa] | 3.813825 | 0.6902082 | 3.189825 | 0.85013522 | -1.195622017 | 0.340832216 |
| PREDICTED: lupus La protein homolog isoform X1 [Sus scrofa] | 1.514255 | 0.51124989 | 1.267325 | 0.48263389 | -1.19484347 | 0.640784595 |
| heterogeneous nuclear ribonucleoprotein A1 isoform b [Homo sapiens] | 3.543475 | 0.70097196 | 2.966975 | 0.34677735 | -1.194305648 | 0.569768461 |
| PREDICTED: transgelin-2 [Ochotona princeps] | 25.27875 | 2.84307267 | 21.1675 | 2.54238082 | -1.194224637 | 0.208550173 |
| PREDICTED: cytoplasmic dynein 1 heavy chain 1 [Eptesicus fuscus] | 20.9735 | 3.67103685 | 17.56675 | 3.69280709 | -1.193931718 | 0.587030187 |
| PREDICTED: macrophage-capping protein isoformX2 [Sus scrofa] | 10.019775 | 0.63893033 | 8.401375 | 1.35565755 | -1.192635134 | 0.474303413 |

| Protein Name | Control MEAN | Control SEM | Leptin MEAN | Leptin SEM | Ratio (Leptin/Control) | P value |
|--|--------------|-------------|-------------|------------|------------------------|-------------|
| PREDICTED: barrier-to-autointegration factor-like isoformX1 [Sus scrofa] | 3.279625 | 0.29987223 | 2.7514 | 0.51395419 | -1.191984081 | 0.488300872 |
| voltage-dependent anion-selective channel protein 1 [Oryctolagus cuniculus] | 8.32845 | 1.34871331 | 6.996425 | 0.52559708 | -1.190386519 | 0.358354165 |
| PREDICTED: galactokinase isoform X1 [Sus scrofa] | 2.029505 | 0.60057404 | 1.705725 | 0.599835 | -1.189819578 | 0.757599425 |
| PREDICTED: NADH-cytochrome b5 reductase 3-like isoform X1 [Sus scrofa] | 14.91325 | 1.33256678 | 12.538775 | 1.2609289 | -1.189370572 | 0.200156128 |
| PREDICTED: N(G),N(G)-dimethylarginine dimethylaminohydrolase 2 [Sorex araneus] | 13.90805 | 1.83229177 | 11.69625 | 0.38914787 | -1.189103345 | 0.279579974 |
| RecName: Full=ATP synthase-coupling factor 6, mitochondrial; Short=ATPase subunit F6 [Sus scrofa] | 1.774355 | 0.49683465 | 1.49279 | 0.2864035 | -1.188616617 | 0.573588726 |
| putative cation-transporting ATPase 13A2 isoform 2 [Camelus ferus] | 1.784305 | 0.51378486 | 1.5014775 | 0.29988551 | -1.188366126 | 0.743544712 |
| superoxide dismutase [Mn], mitochondrial [Sus scrofa] | 17.41775 | 2.88180853 | 14.69275 | 1.36084823 | -1.185465621 | 0.227723188 |
| T-complex protein 1 subunit alpha [Sus scrofa] | 1.784305 | 0.51378486 | 1.506125 | 0.65659907 | -1.184699145 | 0.3051032 |
| PREDICTED: LOW QUALITY PROTEIN: neuroblast differentiation-associated protein AHNAK [Myotis davidii] | 30.0005 | 3.16808129 | 25.3445 | 2.73484568 | -1.183708497 | 0.057801799 |

| Protein Name | Control MEAN | Control SEM | Leptin MEAN | Leptin SEM | Ratio (Leptin/Control) | P value |
|---|--------------|-------------|-------------|------------|------------------------|-------------|
| PREDICTED: neuroblast differentiation-associated protein AHNAK [Sorex araneus] | 17.64575 | 1.8930727 | 14.9289 | 2.59028699 | -1.181985947 | 0.174634577 |
| PREDICTED: basement membrane-specific heparan sulfate proteoglycan core protein [Erinaceus europaeus] | 20.35875 | 2.15909354 | 17.230775 | 5.80682729 | -1.181534203 | 0.71339185 |
| PREDICTED: neuroblast differentiation-associated protein AHNAK [Mustela putorius furo] | 20.48825 | 3.15589442 | 17.3825 | 1.04336319 | -1.178671077 | 0.241518847 |
| PREDICTED: actin-related protein 2/3 complex subunit 5-like protein-like [Macaca mulatta] | 1.7554 | 0.24539619 | 1.490165 | 0.28137997 | -1.177990357 | 0.58143468 |
| SYNCRIP protein [Bos taurus] | 1.75915 | 0.25198929 | 1.4962275 | 0.66716352 | -1.175723612 | 0.639290834 |
| PREDICTED: transmembrane emp24 domain-containing protein 10 [Sus scrofa] | 5.253475 | 0.99852019 | 4.4731 | 0.60023216 | -1.174459547 | 0.603456822 |
| PREDICTED: PDZ and LIM domain protein 5 isoformX3 [Sus scrofa] | 5.805425 | 0.8198995 | 4.950075 | 0.60229262 | -1.172795362 | 0.086345087 |
| ras-related protein Rab-18 isoform 1 [Homo sapiens] | 2.03198 | 0.43064859 | 1.735625 | 0.23786866 | -1.17074829 | 0.576095035 |
| Annexin A6, partial [Bos mutus] | 35.3525 | 9.46636129 | 30.2635 | 1.2782723 | -1.16815636 | 0.591966354 |
| PREDICTED: actin-related protein 2/3 complex subunit 5 [Ornithorhynchus anatinus] | 2.013025 | 0.04569851 | 1.724315 | 0.44021889 | -1.167434604 | 0.532588548 |

| Protein Name | Control MEAN | Control SEM | Leptin MEAN | Leptin SEM | Ratio (Leptin/Control) | P value |
|---|--------------|-------------|-------------|------------|------------------------|-------------|
| Chain A, Refined Structure Of Mitochondrial Malate Dehydrogenase From Porcine Heart And The Consensus Structure For Dicarboxylic Acid Oxidoreductases | 25.472 | 1.84719684 | 21.8555 | 1.61009531 | -1.165473222 | 0.153098556 |
| PREDICTED: proteasome subunit beta type-6 isoform X1 [Equus caballus] | 2.013025 | 0.04569851 | 1.733 | 0.23271051 | -1.161583958 | 0.32917887 |
| PREDICTED: LOW QUALITY PROTEIN: ezrin [Equus caballus] | 8.2309 | 3.06107739 | 7.08665 | 2.44674386 | -1.161465573 | 0.829448341 |
| ras-related protein Rab-2A [Bos taurus] | 2.251725 | 0.46410772 | 1.9425 | 0.63780214 | -1.159189189 | 0.494636811 |
| PREDICTED: rab GDP dissociation inhibitor alpha isoform 1 [Sus scrofa] | 11.507475 | 1.25466249 | 9.927475 | 0.91987211 | -1.159154266 | 0.410417609 |
| PREDICTED: ras-related protein Rab-7a [Equus caballus] | 8.626525 | 1.38022067 | 7.446175 | 0.5367193 | -1.158517628 | 0.470918575 |
| PREDICTED: proteasome subunit alpha type-4 [Ornithorhynchus anatinus] | 1.77188 | 0.49463337 | 1.5307775 | 0.90110268 | -1.157503295 | 0.845743891 |
| TPA: ras-related C3 botulinum toxin substrate 1 precursor [Bos taurus] | 1.9941 | 0.37085747 | 1.724315 | 0.44021889 | -1.156459232 | 0.659725704 |
| ATP synthase subunit O, mitochondrial precursor [Sus scrofa] | 6.32055 | 0.84772936 | 5.472925 | 0.60716323 | -1.154876049 | 0.428793679 |
| PREDICTED: annexin A5 [Ovis aries] | 44.821 | 5.65734434 | 38.898 | 3.34266311 | -1.15227004 | 0.330048421 |

| Protein Name | Control MEAN | Control SEM | Leptin MEAN | Leptin SEM | Ratio (Leptin/Control) | P value |
|---|--------------|-------------|-------------|------------|------------------------|-------------|
| leucine-rich repeat-containing protein 59 [Sus scrofa] | 2.016775 | 0.42627688 | 1.75159 | 0.26467881 | -1.151396731 | 0.642268063 |
| 60S ribosomal protein L14 [Sus scrofa] | 2.054675 | 0.72348057 | 1.784925 | 0.64864985 | -1.151126798 | 0.824912129 |
| ADP-ribosylation factor 3 [Ovis aries] | 8.7908 | 1.02977428 | 7.644275 | 1.36818537 | -1.149984793 | 0.561456455 |
| PREDICTED: annexin A5 [Sus scrofa] | 60.41675 | 6.8273921 | 52.5405 | 4.13781185 | -1.149908166 | 0.288460397 |
| PREDICTED: alpha-enolase isoform X1 [Lipotes vexillifer] | 33.29575 | 4.63001266 | 28.957 | 2.0921992 | -1.149834237 | 0.211755742 |
| transketolase [Sus scrofa] | 8.598725 | 1.93813134 | 7.49245 | 1.53471202 | -1.14765197 | 0.602870314 |
| heat shock 70 kDa protein 1B [Sus scrofa] | 22.63725 | 2.82906614 | 19.73075 | 1.52781256 | -1.147308136 | 0.492521939 |
| Chain B, Crystal Structure Of Bovine Arp23 COMPLEX CO-Crystallized With Atp And Crosslinked With Glutaraldehyde | 2.806005 | 0.78805669 | 2.44879 | 1.15592546 | -1.145874085 | 0.812545983 |
| PREDICTED: 40S ribosomal protein S7 [Equus caballus] | 4.55895 | 0.70613795 | 3.9862 | 0.42860523 | -1.143683207 | 0.549420249 |
| PREDICTED: ras-related protein R-Ras [Sus scrofa] | 6.007725 | 0.64400147 | 5.253525 | 0.54155139 | -1.143560752 | 0.504894879 |
| PREDICTED: integrin alpha-3 isoform X2 [Sus scrofa] | 6.232375 | 0.78799086 | 5.479 | 0.28951373 | -1.137502281 | 0.487641237 |
| Chain A, Structure Of Porcine Class Pi Glutathione S-Transferase | 16.314 | 0.2736351 | 14.36875 | 1.41164262 | -1.1353806 | 0.200787588 |
| PREDICTED: integrin alpha-3 isoform X1 [Pteropus alecto] | 4.774925 | 0.24247829 | 4.207025 | 0.39396367 | -1.134988501 | 0.410024298 |
| annexin A4 [Sus scrofa] | 22.183 | 3.93306401 | 19.55525 | 1.70141732 | -1.134375679 | 0.468396688 |

| Protein Name | Control MEAN | Control SEM | Leptin MEAN | Leptin SEM | Ratio (Leptin/Control) | P value |
|--|--------------|-------------|-------------|------------|------------------------|-------------|
| PREDICTED: myosin light polypeptide 6 isoform X2 [Bubalus bubalis] | 77.29325 | 6.3036946 | 68.233 | 4.92754007 | -1.13278399 | 0.46467675 |
| PREDICTED: serine/threonine-protein phosphatase PP1-beta catalytic subunit [Panthera tigris altaica] | 7.8901 | 1.45352968 | 6.969175 | 0.56139177 | -1.132142614 | 0.424763401 |
| PREDICTED: fermitin family homolog 2, partial [Sus scrofa] | 18.916 | 2.12793425 | 16.7564 | 2.52569672 | -1.128882099 | 0.370481388 |
| ARP3 actin-related protein 3 homolog (yeast) [Bos taurus] | 7.55055 | 0.90752262 | 6.6918 | 0.50846839 | -1.128328701 | 0.164120212 |
| armadillo repeat containing 10 [Sus scrofa] | 3.068705 | 1.12958694 | 2.721525 | 0.42832117 | -1.127568183 | 0.668504137 |
| PREDICTED: basement membrane-specific heparan sulfate proteoglycan core protein [Vicugna pacos] | 44.06 | 6.21747018 | 39.0955 | 9.40416728 | -1.126983924 | 0.760242864 |
| PREDICTED: serine/threonine-protein phosphatase 2A 65 kDa regulatory subunit A alpha isoform-like isoform 1 [Equus caballus] | 5.011175 | 0.5315006 | 4.4519 | 0.92877797 | -1.125626137 | 0.587353944 |
| histidine triad nucleotide-binding protein 2, mitochondrial isoform 1 precursor [Sus scrofa] | 2.78085 | 0.50726747 | 2.471425 | 0.22651322 | -1.125201048 | 0.696698187 |
| PREDICTED: basement membrane-specific heparan sulfate proteoglycan core protein [Orcinus orca] | 37.8465 | 4.85194608 | 33.63825 | 9.20422111 | -1.125103119 | 0.769080254 |
| PREDICTED: myelin protein P0 [Sus scrofa] | 6.48625 | 0.69993042 | 5.7865025 | 1.8634034 | -1.120927538 | 0.625764461 |

| Protein Name | Control MEAN | Control SEM | Leptin MEAN | Leptin SEM | Ratio (Leptin/Control) | P value |
|---|--------------|-------------|-------------|------------|------------------------|-------------|
| PREDICTED: plastin-3 isoformX1 [Sus scrofa] | 14.7305 | 1.54279322 | 13.1515 | 1.06818674 | -1.12006235 | 0.444717897 |
| PREDICTED: neuroblast differentiation-associated protein AHNAK [Mustela putorius furo] | 26.722 | 3.43361816 | 23.8585 | 1.27434679 | -1.120020119 | 0.318463806 |
| PREDICTED: vesicle-associated membrane protein 2 [Ornithorhynchus anatinus] | 2.7846 | 0.30212183 | 2.487375 | 0.27982541 | -1.119493442 | 0.289147949 |
| actin-related protein 2/3 complex subunit 3 [Bos taurus] | 5.5251 | 0.25014426 | 4.957375 | 1.21413038 | -1.114521294 | 0.655745917 |
| T-complex protein 1 subunit beta [Sus scrofa] | 8.57595 | 0.76917748 | 7.729625 | 0.90905514 | -1.109491081 | 0.098073633 |
| PREDICTED: fructose-bisphosphate aldolase A isoform X1 [Camelus ferus] | 23.21675 | 2.35707143 | 20.94525 | 1.35524434 | -1.10844941 | 0.366209047 |
| PREDICTED: stress-70 protein, mitochondrial [Felis catus] | 8.803375 | 0.66575315 | 7.945175 | 1.05824738 | -1.108015242 | 0.489185811 |
| RecName: Full=Neurofilament light polypeptide; Short=NF-L; AltName: Full=68 kDa neurofilament protein; AltName: Full=Neurofilament triplet L protein [Sus scrofa] | 1.87945 | 1.87945 | 1.699875 | 1.699875 | -1.105640121 | 0.391002219 |
| PREDICTED: collagen alpha-1(XII) chain [Sus scrofa] | 8.565225 | 3.7329803 | 7.7482 | 0.94495428 | -1.105447072 | 0.86527439 |
| Alpha-centractin [Pteropus alecto] | 3.273425 | 0.27149294 | 2.964375 | 0.34109145 | -1.104254691 | 0.627075641 |
| rho-related GTP-binding protein RhoC precursor [Homo sapiens] | 5.76005 | 0.36810942 | 5.22485 | 1.01179706 | -1.102433563 | 0.686818778 |

| Protein Name | Control MEAN | Control SEM | Leptin MEAN | Leptin SEM | Ratio (Leptin/Control) | P value |
|---|--------------|-------------|-------------|------------|------------------------|-------------|
| mitochondrial succinate dehydrogenase complex subunit A [Sus scrofa] | 3.0068 | 0.69946256 | 2.7276 | 0.6368844 | -1.10236105 | 0.258090622 |
| ATP synthase subunit alpha, mitochondrial [Sus scrofa] | 30.6055 | 1.53563583 | 27.81175 | 1.31957041 | -1.100452147 | 0.153177958 |
| PREDICTED: 14-3-3 protein zeta/delta [Myotis brandtii] | 26.96975 | 1.31090792 | 24.5185 | 1.71325054 | -1.099975529 | 0.328273634 |
| 14-3-3 protein zeta chain [cattle, brain, Peptide, 245 aa] | 27.22975 | 1.46981276 | 24.78575 | 1.32330831 | -1.098605045 | 0.341554376 |
| peroxiredoxin-6 [Sus scrofa] | 11.13345 | 1.45950377 | 10.1417 | 0.97913727 | -1.097789325 | 0.650866097 |
| PREDICTED: T-complex protein 1 subunit theta isoform 1 [Sus scrofa] | 3.79735 | 0.54756535 | 3.466 | 0.46542102 | -1.095600115 | 0.547043947 |
| hypothetical protein PANDA_015972 [Ailuropoda melanoleuca] | 4.026075 | 0.09136907 | 3.6781 | 0.74665276 | -1.09460727 | 0.679662553 |
| four and a half LIM domains 1 protein, isoform C [Sus scrofa] | 12.703025 | 2.44925296 | 11.61115 | 1.44630693 | -1.094036766 | 0.496633493 |
| ran-specific GTPase-activating protein [Sus scrofa] | 0.7778 | 0.49760689 | 0.71114 | 0.44995723 | -1.093736817 | 0.930636518 |
| PREDICTED: ubiquitin carboxyl-terminal hydrolase 5 isoform 1 [Sus scrofa] | 0.5115 | 0.29533054 | 0.4683 | 0.4683 | -1.092248559 | 0.916695964 |
| PREDICTED: peroxiredoxin-1 [Oryctolagus cuniculus] | 10.61445 | 1.1847935 | 9.722625 | 1.66487748 | -1.091726771 | 0.625025575 |

| Protein Name | Control MEAN | Control SEM | Leptin MEAN | Leptin SEM | Ratio (Leptin/Control) | P value |
|--|--------------|-------------|-------------|------------|------------------------|-------------|
| RecName: Full=Mimecan; AltName: Full=Osteoglycin; Contains: RecName: Full=Corneal keratan sulfate proteoglycan 25 core protein; Short=KSPG25 protein; Contains: RecName: Full=Osteoinductive factor; Short=OIF; Flags: Precursor [Bos taurus] | 12.602925 | 3.31146521 | 11.547525 | 2.99502017 | -1.091396208 | 0.704597335 |
| Annexin A5 [Tupaia chinensis] | 34.3385 | 4.39287329 | 31.46975 | 3.07340312 | -1.09115897 | 0.668391307 |
| PREDICTED: lipoma-preferred partner [Sus scrofa] | 4.318825 | 1.10518255 | 3.974925 | 0.92083803 | -1.086517356 | 0.438931126 |
| pyruvate kinase PKM [Bos taurus] | 41.747 | 2.33290666 | 38.48775 | 2.55487189 | -1.084682789 | 0.200318345 |
| RecName: Full=Caveolin-1 [Rhinolophus ferrumequinum] | 5.992375 | 1.31314029 | 5.527075 | 1.52150848 | -1.084185577 | 0.624502275 |
| PREDICTED: dnaJ homolog subfamily B member 4 isoform X1 [Equus caballus] | 0.769125 | 0.49267537 | 0.71114 | 0.44995723 | -1.081538094 | 0.895967902 |
| RecName: Full=Eukaryotic translation initiation factor 5A-1; Short=eIF-5A-1; Short=eIF-5A1; AltName: Full=Eukaryotic initiation factor 5A isoform 1; Short=eIF-5A; AltName: Full=eIF-4D [Oryctolagus cuniculus] | 4.252325 | 0.73065954 | 3.9456 | 0.47727335 | -1.077738494 | 0.657162971 |

| Protein Name | Control MEAN | Control SEM | Leptin MEAN | Leptin SEM | Ratio (Leptin/Control) | P value |
|--|--------------|-------------|-------------|------------|------------------------|-------------|
| PREDICTED: 40S ribosomal protein S25 [Ornithorhynchus anatinus] | 3.302325 | 0.54006412 | 3.065575 | 1.26888248 | -1.077228579 | 0.872469409 |
| 14-3-3 protein eta [Oryctolagus cuniculus] | 9.3125 | 0.34698797 | 8.6517 | 0.93249808 | -1.076378053 | 0.639626178 |
| GTP-binding nuclear protein Ran, partial [Bos mutus] | 5.290175 | 0.31627978 | 4.915525 | 0.77931367 | -1.076217698 | 0.625781682 |
| enoyl-CoA hydratase, mitochondrial [Sus scrofa] | 4.8001 | 0.55525912 | 4.465825 | 0.17931059 | -1.074851791 | 0.675676155 |
| PREDICTED: poly [ADP-ribose] polymerase 6 isoformX1 [Sus scrofa] | 78.8525 | 5.55985792 | 73.535 | 4.33516161 | -1.072312504 | 0.142445178 |
| hypothetical protein PANDA_006098 [Ailuropoda melanoleuca] | 9.53835 | 0.81024023 | 8.903025 | 1.21843458 | -1.071360577 | 0.616516687 |
| PREDICTED: myosin-10, partial [Sus scrofa] | 131.5275 | 10.4840103 | 122.775 | 8.5520022 | -1.071288943 | 0.515237189 |
| vesicle-trafficking protein SEC22b precursor [Bos taurus] | 1.0292 | 0.42073099 | 0.96125 | 0.66273479 | -1.070689207 | 0.863126164 |
| peroxiredoxin-2 [Sus scrofa] | 19.12525 | 0.85722774 | 17.919 | 0.83041867 | -1.067316815 | 0.308175688 |
| hypothetical protein PANDA_010030 [Ailuropoda melanoleuca] | 5.7725 | 0.93666766 | 5.424475 | 0.93327894 | -1.064158283 | 0.638223917 |
| hypothetical protein PANDA_020401 [Ailuropoda melanoleuca] | 12.32615 | 1.91734325 | 11.5866 | 1.7732813 | -1.063828043 | 0.32116651 |
| peptidyl-prolyl cis-trans isomerase A [Sus scrofa] | 47.32375 | 2.98390771 | 44.6705 | 2.45889299 | -1.059396022 | 0.612418637 |
| PREDICTED: protein canopy homolog 4 [Equus caballus] | 0.771575 | 0.25724221 | 0.729725 | 0.45390642 | -1.057350372 | 0.920470443 |

| Protein Name | Control MEAN | Control SEM | Leptin MEAN | Leptin SEM | Ratio (Leptin/Control) | P value |
|--|--------------|-------------|-------------|------------|------------------------|-------------|
| macrophage migration inhibitory factor [Sus scrofa] | 12.1135 | 1.10487175 | 11.479525 | 0.74578394 | -1.055226588 | 0.697340924 |
| PREDICTED: vimentin isoform X1 [Sus scrofa] | 384.66 | 18.8224011 | 365.59 | 23.1313975 | -1.052162258 | 0.171569586 |
| PREDICTED: acidic leucine-rich nuclear phosphoprotein 32 family member A isoform X1 [Equus caballus] | 0.492555 | 0.28497986 | 0.4683 | 0.4683 | -1.051793722 | 0.951078813 |
| nucleoside diphosphate kinase B [Sus scrofa] | 8.84505 | 0.89644578 | 8.412575 | 0.99803469 | -1.05140816 | 0.767507612 |
| PREDICTED: dihydropyrimidinase-related protein 2 isoform X2 [Loxodonta africana] | 11.966 | 1.90159216 | 11.383025 | 0.97822823 | -1.051214418 | 0.759338806 |
| Cofilin-1, partial [Bos mutus] | 23.26025 | 2.4078032 | 22.19125 | 4.15564294 | -1.04817214 | 0.777088432 |
| clathrin heavy chain 1 [Bos taurus] | 24.925 | 1.54139936 | 23.78375 | 2.76416085 | -1.047984443 | 0.516480751 |
| superoxide dismutase [Cu-Zn] [Sus scrofa] | 10.62725 | 1.81888807 | 10.1411 | 1.03745386 | -1.047938587 | 0.815802279 |
| erythrocyte band 7 integral membrane protein [Bos taurus] | 7.074475 | 0.70426834 | 6.752375 | 0.81069818 | -1.047701735 | 0.803385053 |
| hypothetical protein PANDA_012739 [Ailuropoda melanoleuca] | 1.26413 | 0.26648333 | 1.206715 | 0.58504704 | -1.047579586 | 0.886152766 |
| RecName: Full=ATP synthase subunit e, mitochondrial; Short=ATPase subunit e [Sus scrofa] | 6.521675 | 0.60742213 | 6.2261 | 0.24137727 | -1.047473539 | 0.6609292 |
| PREDICTED: pyruvate kinase isozymes M1/M2 isoform 2 [Dasypus novemcinctus] | 44.54275 | 3.60412626 | 42.54575 | 3.42249018 | -1.046937708 | 0.63949077 |

| Protein Name | Control MEAN | Control SEM | Leptin MEAN | Leptin SEM | Ratio (Leptin/Control) | P value |
|---|--------------|-------------|-------------|------------|------------------------|-------------|
| PREDICTED: T-complex protein 1 subunit gamma isoform 1 [Equus caballus] | 1.53043 | 0.67716146 | 1.46289 | 0.61677142 | -1.046168885 | 0.866973354 |
| 60S ribosomal protein L11 [Mus musculus] | 1.80325 | 0.65233432 | 1.724315 | 0.44021889 | -1.045777599 | 0.893870769 |
| PREDICTED: myb-binding protein 1A isoform X1 [Sus scrofa] | 0.767825 | 0.48725115 | 0.7357925 | 0.2461123 | -1.043534692 | 0.966551466 |
| PREDICTED: peptidyl-prolyl cis-trans isomerase A-like [Physeter catodon] | 39.798 | 1.92668242 | 38.22775 | 1.78456542 | -1.041076182 | 0.638995453 |
| PREDICTED: ras-related protein Rab-10 [Monodelphis domestica] | 8.823675 | 0.43771078 | 8.476725 | 0.70080432 | -1.040929722 | 0.707554362 |
| aldolase C | 12.1045 | 0.89141147 | 11.63365 | 1.22156629 | -1.04047311 | 0.742859698 |
| tubulin-specific chaperone A [Bos taurus] | 0.765375 | 0.48680041 | 0.7357925 | 0.2461123 | -1.040204949 | 0.969623824 |
| PREDICTED: heat shock protein beta-1-like isoform 1 [Sus scrofa] | 37.3635 | 2.91939402 | 36.0625 | 1.78203687 | -1.036076256 | 0.703369425 |
| PREDICTED: synemin [Sus scrofa] | 1.52668 | 0.5318112 | 1.4742 | 0.25083635 | -1.035598969 | 0.945763145 |
| PREDICTED: heterogeneous nuclear ribonucleoprotein L-like [Elephantulus edwardii] | 2.01055 | 0.42105586 | 1.9425 | 0.63780214 | -1.035032175 | 0.854062683 |
| PREDICTED: transgelin [Dasypus novemcinctus] | 301.895 | 26.2347322 | 291.6825 | 24.2320646 | -1.035012385 | 0.669083906 |
| PREDICTED: heat shock-related 70 kDa protein 2 [Sus scrofa] | 22.8735 | 1.71882045 | 22.106 | 1.12857764 | -1.034719081 | 0.695449464 |
| PREDICTED: small nuclear ribonucleoprotein Sm D2-like [Macaca mulatta] | 1.031675 | 0.42476168 | 0.9972175 | 0.026037 | -1.034553646 | 0.938684944 |

| Protein Name | Control MEAN | Control SEM | Leptin MEAN | Leptin SEM | Ratio (Leptin/Control) | P value |
|--|--------------|-------------|-------------|------------|------------------------|-------------|
| acylphosphatase-1 isoform 1 [Sus scrofa] | 2.060875 | 0.73224263 | 1.994425 | 0.05207953 | -1.033317874 | 0.932963789 |
| PREDICTED: LOW QUALITY PROTEIN: IQ motif containing GTPase activating protein 1 [Sus scrofa] | 14.6655 | 1.60058346 | 14.203125 | 2.89162068 | -1.032554455 | 0.773900075 |
| PREDICTED: poly(rC)-binding protein 2-like isoform X1 [Monodelphis domestica] | 1.5407 | 0.66266705 | 1.49279 | 0.2864035 | -1.032094266 | 0.92180872 |
| PREDICTED: integrin-linked protein kinase-like [Ailuropoda melanoleuca] | 2.832475 | 0.97884412 | 2.746175 | 0.50194035 | -1.031425528 | 0.913259084 |
| Translational activator GCN1 [Myotis davidii] | 9.145625 | 1.61278467 | 8.88705 | 1.11377917 | -1.029095707 | 0.848024234 |
| hypothetical protein PANDA_006420 [Ailuropoda melanoleuca] | 1.26413 | 0.26648333 | 1.22874 | 0.47432116 | -1.028801862 | 0.938255035 |
| voltage-dependent anion-selective channel protein 2 [Oryctolagus cuniculus] | 10.26505 | 0.88826586 | 9.990575 | 0.60300931 | -1.027473394 | 0.790414175 |
| PREDICTED: proteasome subunit alpha type-3 [Monodelphis domestica] | 1.26413 | 0.26648333 | 1.231365 | 0.21457457 | -1.026608682 | 0.57592442 |
| PREDICTED: mimecan [Orycteropus afer afer] | 13.4109 | 3.42582852 | 13.0673 | 2.90139249 | -1.026294644 | 0.923011558 |
| PREDICTED: calponin-1 [Chrysochloris asiatica] | 154.2825 | 18.7091343 | 150.4475 | 9.1840227 | -1.02549062 | 0.781386303 |
| PREDICTED: carbonyl reductase [NADPH] 1 [Physeter catodon] | 2.520775 | 0.51573535 | 2.4601 | 0.60135043 | -1.024663632 | 0.957143961 |
| obg-like ATPase 1 [Bos taurus] | 1.734 | 0.43608581 | 1.6924 | 0.70849443 | -1.024580477 | 0.917659381 |

| Protein Name | Control MEAN | Control SEM | Leptin MEAN | Leptin SEM | Ratio (Leptin/Control) | P value |
|--|--------------|-------------|-------------|------------|------------------------|-------------|
| F-actin-capping protein subunit alpha-2 [Sus scrofa] | 4.32775 | 0.81651619 | 4.23895 | 0.4859385 | -1.020948584 | 0.844063067 |
| PREDICTED: LOW QUALITY PROTEIN: collagen alpha-1(XV) chain [Vicugna pacos] | 3.068705 | 1.12958694 | 3.007575 | 0.45405795 | -1.020325345 | 0.959334485 |
| PREDICTED: actin-related protein 2/3 complex subunit 4 [Sarcophilus harrisii] | 8.5801 | 0.96384122 | 8.416175 | 0.88394137 | -1.019477375 | 0.908160292 |
| PREDICTED: glyoxalase domain-containing protein 4 [Sus scrofa] | 1.75915 | 0.25198929 | 1.72694 | 0.44298441 | -1.018651488 | 0.956992512 |
| PREDICTED: hsc70-interacting protein isoform 1 [Sus scrofa] | 1.006505 | 0.02283821 | 0.988525 | 0.38354477 | -1.018188716 | 0.963741837 |
| ribosomal protein, large, P2 [Sus scrofa] | 6.2892 | 0.65088928 | 6.181475 | 0.80195676 | -1.01742707 | 0.938272005 |
| PREDICTED: phosphoglycerate mutase 1 isoform 4 [Canis lupus familiaris] | 8.330075 | 1.05060864 | 8.193275 | 0.30657799 | -1.01669662 | 0.909452389 |
| charged multivesicular body protein 4b [Bos taurus] | 1.26038 | 0.25786916 | 1.2400525 | 0.23550094 | -1.016392451 | 0.963270496 |
| PREDICTED: serine--tRNA ligase, cytoplasmic [Sus scrofa] | 1.514255 | 0.51124989 | 1.490165 | 0.28137997 | -1.016165995 | 0.97447564 |
| PREDICTED: 14-3-3 protein gamma [Chrysochloris asiatica] | 13.616 | 1.47600322 | 13.405 | 0.56572579 | -1.015740395 | 0.849944079 |
| PREDICTED: stress-induced-phosphoprotein 1 [Sus scrofa] | 0.9851 | 0.56995448 | 0.96994 | 0.38307126 | -1.015629833 | 0.972224381 |
| ras-related protein Rab-11B [Rattus norvegicus] | 3.582655 | 1.09429246 | 3.5278 | 0.71725886 | -1.015549351 | 0.963578787 |
| PREDICTED: protein phosphatase 1 regulatory subunit 12B-like isoform X1 [Sus scrofa] | 5.0288 | 0.4176627 | 4.9614 | 0.31475411 | -1.013584875 | 0.915710816 |

| Protein Name | Control MEAN | Control SEM | Leptin MEAN | Leptin SEM | Ratio (Leptin/Control) | P value |
|---|--------------|-------------|-------------|------------|------------------------|-------------|
| guanine nucleotide-binding protein G(I)/G(S)/G(O) subunit gamma-12 [Sus scrofa] | 4.330225 | 0.92479788 | 4.272275 | 0.71039656 | -1.013564202 | 0.942349406 |
| calponin-1 [Sus scrofa] | 170.96 | 19.9725324 | 168.97 | 7.27052153 | -1.011777239 | 0.908010134 |
| triosephosphate isomerase 1 [Sus scrofa] | 33.11025 | 3.88675111 | 32.8385 | 0.96614574 | -1.008275348 | 0.933895635 |
| Myosin regulatory light polypeptide 9 [Tupaia chinensis] | 40.485 | 6.16460668 | 40.20525 | 2.3241429 | -1.006958047 | 0.960768187 |
| ribosomal protein L17 (predicted) [Oryctolagus cuniculus] | 0.50775 | 0.50775 | 0.504265 | 0.29153273 | -1.006911049 | 0.993585989 |
| PREDICTED: tropomyosin alpha-1 chain isoform X2 [Sus scrofa] | 153.7025 | 8.31118361 | 152.8775 | 3.15580517 | -1.005396478 | 0.941642608 |
| acyl-CoA-binding protein [Sus scrofa] | 2.745425 | 0.7350286 | 2.732825 | 0.23111146 | -1.004610614 | 0.989576269 |
| tropomyosin 3, gamma isoform 19-like protein [Camelus ferus] | 69.4605 | 4.22639045 | 69.151 | 0.6756191 | -1.004475713 | 0.948874313 |
| PREDICTED: gelsolin isoform X5 [Orycteropus afer afer] | 11.86605 | 0.86232527 | 11.8228 | 1.90746455 | -1.003658186 | 0.986787531 |
| PREDICTED: tropomyosin alpha-4 chain isoform 6 [Orcinus orca] | 164.835 | 9.69610102 | 164.4525 | 3.43483472 | -1.0023259 | 0.973819965 |
| transforming protein ras - rabbit | 1.7554 | 0.24539619 | 1.75159 | 0.26467881 | -1.002175167 | 0.992177908 |
| PREDICTED: synaptic vesicle membrane protein VAT-1 homolog [Sus scrofa] | 1.4953 | 0.26732804 | 1.49279 | 0.2864035 | -1.001681415 | 0.994846711 |
| nucleophosmin [Bos taurus] | 1.26038 | 0.25786916 | 1.2586425 | 0.27833549 | -1.001380456 | 0.961912311 |
| PREDICTED: cell surface glycoprotein MUC18 isoform X1 [Sus scrofa] | 2.5105 | 0.66085529 | 2.5094 | 0.91191523 | -1.000438352 | 0.998498186 |

| Protein Name | Control MEAN | Control SEM | Leptin MEAN | Leptin SEM | Ratio (Leptin/Control) | P value |
|---|--------------|-------------|-------------|------------|------------------------|-------------|
| PREDICTED: 60S ribosomal protein L23a-like [Equus caballus] | 0.5177 | 0.29890093 | 0.5176 | 0.5176 | -1.000193199 | 0.999825232 |
| RecName: Full=Sodium/potassium-transporting ATPase subunit alpha-1; Short=Sodium pump subunit alpha-1; AltName: Full=Na(+)/K(+) ATPase alpha-1 subunit; Flags: Precursor [Equus caballus] | 0.98755 | 0.38462955 | 0 | 0 | 0 | 0.082670109 |
| PREDICTED: alpha-aminoadipic semialdehyde dehydrogenase-like [Sus scrofa] | 0.98755 | 0.38462955 | 0 | 0 | 0 | 0.082670109 |
| coatomer subunit alpha [Bos taurus] | 1.80945 | 0.88970696 | 0 | 0 | 0 | 0.134854524 |
| PREDICTED: PRA1 family protein 3 [Camelus ferus] | 2.4437 | 1.24751852 | 0 | 0 | 0 | 0.145015048 |
| PREDICTED: adipocyte plasma membrane-associated protein [Sus scrofa] | 1.68615 | 1.03269894 | 0 | 0 | 0 | 0.201024176 |
| tenascin-X precursor [Sus scrofa] | 0.729925 | 0.45489984 | 0 | 0 | 0 | 0.206926313 |
| PREDICTED: mitochondrial inner membrane protein, partial [Sus scrofa] | 0.765375 | 0.48680041 | 0 | 0 | 0 | 0.213938092 |
| PREDICTED: ATP-dependent RNA helicase DDX1 [Equus caballus] | 0.7778 | 0.49760689 | 0 | 0 | 0 | 0.21597607 |

| Protein Name | Control MEAN | Control SEM | Leptin MEAN | Leptin SEM | Ratio (Leptin/Control) | P value |
|--|--------------|-------------|-------------|------------|------------------------|-------------|
| PREDICTED: non-histone chromosomal protein HMG-17 [Monodelphis domestica] | 0.7778 | 0.49760689 | 0 | 0 | 0 | 0.21597607 |
| PREDICTED: protein NipSnap homolog 3A [Sus scrofa] | 0.769125 | 0.49267537 | 0 | 0 | 0 | 0.21641467 |
| ch4 and secrete domains of swine IgM [Sus scrofa] | 0.50775 | 0.50775 | 0 | 0 | 0 | 0.391002219 |
| PREDICTED: NADH dehydrogenase [ubiquinone] 1 alpha subcomplex subunit 5 isoform X1 [Camelus ferus] | 0.520175 | 0.520175 | 0 | 0 | 0 | 0.391002219 |
| PREDICTED: ribosome maturation protein SBDS [Equus caballus] | 0.51525 | 0.51525 | 0 | 0 | 0 | 0.391002219 |
| DDRGK domain-containing protein 1 precursor [Bos taurus] | 0.51525 | 0.51525 | 0 | 0 | 0 | 0.391002219 |
| phosphatidylinositol 4-kinase alpha [Bos taurus] | 0.51525 | 0.51525 | 0 | 0 | 0 | 0.391002219 |
| PREDICTED: keratin, type II cytoskeletal 78 [Galeopterus variegatus] | 1.8034 | 1.8034 | 0 | 0 | 0 | 0.391002219 |
| fascin [Sus scrofa] | 0.46985 | 0.46985 | 0 | 0 | 0 | 0.391002219 |
| phosphatidate cytidyltransferase 2 [Bos taurus] | 0.46985 | 0.46985 | 0 | 0 | 0 | 0.391002219 |
| PREDICTED: elongation factor Tu, mitochondrial-like [Pantholops hodgsonii] | 0.7048 | 0.7048 | 0 | 0 | 0 | 0.391002219 |
| nitrogen regulatory protein P-II 1 [Methylothera sp. 1P/1] | 0.939725 | 0.939725 | 0 | 0 | 0 | 0.391002219 |

| Protein Name | Control MEAN | Control SEM | Leptin MEAN | Leptin SEM | Ratio (Leptin/Control) | <i>P</i> value |
|--|-------------------------|------------------------|------------------------|-----------------------|-----------------------------------|-----------------------|
| PREDICTED: 2',3'-cyclic-nucleotide 3'-phosphodiesterase [Sus scrofa] | 1.17465 | 1.17465 | 0 | 0 | 0 | 0.391002219 |
| MHC class I antigen [Sus scrofa] | 1.409575 | 1.409575 | 0 | 0 | 0 | 0.391002219 |
| MULTISPECIES: molecular chaperone GroEL [Mesorhizobium] | 2.3493 | 2.3493 | 0 | 0 | 0 | 0.391002219 |

APPENDIX B: Supplemental Figures

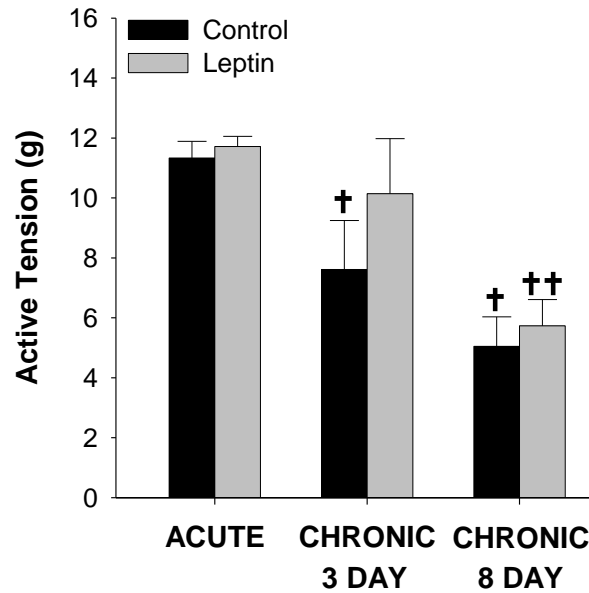


Figure I Effects of acute versus chronic leptin treatment on coronary contraction. Leptin treatment had no effect on vasoconstriction to the thromboxane A₂ receptor agonist, U46619 (1 μM) following acute, chronic 3 day, or chronic 8 day exposure. Contractile responses in untreated, control arteries were progressively reduced throughout the culture time course. Contractile responses in leptin treated arteries were also reduced following 8 days of exposure. All groups n = 4. †*P*<0.05 versus acute control. ††*P*<0.05 versus acute leptin

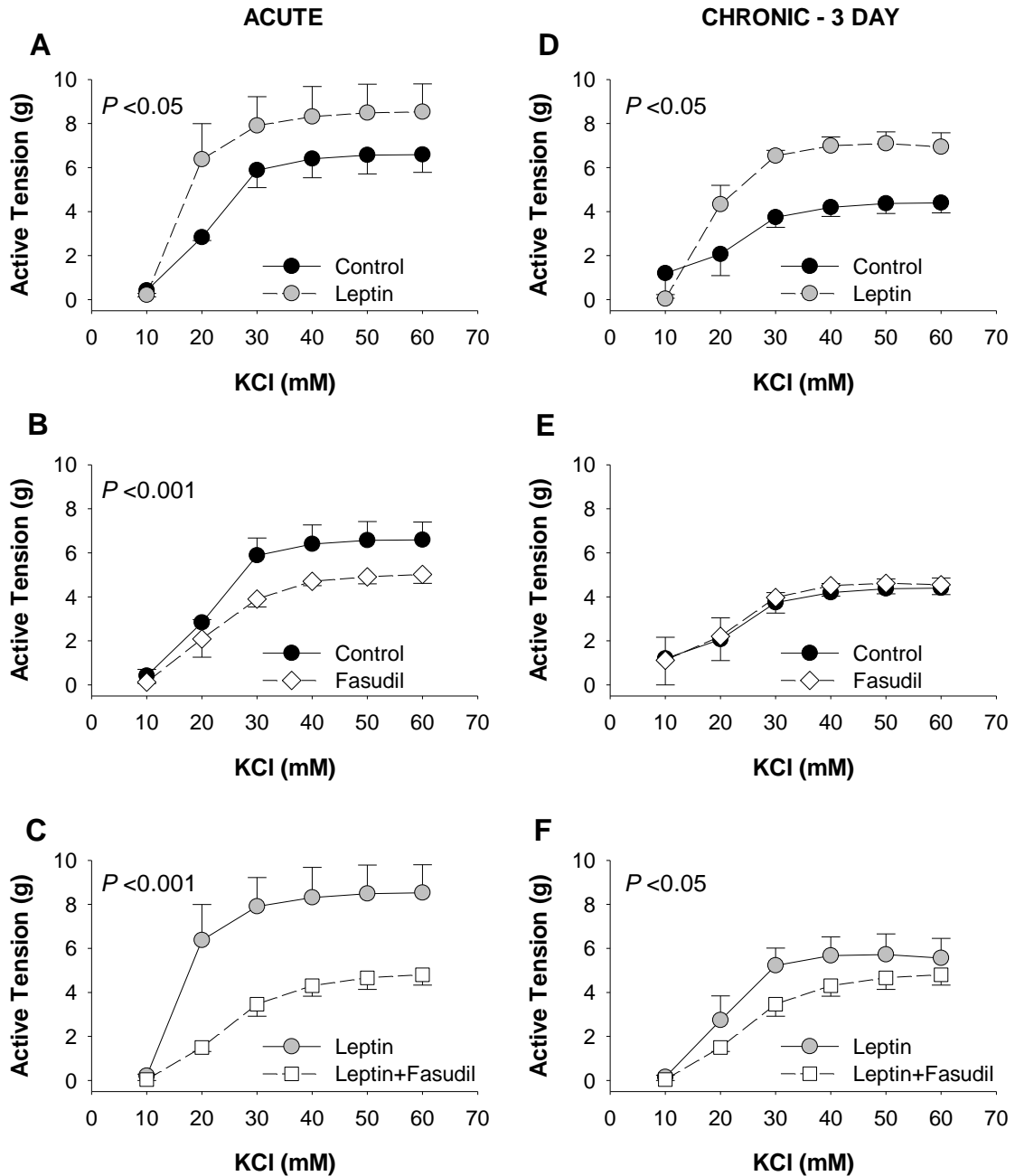


Figure II Effects of leptin and/or fasudil treatment in the absence of coronary endothelium. Functional responses observed in endothelium intact arteries following acute (Fig. 1A, 2A, 2C) and chronic (Fig. 1B, 2B, 2D) leptin administration were similar to those observed in endothelium denuded arteries following acute (A-C) and chronic, 3 day (D-F) exposure. All groups $n = 3$

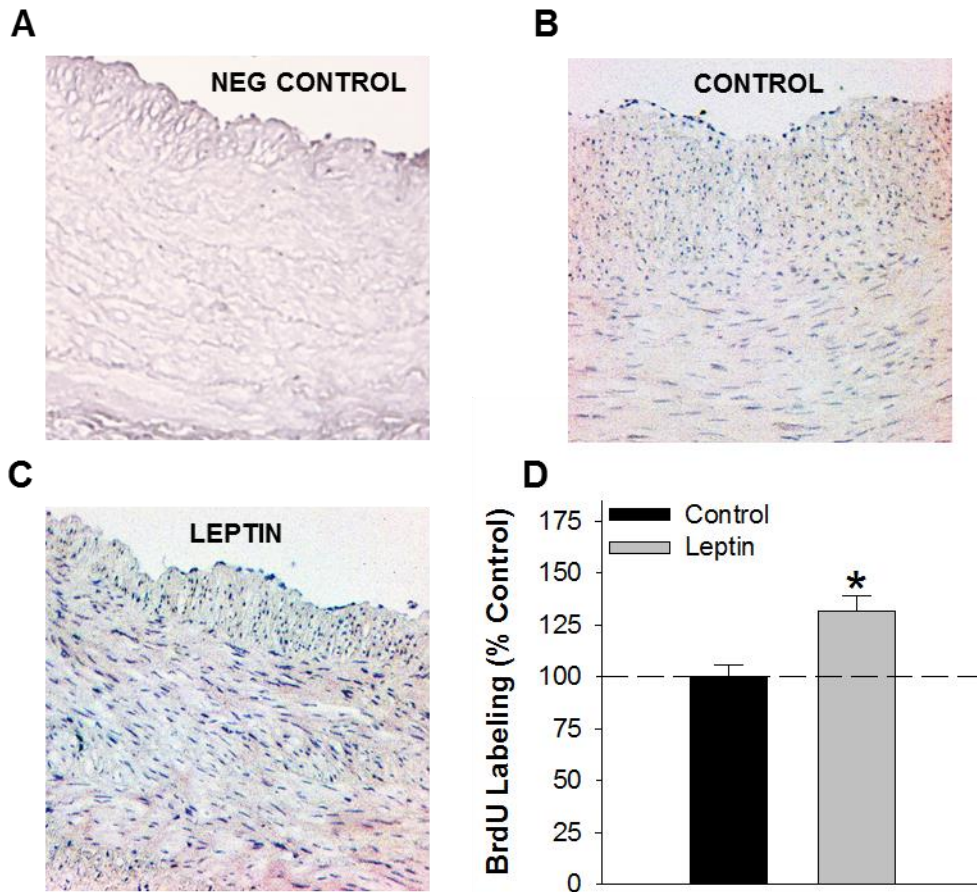


Figure III Leptin augments cellular proliferation in coronary arteries. Representative images of BrdU-proliferation assays in negative control (no BrdU added to culture media [A]), untreated, control (B) and leptin treated (C) arteries (8 day culture in serum containing media). A significantly higher percentage of BrdU-positive nuclei was detected in leptin treated, relative to untreated arteries (D). Each group n = 5. * $P < 0.05$, leptin versus control

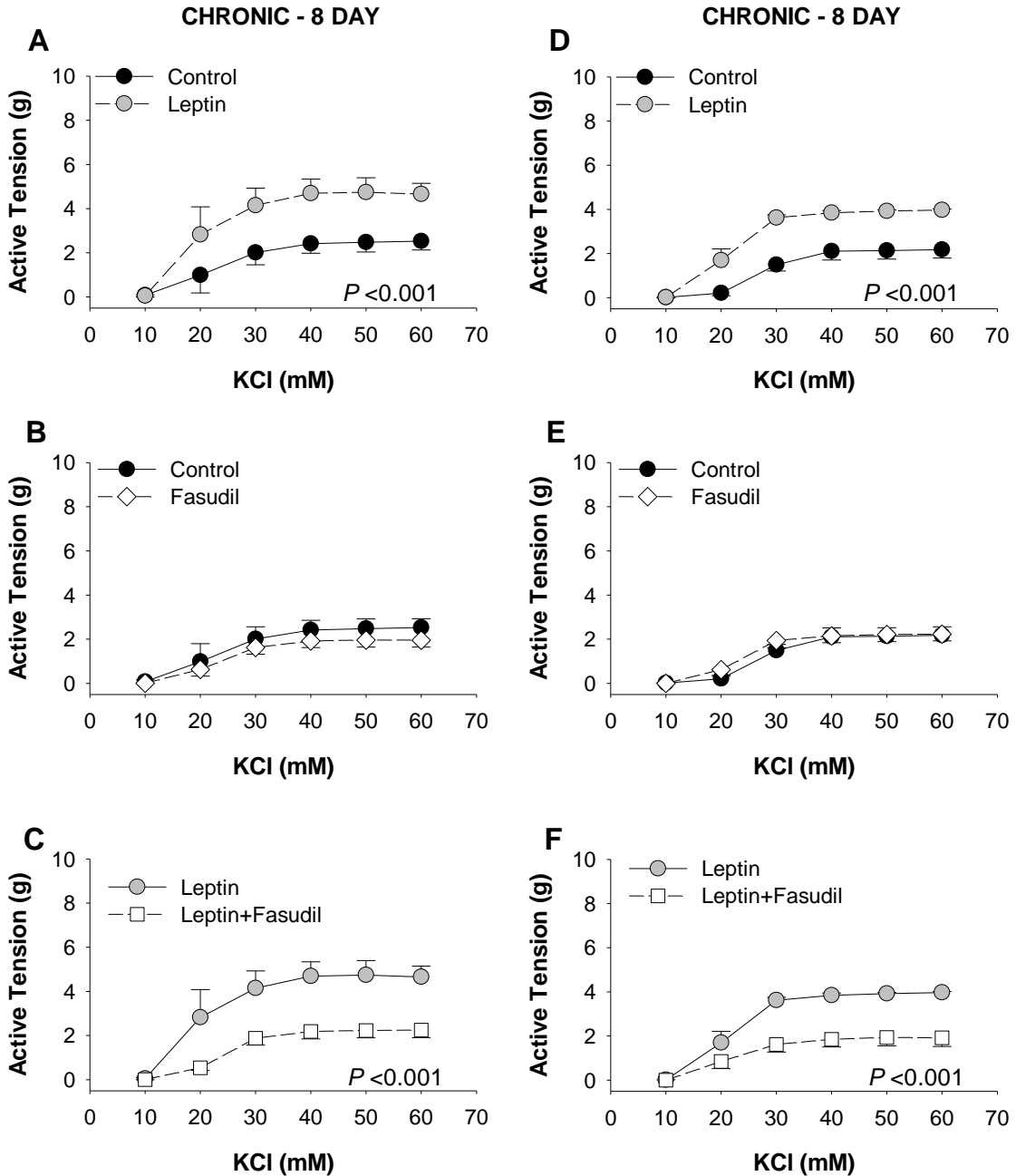


Figure IV Effects of chronic, 8 day leptin and/or fasudil treatment on depolarization-induced contractions. Chronic leptin administration (8 day culture, serum-containing media) increased KCl-induced contractions ~2.2 g at doses >40 mM (A). Inhibition of Rho kinase with fasudil (1 μ M) had no effect on vasoconstriction to KCl in the absence of leptin (B), but reduced the effect of leptin administration on KCl-induced contractions (C). Functional responses of all treatment groups were similar in endothelium denuded arteries (D-F). All groups n = 3

Reference List

- (1) Borbouse L, Dick GM, Asano S et al. Impaired function of coronary BK(Ca) channels in metabolic syndrome. *Am J Physiol Heart Circ Physiol* 2009;297:H1629-H1637.
- (2) Payne GA, Borbouse L, Kumar S et al. Epicardial perivascular adipose-derived leptin exacerbates coronary endothelial dysfunction in metabolic syndrome via a protein kinase C-beta pathway. *Arterioscler Thromb Vasc Biol* 2010;30:1711-1717.
- (3) World Health Organization. Global target 7: halt the rise in diabetes and obesity. Global status report on noncommunicable diseases, 2014. Geneva: WHO Press; 2014;79-94.
- (4) Berwick ZC, Dick GM, Tune JD. Heart of the matter: coronary dysfunction in metabolic syndrome. *J Mol Cell Cardiol* 2012;52:848-856.
- (5) Lohn M, Dubrovskaja G, Lauterbach B, Luft FC, Gollasch M, Sharma AM. Periadventitial fat releases a vascular relaxing factor. *Federation of American Societies for Experimental Biology* 2002;16:1057-1063.
- (6) Taube A, Schlich R, Sell H, Eckardt K, Eckel J. Inflammation and metabolic dysfunction: links to cardiovascular diseases. *Am J Physiol Heart Circ Physiol* 2012;302:H2148-H2165.
- (7) Mozaffarian D, Benjamin E, Go A et al. Heart disease and stroke statistics-2015 update: a report from the American Heart Association. *Circulation* 2015;131:e29-e322.
- (8) Brown NK, Zhou Z, Zhang J et al. Perivascular adipose tissue in vascular function and disease: a review of current research and animal models. *Arterioscler Thromb Vasc Biol* 2014;34:1621-1630.
- (9) Owen MK, Witzmann FA, McKenney ML et al. Perivascular Adipose Tissue Potentiates Contraction of Coronary Vascular Smooth Muscle: Influence of Obesity. *Circulation* 2013;128:9-18.
- (10) Bartell S, Rayalam S, Ambati S et al. Central (IVC) leptin injection increases bone formation, bone mineral density, muscle mass, serum IGF-1, and the expression of osteogenic genes in leptin-deficient ob/ob mice. *J Bone Miner Res* 2011;26:1710-1720.
- (11) Ng M, Fleming T, Robinson M et al. Global, regional, and national prevalence of overweight and obesity in children and adults during 1980-2013: a systematic analysis for the Global Burden of Disease Study 2013. *Lancet* 2014;384:766-781.
- (12) Freitas Lima L, Braga V, do Socorro de Franca Silva M et al. Adipokines, diabetes and atherosclerosis: an inflammatory association. *Front Physiol* 2015;6.
- (13) Ouchi N, Parker JL, Lugus JJ, Walsh K. Adipokines in inflammation and metabolic disease. *Nat Rev Immunol* 2011;11:85-97.

- (14) Skeoch S, Bruce I. Atherosclerosis in rheumatoid arthritis: is it all about inflammation? *Nat Rev Rheumatol* 2015;11:400.
- (15) Payne GA, Kohr MC, Tune JD. Epicardial perivascular adipose tissue as a therapeutic target in obesity-related coronary artery disease. *Br J Pharmacol* 2012;165:659-669.
- (16) Knudson JD, Dick GM, Tune JD. Adipokines and coronary vasomotor dysfunction. *Exp Biol Med (Maywood)* 2007;232:727-736.
- (17) Owen M, Noblet J, Sassoon D, Conteh A, Goodwill A, Tune J. Perivascular adipose tissue and coronary disease. *Arterioscler Thromb Vasc Biol* 2014;34:1643-1649.
- (18) Tousoulis D, Siasos G, Maniatis K et al. Serum osteoprotegerin and osteopontin levels are associated with arterial stiffness and the presence and severity of coronary artery disease. *Int J Cardiol* 2013;167:1924-1928.
- (19) Collin-Osdoby P. Regulation of vascular calcification by osteoclast regulatory factors RANKL and osteoprotegerin. *Circ Res* 2004;95:1046-1057.
- (20) Sacks HS, Fain JN. Human epicardial adipose tissue: a review. *Am Heart J* 2007;153:907-917.
- (21) Berwick ZC, Dick GM, Moberly SP, Kohr MC, Sturek M, Tune JD. Contribution of voltage-dependent K(+) channels to metabolic control of coronary blood flow. *J Mol Cell Cardiol* 2012;52:912-919.
- (22) Parhami F, Tintut Y, Ballard A, Fogelman A, Demer L. Leptin enhances the calcification of vascular cells: artery wall as a target of leptin. *Circ Res* 2001;88:954-960.
- (23) Roth J, Qiang X, Marban S, Redelt H, Lowell B. The obesity pandemic: where we have been and where are we going? *Obes Res* 2004;12:88S-101S.
- (24) Swinburn B, Sacks G, Hall K et al. The global obesity pandemic: shaped by global drivers and local environments. *Lancet* 2011;378:804-814.
- (25) Seidell J, Halberstadt J. The global burden of obesity and the challenges of prevention. *Ann Nutr Metab* 2015;66 (suppl 2):7-12.
- (26) Finucane M, Stevens G, Cowan M et al. National, regional, and global trends in body-mass index since 1980: systematic analysis of health examination surveys and epidemiological studies with 960 country-years and 9.1 million participants. *Lancet* 2011;377:557-567.
- (27) Flegal K, Carroll M, Ogden C, Curtin L. Prevalence and trends in obesity among US adults, 1999-2008. *JAMA* 2010;303:235-241.
- (28) Rokholm B, Baker J, Sorensen T. The levelling off of the obesity epidemic since the year 1999-a review of evidence and perspectives. *Obes Rev* 2010;11:835-846.

- (29) Flegal KM, Carroll MD, Kit BK, Ogden CL. Prevalence of obesity and trends in the distribution of body mass index among US adults, 1999-2010. *JAMA* 2012;307:491-497.
- (30) Ogden C, Carroll M, Kit B, Flegal K. Prevalence of childhood and adult obesity in the United States. *JAMA* 2014;311:806-814.
- (31) Sturm R. Increases in morbid obesity in the USA: 2000-2005. *Public Health* 2007;121:492-496.
- (32) Finkelstein E, Trogon J, Cohen J, Dietz W. Annual medical spending attributable to obesity: payer-and service-specific estimates. *Health Aff (Millwood)* 2009;28:w822-w831.
- (33) Hammond R, Levine R. The economic impact of obesity in the United States. *Diabetes Metab Syndr Obes* 2010;3:285-295.
- (34) Wolf A. What is the economic case for treating obesity? *Obes Res* 1998;6:2S-7S.
- (35) Khaodhiar L, McCowen K, Blackburn G. Obesity and its comorbid conditions. *Clin Cornerstone* 1999;2:17-31.
- (36) Haslam D, James W. Obesity. *Lancet* 2005;366:1197-1209.
- (37) Reaven G. Banting lecture 1988: role of insulin resistance in human disease. *Diabetes* 1988;37:1595-1607.
- (38) Grundy SM, Brewer HB, Jr., Cleeman JI, Smith SC, Jr., Lenfant C. Definition of metabolic syndrome: Report of the National Heart, Lung, and Blood Institute/American Heart Association conference on scientific issues related to definition. *Circulation* 2004;109:433-438.
- (39) Eckel R, Grundy S, Zimmet P. The metabolic syndrome. *Lancet* 2005;365:1415-1428.
- (40) Park Y, Zhu S, Palaniappan L, Heshka S, Carnethon M, Heymsfield S. The metabolic syndrome prevalence and associated risk factor findings in the US population from the Third National Health and Nutrition Examination Survey, 1988-1994. *Arch Intern Med* 2003;163:427-436.
- (41) Cameron A, Shaw J, Zimmet P. The metabolic syndrome: prevalence in worldwide populations. *Endocrinol Metab Clin North Am* 2004;33:351-375.
- (42) Lakka HM, Laaksonen DE, Lakka TA et al. The metabolic syndrome and total and cardiovascular disease mortality in middle-aged men. *JAMA* 2002;288:2709-2716.
- (43) Isomaa B, Almgren P, Tuomi T et al. Cardiovascular morbidity and mortality associated with the metabolic syndrome. *Diabetes Care* 2001;24:683-689.
- (44) Hubert H, Feinleib M, McNamara P, Castelli W. Obesity is an independent risk factor for cardiovascular disease: a 26 year follow-up of participants in the Framingham Heart Study. *Circulation* 1983;67:968-977.

- (45) Eckel R. Obesity and heart disease: a statement for healthcare professional from the Nutrition Committee. *Circulation* 1997;96:3248-3250.
- (46) Cho E, Manson J, Stampfer M et al. A prospective study of obesity and risk of coronary heart disease among diabetic women. *Diabetes Care* 2002;25:1142-1148.
- (47) Berg A, Chérer P. Adipose tissue, inflammation, and cardiovascular disease. *Circ Res* 2005;96:939-949.
- (48) Lau DC, Dhillon B, Yan H, Szmitko PE, Verma S. Adipokines: molecular links between obesity and atherosclerosis. *Am J Physiol Heart Circ Physiol* 2005;288:H2031-H2041.
- (49) Trayhurn P, Beattie J. Physiological role of adipose tissue: white adipose tissue as an endocrine and secretory organ. *Proc Nutr Soc* 2001;60:329-339.
- (50) Rosen E. What we talk about when we talk about fat. *Cell* 2014;156:20-44.
- (51) Hajer G, van Haeften T, Visseren F. Adipose tissue dysfunction in obesity, diabetes, and vascular diseases. *Eur Heart J* 2008;29:2959-2971.
- (52) O'Rourke R, White A, Metcalf M et al. Hypoxia-induced inflammatory cytokine secretion in human adipose tissue stromovascular cells. *Diabetologica* 2011;54:1480-1490.
- (53) Skuple P, Harder C, Kraft I, Müller-Schölze S, Hauner H, Kolb H. Production and release of macrophage migration inhibitory factor from human adipocytes. *Endocrinology* 2005;146:1006-1011.
- (54) Lau D, Schillabeer G, Li Z, Wong K, Varzaneh F, Tough S. Paracrine interactions in adipose tissue development and growth. *J Obes Relat Metab Disord* 1996;20:S16-S25.
- (55) Hirsch J, Batchelor B. Adipose tissue cellularity in human obesity. *Endocrinol Metab* 1976;5:299-311.
- (56) Juge-Aubry CE, Henrichot E, Meier CA. Adipose tissue: a regulator of inflammation. *Best Pract Res Clin Endocrinol Metab* 2005;19:547-566.
- (57) Skurk T, Alberti-Huber C, Herder C, Hauner H. Relationship between adipocyte size and adipokine expression and secretion. *J Clin Endocrinol Metab* 2007;92:1023-1033.
- (58) Weisberg S, McCann D, Desai M, Rosenbaum M, Leibel R, Ferrante A. Obesity is associated with macrophage accumulation in adipose tissue. *J Clin Invest* 2003;112:1796-1808.
- (59) Ouchi N, Shibata R, Walsh K. Cardioprotection by adiponectin. *Trends Cardiovasc Med* 2006;16:141-146.
- (60) Beltowski J, Jamroz-Wisniewska A, Widomska S. Adiponectin and its role in cardiovascular diseases. *Cardiovasc Hematol Disord Drug Targets* 2008;8:7-46.

- (61) Ouchi N, Shibata R, Walsh K. Targeting adiponectin for cardioprotection. *Expert Opin Ther Targets* 2006;10:573-581.
- (62) Withers SB, Bussey CE, Saxton SN, Melrose HM, Watkins AE, Heagerty AM. Mechanisms of adiponectin-associated perivascular function in vascular disease. *Arterioscler Thromb Vasc Biol* 2014;34:1637-1642.
- (63) Hu E, Liang P, Spiegelman B. AdipoQ is a novel adipose-specific gene dysregulated in obesity. *J Biol Chem* 1996;271:10697-10703.
- (64) Packerd R, Libby P. Inflammation in atherosclerosis: from vascular biology to biomarker discovery and risk prediction. *Clin Chem* 2008;54:24-38.
- (65) Libby P, Ridker P, Maseri A. Inflammation and atherosclerosis. *Circulation* 2002;105:1135-1143.
- (66) Verma S, Anderson T. Fundamentals of endothelial function for the clinical cardiologist. *Circulation* 2002;105:546-549.
- (67) Lusis AJ. Atherosclerosis. *Nature* 2000;407:233-241.
- (68) Ross R. Atherosclerosis --an inflammatory disease. *N Engl J Med* 1999;340:115-126.
- (69) Tuttolomondo A, Di RD, Pecoraro R, Arnao V, Pinto A, Licata G. Atherosclerosis as an inflammatory disease. *Curr Pharm Des* 2012;18:4266-4288.
- (70) Beltowski J. Leptin and atherosclerosis. *Atherosclerosis* 2006;189:47-60.
- (71) Beltowski J. Leptin and the regulation of endothelial function in physiological and pathological conditions. *Clin Exp Pharmacol Physiol* 2011;39:168-178.
- (72) Samaras K, Botelho N, Chisholm D, Lord R. Subcutaneous and visceral adipose tissue gene expression of serum adipokines that predict type 2 diabetes. *Obesity* 2010;18:884-889.
- (73) Chatterjee TK, Aronow BJ, Tong WS et al. Human coronary artery perivascular adipocytes overexpress genes responsible for regulating vascular morphology, inflammation, and hemostasis. *Physiol Genomics* 2013;45:697-709.
- (74) Wajchenberg B. Subcutaneous and visceral adipose tissue: their relation to the metabolic syndrome. *Endocr Rev* 2000;21:697-738.
- (75) Chatterjee TK, Stoll LL, Denning GM et al. Proinflammatory phenotype of perivascular adipocytes: influence of high-fat feeding. *Circ Res* 2009;104:541-549.
- (76) Alvarez-Llamas G, Szalowska E, de Vries M et al. Characterization of the human visceral adipose tissue secretome. *Mol Cell Proteomics* 2007;6:589-600.
- (77) Montani JP, Carroll JF, Dwyer TM, Antic V, Yang Z, Dulloo AG. Ectopic fat storage in heart, blood vessels and kidneys in the pathogenesis of cardiovascular diseases. *Int J Obes Relat Metab Disord* 2004;28 Suppl 4:S58-S65.

- (78) Gil-Ortega M, Somoza B, Huang Y, Gollasch M, Fernandez-Alfonso M. Regional differences in perivascular adipose tissue impacting vascular homeostasis. *Trends Endocrinol Metab* 2015;26:367-375.
- (79) Eringa E, Bakker W, van Hinsbergh W. Paracrine regulation of vascular tone, inflammation and insulin sensitivity by perivascular adipose tissue. *Vascul Pharmacol* 2012;56:204-209.
- (80) Thalmann S, Meier CA. Local adipose tissue depots as cardiovascular risk factors. *Cardiovasc Res* 2007;75:690-701.
- (81) Omar A, Chatterjee T, Tang Y, Hui D, Weintraub N. Proinflammatory phenotype of perivascular adipocytes. *Arterioscler Thromb Vasc Biol* 2014;34:1634-1636.
- (82) Ouwens DM, Sell H, Greulich S, Eckel J. The role of epicardial and perivascular adipose tissue in the pathophysiology of cardiovascular disease. *J Cell Mol Med* 2010;14:2223-2234.
- (83) Henrichot E, Juge-Aubry CE, Pernin A et al. Production of chemokines by perivascular adipose tissue: a role in the pathogenesis of atherosclerosis? *Arteriosclerosis Thrombosis & Vascular Biology* 2005;25:2594-2599.
- (84) Houben A, Eringa E, Jonk A, Serne E, Smulders Y, Stehouwer C. Perivascular fat and the microcirculation: relevance to insulin resistance, diabetes, and cardiovascular disease. *Curr Cardiovasc Risk Rep* 2012;6:80-90.
- (85) Fox C, Massaro J, Schlett C et al. Periaortic fat deposition is associated with peripheral arterial disease: the Framingham heart study. *Circ Cardiovasc Imaging* 2010;3:515-519.
- (86) Iozzo P. Myocardial, perivascular, and epicardial fat. *Diabetes Care* 2011;34(Suppl 2):S371-S379.
- (87) Sacks H, Fain J, Holman B et al. Uncoupling protein-1 and related messenger ribonucleic acids in human epicardial and other adipose tissues: epicardial fat functioning as brown fat. *J Clin Endocrinol Metab* 2009;94:3611-3615.
- (88) Cai X, Lin Y, Hauschka P, Grottkau B. Adipose stem cells originate from perivascular cells. *Biol Cell* 2011;103:435-447.
- (89) Zhao X, Gong P, Lin Y, Wang J, Yang X, Cai X. Characterization of α -smooth muscle actin positive cells during multilineage differentiation of dental pulp stem cells. *Cell Prolif* 2012;45:259-265.
- (90) Iacobellis G, Willens HJ. Echocardiographic epicardial fat: a review of research and clinical applications. *J Am Soc Echocardiogr* 2009;22:1311-1319.
- (91) Verhagen SN, Visseren FL. Perivascular adipose tissue as a cause of atherosclerosis. *Atherosclerosis* 2011;214:3-10.
- (92) Iacobellis G, Assael F, Ribaldo M et al. Epicardial fat from echocardiography: a new method for visceral adipose tissue prediction. *Obes Res* 2003;11:304-310.

- (93) Wheeler G, Shi R, Beck S et al. Pericardial and visceral adipose tissues measured volumetrically with computed tomography are highly associated in type 2 diabetic families. *Invest Radiol* 2005;40:97-101.
- (94) Sarin S, Wenger C, Marwaha A et al. Clinical significance of epicardial fat measured using cardiac multislice computed tomography. *Am J Cardiol* 2008;102:767-771.
- (95) Greif M, Becker A, von ZF et al. Pericardial adipose tissue determined by dual source CT is a risk factor for coronary atherosclerosis. *Arterioscler Thromb Vasc Biol* 2009;29:781-786.
- (96) Ahn S, Lim H, Joe D et al. Relationship of epicardial adipose tissue by echocardiography to coronary artery disease. *Heart* 2008;94:e7.
- (97) Jeong J, Jeong M, Yun K et al. Echocardiographic epicardial fat thickness and coronary artery disease. *Circ J* 2007;71:536-539.
- (98) Ding J, Hsu FC, Harris TB et al. The association of pericardial fat with incident coronary heart disease: the Multi-Ethnic Study of Atherosclerosis (MESA). *Am J Clin Nutr* 2009;90:499-504.
- (99) Mahabadi AA, Reinsch N, Lehmann N et al. Association of pericoronary fat volume with atherosclerotic plaque burden in the underlying coronary artery: a segment analysis. *Atherosclerosis* 2010;211:195-199.
- (100) Verhagen S, Vink A, van der Graaf Y, Visseren F. Coronary perivascular adipose tissue characteristics are related to atherosclerotic plaque size and composition. A post-mortem study. *Atherosclerosis* 2012;225:99-104.
- (101) McKenney M, Schultz K, Boyd J, Byrd J, Alloosh M. Epicardial adipose excision slows the progression of porcine coronary atherosclerosis. *J Cardiothorac Surg* 2014;9.
- (102) Schlett CL, Massaro JM, Lehman SJ et al. Novel measurements of periaortic adipose tissue in comparison to anthropometric measures of obesity, and abdominal adipose tissue. *Int J Obes (Lond)* 2009;33:226-232.
- (103) Lehman SJ, Massaro JM, Schlett CL, O'Donnell CJ, Hoffmann U, Fox CS. Periaortic fat, cardiovascular disease risk factors, and aortic calcification: the Framingham Heart Study. *Atherosclerosis* 2010;210:656-661.
- (104) Tune JD, Gorman MW, Feigl EO. Matching coronary blood flow to myocardial oxygen consumption. *J Appl Physiol* 2004;97:404-415.
- (105) Tune J, Richmond K, Gorman M, Feigl E. Control of coronary blood flow during exercise. *Exp Biol Med (Maywood)* 2002;227:238-250.
- (106) Duncker D, Bache R. Regulation of coronary blood flow during exercise. *Physiol Rev* 2008;88:1009-1086.

- (107) He M, Downey H. Downregulation of ventricular contractile function during early ischemia is flow but not pressure dependent. *Am J Physiol* 1998;275:H1520-H1523.
- (108) He M, Wang S, Downey H. Correlation between myocardial contractile force and cytosolic inorganic phosphate during early ischemia. *Am J Physiol* 1997;272:H1333-H1341.
- (109) Ross Jr. Myocardial perfusion-contraction matching. Implications for coronary heart disease and hibernation. *Circulation* 1991;83:1076-1083.
- (110) Feigl EO. Coronary physiology. *Physiol Rev* 1983;63:1-205.
- (111) Pirat B, Bozbas H, Simsek V et al. Impaired coronary flow reserve in patients with metabolic syndrome. *Atherosclerosis* 2008;201:112-116.
- (112) Schindler T, Cardenas J, Prior J et al. Relationship between increasing body weight, insulin resistance, inflammation, adipocytokine leptin, and coronary circulatory function. *J Am Coll Cardiol* 2006;47:1188-1195.
- (113) Setty S, Sun W, Tune JD. Coronary blood flow regulation in the prediabetic metabolic syndrome. *Basic Res Cardiol* 2003;98:416-423.
- (114) Zhang C, Knudson JD, Setty S et al. Coronary arteriolar vasoconstriction to angiotensin II is augmented in prediabetic metabolic syndrome via activation of AT1 receptors. *Am J Physiol Heart Circ Physiol* 2005;288:H2154-H2162.
- (115) Teragawa H, Morita K, Shishido H et al. Impaired myocardial blood flow reserve in subjects with metabolic syndrome analyzed using positron emission tomography and N-13 labeled ammonia. *Eur J Nucl Med Mol Imaging* 2010;37:368-376.
- (116) Kondo I, Mizushige K, Hirao K et al. Ultrasonographic assessment of coronary flow reserve and abdominal fat in obesity. *Ultrasound Med Biol* 2001;27:1199-1205.
- (117) Kiviniemi T, Snapir A, Saraste M et al. Determinants of coronary flow velocity reserve in healthy young men. *Am J Heart Circ Physiol* 2006;291:H564-H569.
- (118) De BB, Hersbach F, Pijls NH et al. Abnormal epicardial coronary resistance in patients with diffuse atherosclerosis but "Normal" coronary angiography. *Circulation* 2001;104:2401-2406.
- (119) Borbouse L, Dick GM, Payne GA et al. Metabolic syndrome reduces the contribution of K⁺ channels to ischemic coronary vasodilation. *Am J Physiol Heart Circ Physiol* 2010;298:H1182-H1189.
- (120) Galassi A, Reynolds K, He J. Metabolic syndrome an drisk of cardiovascular disease: a meta-analysis. *Am J Med* 2006;119:812-819.
- (121) Lambert G, Straznicky N, Lambert E, Dixon J, Schlaich M. Sympathetic nervous system activation in obesity and the metabolic syndrome - causes, consequences and therapeutic implications. *Pharmacol Ther* 2010;126:156-172.

- (122) Straznicky N, Eikelis N, Lambert E, Esler M. Mediators of sympathetic activation in metabolic syndrome obesity. *Curr Hypertens Rep* 2008;10:440-447.
- (123) Grasi G, Dell'oro R, Quarti-Trevano F et al. Neuroadrenergic and reflex abnormalities in patients with metabolic syndrome. *Diabetologia* 2005;48:1359-1365.
- (124) Huggett R, Burns J, Mackintosh A, Mary D. Sympathetic neural activation in nondiabetic metabolic syndrome and its further augmentation by hypertension. *Hypertension* 2004;44:847-852.
- (125) Dincer UD, Araiza AG, Knudson JD, Molina PE, Tune JD. Sensitization of coronary alpha-adrenoceptor vasoconstriction in the prediabetic metabolic syndrome. *Microcirculation* 2006;13:587-595.
- (126) Grisk O, Frauendorf T, Schluter T et al. Impaired coronary function in Wistar Ottawa Karlsburg W rats - a new model of the metabolic syndrome. *Pflugers Arch* 2007;454:1011-1021.
- (127) Kushibiki M, Yamada M, Oikawa K, Tomita H, Osani T, Okumura K. Aldosterone causes vasoconstriction in coronary arterioles of rats via angiotensin II type-1 receptor: influence of hypertension. *Eur J Pharmacol* 2007;572:182-188.
- (128) Fujita M, Minamino T, Asanuma H et al. Aldosterone nongenomically worsens ischemia via protein kinase C-dependent pathways in hypoperfused canine hearts. *Hypertension* 2005;46:113-117.
- (129) Dick GM, Tune JD. Role of potassium channels in coronary vasodilation. *Exp Biol Med (Maywood)* 2010;235:10-22.
- (130) Ganitkevich V, Isenberg G. Contribution of two types of calcium channels to membrane conductance of single myocytes from guinea-pig coronary artery. *Am J Physiol* 1990;19:42.
- (131) Matsuda J, Volk K, Shibata E. Calcium currents in isolated rabbit coronary arterial smooth muscle myocytes. *J Physiol* 1990;427:657-680.
- (132) Dick G, Bratz I, Borbouse L et al. Voltage-dependent K⁺ channels regulate the duration of reactive hyperemia in the canine coronary circulation. *Circulation* 2008;118:H2371-H2381.
- (133) Rogers PA, Chilian WM, Bratz IN, Bryan RM, Jr., Dick GM. H₂O₂ activates redox- and 4-aminopyridine-sensitive K_v channels in coronary vascular smooth muscle. *Am J Physiol Heart Circ Physiol* 2007;292:H1404-H1411.
- (134) Miura H, Liu Y, Gutterman D. Human coronary arteriolar dilation to bradykinin depends on membrane hyperpolarization: contribution of nitric oxide and Ca²⁺-activated K⁺ channels. *Circulation* 1999;99:3132-3138.
- (135) Miura H, Wachtel R, Liu Y, Loberiza Jr F, Saito T, Miura M. Flow-induced dilation of human coronary arterioles: important role of Ca²⁺-activated K⁺ channels. *Circulation* 2001;103:1992-1998.

- (136) Borbouse L, Dick GM, Payne GA et al. Contribution of BK(Ca) channels to local metabolic coronary vasodilation: Effects of metabolic syndrome. *Am J Physiol Heart Circ Physiol* 2010;298:H966-H973.
- (137) Mokolke E, Dietz N, Eckman D, Nelson M, Sturek M. Diabetic dyslipidemia and exercise affect coronary tone and differential regulation of conduit microvessel K⁺ current. *Am J Physiol Heart Circ Physiol* 2005;288:H1223-H1241.
- (138) Witczak CA, Wamhoff BR, Sturek M. Exercise training prevents Ca²⁺ dysregulation in coronary smooth muscle from diabetic dyslipidemic yucatan swine. *J Appl Physiol* 2006;101:752-762.
- (139) Bowles D, Heaps C, Turk J, Maddali K, Price E. Hypercholesterolemia inhibits L-type calcium current in coronary macro-, not microcirculation. *J Appl Physiol* 2004;96:2240-2248.
- (140) Knudson JD, Dincer UD, Bratz IN, Sturek M, Dick GM, Tune JD. Mechanisms of coronary dysfunction in obesity and insulin resistance. *Microcirculation* 2007;14:317-338.
- (141) Berwick ZC, Dick GM, O'Leary HA et al. Contribution of electromechanical coupling between KV and CaV1.2 channels to coronary dysfunction in obesity. *Basic Res Cardiol* 2013;108:370.
- (142) Murthy VL, Naya M, Foster CR et al. Association between coronary vascular dysfunction and cardiac mortality in patients with and without diabetes mellitus. *Circulation* 2012;126:1858-1868.
- (143) Chilian WM, Eastham CL, Marcus ML. Microvascular distribution of coronary vascular resistance in beating left ventricle. *Am J Physiol* 1986;251:H779-H788.
- (144) Sturek M. Ca²⁺ regulatory mechanisms of exercise protection against coronary artery disease in metabolic syndrome and diabetes. *J Appl Physiol* 2011;111:573-586.
- (145) Adams MR, Robinson J, McCredie R et al. Smooth muscle dysfunction occurs independently of impaired endothelium-dependent dilation in adults at risk of atherosclerosis. *J Am Coll Cardiol* 1998;32:123-127.
- (146) Gomez D, Owens GK. Smooth muscle cell phenotypic switching in atherosclerosis. *Cardiovasc Res* 2012;95:156-164.
- (147) Berra-Romani R, Mazzocco-Spezia A, Pulina M, Golovina V. Ca²⁺ handling is altered when arterial myocytes progress from a contractile to a proliferative phenotype in culture. *Am J Physiol Cell Physiol* 2008;295:C790.
- (148) Campbell J, Campbell G. Smooth muscle phenotypic modulation - a personal experience. *Arterioscler Thromb Vasc Biol* 2012;32:1789.
- (149) Soltis EE, Cassis LA. Influence of perivascular adipose tissue on rat aortic smooth muscle responsiveness. *Clin Exp Hypertens A* 1991;13:277-296.

- (150) Dubrovskaja G, Verlohren S, Luft FC, Gollasch M. Mechanisms of ADRF release from rat aortic adventitial adipose tissue. *Am J Physiol Heart Circ Physiol* 2004;286:H1107-H1113.
- (151) Gao YJ, Lu C, Su LY, Sharma AM, Lee RM. Modulation of vascular function by perivascular adipose tissue: the role of endothelium and hydrogen peroxide. *Br J Pharmacol* 2007;151:323-331.
- (152) Galvez B, de Castro J, Herold D et al. Perivascular adipose tissue and mesenteric vascular function in spontaneously hypertensive rats. *Arterioscler Thromb Vasc Biol* 2006;26:1297-1302.
- (153) Schleifenbaum J, Kohn C, Voblova N et al. Systemic peripheral artery relaxation by KCNQ channel openers and hydrogen sulfide. *J Hypertens* 2010;28:1875-1882.
- (154) Verlohren S, Dubrovskaja G, Tsang SY et al. Visceral periadventitial adipose tissue regulates arterial tone of mesenteric arteries. *Hypertension* 2004;44:271-276.
- (155) Lee RM, Lu C, Su LY, Gao YJ. Endothelium-dependent relaxation factor released by perivascular adipose tissue. *J Hypertens* 2009;27:782-790.
- (156) Gao YJ, Takemori K, Su LY et al. Perivascular adipose tissue promotes vasoconstriction: the role of superoxide anion. *Cardiovasc Res* 2006;71:363-373.
- (157) Gollasch M. Vasodilator signals from perivascular adipose tissue. *Br J Pharmacol* 2012;165:633-642.
- (158) Gao YJ, Zeng ZH, Teoh K et al. Perivascular adipose tissue modulates vascular function in the human internal thoracic artery. *J Thorac Cardiovasc Surg* 2005;130:1130-1136.
- (159) Malinowski M, Deja MA, Golba KS, Roleder T, Biernat J, Wos S. Perivascular tissue of internal thoracic artery releases potent nitric oxide and prostacyclin-independent anticontractile factor. *Eur J Cardiothorac Surg* 2008;33:225-231.
- (160) Greenstein AS, Khavandi K, Withers SB et al. Local inflammation and hypoxia abolish the protective anticontractile properties of perivascular fat in obese patients. *Circulation* 2009;119:1661-1670.
- (161) Fesus G, Dubrovskaja G, Gorzelniak K et al. Adiponectin is a novel humoral vasodilator. *Cardiovasc Res* 2007;75:719-727.
- (162) Tano JY, Schleifenbaum J, Gollasch M. Perivascular adipose tissue, potassium channels, and vascular dysfunction. *Arterioscler Thromb Vasc Biol* 2014;34:1827-1830.
- (163) Zavaritskaya O, Zhuravleva N, Schleifenbaum J et al. Role of KCNQ channels in skeletal muscle arteries and periadventitial vascular dysfunction. *Hypertension* 2013;61:151-159.

- (164) Lynch F, Withers S, Yao Z et al. Perivascular adipose tissue-derived adiponectin activates BK(Ca) channels to induce anticontractile responses. *Am J Physiol Heart Circ Physiol* 2013;304:H786-H795.
- (165) Rivers R, Hein T, Zhang C, Kuo L. Activation of barium-sensitive inward rectifier potassium channels mediates remote dilation of coronary arteries. *Circulation* 2001;104:1479-1753.
- (166) Lu C, Su LY, Lee RM, Gao YJ. Mechanisms for perivascular adipose tissue-mediated potentiation of vascular contraction to perivascular neuronal stimulation: the role of adipocyte-derived angiotensin II. *Eur J Pharmacol* 2010;634:107-112.
- (167) Ma L, Ma S, He H, Yang D, Chen X, Luo Z. Perivascular fat-mediated vascular dysfunction and remodeling through the AMPK/mTOR pathway in high-fat diet-induced obese rats. *Hypertens Res* 2010;33:446-453.
- (168) Marchesi C, Ebrahimian T, Angulo O, Paradis P, Schiffrin EL. Endothelial nitric oxide synthase uncoupling and perivascular adipose oxidative stress and inflammation contribute to vascular dysfunction in a rodent model of metabolic syndrome. *Hypertension* 2009;54:1384-1392.
- (169) Ketonen J, Shi J, Martonen E, Mervaala E. Periadventitial adipose tissue promotes endothelial dysfunction via oxidative stress in diet-induced obese C57Bl/6 mice. *Circ J* 2010;74:1479-1487.
- (170) Watts S, Dorrance A, Penfold M et al. Chemerin connects fat to arterial contraction. *Arterioscler Thromb Vasc Biol* 2013;33:1320-1328.
- (171) Payne GA, Borbouse L, Bratz IN et al. Endogenous adipose-derived factors diminish coronary endothelial function via inhibition of nitric oxide synthase. *Microcirculation* 2008;15:417-426.
- (172) Payne GA, Bohlen HG, Dincer UD, Borbouse L, Tune JD. Periadventitial adipose tissue impairs coronary endothelial function via PKC-beta-dependent phosphorylation of nitric oxide synthase. *Am J Physiol Heart Circ Physiol* 2009;297:H460-H465.
- (173) Reifenberger MS, Turk JR, Newcomer SC, Booth FW, Laughlin MH. Perivascular fat alters reactivity of coronary artery: effects of diet and exercise. *Med Sci Sports Exerc* 2007;39:2125-2134.
- (174) Bunker AK, Laughlin MH. Influence of exercise and perivascular adipose tissue on coronary artery vasomotor function in a familial hypercholesterolemic porcine atherosclerosis model. *J Appl Physiol* 2010;108:490-497.
- (175) Lim S, Meigs J. Ectopic fat and cardiometabolic and vascular risk. *Int J Cardiol* 2013;169:166-176.
- (176) Baker AR, Silva NF, Quinn DW et al. Human epicardial adipose tissue expresses a pathogenic profile of adipocytokines in patients with cardiovascular disease. *Cardiovasc Diabetol* 2006;5:1.

- (177) Cheng KH, Chu CS, Lee KT et al. Adipocytokines and proinflammatory mediators from abdominal and epicardial adipose tissue in patients with coronary artery disease. *Int J Obes (Lond)* 2008;32:268-274.
- (178) Karastergiou K, Fried S. Multiple adipose depots increase cardiovascular risk via local and systemic effects. *Curr Atheroscler Rep* 2013;15:361.
- (179) Shibasaki I, Nishikimi T, Mochizuki Y et al. Greater expression of inflammatory cytokines, adrenomedullin, and natriuretic peptide receptor-C in epicardial adipose tissue in coronary artery disease. *Regul Pept* 2010;165:210-217.
- (180) Ikeda T, Shirasawa T, Esaki Y, Yoshiki S, Hirokawa K. Osteopontin mRNA is expressed by smooth muscle-derived foam cells in human atherosclerotic lesions of the aorta. *J Clin Invest* 1993;92:2814-2820.
- (181) Langheim S, Dreas L, Veschini L et al. Increased expression and secretion of resistin in epicardial adipose tissue of patients with acute coronary syndrome. *Am J Physiol Heart Circ Physiol* 2010;298:H746-H753.
- (182) Iacobellis G, Pistilli D, Gucciardo M et al. Adiponectin expression in human epicardial adipose tissue in vivo is lower in patients with coronary artery disease. *Cytokine* 2005;29:251-255.
- (183) Tesouro M, Cardillo C. Obesity, blood vessels and metabolic syndrome. *Acta Physiol (Oxf)* 2011;203:279-286.
- (184) Mazurek T, Zhang L, Zalewski A et al. Human epicardial adipose tissue is a source of inflammatory mediators. *Circulation* 2003;108:2460-2466.
- (185) Herrmann J, Lerman LO, Rodriguez-Porcel M et al. Coronary vasa vasorum neovascularization precedes epicardial endothelial dysfunction in experimental hypercholesterolemia. *Cardiovasc Res* 2001;51:762-766.
- (186) Moreno P, Purushothaman K, Sirol M, Levy A, Fuster V. Neovascularization in human atherosclerosis. *Circulation* 2006;113:2245-2252.
- (187) Gossel M, Versari D, Mannheim D, Ritman EL, Lerman LO, Lerman A. Increased spatial vasa vasorum density in the proximal LAD in hypercholesterolemia--implications for vulnerable plaque-development. *Atherosclerosis* 2007;192:246-252.
- (188) Staub D, Schinkel A, Coll B et al. Contrast-enhanced ultrasound imaging of the vasa vasorum: from early atherosclerosis to the identification of unstable plaques. *JACC Cardiovasc Imaging* 2010;3:761-771.
- (189) Kumamoto M, Nakashima Y, Sueishi K. Intimal neovascularization in human coronary atherosclerosis: its origin and pathophysiological significance. *Hum Pathol* 1995;26:450-456.
- (190) Masuzaki H, Ogawa Y, Isse N et al. Human obese gene expression. Adipocyte-specific expression and regional differences in the adipose tissue. *Diabetes* 2015;44:855-858.

- (191) Friedman JM, Halaas JL. Leptin and the regulation of body weight in mammals. *Nature* 1998;395:763-770.
- (192) Shek EW, Brands MW, Hall JE. Chronic leptin infusion increases arterial pressure. *Hypertension* 1998;31:409-414.
- (193) Konstantinides S, Schafer K, Loskutoff D. The prothrombotic effects of leptin: possible implications for the risk of cardiovascular disease in obesity. *Ann N Y Acad Sci* 2001;947:134-141.
- (194) Knudson JD, Dincer UD, Zhang C et al. Leptin Receptors are Expressed in Coronary Arteries and Hyperleptinemia Causes Significant Coronary Endothelial Dysfunction. *Am J Physiol Heart Circ Physiol* 2005.
- (195) Gruen M, Hao M, Piston D, Hasty A. Leptin requires canonical migratory signaling pathways for induction of monocyte and macrophage chemotaxis. *Am J Physiol Cell Physiol* 2007;293:C1481-C1488.
- (196) O'Rourke L, eaman S, hepherd P. Insulin and lepin acutely regulate cholesterol ester metabolism in macrophages by novel signaling pathways. *Diabetes* 2001;50:955-961.
- (197) Huang F, Xiong X, Wang H, You S, Zneg H. Leptin-induced vascular smooth muscle cell proliferation via regulating cell cycle, activating ERK1/2 and NF-kB. *Acta Biochim Biophys Sin* 2010;42:325-331.
- (198) Oda A, Taniguchi T, Yokoyama M. Leptin stimulates rat aortic smooth muscle cell proliferation and migration. *Kobe J Med Sci* 2001;47:141-150.
- (199) Gormez S, Demirkan A, Atalar F et al. Adipose tissue gene expression of adiponectin, tumor necrosis factor-alpha and leptin in metabolic syndrome patients with coronary artery disease. *Intern Med* 2011;50:805-810.
- (200) Jaffer I, Riederer M, Shah P et al. Expression of fat mobilizing genes in human epicardial adipose tissue. *Atherosclerosis* 2012;220:122-127.
- (201) Karastergiou K, Evans I, Ogston N et al. Epicardial adipokines in obesity and coronary artery disease induce atherogenic changes in monocytes and endothelial cells. *Arterioscler Thromb Vasc Biol* 2010;30:1340-1346.
- (202) Fortuno A, Rodriguez A, Gomez-Ambrosi J et al. Leptin inhibits angiotensin II-induced intracellular calcium increase and vasoconstriction in the rat aorta. *Endocrinology* 2002;143:3555-3560.
- (203) Rodriguez A, Fortuno A, Gomez-Ambrosi J, Zalba G, Diez J, Fruhbeck G. The inhibitory effect of leptin on angiotensin II-induced vasoconstriction in vascular smooth muscle cells is mediated via a nitric oxide-dependent mechanism. *Endocrinology* 2007;148:324-331.
- (204) Rodriguez A, Fruhbeck G, Gomez-Ambrosi J et al. The inhibitory effect of leptin on angiotensin II-induced vasoconstriction is blunted in spontaneously hypertensive rats. *J Hypertens* 2006;24:1589-1597.

- (205) Barandier C, Montani J, Yang Z. Mature adipocytes and perivascular adipose tissue stimulate vascular smooth muscle cell proliferation: effects of aging and obesity. *Am J Physiol Heart Circ Physiol* 2005;289:H1807-H1813.
- (206) Schafer K, Halle M, Goeschen C et al. Leptin promotes vascular remodeling and neointimal growth in mice. *Arterioscler Thromb Vasc Biol* 2004;24:112-117.
- (207) Schroeter MR, Eschholz N, Herzberg S et al. Leptin-dependent and leptin-independent paracrine effects of perivascular adipose tissue on neointima formation. *Arterioscler Thromb Vasc Biol* 2013;33:980-987.
- (208) Minobe E, Asmara H, Saud ZA, Kameyama M. Calpastatin domain L is a partial agonist of the calmodulin-binding site for channel activation in Cav1.2 Ca²⁺ channels. *J Biol Chem* 2011;286:39013-39022.
- (209) Saud Z, Minobe E, Wang W et al. Calpastatin binds to a calmodulin-binding site of cardiac CaV1.2 Ca²⁺ channels. *Biochem Biophys Res Commun* 2007;364:372-377.
- (210) Sun W, Feng R, Hu H et al. The Ca²⁺-dependent interaction of calpastatin domain L with the C-terminal tail of the CaV1.2 channel. *FEBS Letters* 2014;588:665-671.
- (211) De Rosa S, Cirillo P, Pacileo M, Di Palma V, Paglia A, Chiariello M. Leptin stimulated C-reactive protein production by human coronary artery endothelial cells. *J Vasc Res* 2009;46:609-617.
- (212) Casellini C, Barlow P, Rice A et al. A 6-month, randomized, double-masked, placebo-controlled study evaluating the effects of the protein kinase C-beta inhibitor ruboxistaurin on skin microvascular blood flow and other measures of diabetic peripheral neuropathy. *Diabetes Care* 2007;30:896-902.
- (213) Mehta N, Sheetz M, Price K et al. Selective PKC beta inhibition with ruboxistaurin and endothelial function in type-2 diabetes mellitus. *Cardiovasc Drugs Ther* 2009;23:17-24.
- (214) Bohlen H. Mechanisms for early microvascular injury in obesity and type II diabetes. *Curr Hypertens Rep* 2004;6:60-65.
- (215) Kadowaki T, Yamauchi T, Kubota N, Hara K, Ueki K, Tobe K. Adiponectin and adiponectin receptors in insulin resistance, diabetes, and the metabolic syndrome. *J Clin Invest* 2006;116:1784-1792.
- (216) Lee S, Zhang H, Chen J, Dellsperger K, Hill M, Zhang C. Adiponectin abates diabetes-induced endothelial dysfunction by suppressing oxidative stress, adhesion molecules, and inflammation in type 2 diabetic mice. *303* 2012;H106:H115.
- (217) Deng G, Long Y, Yu Y, Li M. Adiponectin directly improves endothelial dysfunction in obese rats through the AMPK-eNOS pathway. *Int J Obes (Lond)* 2010;34:165-171.

- (218) Riento K, Ridley A. ROCKs: multifunctional kinases in cell behavior. *Nat Rev Mol Cell Biol* 2003;4:446-456.
- (219) Etienne-Manneville S, Hall A. Rho GTPases in cell biology. *Nature* 2002;420:629-635.
- (220) Loirand G, Guerin P, Pacaud P. Rho kinases in cardiovascular physiology and pathophysiology. *Circ Res* 2006;98:322-334.
- (221) Somlyo A, Somlyo A. Ca²⁺ sensitivity of smooth muscle and non-muscle myosin II. Modulated by G proteins, kinases, and myosin phosphatase. *Physiol Rev* 2003;83:1325-1358.
- (222) Kamiyama M, Utsunomia K, Taniguchi K et al. Contribution of RhoA and Rho kinase to platelet-derived growth factor-BB-induced proliferation of vascular smooth muscle cells. *J Atheroscler Thromb* 2003;10:117-123.
- (223) Seasholtz T, Majumdar M, Kaplan D, Brown J. Rho and Rho kinase mediate thrombin-stimulated vascular smooth muscle cell DNA synthesis and migration. *Circ Res* 1999;84:1186-1193.
- (224) Pearce J, Li J, Edwards M, English W, Geary R. Differential effects of Rho-kinase inhibition on artery wall mass and remodeling. *J Vasc Surg* 2004;39:223-228.
- (225) Eto Y, Shimokawa H, Hiroki J et al. Gene transfer of dominant negative Rho kinase suppresses neointimal formation after balloon injury in pigs. *Am J Heart Circ Physiol* 2000;278:H1744-H1750.
- (226) Shibata R, Kai H, Seki Y et al. Role of Rho-associated kinase in neointima formation after vascular injury. *Circulation* 2001;103:284-289.
- (227) Negoro N, Hoshiga M, Seto M et al. The kinase inhibitor fasudil (HA-1077) reduces neointimal hyperplasia through inhibiting migration and enhancing cell loss of vascular smooth muscle cells. *Biochem Biophys Res Commun* 1999;262:211-215.
- (228) Boydens C, Maenhaut N, Pauwels B, Decaluwe K, Van d, V. Adipose tissue as regulator of vascular tone. *Curr Hypertens Rep* 2012;14:270-278.
- (229) Lohn M, Dubrovskaja G, Lauterbach B, Luft FC, Gollasch M, Sharma AM. Periadventitial fat releases a vascular relaxing factor. *FASEB J* 2002;16:1057-1063.
- (230) Letavernier E, Perez J, Bellocq A et al. Targeting the calpain/calpastatin system as a new strategy to prevent cardiovascular remodeling in angiotensin II-induced hypertension. *Circ Res* 2008;102:720-728.
- (231) Lau S, Chu P, Weiss L. A specific marker of macrophages in paraffin-embedded tissue samples. *Hematopathology* 2004;122:794-801.
- (232) Schindelin J, Arganda-Carreras I, Frise E et al. Fiji: an open-source platform for biological-image analysis. *Nature Methods* 2012;9:676-682.

- (233) Samora JB, Goodwill AG, Frisbee JC, Boegehold MA. Growth-dependent changes in the contribution of carbon monoxide to arteriolar function. *J Vasc Res* 2010;47:23-24.
- (234) Dyson MC, Alloosh M, Vuchetich JP, Mokolke EA, Sturek M. Components of metabolic syndrome and coronary artery disease in femal Ossabaw swine fed excess atherogenic diet. *Comp Med* 2006;56:35-45.
- (235) Edwards JM, Neeb ZP, Alloosh MA et al. Exercise training decreases store-operated Ca²⁺entry associated with metabolic syndrome and coronary atherosclerosis. *Cardiovasc Res* 2010;85:631-640.
- (236) Neeb Z, Edwards J, Aloosh M, Long X, Mokolke E, Sturek M. Metabolic syndrome and coronary artery disease in Ossabaw comapred with Yucatan swine. *Comparative Medicine* 2010;60:300-315.
- (237) Turk J, Carroll J, Laughlin H et al. C-reactive protein correlates with macrophage accumulation in coronary arteries of hypercholesterolemic pigs. *J Appl Physiol* 2003;95:1301-1304.
- (238) Agabiti-Rosei C, De Ciuceis C, Rossini C et al. Anticontractile activity of perivascular fat in obese mice and the effect of long-term treatment with melatonin. *J Hypertens* 2014;32:1264-1274.
- (239) Withers S, Simpson L, Fattah S, Werner M, Heagerty A. cGMP-dependent protein kinase (PKG) mediates the anticontractile capacity of perivascular adipose tissue. *Cardiovasc Res* 2014;101:130-137.
- (240) Berwick ZC, Dick GM, Tune JD. Heart of the matter: coronary dysfunction in metabolic syndrome. *J Mol Cell Cardiol* 2012;52:848-856.
- (241) Lu T, Ye D, He T, Wang X, Wang H, Lee H. Imparied Ca²⁺-dependent activation of large-conductance Ca²⁺-activated K⁺ channels in the coronary artery smooth muscle cells of Zucker diabetic fatty rats. *Biophys J* 2008;95:5165-5177.
- (242) Yang Y, Jones A, Thomas T, Rubin L. Influence of sex, high-fat diet, and exercise training on potassium currents of swine coronary smooth muscle. *Am J Physiol Heart Circ Physiol* 2007;293:H1553-H1563.
- (243) Sellers A, Ashford M. Activation of BKCa channels in acutely dissociated neurones from the rat ventromedial hypothalamus by NS1619. *Br J Parmacol* 1994;113:659-661.
- (244) Seebohm G, Pusch M, Chen J, Sanguinetti M. Parmacological activation of normal and arrhythmia-associated mutant KCNQ1 potassium channels. *Circ Res* 2003;93:941-947.
- (245) D'hahan N, Jacquet H, Moreau C, Catty P, Vivaudou M. A transmembrane domain of hte sulfonylurea receptor mediates activation of ATP-sensitive K(+) channels by K(+) channel openers. *Mol Pharmacol* 1999;56:308-315.

- (246) Zuidema M, Yang Y, Wang M et al. Antecedent hydrogen sulfide elicits an anti-inflammatory phenotype in postischemic murine small intestine: role of BK channels. *Am J Physiol Heart Circ Physiol* 2010;299:H1554-H1567.
- (247) Hu Y, Yang G, Xiao X, Liu L, Li T. Bkca opener, NS1619 pretreatment protects against shock-induced vascular hyporeactivity through PDZ-Rho GEF-RhoA-Rho kinase pathway in rats. *J Trauma Acute Care Surg* 2014;76:394-401.
- (248) Bardou O, Prive A, Migneault F et al. K⁺ channels regulate ENaC expression via changes in promoter activity and control fluid clearance in alveolar epithelial cells. *Biochem Biophys Acta* 2012;1818:1682-1690.
- (249) Kubo M, Quayle J, Standen N. Angiotensin II inhibition of ATP-sensitive K⁺ currents in rat arterial smooth muscle cells through protein kinase C. *J Physiol* 1997;503:489-496.
- (250) Chatterjee T, Idelman G, Blanco V et al. Histone deacetylase 9 is a negative regulator of adipogenic differentiation. *J Biol Chem* 2011;286:27836-27847.
- (251) Drolet R, Belanger C, Fortier M et al. Fat depot-specific impact of visceral obesity on adipocyte adiponectin release in women. *Obesity (Silver Spring)* 2009;17:424-430.
- (252) Noblet JN, Owen MK, Goodwill AG, Sassoon DJ, Tune JD. Lean and obese coronary perivascular adipose tissue impairs vasodilation via differential inhibition of vascular smooth muscle K⁺ channels. *Arterioscler Thromb Vasc Biol* 2015;35:1393-1400.
- (253) Gorter PM, van Lindert AS, de Vos AM et al. Quantification of epicardial and pericoronary fat using cardiac computed tomography; reproducibility and relation with obesity and metabolic syndrome in patients suspected of coronary artery disease. *Atherosclerosis* 2008;197:896-903.
- (254) Beltowski J. Leptin and the regulation of endothelial function in physiological and pathological conditions. *Clin Exp Pharmacol Physiol* 2012;39:168-178.
- (255) Knudson JD, Dincer UD, Zhang C et al. Leptin Receptors are Expressed in Coronary Arteries and Hyperleptinemia Causes Significant Coronary Endothelial Dysfunction. *Am J Physiol Heart Circ Physiol* 2005.
- (256) Bohlen F, Kratzsh J, Mueller M et al. Leptin inhibits cell growth of human vascular smooth muscle cells. *Vascul Pharmacol* 2007;46:67-71.
- (257) Bouloumie A, Marumo T, Lafontan M, Busse R. Leptin induces oxidative stress in human endothelial cells. *FASEB J* 1999;13:1231-1238.
- (258) Korda M, Kubant R, Patton S, Malinski T. Leptin-induced endothelial dysfunction in obesity. *Am J Physiol Heart Circ Physiol* 2008;295:H1514-H1521.
- (259) Zeidan A, Javadov S, Karmazyn M. Essential role of Rho/ROCK-dependent processes and actin dynamics in mediating leptin-induced hypertrophy in rat neonatal ventricular myocytes. *Cardiovasc Res* 2006;72:101-111.

- (260) Zeidan A, Paylor B, Steinhoff K et al. Actin cytoskeleton dynamics promotes leptin-induced vascular smooth muscle hypertrophy via RhoA/ROCK- and phosphatidylinositol 3-kinase/protein kinase B-dependent pathways. *J Pharmacol Exp Ther* 2007;322:1110-1116.
- (261) Zeidan A, Javadov S, Chakrabarti S, Karmazyn M. Leptin-induced cardiomyocyte hypertrophy involves selective caveolae and RhoA/ROCK-dependent p38 MAPK translocation to nuclei. *Cardiovasc Res* 2008;77:64-72.
- (262) Shan J, Nguyen TB, Totary-Jain H, Dansky H, Marx SO, Marks AR. Leptin-enhanced neointimal hyperplasia is reduced by mTOR and PI3K inhibitors. *Proc Natl Acad Sci USA* 2008;105:19006-19011.
- (263) Liu B, Itoh H, Louie O, Kubota K, Kent K. The signaling protein Rho is necessary for vascular smooth muscle migration and survival but not for proliferation. *Surgery* 2002;132:317-325.
- (264) Pardina E, Ferrer R, Baena-Fustegueras J et al. The relationships between IGF-1 and CRP, NO, leptin, and adiponectin during weight loss in the morbidly obese. *Obes Surg* 2010;40:623-632.
- (265) Lin YC, Huang J, Kan H, Castranova V, Frisbee JC, Yu HG. Defective calcium inactivation causes long QT in obese insulin-resistant rat. *Am J Physiol Heart Circ Physiol* 2012;302:H1013-H1022.
- (266) Owens GK, Kumar MS, Wamhoff BR. Molecular regulation of vascular smooth muscle cell differentiation in development and disease. *Physiol Rev* 2004;84:767-801.
- (267) Wamhoff BR, Bowles DK, McDonald OG, Sinha S, Somlyo AP, Owens GK. L-type voltage-gated Ca²⁺ channels modulate expression of smooth muscle differentiation marker genes via a Rho kinase/myocardin/SRF-dependent mechanism. *Circ Res* 2004;95:406-414.
- (268) Ozer C, Gulen S, Dilekoz E, Babul A, Ercan ZS. The effect of systemic leptin administration on aorta smooth muscle responses in diabetic rats. *Mol Cell Biochem* 2006;282:187-191.
- (269) Shin HJ, Oh J, Kang SM et al. Leptin induces hypertrophy via p38 mitogen-activated protein kinase in rat vascular smooth muscle cells. *Biochem Biophys Res Commun* 2005;329:18-24.
- (270) Rodriguez A, Gomez-Ambrosi J, Catalan V, Fortuno A, Fruhbeck G. Leptin inhibits the proliferation of vascular smooth muscle cells induced by angiotensin II through nitric oxide-dependent mechanisms. *Mediator Inflamm* 2010;2010.
- (271) Davies S, Reddy H, Caivano M, Cohen P. Specificity and mechanism of action of some commonly used protein kinase inhibitors. *Biochem J* 2000;351:95-105.
- (272) Bain J, Plater L, Elliott M et al. The selectivity of protein kinase inhibitors: a further update. *Biochem J* 2007;408:297-315.

- (273) Rikitake Y, Kim H, Huang Z et al. Inhibition of Rho kinase (ROCK) leads to increased cerebral blood flow and stroke protection. *Stroke* 2005;36:2251-2257.
- (274) Despres J, Lemieux I. Abdominal obesity and metabolic syndrome. *Nature* 2006;444:881-887.
- (275) World Health Organization. Obesity: preventing and managing the global epidemic. WHO Technical Report Series 2000;894.
- (276) World Health Organization. Global strategy on diet, physical activity and health. World Health Assembly resolution 2004;WHA57.17.
- (277) Britton KA, Fox CS. Perivascular adipose tissue and vascular disease. *Clin Lipidol* 2011;6:79-91.
- (278) Foo J, Polyzos S, Anastasilakis A, Chou S, Mantzoros C. The effect of leptin replacement on parathyroid hormone, RANKL-osteoprotegerin axis, and Wnt inhibitors in young women with hypothalamic amenorrhea. *J Clin Endocrinol Metab* 2014;99:E2252-E2258.
- (279) Guzel S, Seven A, Kocaoglu A et al. Osteoprotegerin, leptin and IL-6: association with silent myocardial ischemia in type 2 diabetes mellitus. *Diab Vasc Dis Res* 2013;10:25-31.
- (280) Liu G, Liang Q, Cui R et al. Leptin promotes the osteoblastic differentiation of vascular smooth muscle cells from female mice by increasing RANKL expression. *Endocrinology* 2014;155:558-567.
- (281) Venuraju S, Yerramasu A, Corder R, Lahiri A. Osteoprotegerin as a predictor of coronary artery disease and cardiovascular mortality and morbidity. *J Am Coll Cardiol* 2010;55:2049-2061.
- (282) Dhore C, Cleutjens J, Lutgens E et al. Differential expression of bone matrix proteins in human atherosclerotic plaques. *Arterioscler Thromb Vasc Biol* 2001;21:1998-2003.
- (283) Sandberg W, Yndestad A, Oie E et al. Enhanced T-cell expression of RANK ligand in acute coronary syndrome: possible role in plaque destabilization. *Arterioscler Thromb Vasc Biol* 2006;26:857-863.

CURRICULUM VITAE

Jillian Nicole Noblet

EDUCATION

Indiana University

April 2016

Doctor of Philosophy, Cellular & Integrative Physiology

GPA: 4.0

Indiana University – Purdue University Indianapolis

May 2012

Bachelor of Science, Biology

GPA: 4.0

RESEARCH EXPERIENCE

Johnathan D. Tune, PhD Laboratory

2013 – 2016

Cellular & Integrative Physiology, IU School of Medicine

PROFESSIONAL EXPERIENCE

Indiana University School of Medicine

2015 – present

Council Member, Networking Committee

- Facilitating network development among IUSM and industry/biotech professionals
- Recruiting industry professionals to attend bi-annual networking events
- Supporting professional development programs for IUSM graduate students

Indiana Physiological Society

2014 – present

Council Member

- Working to unite physiologists and promote the discipline in the state Indiana
- Establishing outreach programs to foster K-12 interest in physiology
- Organizing the annual meeting of the society's ~250 members

American Physiological Society

2015 – present

Chair-elect, Cardiovascular Section Trainee Council

- Serving as the representative for ~500 cardiovascular trainees nationwide
- Advocating for the needs of trainees within the American Physiological Society
- Promoting cardiovascular trainee participation at national conferences

TEACHING ASSIGNMENTS

Indiana University School of Medicine

G717 – Cellular Basis of Systems Biology

Teaching Assistant

2013 – 2015

G735 – Cardiovascular, Renal, and Respiratory Function in Health and Disease 2015
Teaching Assistant

GRANTS AND FELLOWSHIPS

Indiana Clinical & Translational Sciences Predoctoral Fellowship 2014 – present
NIH, National Center for Advancing Translational Sciences
Grant application-based award for translational research projects, supports annual stipend

Moenkhaus Physiology Fellowship 2013
Indiana University School of Medicine
Awarded to first year students with exemplary academic records, supports annual stipend

HONORS AND AWARDS

Young Investigator Award 2016
Society for Experimental Biology and Medicine
Abstract-based award at the national Experimental Biology meeting

Dr. Stier Physiology Award 2015
Indiana University School of Medicine
Awarded to physiology students for excellence in research, supplements annual stipend

Caroline tum Suden/Frances Hellebrandt Professional Opportunity Award 2015
American Physiological Society
Abstract-based award, supports travel to the national Experimental Biology meeting

PUBLICATIONS

Peer-Reviewed Journal Articles

1. **Noblet JN**, Goodwill AG, Sassoon DJ, Kiel AM, Tune JD. Leptin augments coronary vasoconstriction and smooth muscle proliferation via a Rho kinase dependent pathway. *Basic Res Cardiol.* 2016. *In press.*
2. Goodwill AG, **Noblet JN**, Sassoon DJ, Fu L, Kassab GS, Schepers L, Tune JD, Dick GM. Critical contribution of K_v1 channels to the regulation of coronary blood flow. *Basic Res Cardiol.* 2016. *In review.*
3. Sassoon DJ, Goodwill AG, **Noblet JN**, Conteh AM, Herring B, McClintick J, Tune JD, Mather KJ. Obesity alters molecular and functional cardiac responses to ischemia-reperfusion and glucagon-like peptide-1 receptor agonism. *Basic Res Cardiol.* 2016. *In review.*
4. Goodwill AG, Fu L, **Noblet JN**, Casalini ED, Sassoon DJ, Berwick Z, Kassab GS, Tune JD, Dick GM. K_v7 channels contribute to paracrine, but not metabolic or ischemic, regulation of coronary vascular reactivity in swine. *Am J Physiol Heart Circ Physiol.* 2016.

5. **Noblet JN**, Owen MK, Goodwill AG, Sassoon DJ, Tune JD. Coronary perivascular adipose tissue impairs K⁺ channel mediated vasodilation in lean and obese hearts. *Arterioscler Thromb Vasc Biol.* 2015.
6. Owen MK, **Noblet JN**, Sassoon DJ, Conteh AM, Goodwill AG, Tune JD. Perivascular adipose tissue and coronary vascular disease. *Arterioscler Thromb Vasc Biol.* 2014.
7. Goodwill AG, Tune JD, **Noblet JN**, Conteh AM, Sassoon DJ, Casalini ED, Mather KJ. Glucagon like peptide-1 (7-36) but not (9-36) augments cardiac output during myocardial ischemia via a Frank-Starling Mechanism. *Basic Res Cardiol.* 2014.
8. Goodwill AG, Mather KJ, Conteh AM, Sassoon DJ, **Noblet JN**, Tune JD. Cardiovascular and hemodynamic effects of glucagon-like peptide-1. *Rev Endocr Metab Disord.* 2014.
9. Hiatt SC, Owen MK, Li W, Chen X, Riley AM, **Noblet JN**, Flores S, Sturek M, Tune JD, Obukhov AG. Mechanisms underlying capsaicin effects in canine coronary artery: implications for coronary spasm. *Cardiovasc Res.* 2014.

Published Abstracts at National Meetings

1. **Noblet JN**, Goodwill AG, Dassoon DJ, Kiel AM, Tune JD. Role of leptin in coronary vascular dysfunction and proliferation. Experimental Biology, 2016.
2. Goodwill AG, **Noblet JN**, Sassoon DJ, Fu L, Schepers L, Sturek J, Tune JD, Dick GM. K_v1 channels are critical regulators of coronary blood flow in swine. Experimental Biology, 2016.
3. Goodwill AG, Sassoon DJ, **Noblet JN**, Conteh AM, Mather KJ, Tune JD. The long acting GLP-1 receptor agonist, liraglutide, augments myocardial contractile responses and cardiac efficiency under sympathetic stimulation in obesity and myocardial infarction. Experimental Biology, 2016.
4. Sassoon DJ, Goodwill AG, **Noblet JN**, Conteh AM, Herring BP, McClintick J, Tune JD, Mather KJ. Obesity distinctly influences cardiac function and molecular responses to ischemia-reperfusion and GLP-1 receptor agonism. Experimental Biology, 2016.
5. Kiel AM, Goodwill AG, **Noblet JN**, Sassoon DJ, Tune JD. Determinants of myocardial oxygen delivery in response to moderate and severe reductions in hematocrit. Experimental Biology, 2016.
6. **Noblet JN**, Goodwill AG, Sassoon DJ, Tune JD. Coronary vascular effects of leptin and calpastatin in lean vs. obese hearts. Experimental Biology, 2015.
7. **Noblet JN**, Owen MK, Goodwill AG, Sassoon DJ, Tune JD. Perivascular adipose tissue and vascular reactivity in obesity-induced coronary disease. Translational Science, 2015.

8. Goodwill AG, Mather KJ, **Noblet JN**, Sassoos DJ, Conteh AM, Tune JD. Effects of liraglutide on cardiac function and myocardial infarct size in the setting of obesity. *Experimental Biology*, 2015.
9. **Noblet JN**, Owen MK, Goodwill AG, Dick GM, Tune JD. Coronary perivascular adipose tissue and K⁺ channel-mediated vasodilation in lean and obese hearts. *Experimental Biology*, 2014.
10. Goodwill AG, Casalini ED, Conteh AM, **Noblet JN**, Sassoos DJ, Tune JD, Mather KJ. GLP-1 (7-36) augments cardiac output during regional myocardial ischemia via increases in ventricular preload, independent of changes in cardiac inotropy. *Experimental Biology*, 2014.
11. Goodwill AG, Casalini ED, **Noblet JN**, Christe ME, Kowala M, Zhen EY, Berwick ZC, Moberly SP, Tune JD. Effects of systemic [Pyr] Apelin-13 administration on coronary and peripheral hemodynamics. *Experimental Biology*, 2014.
12. Conteh AM, Goodwill AG, **Noblet JN**, Sassoos DJ, Tune JD, Mather KJ. Exendin-4 treatment increases contractile function during ischemia in lean but not obese swine. *Experimental Biology*, 2014.
13. Sassoos DJ, Goodwill AG, Conteh AM, **Noblet JN**, Mather KJ, Tune JD. Characterization of cardiovascular performance during ischemia-reperfusion injury in obese vs. lean Ossabaw swine. *Experimental Biology*, 2014.
14. McKenney ML, Dineen SL, **Noblet JN**, Tune JD, Sturek M. Increased Ca²⁺-activated Ca²⁺ influx and impaired Ca²⁺-buffering in coronary smooth muscle from metabolic syndrome Ossabaw swine. *Experimental Biology*, 2014.
15. Fancher IS, **Noblet JN**, Goodwill AG, Tune JD, Dick GM. Mechanism of inhibition of delayed rectifier K⁺ current (K_{DR}) by diphenyl phosphine oxide-1 (DPO-1) in porcine coronary smooth muscle. *Experimental Biology*, 2014.